B Cell Responses to Protein Adducts

Lachlan Deimel



Supervisors: Profs Quentin J. Sattentau & Benjamin G. Davis

A thesis submitted for the degree of Doctor of Philosophy in Molecular Cell Biology in Health and Disease at the Sir William Dunn School of Pathology, University of Oxford

(This page is intentionally left blank)

“Science is not a heartless pursuit of objective information; it is a creative human activity”

- Stephen Jay Gould

(This page is intentionally left blank)

Aspects of this thesis are included in publications, as listed below:

- **Deimel, L. P.**, Xue, X., Khan, A., Moynie, L., Buchanan, C. J., Sun, G., McBride, R., Schuster, H., Gauthier, C., Saliba, R., Leonavicus, K., Minall, L., Bort, G., Russell, R. A., Sezgin, E., Paulson, J. C., Anthony, D. C., Baldwin, A. J., Naismith, J., … Sattentau, Q. J. (2023). Engineered display of ganglioside-sugars on protein elicits a clonally and structurally constrained B cell response. *BioRxiv*, 2023.06.03.543556. https://doi.org/10.1101/2023.06.03.543556
- **Deimel, L. P.**, Xue, X., & Sattentau, Q. J. (2022). Glycans in HIV-1 vaccine design - engaging the shield. *Trends in Microbiology*. https://doi.org/10.1016/j.tim.2022.02.004
- **Deimel, L. P.**, Liu, X., Gilbert-Jaramillo, J., Liu, S., James, W. S., & Sattentau, Q. J. (2022). Intranasal SARS-CoV-2 spike-based immunisation adjuvanted with polyethyleneimine elicits mucosal and systemic humoral responses in mice. *Journal of Immunological Methods*, *511*, 113380. https://doi.org/https://doi.org/10.1016/j.jim.2022.113380
- Buchanan, C. J., Gaunt, B., Harrison, P. J., Yang, Y., Liu, J., Khan, A., Giltrap, A. M., le Bas, A., Ward, P. N., Gupta, K., Dumoux, M., Tan, T. K., Schimaski, L., Daga, S., Picchiotti, N., Baldassarri, M., Benetti, E., Fallerini, C., Fava, F., … **Deimel, L. P.**, … Davis, B. G. (2022). Pathogen-sugar interactions revealed by universal saturation transfer analysis. *Science*, *377*(6604), eabm3125. https://doi.org/10.1126/science.abm3125

(This page is intentionally left blank)

Abstract

Protein adducts are covalent additions between electrophiles and nucleophilic protein sites, such as amines of some sidechain residues. These adducts may form functional antigenic complex that elicit downstream anti-adduct responses: surfaces encompassing the adduct may be recognised by cognate B cells, while associated peptide may be presented to T cells. In this thesis, I investigate protein adducts in two discrete contexts: 1) as a potential vaccine design tool in overcoming tolerance barriers to an immunorecessive glycan, and 2) the immunogenicity of a protein-reactive small-molecule drug.

…

Tumour-associated carbohydrate antigens (TACAs) are long-proposed targets for vaccination and therapeutic antibody production, but their self-like character imparts immunorecessiveness that classical vaccination approaches have failed to overcome. One prominent TACA, the glycan component of ganglioside sugar GM3 (GM3g), is over-expressed on diverse tumours and is notoriously immunorecessive. Weak adaptive responses to GM3 are believed to be associated with both lack of associated T cell help and lack of cognate naïve B cells in the repertoire. Here, I report on the immunogenicity of a novel synthetic protein chemistry pipeline wherein artificial conjugates of GM3g are presented via a short, bespoke synthetic linker, [–amidine-GM3g], on primary amines of lysine sidechains of carrier proteins. These long orthogonal glycoconjugates (LOGs) are highly immunogenic in mice, raising a robust GM3g-specific IgG response. Thorough antigen-specific clonotyping of the B cell response revealed a novel lectin-like clonal class raised against the LOG, with a defined germline configuration dominated by members of the *IGHV2* subgroup. Subsequent

structural, biophysical and biochemical characterisation of the response demonstrated how the artificial display of GM3g accesses this unique clonotype, but also explains why antibodies do not cross-react with native, ceramide-docked GM3g. These findings represent the first potential step towards a novel germline targeting-like approach to vaccine design against this and other TACAs.

…

β-lactam antibiotics, such as penicillin G (PenG) are chemically unstable under carbonate buffer systems, such as that in serum. Lactam-based adducts have long been hypothesised as a key antigenic driver of antibody-mediated hypersensitivity, both IgE and IgG, although the molecular basis for these reactions and the determinants of drug adduct immunogenicity are poorly understood. Using a murine model, I investigate both the pharmacokinetic and immunological factors that determine the penicilloyl-specific antibody responses. I demonstrate that free drug availability, innate immune activation and protein carrier factors are critical in determining the serological response. Clonotyping of the anti-PenG response revealed a single dominant clonotype raised against the drug, comprised of phylogeneticially-related *IGHV1*, *IGHV5*, *IGHV10* and *IGHV14* family members. Further structural and biochemical characterisation of the clonal family raised against the drug may inform the design of a PenG analogues that cannot bind this B cell clonal class, representing a candidate no/low allergenic drug alternative in a mouse model.

…

In summary, protein adducts have broad implications for immunity and pathology. This thesis contributes to how we may utilise these adducts as tools both for vaccine design and to study the role of adducts in disease.

Acknowledgements

First, I am thoroughly grateful for the support of my supervisor, Quentin Sattentau: Quentin, I hope to be even half the scientist and mentor you are—deeply thoughtful, always kind and boundlessly creative. It has been a blast and am so proud of the work we have done together. Thank you also to my co-supervisor, Ben Davis, for his guidance and wisdom throughout my doctoral training. Ben's excitement and lateral thinking deeply encouraged me to push the science forward, and I've learned a lot from him.

A particular appreciation goes out to Xiaochao Xue, whose chemical wizardry made much of the glycoconjguate work possible. Chao, I am so thankful for your hard work on these projects, and for your friendship. These thanks also extend to Aziz Khan, Guoxuan Sun and many other past members of the Davis lab who have contributed to aspects of the synthetic carbohydrate chemistry utilised in this thesis.

I've been fortunate to benefit from the talent and expertise of many of our collaborators. Thank you to Lucile Moynie and James Naismith for your structural biology support and expertise, to Ryan McBride and James Paulson for sharing your glycan array, to Toshiki Eri and James di Santo for generating and maintaining humanised mice for us, to Dominik Damm and Klaus Überla for maintaining and immunising TRIANNI mice, and to Sean Burnap for your support in running mass spectral analyses on my protein adducts. These contributions have really strengthened my thesis and I am very grateful.

Thanks also extends to the many facilities staff at the Dunn School of Pathology. I'd like to thank the animal support staff who took care of my mice day-to-day. In particular, I'm so grateful to Nicky Hamp: the care and support you show all of the researchers who use the animal facility is amazing—we are in complete awe of the work you put in. I'm also grateful for the help from Robert Hedley and Vasiliki Tsioligka, who manage and run the cell sorting facility.

The Sattentau lab members have shown me much friendship and support. A particular shout-out to Rebecca Moore—thank you for your incredible kindness, unmatched organisation, technical prowess, and all-round lab superstardom. We miss you terribly. To Lu Li Jovanoska, Linnea Drexhage, Kate Dicker, Shengpan Zhang and Scarlett Harris—it has been so wonderful to work alongside you all and am deeply excited to see your careers continue to take-off and flourish.

I have such a fabulous group of friends in Oxford who have made my time just so amazingly positive. Sam Day, Bill de la Rosa, Claudia McHardy, Sophie van Leur, Asmaa Hachim, Paul Metz, Anne Sophie Larsen, Jacob Wall, Annie Shaw, Oresis Zavlis, Anish Gawande—you're all so wonderful. Thank you for keeping me sane and for dragging me out of the lab.

Finally, to my dad, Ashley, my sister, Isobel, and my Oma, Henny: thank you for the love you've shown me throughout this crazy time in Oxford. Last and most importantly, Bryce, my love, thank you for the care and compassion you've shown me, especially during the toughest times of my DPhil. I'm grateful every day for the sacrifices you make for me to be in Oxford. I love you immensely.

x

Table of contents

Abstract ..... **vii**

Acknowledgements ..... **ix**

Table of contents ..... **xi**

Abbreviations ..... **xviii**

Chapter 1—Introduction **1**

1.1. B cell biology and antibody development 1

1.1.1. The role of T cells: a classical hapten-carrier biology perspective 6

1.1.2. Outstanding problems in protein conjugate antigens 8

1.2. Introduction to glycan immunogenicity 9

1.3. Introduction to glycosylation in cancer 11

1.4. Immunogenicity of TACAs 15

1.4.1. Constraints of the naïve B cell repertoire in TACA recognition 15

1.4.2. T cell immunorecessiveness to TACAs 17

1.4.3. Inherent immunoinhibitory effects of some TACAs 21

1.5. TACA-directed vaccination design strategies to improve B cell responses 22

1.6. Key challenges in TACA-directed vaccination design 26

1.6.1. Lack of anti-TACA B cell clonotyping 26

1.6.2. Potential consequences of synthetic linkers 28

1.6.3. Heterogeneity in TACA profiles and tumour adaptability 29

1.6.4. Breaking self-glycan tolerance: a word of caution 30

1.7. Summary of TACA vaccination 30

1.8. Overview of anti-drug antibodies..... 31

1.8.1. β-lactam antibiotics..... 32

1.8.2. Immunogenicity of penicillin adducts..... 34

1.9. Aims and hypotheses..... 36

Chapter 2—Materials and Methods..... 39

2.1. Immunogen synthesis and chemical characterisation 39

2.1.1. Molecular cloning..... 39

2.1.2. Mammalian protein expression..... 40

2.1.3. Protein purification..... 41

2.1.4. Protein quantification..... 43

2.1.5. Synthesis and conjugation of semi-synthetic glycoconjugates..... 43

2.1.6. Ex vivo drug modification of proteins..... 46

2.1.7. Evaluation of endotoxin 47

2.1.8. Protein gel electrophoresis..... 48

2.1.9. Mass spectrometry (MS) 49

2.1.10. PNAse F treatment of glycoproteins..... 50

2.1.11. Liposome synthesis..... 50

2.2. Animal work and immunisation schedules 51

2.2.1. Animal handling and maintenance 51

2.2.2. Formulation of immunisations..... 52

2.3. ELISA 53

2.3.1. Direct ELISA 53

2.3.2. Competition ELISA 54

2.3.3. Free primary amine ELISA 54

2.3.4. Capture cytokine ELISA 55

2.4. T cell analyses 55

2.4.1. Preparation of murine single cell suspensions 55

2.4.2. Thymidine proliferation assay 56

2.4.3. Intracellular cytokine staining 56

2.4.4. Tfh quantification 57

2.5. Glycan array 57

2.6. Isolation of single antigen-specific B cells 58

2.6.1. Molecular probe synthesis 58

2.6.2. Single cell sorting 59

2.6.3. Recovery of variable region sequences 60

2.6.4. Vectorisation and recombinant mAb expression 62

2.6.5. Immunogenetic analysis 65

2.7. Isothermal titration calorimetry (ITC) 65

2.8. X-ray crystallography 66

2.9. Bacterial growth assays 67

2.9.1. Culturing and maintenance of Streptococcus pneumoniae 67

2.9.2. Liquid minimal inhibitory concentration (MIC) recovery assay 67

2.9.3. Disk diffusion assay 68

2.10. Data processing and statistical analysis 68

Chapter 3—Immunogenicity of semi-synthetic GM3g glycoconjugates in mice 69

3.1 Background 69

3.1.1 Immunorecessiveness of self-carbohydrate antigens 69

3.1.2 Conceptual framework for the glycan blind spot: the BCR–epitope recognition requirement 71

3.1.3 SiaLac as a model glycan 72

3.1.4 Rationale for a semi-synthetic glyco-hapten-based vaccination strategy 74

3.1.5 Aims 74

3.2 Results 75

3.2.1. Immunogenicity of native GM3 on liposomes 75

3.2.2. Differing presentation of GM3g modulates B cell immunogenicity .. 77

3.2.3. Evaluation of HEL-[–amidine-GM3g]$_6$ antigenicity and intrinsic immunogenicity of the GM3g modification 82

3.2.4. Evaluation of the glycoconjugate-specific antibody response 84

3.2.5. Precise LOG editing maps the role of glycan site and glycan display stoichiometry in modulating immunogenicity 86

3.2.6. Evaluating the immunogenicity of gp120-[–amidine-GM3g]$_{16}$ 93

3.2.7. Effects of sex and background on glycoconjugate-specific responses 98

3.2.8. Immunogenicity of [–amidine-GD3] LOGs..... 101

3.2.9. Evaluating the glycan specificity and linker-dependency of the anti-LOG serological response..... 103

3.2.10. Determining context-dependency in glycan recognition..... 106

3.3 Discussion..... 109

3.3.1. LOG-raised antiserum exhibits narrow glycan reactivity: a comparison with professional carbohydrate binding proteins 110

3.3.2. Context dependent glycan recognition: evaluating the translational potential of the LOG-raised antibody response..... 111

3.3.3. Relationship between LOG occupancy and immunogenicity: how important is avidity?..... 115

3.3.4. GM3 but not GD3: the implications of stochasticity in linker–glycan immunogenicity 117

3.3.5. Conclusions..... 118

Chapter 4—Molecular underpinnings of the LOG-specific antibody response..... 121

4.1 Background..... 121

4.1.1 Introduction to molecular immunology 121

4.1.2 Overview of B cell molecular cloning techniques 122

4.1.3 Rationale for a molecular approach to dissecting the anti-GM3g response..... 124

4.1.4 Aims..... 124

4.2 Results 125

4.2.1. Dissecting the clonality of the anti-GM3g-specific antibody response 125

4.2.2. The role of the protein backbone on GM3g-specific outcomes 131

4.2.3. Evaluating the effects of SHM on GM3g-specific antibody clones 136

4.2.4. Biophysical, structural and biochemical characterisation of prototypical monoclonal antibody, BAR-1..... 137

4.2.5. Predicting the translational potential of the [–amidine-GM3g] LOG 144

4.3 Discussion..... 149

4.3.1. Clonal responses to LOGs: lectin-like motifs in the germline 151

4.3.2. Carrier protein toggles GC experience but not LOG-specific clonality 152

4.3.3. SHM without affinity maturation: affinity ceiling reached or tertiary negative selective forces? 154

4.3.4. 'Walking' the BAR-1 class: challenges and feasibility 156

4.3.5. Translational limitations of the murine model 157

4.3.6. Conclusions 158

Chapter 5—Antibody responses against β-lactam antibiotics..... 159

5.1 Background 159

5.1.1. Penicillins as haptens 159

5.1.2. PenG-specific immunity and allergy: gaps in the literature 160

5.1.3. Aims 161

5.2 Results 162

5.2.1. Evaluation of pre-coupled PenG–protein complexes in mice 162

5.2.2. Determining the humoral responses following free PenG administration 167

5.2.3. Establishing the B cell clonality against PenG 172

5.2.4. Characterisation of B cell clones against PenG 175

5.3. Discussion 177

5.3.1. Factors affecting drug immunogenicity 178

5.3.2. Relationship between drug conjugation chemistry and antibody function 181

5.3.3. Future directions: Implications for germline-informed drug design 183

5.3.4. Conclusions 184

Chapter 6—General Discussion 185

6.1 Thesis summary 185

6.2 LOG-based vaccination: benefits and penalties to improved antigenicity 187

6.3 The implications of drug-adduct immunogenicity 189

6.4 Conclusions 191

References 193

Abbreviations

Ab/mAb	Antibody/monoclonal Ab
ADA	Anti-drug antibodies
ADCC	Antigen-dependent cellular cytotoxicity
ADCP	Antigen-dependent cellular phagocytosis
AID	Activation-induced cytidine deaminase
Ag	Antigen
AUC	Area under the curve
BCR	B cell receptor
BFA	Brefeldin A
BSA	Bovine serum albumin
CBM	Carbohydrate-binding modules
CDRx	Complimentary determining region
CDx	Cluster of differentiation x
DAMP	Damage-associated molecular pattern
DMF	Dimethylformamide
EC_{50}	50% effective concentration
ELISA	Enzyme-linked immunosorbent assay
ELISpot	Enzyme-linked immune absorbent spot
Env	Envelope glycoprotein of HIV-1
EPT	Endpoint titre
ESI	Electron spray ionization
Fc	Antibody common chain
FRx	Framing region x
FDC	Follicular dendritic cell

FUT7	α-1,3-fucosyltransferase
Gal	Galactose
GalNAc/Tn	*N*-acetylgalactosamine
GC	Germinal centre
Glc	Glucose
GlcNAc	*N*-acetylglucosamine
GL/iGL	Germline/inferred GL
GM3g	Glycan of ganglioside, GM3; α-2,3-sialyllactose
GPI	Glycosylphosphatidylinositol
Gp120	Glycoprotein 120
FMO	Fluorescence minus one
HA	Hemagglutinin
HC	Antibody heavy chain
HEL	Hen egg lysozyme
HIF-1	Hypoxia-inducible factor-1
HIS	Human immune system
HIV	Human immunodeficiency virus
HRP	Horseradish peroxidase
HSA	Human serum albumin
IAV	Influenza A virus
ICS	Intracellular cytokine staining
IC_{50}	50% inhibitory concentration
IFN	Interferon
Ig	Immunoglobin
IL-x	Interleukin-x

IME	2-imino-2-methoxyl-1-thiol
ITC	Isothermal calitometry
KC	Antibody kappa chain
KLH	Keyhole limpet hemocyanin
Le^A	Lewis A
Le^X	Lewis X
LN	Lymph node
LOG	Long orthogonal glycoconjugate
LPS	Lipopolysaccharide
MHC/pMHC	Major histocompatibility complex/peptide-loaded MHC
MMCCH	4-(4-*N*-maleimidomethyl) cyclohexane-1-carboxyl hydrazine
MPLA	Monophosphoryl lipid A
MS/LC-MS	Mass spectrometry/liquid chromatography MS
MSA	Mouse serum albumin
MUC-1	Mucin-1
Neu5Ac	*N*-acetylneuraminic acid
Neu5Gc	*N*-glycolulneuraminic acid
NF-κB	Nuclear factor kappa-light-chain-enhancer of activated B cells
NK	Natural killer
NP	Nitrophenol
OD	Optical density
OVA	Ovalbumin
PAMP	Pathogen-associated molecular pattern
PB	Plasmablast
PBS/PBST	Phosphate buffered saline/PBS tween-20

PC (cell)	Plasma cell
PC (lipid)	Phosphatidylcholine
PG	Phosphatidylglycerol
PD-L1	Programmed death ligand-1
PEG	Polyethylene glycol
PenG	Penicillin G
PenG-Ben	PenG benzathine
PGN	Peptidoglycan
PNGase F	Peptide:*N*-glycosidase F
PNGS	Potential *N*-linked glycosylation site
PTM	Post-translational modification
RAFTs	Regioselectively addressable functionalised templates
SARS-CoV-2	Severe acute respiratory syndrome coronavirus 2
SHM	Somatic hypermutation
SMD	Small-molecule drug
SPR	Surface plasmon resonance
SSEA-4	Stage-specific embryonic antigen-4
ST3O	Sialyllatransferase ST3Gla-1
TACA	Tumour-associated carbohydrate antigen
TAP	Transporter associated with antigen processing
TCR	T cell receptor
TLP	Tertiary lymphoid organ
TNBSA	2,4,6-trinitrobenzenesulfonic acid
TSLP	Thymic stromal lymphopoietin
Tfh	Follicular helper T cell

Th	Helper T cell
TLR-x	Toll-like receptor x
TNF	Tumour necrosis factor
$V_H/D_H/J_H$	V-/D-/J-gene segments of the antibody heavy chain
VH/VK	Variable region of antibody heavy/kappa chain

Chapter 1—Introduction

1.1. B cell biology and antibody development

The 1930 Nobel prize in Medicine was awarded to Karl Landstiner for, among other things, his contribution in identifying that the immune system could mount an antibody response (usually high affinity) of tremendous specificity against almost any antigen (Landsteiner, 2013). Indeed, antibody responses protect from diverse pathological agents, spanning from toxins to multicellular parasites, but may also inadvertently trigger allergy or be misdirected towards self-antigen, resulting in autoimmunity (Elkon and Casali, 2008; Karagiannis et al., 2013; Lu et al., 2018; Prüss, 2021). Indeed, the proper functioning of the humoral compartment of the adaptive immune response is critical to the maintenance of human health.

One of the founding questions for the field post-Landstiner was how such diverse antibody responses could be generated, especially in the context of a limited genome size. Two discrete findings underpinned this: V(D)J recombination and

clonal selection. First, the germline underpinnings of this diversity were discovered by David Baltimore and others, who described how during early development in the bone marrow, B cells undergo V(D)J recombination wherein germline-encoded gene-segments are arranged to encode a potential precursor potential antibody product (**Fig 1.1a**) (Alt and Baltimore, 1982; Tonegawa, 1983). The combinatorial effect of this hard-wired developmental mechanism results in a highly diverse B repertoire from relatively few gene segments; for example, in the case of a mouse, approximately 300 gene segments produce a theoretical repertoire of ~3 million segment combinations. Second, the concept of clonal selection states that, upon antigen exposure, the diverse B cell repertoire is tested against the antigen and, by chance, a subset of B cells cross-link via the B cell receptor (BCR), undergo expansion and produce their antibody products (Burnet, 1976). While these phenomena explain the initial B cell response, the antigen pre-exposure B cell repertoire does not account for the vast number of high-affinity responses observed post-exposure.

The underpinnings of further B cell diversification were first observed in 1964, when Herman Eisen reported in rabbits that antibody responses progressively gained affinity over time post-vaccination (Eisen, 2014; Eisen and Siskind, 1964). This process of *affinity maturation* was later shown to be caused by immunoglobin gene diversification via somatic hypermutation (SHM) that would take place post-antigen encounter (**Fig 1.1b**) (Berek and Milstein, 1987; Weigert et al., 1970). While Walther Flemming first observed the tertiary lymphoid organs where affinity maturation takes place in 1884 (Nieuwenhuis and Opstelten, 1984), only later were the mechanics of these so-called germinal

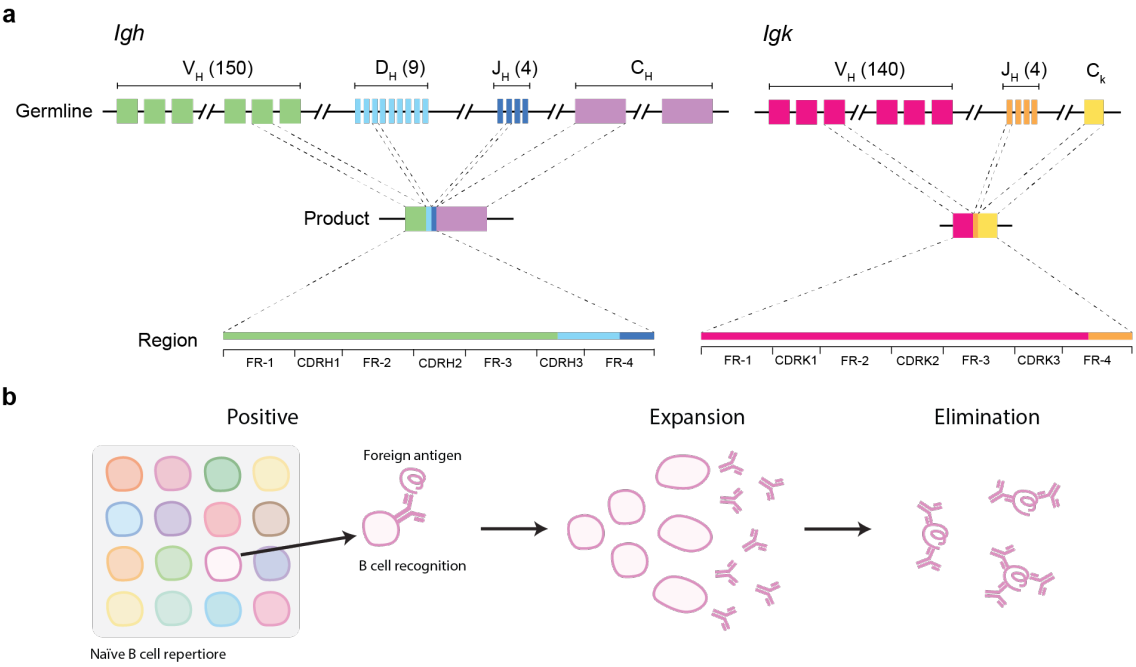


Figure 1.1: B cell clonal selection.

(a) Murine V(D)J recombination during early B cell development in the bone marrow results in a combinatorial outcome wherein a given B cell has a specific gene segment configuration on both the heavy and light chains. **(b)** Antigen is tested against the diverse B cell repertoire. B cells that bind antigen and activate can undergo rapid clonal expansion, fate differentiation, migration and formation of tertiary lymphoid organs, and antibody production.

centres (GCs) better understood, including the demonstration that the GCs were the site where both SHM and affinity-based selection occurs (Jacob et al., 1991; Küppers et al., 1993).

The contemporary working model for germinal centre biology is relatively sophisticated and describes the molecular and cellular underpinnings of B cell outcomes (**Fig 1.2**). Briefly, it involves the seeding of activated B cells that differentiate into specialised GC B cells in the GC follicle. The GC is segmented into two distinct zones. The dark zone is the site where GC B cells undergo rapid proliferation and use of activation-induced cytidine deaminase (AID) (Maul and Gearhart, 2010), which mediates SHM of the encoded antibody variable region.

The daughter B cells with their variable BCRs migrate into the light zone, where a specialised stromal cell population—follicular dendritic cells (FDCs), which express high levels of complement receptors and Fc receptors—capture antigen/immune complexes for presentation to GC B cells (Allen and Cyster, 2008). The GC B cells test their BCRs against antigen in the light zone and

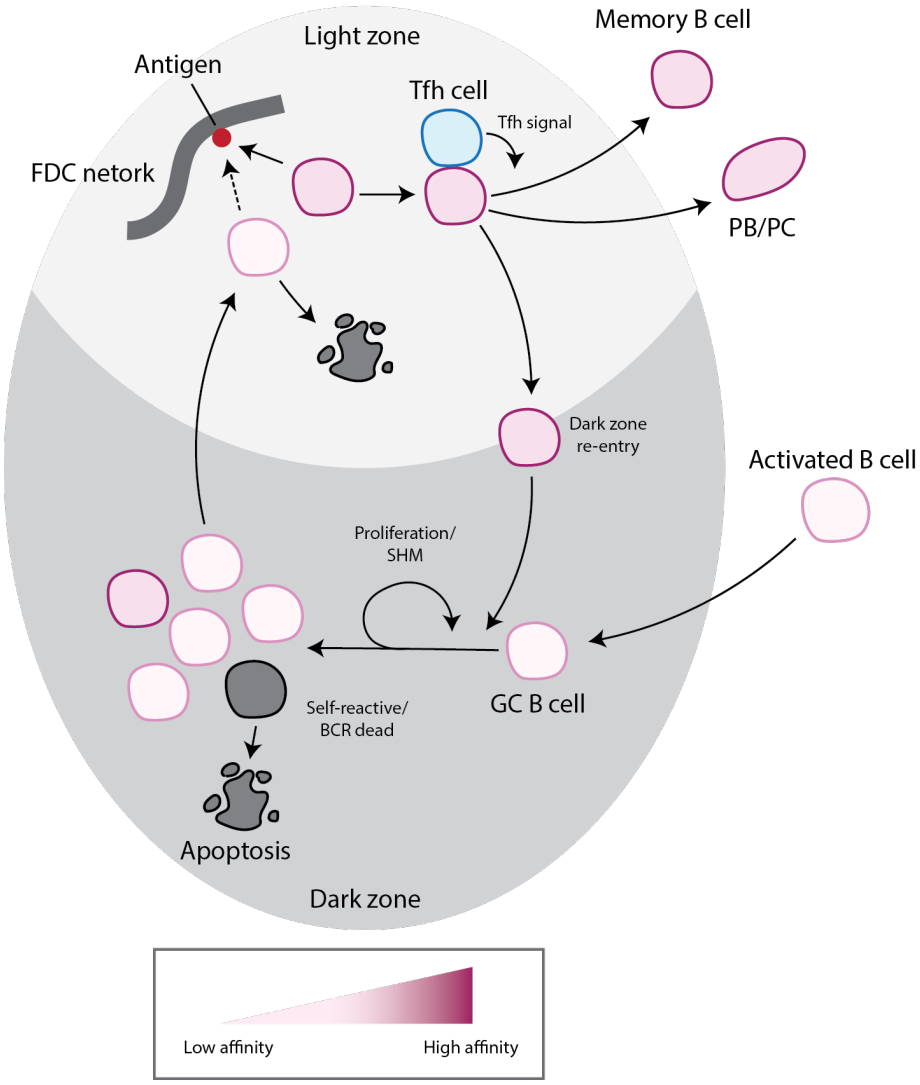


Figure 1.2: Reductionist GC model.

GC B cells rapidly proliferate in the dark zone, incorporating mutations into the variable region via AID. Cells migrate to the light zone where B cell clones compete for antigen displayed on the FDC network. Proportionally to affinity, cells take-up antigen and cross-present to Tfh cells, which supply B cells with survival and fate-differentiating signals. This process iteratively over time improves the affinity of antigen-specific cells. Adapted from Victora and Nussenzweig (2023).

competitively take up antigen to cross-present to a specialised helper T cell subset, the follicular helper T cell (Tfh) (Chen et al., 2023; Vinuesa et al., 2016a). Tfh cell-derived signals drive positive selection, permitting the GC B cell to re-enter the dark zone, become a plasmablast (PB)/plasma cell (PC) or become a memory B cell. Failure to receive these Tfh signals results in apoptosis. Since GC cycling is an iterative and competitive process, over time, B cells with a higher affinity for available antigen are more likely to internalise and present antigen to survive. This explains the observations made by Eisen.

There are several hallmark properties of the B cell compartment that allows for long-term protection against secondary encounters: 1) the maintenance of antibody supply to offer continuous protection, mediated by long-lived PCs that will secrete antibodies for months to a lifetime (Manz et al., 1997; Nutt et al., 2015), and 2) offer a memory B cell population that are pre-programmed to rapidly expand and differentiate into PBs to supply a substantial and rapid antibody supply upon antigen re-exposure (Mesin et al., 2020). These immune traits explain the protective functions of vaccination that Edward Jenner described in 1821 (Jenner, 1821). Indeed, the export of both PCs and memory B cells is the basis for vaccination: that of deliberately and safely exposing an individual to antigen such that encounter with a harmful agent is met by the efficiency and magnitude of a secondary adaptive immune response. Thus, the cellular and molecular processes described determine the diversity and quality of antibodies against a given target. These concepts are the basis of the humoral response and are relied upon heavily throughout this thesis.

1.1.1. The role of T cells: a classical hapten-carrier biology perspective

Effective and long-lasting B cell responses are almost universally T cell dependent, classically requiring antigen uptake and presentation to T cells. This is because of the critical and broad roles of T cell signals in B cell support: pMHC-II–TCR, cytokine and co-stimulatory signalling drives B cell proliferation, fate differentiation, isotype switching (an AID-mediated phenomenon that determines Fc effector functions of antibody products) and cell survival (**Fig 1.3**) (Crotty, 2015). Therefore, antigen that lack associated T cell help (especially antigenic complexes that are without a peptidic component) will be unable to elicit robust, long-lived class-switched B cell responses. Some classic examples include small-molecule toxins (e.g. Staphylococcal enterotoxin B and aflatoxin) (Ertekin et al., 2016; Yolaç et al., 2012) and carbohydrates (e.g. capsular polysaccharides isolated from bacteria such as *Pneumococci* species and *Haemophilus influenzae*) (Astronomo and Burton, 2010; Galiza and Heath, 2007; Gessner and Adegbola, 2008).

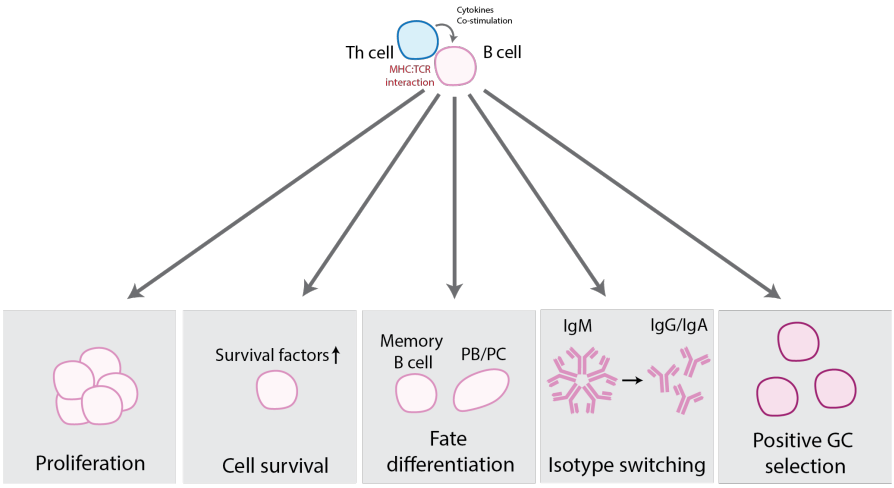


Figure 1.3: Role of T cell help in the propagation of B cell immunity.

B cells cross-present antigen to corresponding T cells. Helper T cells respond by supplying cytokines and co-stimulatory factors. This ultimately drives B cell proliferation, cell survival, fate differentiation, isotype switching and positive GC selection.

Positive antigenic signals provided to both T cells and B cells are not sufficient for a robust serological outcome; indeed, antigenicity (that is, the presence cognate antigen-specific lymphocytes) is necessary rather than sufficient for a potent humoral response. Immunogenicity (the overall quality and magnitude of an adaptive response) is influenced by factors, such as innate inflammatory and other cues, that form an immune environment capable of potentiating the adaptive response. In vaccine settings, this is achieved by administering adjuvanted formulations, such using alum or monophosphoryl lipid A (MPLA), that interact with innate pathogen-/damage-associated molecular patterns (PAMPs/DAMPs) (Akira, 2011; Aoshi, 2017; Awate et al., 2013; Iho et al., 2015; Tizard, 2021). The subsequent activation of innate and other immune cells helps to potentiate the downstream adaptive outcome.

Landsteiner and Jacobs first described the phenomenon whereby otherwise immunosilent molecules, such as urushiol, benzyl chlorides and acyl chlorides, could become immunogenic when conjugated to carrier proteins and administered to animals with alum (Landsteiner and Jacobs, 1936). For example, they showed that chlorobenzoyl-based hapten-carrier complexes when administered in formulation with alum sensitised Guinea pigs, inducing a robust serological response associated with anaphylaxis following subsequent p-chlorobenzoyl chloride exposure (Landsteiner and Jacobs, 1936). In the following decades, the functionalisation of many otherwise small molecules and other immunorecessive moieties has been exploited by conjugating them to carrier proteins to elicit high-affinity antibody responses (Bennett et al., 1987; Green et al., 1968; Landsteiner and Jacobs, 1936; Mitchison, 1971). These findings have

collectively given rise to protein-conjugate-based vaccine design, wherein immunorecessive targets can readily elicit antibody responses if the basis for immunorecessiveness is underpinned by lack of T cell help. This is exemplified by bacterial pathogens such as *Streptococcus pneumoniae, Haemophilus influenzae* and *Neisseria meningitidis*, against which highly effective FDA-approved glycoconjugate-based vaccines have been developed (Zhu et al., 2021).

1.1.2. Outstanding problems in protein conjugate antigens

In this thesis, two discrete problems are investigated:

1. There are some antigenic targets that are immunorecessive for both T cells and B cells. For example, carbohydrates may lack associated T cell immunogenic components but retain their immunorecessive character even when conjugated to carrier proteins for associated T cell help (Livingston and Ragupathi, 2006). This is presumably a function of an absence of relevant reactive naïve B cells in the mature repertoire. How could vaccines be developed to overcome this apparent 'blind spot' in the repertoire?
2. Many small molecules, such as those used therapeutically, are chemically unstable. The relationships between drug propensity to form functional hapten-carrier immune complexes *in vivo*, the immunogenicity of the resultant complex, and the effect of the downstream antibody response is largely unknown. For example, what is the relationship between small-molecule–protein conjugation chemistry and the propensity to initiate a humoral response?

These are the central questions investigated here, and each of these topics are specifically introduced below.

…

1.2. Introduction to glycan immunogenicity

Glycosylation is a common modification made to both proteins and lipids, playing a crucial role in mediating the structure and function of glycoproteins and glycolipids in eukaryotic organisms. Glycosylation is also utilised by various pathogenic agents, such as viruses and cancer, as reviewed elsewhere (Reily et al., 2019). Reflecting the broad and critical roles of glycans *in vivo*, abnormal glycan patterns have been linked to various diseases, including cognitive and physical disability, organ damage, immune dysfunction, chronic inflammation, and immune disorders (Reily et al., 2019; Varki, 2017). Since mammalian glycans are endogenously added and processed, they and their native protein glycoconjugates have restricted immunogenicity to avoid autoreactive responses.

Immunogenicity of glycans may be limited by different mechanisms, including central and peripheral immunological tolerance (later detailed) and intrinsic lack of antigen immunogenicity due to biophysical constraints such as antigen size, charge and accessibility. Several well-understood adaptive tolerance mechanisms exist, such as B cell negative selection in the bone marrow to eliminate self-glcyan-reactive precursors (New et al., 2016), interactions between carbohydrate-based antigens and immunoinhibitory lectins (Lübbers et al., 2018;

Müller and Nitschke, 2014), and the absence of T cell help for clonal expansion, class-switching and affinity maturation of B cells (Avci et al., 2013; Avci and Kasper, 2010). However, unlike self-glycans, foreign glycans such as those derived from bacteria can easily induce antibody responses, such as those derived from bacteria, as they are not subjected to the same antigenicity-based tolerance constraints: correspondingly, classical glycoconjugate vaccines display bacterial polysaccharides in a format where the sugar polymer is typically presented by conjugation to a carrier protein, wherein cognate B cells recognise the carbohydrate, and the associated carrier is cross-presented to T cells (Avery and Goebel, 1929; Rappuoli et al., 2019). In contrast, the immunological 'blind-spots' present for self-like glycans and glycoconjugates may render the host vulnerable to pathogen attack and other pathologies such as cancers that routinely exploit glycosylation processes as an immune evasion tactic. Thus, self-glycosylation as an immune evasion strategy leaves the host susceptible to attack.

The selective breaking of B cell tolerance to glycans can have significant consequences in specific settings. For instance, TACAs are glycosylation patterns (self or 'self-like') that may be over-expressed or modified on tumour cells compared to their healthy counterparts (Haji-Ghassemi et al., 2015). TACAs are promising targets for therapeutic antibodies or active vaccination, being subject to considerable study over several decades (Bilodeau et al., 1995; Kim et al., 2000; Kudryashov et al., 1998; Kuduk et al., 1998a; Livingston et al., 1989; Livingston and Ragupathi, 2006; Zhu et al., 2009). However, designing vaccines targeting TACAs poses several challenges that remain largely unaddressed: i)

several major classes of TACAs are presented on glycosphingolipids (including gangliosides) rather than proteins, removing the Th component of the adaptive response, and ii) proximity of the carbohydrate to the membrane may limit B cell receptor accessibility and downstream antibody engagement (Lloyd et al., 1992).

1.3. Introduction to glycosylation in cancer

As previously outlined, the functional roles of glycans are highly diverse, but include facilitating protein folding, governing physiochemical stability, and mediating ligand interactions which modulate cell–cell adhesion (Varki, 2016). Interestingly, a long-reported phenomenon occurring during oncogenesis is modified glycosylation during tumor cell progression (Hakomori and Murakami, 1968). The resultant effect of these glycan alterations for the cancer cells is broad, but some specific examples include modulation of cell metabolism, promotion of cell migration and metastasis, and alterations to the inflammatory microenvironment (Dube and Bertozzi, 2005; Glavey et al., 2015).

Although the glycosylation signatures that differentiate cancer cells from healthy cells are heterogenous, there are sets of alterations that are commonly observed in cell- and site-dependent manners, such as changes in sialylation on melanoma, colonic, lung and neuroectodermal cancers (Guthmann et al., 2004; Kim and Varki, 1997; Shimizu et al., 2020). These differences in cancer cell glycosylation are classically characterised by two distinct classes (Hakomori and Kannagi, 1983; Kannagi et al., 2008).

First, incomplete synthesis, wherein glycan structures are abnormally matured during their biosynthesis, generally underpinned by selective epigenetic silencing of specific glycotransferases and other glycan-processing genes. Among the well-characterised examples is the silencing of α-2,6-Sialyltransferase (Miyazaki et al., 2004), necessary for disialyl Lewis A and sialyl-6-Sulfo Lewis X biosynthesis in healthy cells. However, in cancerous cells, glycotransferase silencing instead results in un-sialyllated Lewis A (Le^A) and X (Le^X), respectively.

Second, neosynthesis is the process by which cancer glycan synthesis is actively promoted *de novo*, a principle that can similarly be illustrated by $Le^{A/X}$. For example, in the hypoxic tumour microenvironment, induction of Hypoxia-Inducible Factor-1 (HIF-1) bolsters transcription of necessary glycotransferases α-1,3-fucosyltransferase (FUT7) and sialyltransferase ST3Gal-I (ST3O) to accelerate $Le^{A/X}$ biosynthesis (Koike et al., 2004). Notably, both Le^A and Le^X are vascular selectin ligands, proposed to facilitate endothelial adhesion of cancer cells, angiogenesis, and promote systemic migration and metastasis (Julien et al., 2011; Tei et al., 2002; Trinchera et al., 2017) (**Fig 1.4**). Thus, these changes in glycosylation associated with oncogenesis (onco-glycans) intuitively provide selective advantages to cancer cells.

Deviation in the carbohydrate signatures of cancer cells from that of their healthy counterparts invites the targeting of these glycans as a therapeutic approach.

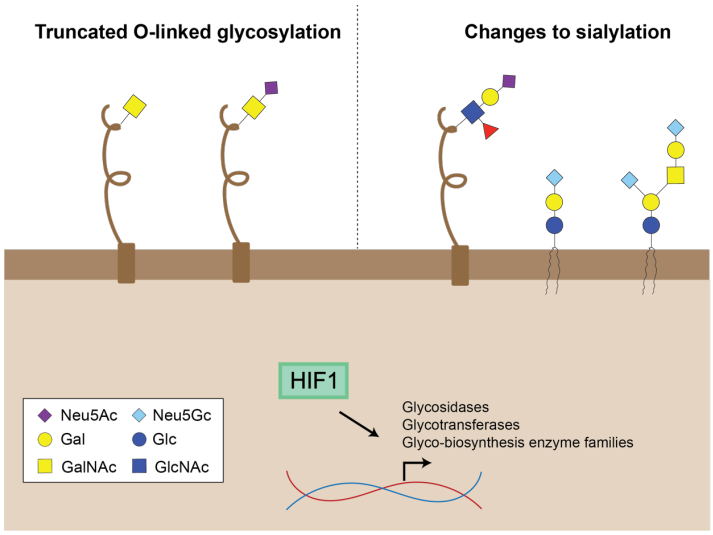


Figure 1.4: Common glycosylation changes in cancer.

As tumours progress, induction of factors such as HIF-1 modulates cell glycosylation machinery. The resultant effect on the glycome typically is associated with truncated *O*-linked glycosylation and changes to the sialylation patterns.

There have been many drug strategies engineered to selectively target tumor-specific glycosylation and interfere with tumour development: small-molecule inhibitors that block glycotransferase function, including GlcNAc-T5, SUT7 and ST6Gal1 (Donovan et al., 1999; Rillahan et al., 2011); infusions of CAR T cells that recognise specific cancer-associated glycoforms, such as that of the Thomsen-nouveau (Tn; monosaccharide GalNAc) glycoform of mucin-1 (MUC1) (Posey et al., 2016), and therapies to block tumour-potentiating glycan–ligand interactions, such as using selectin agonists (DeAngelo et al., 2022). These strategies are at various stages of translational development and clinical trial (Costa et al., 2020).

An alternative therapeutic strategy is the targeting of cancer-specific or cancer-overexpressed carbohydrates via vaccination or therapeutic antibody infusions. These so-called TACAs encompass both aberrant and wild-type glycoforms of

gangliosides and other glycosphingolipids, and glycoproteins including mucins, proteoglycans and glycosylphosphatidylinositol (GPI)-anchored proteins. TACAs represent a continuing focus for the vaccine immunology field, particularly the raising of protective TACA-binding antibodies. The role of such antibodies *in vivo* may facilitate the inhibition of onco-glycan–ligand interactions and promote active tumour killing via antigen-dependent cellular cytotoxicity (ADCC) and antigen-dependent cellular phagocytosis (ADCP) (**Fig 1.5**). However, experimentally, the generation of functional TACA-specific antibodies via vaccination is widely regarded as challenging (Chefalo et al., 2003): TACA immunogenicity is generally extremely low, a cumulative effect of several inherent characteristics that render classical vaccine formulations ineffective. While the high bar to elicit self-derived carbohydrate-reactive antibodies is intuitive to avoid widespread autoimmunity against normal glycan presentations, there is clinical evidence that

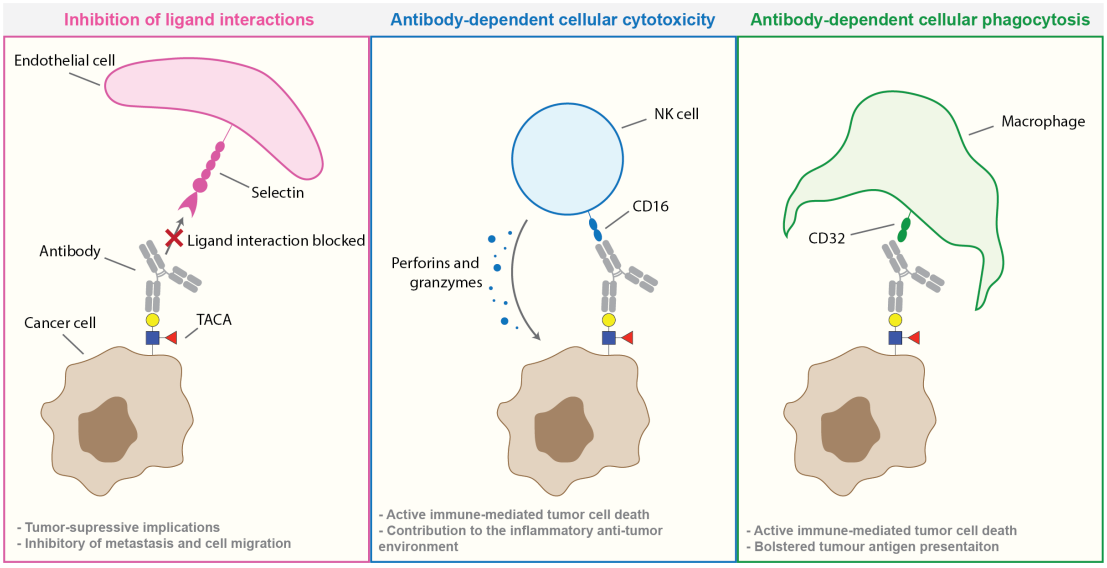


Figure 1.5: Modes of anti-TACA effector functions.

Antibodies raised against TACAs may have several anti-tumour/tumour-suppressive effects. The neutralization of surface TACAs may block ligand interactions that propagate the tumour cell (left). Anitbodies bound to TACAs may also mediate Fc effector functions, such as antibody-dependent cellular cytotoxicity (ADCC) or antibody-dependent cellular phagocytosis (ADCP) (middle, right).

thoughtful vaccination design may elicit protective and cancer-specific TACA-directed humoral responses (Chapman et al., 2000; Holmberg and Sandmaier, 2004). These outcomes encourage further development. Here, I evaluate i) the inherent features of TACAs that causatively make them challenging antibody targets, ii) the progress in TACA-directed vaccination, and iii) emerging and novel vaccination approaches against TACAs.

1.4. Immunogenicity of TACAs

Whether an antibody response is elicited against a given antigen is contingent on a wide set of parameters, relying on the triggering of innate compartments to activate the adaptive immune response, appropriate engagement of the BCR and the generation of T cell help. TACAs are subject to intrinsic immunogenicity constraints through a variety of mechanisms that cumulatively render them challenging vaccination targets (**Fig 1.6**).

1.4.1. Constraints of the naïve B cell repertoire in TACA recognition

The theoretical human naïve B cell repertoire is extremely large, with estimates based on combinatorial calculations as being ~10^{15}–10^{18} (Briney et al., 2019; Rees, 2020). While the total number of peripheral naïve B cells at any given time is estimated to be ~10^{9} (Morbach et al., 2010), it is evident that the repertoire is necessarily highly diverse to allow immune system recognition of and response to highly variant antigenic targets *de novo*. However, while the mature naïve B cell repertoire is certainly diverse, it is highly skewed; intuitively, there is evolutionary incentive that the repertoire is comprised of clones that are useful in eliminating pathogens and other harmful agents while avoiding recognition of

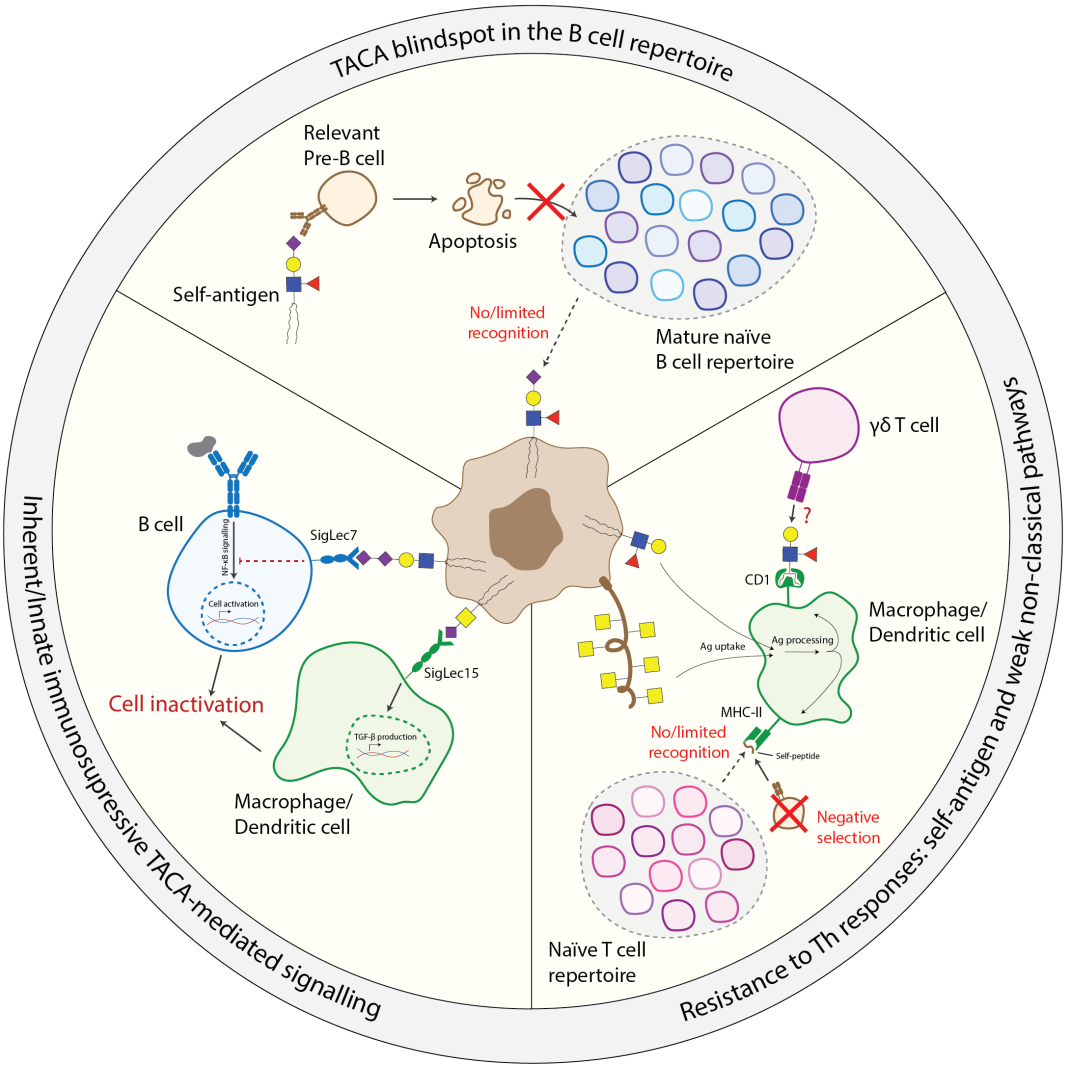


Figure 1.6: Intrinsic immunoevasive properties of TACAs.

TACAs resist antibody-mediated immune attack via several inherent tolerance mechanisms. This includes absence of self-glycan-reactive B cells in the mature naïve repertoire, resistance to associated Th responses to propagate a hypothetical B cell clone and trans-activation of immunosuppressive lectins.

self-antigen. Such biases on the repertoire are imparted at two levels: i) the germline encoding of the V-, D- and J-gene segments are naturally subject to evolutionary pressures, and thus the motifs present in these segments must be selected to provide an advantage, and ii) central tolerance mechanisms, whereby self-reactive B cell precursors that display reactivity to self-antigen undergo either apoptosis or corrective BCR editing (Nemazee, 2017).

Given the self-like nature of TACAs, it is likely that the B cell repertoire is skewed against responding; that is, no or very few BCRs in circulating B cells can be cross-linked with sufficient avidity by TACAs to initiate activation. There is some experimental evidence concerning this phenomenon from mouse models. For example, several TACAs including GM3, Le^X and Le^A have been artificially linked to synthetic peptides or protein carriers to yield a TACA epitope within an antigenic complex allowing generation of Th responses, and formulated with a potent adjuvant (Ravindranath et al., 1998; Yu et al., 2011a). The serological outcome in mice rarely shows carbohydrate-only responses, and it is often difficult to differentiate the antibody response against the TACA-of-interest versus reactivity with the linker used (Livingston et al., 1989; Livingston and Ragupathi, 2006). It is also important to note that the mouse germline differs substantially from that of humans, and there are some TACA–carrier complexes that have generated responses in murine models but failed to translate to humans (Chapman et al., 2000; Holmberg and Sandmaier, 2004; Oyelaran and Gildersleeve, 2010). This implies that the design of TACA-based vaccines would benefit from being germline-informed, noting both TACA species-dependency and B cell repertoire-dependency in the response. Reflections on how a germline-targeted approach could be developed is explored throughout later chapters.

1.4.2. T cell immunorecessiveness to TACAs

To propagate the B cell response after a relevant clone has been engaged, T cell help is required for efficient proliferation, isotype switching, clonal survival and, ultimately, the formation and maintenance of germinal centres. Native

presentation of TACAs is inherently resistant to the elicitation of Th responses (Buskas et al., 2009). For example, the use of native TACA antigens such as purified gangliosides GM1 (monosialyltetrasaccharide), GM3 (sialyllactose) and GD2 (disialyllactose) in vaccination typically invokes no detectable antigen-specific immunoglobin, or rarely a low titre IgM response with no/little functional tumour-killing effect (Livingston et al., 1989). Indeed, T cell help for B cell activation is a major challenge in facilitating high-affinity class-switched glycan-specific antibody responses.

1.4.2.1. Recognition of glycoconjugates by TCRs

In general, T cell receptors fail to directly engage glycans and glycoconjugates. This is due to constraints both in antigen presenting pathways and the narrow depth of antigen the TCR can accommodate (Werdelin et al., 2002). However, the dogma of T cells only being able to recognise protein antigens is being eroded: evidence exists (although still somewhat controversial) for antigenic processing of glycans and other bulky PTMs for their presentation to T cells. Glycopeptides may be routinely presented on both MHC-II and MHC-I (Apostolopoulos et al., 2003; Dengjel and Stevanovic, 2006; Haurum et al., 1999; Malaker et al., 2017; Speir et al., 1999; Wieczorek et al., 2017). There is a consensus that glycosylated epitopes have diverse possible fates in antigen processing pathways, including glycan retention or partial or complete glycan removal (Werdelin et al., 2002). Critically, the general features that dictate whether an MHC molecule will successfully anchor an intact glycopeptide is not currently predictable. In particular, the conditions that allow for lysosomal/proteasomal survival of carbohydrate, as well as passage through

downstream MHC-complexing quality control steps (e.g. TAP and HLA-DM), remains unclear (Haurum et al., 1999; Werdelin et al., 2002). Despite this uncertainty, it is evident that MHC-restricted glycopeptide-specific T cell activation does occur and may be harnessed in vaccine design as typified by experimental glycopeptide-based immunisations (Sun et al., 2020).

Th cell recognition of glycopeptides has been investigated in the contexts of viral infection and cancer. Experimentally, it seems that αβ TCRs can recognise small glycans, generally up to three to four monosaccharides (Abdel-Motal et al., 1996; Galli-Stampino et al., 1997; Pellicci et al., 2011; Speir et al., 1999). Further structural consideration of the αβ TCR indicates that this may be a consequence of the limited depth of the complementary determining region 3 (CDR3), which may only accommodate small PTMs without sterically compromising TCR interactions with α-helical domains of the presenting MHC (Werdelin et al., 2002). The recognition of larger and more diverse glycans (including glycolipids and phosphocarbohydrates) by MHC-unrestricted γδ T cells has been reported, and γδ T cells are probably sufficient to provide B cell help (Rampoldi et al., 2020; Schoel et al., 1994; Speir et al., 1999). Despite the biophysical constraints of αβ Th cell glycan recognition, glycopeptide immunogens routinely stimulate MHC-restricted T cell immunity, such as immunisation with bacterial capsular polysaccharides conjugated to a carrier protein, which generates strong carbohydrate-specific Th cell responses (Sun et al., 2019). However, there is no description of the generation of TACA-specific Th responses: the most successful strategy used to supply Th responses to glycan-specific B cells relies on linking the glycan to a protein carrier. Since linked recognition means that T

helper cells can recognise protein components of an antigen whilst B cells recognise glycan or glycoconjugate epitopes, glycan-specific Th cell responses are not required to produce glycan and glycopeptide-specific antibodies, as reviewed in adjacent systems (Krumm and Doores, 2020) and exemplified by glycoconjugate-based vaccines previously developed and licensed (Zhu et al., 2021). These systems have the added advantage of working with non-self bacterial glycans against, which there is limited risk of generating autoimmunity and therefore have not evolved towards immune tolerance.

1.4.2.2. T cell tolerance of self-glycoproteins

TACAs are often associated with glycoproteins and proteoglycans, which are among the most well-studied cancer vaccination targets. For example, mucins proteoglycan chains may exhibit aberrant glycosylation post-oncotransformation, (Galli-Stampino et al., 1997; Holmberg and Sandmaier, 2004). There are several cancer-specific mucin glycoforms, such as that of Tn MUC1, which is specific to certain breast and lung cancers, and where antibody responses have been detected (Kato et al., 2021). In this specific example, it is implied that the tumor-specific variation in glycosylation removes tolerance restrictions providing a platform for B cell recognition against the Tn component of the mucin. However, vaccination using Tn MUC1 might nevertheless be hindered by T cell immunorecessiveness, since the protein backbone remains unchanged implying T cell tolerance against self-mucin protein, a finding that is reported in both mice and humans (Apostolopoulos et al., 1995). This can be circumvented by modifying the protein carrier to include immunodominant T cell epitopes. These

strategies are being evaluated in the clinic, although their efficacy so far remains unclear (Butts et al., 2014; Palmer et al., 2001).

1.4.2.3. T cell immunity against TACA-carrying glycolipids

Glycolipids such as cancer-associated gangliosides are also highly immunorecessive. This is in large part a function of these lipids being unable to prime T cells in a classical MHC-restricted manner, instead relying on the peptide-independent, lipid-anchoring CD1 family. Indeed, some glycolipids are presented on CD1a–d receptors, which has been explored as a vaccination design strategy against foreign glycolipids, such as those derived from *Pneumococcus* (Bai et al., 2013; Icart et al., 2008). However, T cell reactivity against TACAs has been associated with autoimmunity; for instance, T cell recognition of GM3 is associated with progressive axonal damage in multiple sclerosis patients (Pender et al., 2003). This highlights a key challenge in TACA-directed vaccination design: that the immune response mounted should ideally strictly target pathology-specific elements and avoid reactivity with vulnerable self-determinants.

1.4.3. Inherent immunoinhibitory effects of some TACAs

Intrinsic to many TACAs is the capacity to interact with specific immunomodulatory elements that may have consequences for eliciting a B cell response. For example, increases in the sialoglycan density on tumour cells enables recognition of the immune checkpoint and immunoinhibitory receptors Siglec-7 and Siglec-9. While these lectins have classically been investigated in

the context of natural killer (NK) cell inactivation (Hudak et al., 2014; Jandus et al., 2014), they are also expressed on macrophages and B cells, where their engagement is reported to also blunt humoral responses (Crocker et al., 2007). Therefore, these findings imply that a further TACA immune tolerance mechanism is the exploitation of the Siglec-Sialoglycan axis (Rodrigues Mantuano et al., 2020).

1.5. TACA-directed vaccination design strategies to improve B cell responses

An embedded assumption in TACA-directed vaccine immunology is that the frequency of TACA-reactive germline B cells is low to avoid autoimmunity, and thus the probability that administering formulations of TACAs *in vivo* would be unlikely to activate a relevant B cell. Consequently, for the last several decades, there have been many attempts to utilise “near-self” TACA analogues (Wilson and Danishefsky, 2013): the implicit principle is that modified non-native glycan mimics that deviate from endogenous structures may be more attractive to the naïve B cell repertoire, and subsequently capable of initiating a response.

First, a major class of TACA-based antigens explored for vaccine development is synthetic mimics. For example, the synthesis of fluorinated TACA antigens has generated a significant amount of attention; these antigens are typically characterised as having C–OH groups substituted by C–F, which offer similar electronegativity properties (Nativi et al., 2019)(**Fig 1.7a**). While several fluorinated Tn antigens have been synthesised (Wagner et al., 2010; Xia et al., 2006), their relative immunogenicity compared to

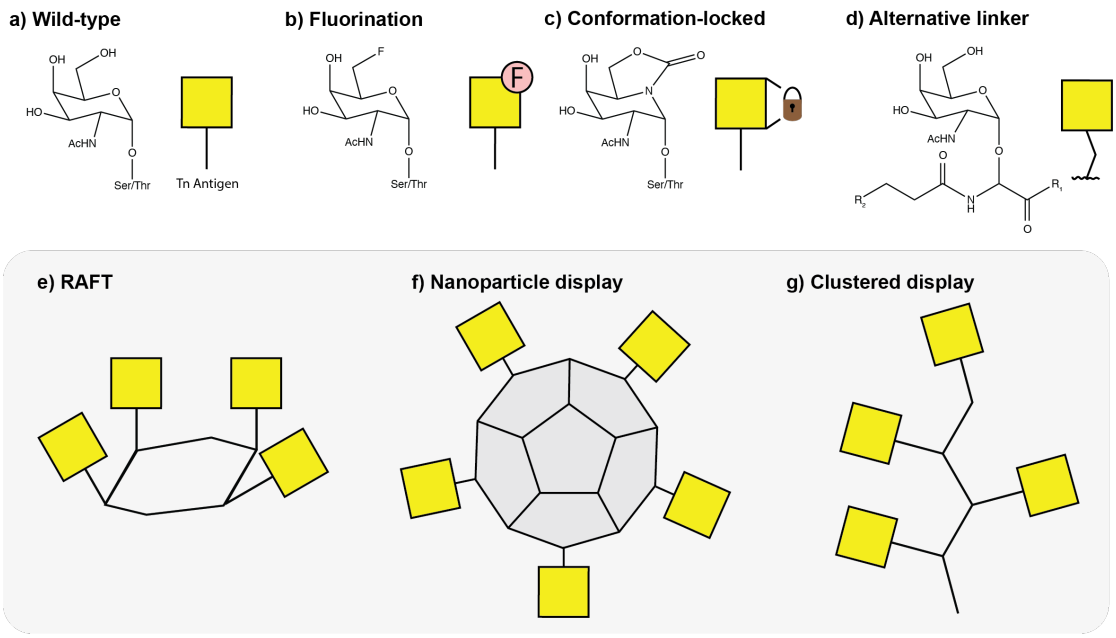


Figure 1.7: TACA analogue principles.

Several semi-synthetic glycan analogues have been developed to overcome some of the inherent immunogenicity challenges of self-glycans. For example, the **(a)** wild-type Tn antigen can be **(b)** fluorinated, **(c)** conformation-locked and **(d)** synthetically linked. **(e–f)** Several multivalent displays have also been established.

their native non-fluorinated parental counterparts is typically null. However, recently, fluorinated sialyl-Tn antigens were shown to improve both TACA-reactive IgG antibody titres and marginally improve survival outcomes in mice (Song et al., 2017). These data are consistent with the hypothesis that altering the antigen's position on the self–non-self spectrum alters its relative immunogenicity.

Notably, many carbohydrates lack structural rigidity, underpinned by the conformational flexibility of the oscillating ring structure, as well as flexibility about the glycosidic bond. This creates something of a "moving target", a behaviour of carbohydrate antigens that has similarly been investigated in the context of human immunodeficiency virus (HIV)-1, where the viral surface envelope glycoprotein (Env) exploits structurally fluid *N*-linked glycans to shroud underlying

neutralizable protein surfaces (Deimel et al., 2022; Ward and Wilson, 2017). To address this phenomenon in TACAs, investigation of various “locked” conformations that limit movement compared to the natural ring structures has been undertaken. For instance, a Tn antigen mimic wherein the saccharide was replaced with an sp^2-iminosugar (**Fig 1.7b**) exhibits substantially less structural flexibility (Fernández et al., 2016). While the immunogenicity of this locked Tn mimic has not been tested *in vivo*, Tn-specific anti-MUC1 scFv-SM3 binds some of these stabilised structures better than the natural Tn motif, potentially suggesting their suitability as an immunogen.

Rather than modifying the carbohydrate component directly, an alternative approach to alter TACA immunogenicity is via modification of the chemical linker. For instance, gangliosides such as GM1 are strongly immunorecessive, which may in part be a function both of its relative inaccessibility for B cells due to its embedding in the membrane and its ceramide tail that fails to induce classical Th responses (Livingston et al., 1989). However, Krug et al. demonstrated that presenting the glycan component, GM1g, via an alternative 4-(4-*N*-maleimidomethyl) cyclohexane-1-carboxyl hydrazine (MMCCH) linker to a carrier protein (**Fig 1.7c**) resulted in antibody production in patients with small lung cell cancer (Krug et al., 2004). This may indicate that the artificial context in which the glycan is presented can result in an otherwise inappropriate B cell clonotype recognising the TACA-linker complex, and that the associated peptidic component may then offer potent Th responses. Indeed, the artificial fixing of TACAs to Th-immunogenic protein carriers is widely accepted as an effective strategy to propagate anti-TACA B cell responses.

In this respect, glycans can be viewed in the same lens as classical haptens (Green et al., 1968): the non-protein conjugate component (in this case, pure TACA) alone is unable to elicit a humoral response, however, fixing the glycan to a carrier protein results in associated Th epitopes within the same antigenic complex. This 'linked' help allows B cells to recognise the carbohydrate component and internalise the antigenic complex for cross-presentation with Th cells. Therefore, the utilisation of highly Th-immunogenic carrier proteins is expected to better propagate the ensuing B cell response (Herzenberg and Tokuhisa, 1982), driving outcomes such as B cell proliferation, fate differentiation and germinal centre formation and maintenance. Thus, in both mouse and human trials, TACA analogues are fixed to Th epitope-rich carriers, such as keyhole limpet hemocyanin (KLH), which dramatically bolsters the serological titres against the carbohydrate component (Holmberg and Sandmaier, 2004; Kim et al., 2000).

Similar linker approaches have been developed for the globo-H TACA (Bilodeau et al., 1995; Kuduk et al., 1998b). Notably, many of these chemical linkers are themselves highly immunodominant; for example, polyethylene glycol (PEG) is a common linker/spacer, however, both mice and humans mount significant anti-PEG responses (Trabbic *et al.*, 2019; Chen, Cheng and Roffler, 2021), which may detract from the anti-TACA response by competition for T cell help in the germinal centre (GC) reaction.

Improving the valency of TACAs on an immune complex has similarly been shown to improve immunogenicity. This is presumably a function of the multivalency imparting an avidity boost that affects BCR cross-linking, but may also enhance antigen trapping and presentation by FDCs in the GC. Several formats have been developed, including “regioselectively addressable functionalised templates” (RAFTs)(**Fig 1.7d**)(Grigalevicius et al., 2005), nanoparticle displays (**Fig 1.7e**)(Trabbic et al., 2021) and monovalent clustered vaccines (**Fig 1.7f**)(Kuduk et al., 1998a). These are associated with improved antibody (although usually IgM) titres compared with their monomeric counterparts (Sabbatini et al., 2007).

1.6. Key challenges in TACA-directed vaccination design

1.6.1. Lack of anti-TACA B cell clonotyping

Modern molecular immunology has revealed the immense benefit of understanding the clonality of the B cell response in vaccination/infection contexts against viruses such as HIV-1, influenza A (IAV) and severe acute respiratory syndrome coronavirus (SARS-CoV)-2 (Gaebler et al., 2021; Leggat et al., 2023; Robbiani et al., 2020). For example, isolating antigen-specific B cells, sequencing their BCR and evaluating the structural, biochemical and biophysical properties of individual antibody clones, provides deep insight into the specific V(D)J configurations and GC outcomes conducive to an effective antibody response (Mesin et al., 2020; Viant et al., 2021; von Boehmer et al., 2016). In understanding the clonal class(es) responsive to a given antigenic target, it allows for the refinement of an immunogen to specifically activate B cells of a desired clonal origin—the principle of so-called ‘germline targeting’ that

underpins the basis of HIV-1 vaccination candidates undergoing clinical trials (Leggat et al., 2023). Indeed, these approaches to evaluating B cell outcomes at the individual cell molecular level provides a nuanced understanding of how antibodies deliver their functional effect and the impact of vaccination design in governing the reliable recapitulation of these outcomes.

B cell responses have been analysed at the clonal level using mouse models. For example, the inferred germline revertant of anti-GM3 antibody raised in a mouse (clone 14F7)(Bjerregaard-Andersen et al., 2021; Carr et al., 2002) is of a mouse *moIGHV1-66*01* origin. However, the closest human germline cousin, *huIGHV1-3*01*, has only 73% amino acid sequence identity (Brochet et al., 2008). It is therefore likely that the phylogenetically-inferred closest human counterpart of the 14F7 clone is not reactive with GM3. Similarly, a mouse-raised stage-specific embryonic antigen-4 (SSEA4) antibody, ch28/11 (Soliman et al., 2020a), is of the *moIGHV2-3*01* origin, but the human closest relative, *huIGHV2-26*01* is similarly diverse (64% identity). These data imply that the B cell response measured in an animal model system cannot be predicted to translate to humans, and that instead humans may either adopt alternative clonal configurations or perhaps fail to respond. I, therefore, suggest that murine models are best for understanding the basic molecular and cellular biology of B cell responses to TACAs, and to provide antibodies with passive therapeutic potential after humanisation.

To our knowledge, no comprehensive TACA-specific clonotyping has been carried out in humans, despite vaccination candidates having entered the clinic

(Hakomori, 2001; Hernández et al., 2008). Without having either isolated or described clonal classes capable of reacting with TACAs, the field lacks a template for the kinds of antibody responses that can be generated and are desirable. A clonal understanding has proved highly beneficial in determinining the molecular basis for effective anti-viral vaccine design against immunoevasive pathogens, including HIV-1 and IAV. However, this work in humans would likely be challenging—needing the isolation of TACA-specific B cells in people with TACA-positive tumours.

1.6.2. Potential consequences of synthetic linkers

As previously discussed, a common vaccination mode to improve the immunogenicity of TACA responses is to use non-native TACA display. These approaches may work, in part, because the synthetic TACA-mimicking epitopes access alternative B cell receptor clonotypes compared to endogenous TACA presentations. Consequently, there is a risk that such synthetic immunogens may mount antibody responses that fail to cross-react with the wild-type TACA—this is a common theme in the literature. For example, semi-synthetic glycoproteins of 5'-*N*-p-methylphenylacetyl GM3 and derivatives thereof are highly immunogenic in mice, eliciting robust antibody responses against the autologous glycoconjugate (Yu et al., 2011b). However, convincing serological cross-reactivity with membrane-docked GM3 ceramide has not been reported. Similar linker-dependency in the antibody response has been found in the context of Le^Y and oligomannose glycoconjugates (Buskas et al., 2004; Ni et al., 2006).

Collectively, these data suggest that antibodies raised against artificial glycoconjugates may incorporate the linker into their epitopes, and the subsequent accommodation of these linkers may ultimately impact the capacity for native TACA recognition. For example, in the case of GM3 glycoconjugates, linker dependency in the antibody response may affect the angle of B cell approach, and the portion of the paratope that was raised to recognise the linker may clash with other structures, such as the plasma membrane, failing to engage the native ganglioside. This further supports the need for thorough clonotyping and subsequent structural analyses to provide insight into the physiological relevance of the clonotypical response mounted by a given glycoconjugate.

1.6.3. Heterogeneity in TACA profiles and tumour adaptability

While some TACAs are associated with certain types of cancer, the expression of TACAs is relatively heterogenous. Therefore, whether an immunisation strategy against a given TACA offers protective benefit will ultimately depend on the tumour glycoform. To address this, heterologous and mosaic vaccination strategies have been designed, such as a pentavalent glycoconjugate comprised of common TACAs Globo-H, sTn, Tn, TF and GM2 (Ragupathi et al., 2006; Zhu et al., 2009). However, the clinical impact of these immunisations remains unclear (O'Cearbhaill et al., 2016). Moreover, it is unclear how readily cancers can adapt to the selective pressures of TACA-specific antibody responses. Crucially, there is significant scope for further exploration of the protective benefit and health outcomes offered by anti-TACA responses—it is likely heavily dependent on cancer type, cancer progression status, immunocompetence of the

patient and the point at which a vaccination is administered. These factors are not well-understood.

1.6.4. Breaking self-glycan tolerance: a word of caution

Since TACAs are self or self-like glycans, it is intuitive that the breaking of tolerance to these moieties might drive downstream autoreactivity and autoimmunity. For example, as previously mentioned, in both humans and animal models, anti-glycan responses are associated with several pathologies, including neurodegeneration (Lin et al., 2023; Yuki et al., 1997), arthritis (Hida et al., 2005) and inflammatory bowel conditions (Dotan et al., 2006; Ruutu et al., 2012; Temme et al., 2021). Perhaps the most well-characterised example is the use of anti-GD2 antibodies to treat melanoma; while there is strong clinical evidence that the passive administration of anti-GD2 prevents tumour progression in some patients (Nazha et al., 2020), it has been shown that these therapies can drive sensorimotor demyelinating polyneuropathy (Yuki et al., 1997). These data highlight that the tampering of glycan tolerance requires significant scrutiny to ensure any potential products are safe.

1.7. Summary of TACA vaccination

It is evident that TACAs present as potentially valuable vaccination targets, with antibody responses likely offering some benefit in particular clinical settings. However, given the unique immunogenicity profile of TACAs—characterised by their self-like nature, their association with poor Th responses and inherent immunoinhibitory properties—they present as distinctly difficult antigenic targets. Over recent decades, there have been considerable efforts to overcome the

immunorecessiveness of TACAs, especially by the development of semi-synthetic TACA mimics; while these approaches have facilitated measurable benefit to the serological response in both mice and some clinical trials, the efficacy of these immunisations remains unclear. I propose that the application of modern molecular immunology tools (especially describing the clonality of anti-TACA responses in humans) remains an open and likely valuable line of inquiry going forward. I envisage that this approach will invite a nuanced vaccine design effort that is structurally and immunogenetically informed to deliver a functional antibody outcome.

…

1.8. Overview of anti-drug antibodies

Many anti-drug antibodies (ADAs) have been identified following passive administration of biologic antibody therapies; for example, both infliximab (a tumour necrosis factor (TNF) inhibitor used to treat various autoimmune conditions) and atezolizumab (programmed death ligand-1 (PD-L1) inhibitor used in combination cancer immunotherapy) are highly immunogenic *in vivo* (Ben-Horin et al., 2011; Enrico et al., 2020; Pratt, 2018; Vaisman-Mentesh et al., 2019). In these cases, the production of ADAs is presumably a function of the corresponding drug meeting two key conditions for adaptive immunogenicity: 1) cognate B cells against the drug, and 2) associated T cell epitopes within the same antigenic complex (which is likely met by virtue of the antibody-based drug being peptidic).

There is overwhelming evidence that ADAs can impact effective drug activity, although the mechanistic underpinnings are seemingly varied (Chirmule et al., 2012; Vultaggio et al., 2014). For example, anti-idiotopic responses are intrinsically inhibitory, competing with the target ligand for the drug binding surface. Moreover, the production of ADAs and the subsequent formation of drug–ADA immune complexes (including subsequent compliment deposition) promotes drug clearance (Kohler et al., 2019; Potocnjak et al., 1982). Both outcomes affect drug pharmacokinetics and may have implications for drug efficacy (Kavai and Szegedi, 2007).

The principle of hapten-carrier biology may similarly extend to some small-molecule drugs (SMD). For example, some SMDs have unstable functional groups that may indiscriminately fix to endogenous proteins upon administration. For instance, it is known that some drugs, such as penicillin, warfarin and diazepam interact endogenously with human serum albumin (HSA) (Larsen et al., 2016); indeed, the phenomenon of non-enzymatic post-translational modifications are widely reported under physiological conditions (Dolhofer and Wieland, 1980; Kragh-Hansen, 1990, 1981; Peters, 1985; Walker, 1976). However, the precise mechanistic relationships between drug–protein interactions, complex immunogenicity and the functional effect of any possible antibody response is not well-described at the molecular level.

1.8.1. β-lactam antibiotics

One major drug class of interest that may serve as an effective model of drug-protein conjugation and its immunological outcomes is β-lactam antibiotics, such

as penicillin-type antibiotics, characterised by their β-lactam, hiazolidine and benzene functional groups. These are widely used as therapeutics for their bactericidal/bacteriostatic effects. PenG was the first clinically-developed antibiotic, produced at-scale by Ernst Chain and Howard Florey in 1940 (Abraham et al., 1992; Chain, 1979; Florey et al., 1943; Kong et al., 2010). However, it was in 1974 that Blumberk and Strominger determined that PenG worked by suicidally binding the catalytic site of peptidoglycans (PGN) by mimicking the termini of D-Ala-D-Ala (Blumberg and Strominger, 1974). The PGN inhibitory function results in a failure for bacteria to maintain osmotic pressure, resulting in cell lysis.

These antibiotics are notoriously chemically unstable, a consequence of the β-lactam ring readily hydrolysing or reacting with amine (Brouwers et al., 2020; Kipper et al., 2018). Studies have shown that salt availability, temperature and pH of the drug in solution drastically affect half-life. When incubating β-lactam drugs in human serum *ex vivo*, the amount of free, intact drug diminishes rapidly at room temperature, in line with drug fastening to bulk serum protein (Bahmany et al., 2023). Clinically, high doses of β-lactam antibiotics result in a significant fraction (up to 60% of drug) binding HSA (Lapresle and Wal, 1979; Yvon et al., 1990; Yvon and Wal, 1988). Analysis indicated that PenG and other β -lactams preferentially react with the primary amines of lysine sidechains (**Fig 1.8**), and may also form minor, more unstable conjugates with arginine and histidine (Levine and Ovary, 1961). The implications for these adducts and their ensuing immunogenicity have not been fully explored.

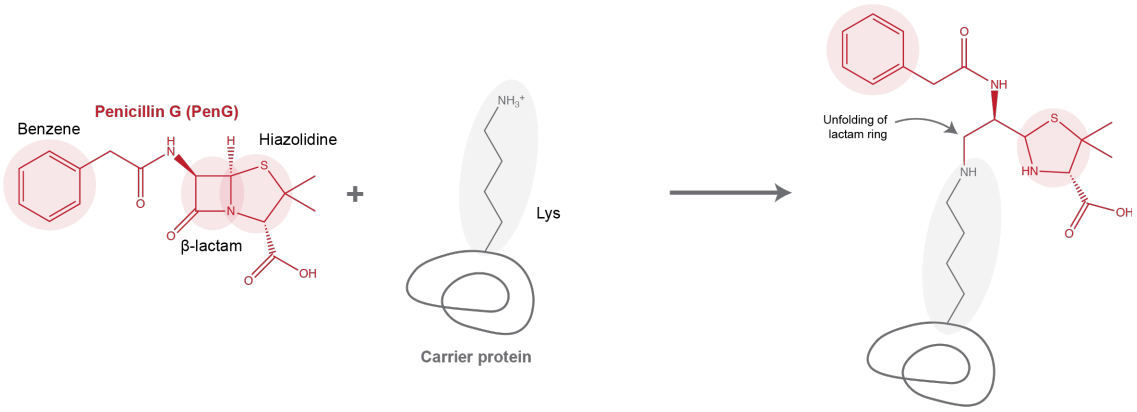


Figure 1.8: Penicillin-type β-lactam class and reactivity with primary amines.

The β-lactam ring of penicillins, such as PenG, are highly reactive with primary amines of lysine sidechains under certain buffer conditions. The reaction results in the unfolding of the β-lactam ring and the covalent fixing of the drug to the sidechain. Structure of the conjugate inferred from Mayorga et al. 2021.

1.8.2. Immunogenicity of penicillin adducts

PenG-protein conjugates are believed to be a key antigenic factor driving drug hypersensitivity. Notably, the underpinnings of the hypersensitivity reaction are believed to be immunologically heterogenous. Most commonly and well-characterised is Th cell-mediated (or type IV) hypersensitivity, which may be elicited in as much as 30% of the population (Dupnik, 2017). This reaction tends to be asymptomatic–mild, with clinical symptomology of fever and rash. The molecular underpinning of this hypersensitivity reaction is predominately caused by the Th cell compartment. For example, the common broad-spectrum β-lactam, piperacillin, is known to be highly immunogenic: when bound to Lys_{541} of HSA, the drug–peptide complex is presented and is highly attractive to Vβ13.1 and Vβ17 T cell clones (Meng et al., 2017a). Similar T cell drug reactogenicity has been observed against PenG, amoxicillin and other β-lactam drugs (Gill, 1967). The immune phenotype of the drug-specific antibody pool is diverse, although in patients with T cell-mediated allergy, they mostly comprise a Th2 phenotype (that is, secreting IL-4, IL-5 and IL-13) in line with the eosinophilic presentation of this

form of hypersensitivity (Blumenthal et al., 2015; Brander et al., 1995; Goh et al., 2021; Lochmatter et al., 2009; Whitaker et al., 2011).

The implications of antibody-mediated responses against PenG and other β-lactams are poorly described. Notably, the capacity for antibody responses to be mounted against penicillin was first described in 1961 by Levine and Ovary. They found that pre-complexing PenG to carrier proteins (HSA, human γ-globin or poly-L-lysine) in sufficiently basic buffer conditions *in vitro* and subsequently immunising rabbits with these conjugates in complete Freund's adjuvant resulted in an anti-PenG serological response (Levine and Ovary, 1961). While these studies provide proof-of-principle that penicilloyls can be immunogenic, the tested immunisation conditions are not representative of the antigenic environment post-administration of free drug: 1) complete Freund's adjuvant is highly immunopotentiating and over-engages the innate compartment compared to free drug administration (Stils, 2005); 2) the use of foreign protein carriers most likely exaggerates T cell help compared to more tolerogenic endogenous conjugates formed upon free drug administration (for example, using HSA rather than rabbit serum albumin), and 3) the pre-complexing strategy was designed to optimise adduct loading and may not reflect the density and quantity of penicilloyls generated *in vivo* following free drug dosing (Levine and Ovary, 1961). Therefore, these early data did not directly implicate these adducts as physiologically relevant antigenic determinants of hypersensitivity.

However, in the clinic, antibody responses against PenG are reported in ~55% of patients treated with the drug, although the disjunct between the rarity of

allergy compared to the frequency of anti-PenG responses was noted (Lafaye and Lapresle, 1988). However, the subset of hypersensitive patients was hypothesised to be a consequence of an IgE response to the drug (the isotype responsible for anaphylaxis-inducing type I hypersensitivity). However, tests for IgE offer poor sensitivity and specificity, with the best predictor of clinically significant IgE-mediated PenG allergy being positive case history (Tannert et al., 2017). Notably, IgG may also be implicated in a less acute form of hypersensitivity (Weiss and Adkinson, 1988). Whether there are any functional effects of anti-penicillin responses in individuals who exhibit a non-allergic phenotype has, to my knowledge, never been investigated. For example, whether these antibodies have a drug sequestering or other effect remains unclear.

…

1.9. Aims and hypotheses

Protein conjugates allow antibody responses to be raised against non-peptidic epitopes, by associating a conjugate-of-interest with associated T cell help from the same antigenic complex. In this thesis, I take this principle to develop two model systems to understand discrete and outstanding challenges for the field:

1. **<u>Overcoming tolerance barriers (results chapters 3 and 4)</u>**

   Conjugate-based vaccinations has been explored in certain settings to overcome T cell help constraints. Some antigenic targets may also lack B cell immunogenicity (such as certain carbohydrate antigens). Using the

model TACA GM3g, I evaluate novel approaches directed to how conjugate-based vaccine design can overcome these tolerogenic barriers.

Hypothesis: Since TACAs and other self-antigens are highly tolerogenic, immunisation with native presentations fail to elicit an antibody response. Artificial presentation of GM3g may access naïve B cell clones otherwise inaccessible to the carbohydrate.

Aims:

i) Develop a semi-synthetic protein chemistry approach to artificially present the model immunorecessive carbohydrate, GM3g, in non-native modes.
ii) Characterise the resultant B cell responses at the clonal and molecular level.
iii) Characterise the antibody response serologically, biophysically and structurally

2. **<u>Immunogenicity of small-molecule-derived complexes and properties of the antibody response (results chapter 5)</u>**

Some chemically unstable small molecules, such as some drugs, react with endogenous protein. The formation of immune complexes may be immunogenic for the drug under certain conditions. The conditions and the functional effects of any antibody responses against the small-molecule conjugates are poorly understood.

Hypothesis: Pre-complexed PenG conjugates may be significantly more immunogenic compared to administration of free drug complexing *in vivo* and will allow a detailed immunogenic and molecular analysis of anti-drug B cell responses.

Aims:

i) Using PenG as a model, to investigate at the molecular level the relationship between drug chemical instability and the formation of functional drug-protein antigenic complexes

ii) Interrogate the downstream B cell response and the clonal and molecular level.

iii) Evaluate functional features of the ensuing antibody response.

Chapter 2—Materials and Methods

2.1. Immunogen synthesis and chemical characterisation

2.1.1. Molecular cloning

Gene constructs for model immunogens (such as modified HIV-1 glycoprotein-120 (gp120), henn egg lysozyme (HEL) and ovalbumin (OVA)) were codon optimised for improved expression in human cells and ordered from GeneArt (Life Technologies) with adapters for a suitable mammalian expression vector, pCMV. The vector was digested with the appropriate restriction enzymes (New England Biotechnologies, NEB) and genes were subcloned using via a Gibson reaction. Gibson mix was made in-house, adapting from previously published protocols (Gibson, 2011). Briefly, 12.5 µL of Gibson master mix (100 mM Tris Cl pH 7.5 (Merck), 10 mM MgCl2 (Merck), 0.2 mM dNTP (NEB), 10 mM DTT (Merck), 5% PEG-800 (Merck), 2 mM NAD (NEB), 0.005 U/µL T5 exonuclease (NEB), 0.033 U/µL Phusion DNA polymerase (NEB) and 5.3 U/µL Taq DNA ligase (NEB)) was combined with 10–100 µg vector and 1:2 molar ratio insert to a total volume of 20 µL. The reaction mixture was incubated at 50°C for 60 mins followed

by a 10 min 80°C denaturing cycle. Product was transformed into DH5α sub-cloning competent bacterial cells (Life Technologies), plasmid extracted from single colonies using Mini-Prep Plasmid Preparation kits (Qiagen) and products confirmed by Sanger sequencing (Source Bioscience).

Site-directed mutagenesis was conducted using primers designed to induce the appropriate mutation flanked by a 15 nt annealing side and an 8 nt overhang. Mutagenesis was conducted using the appropriate reaction mix of 2X DreamTaq Green master mix (Life Technologies), 1–15 ng wild-type plasmid backbone and 0.2 mM primers. Cycling conditions were determined according to the manufacturer's instructions. The PCR product was run on an agarose gel (1.2–1.5% agarose at 130V for 30 mins). The band of the correct length was excised and purified using the Gel Purifcation Kit (Qiagen). The product was treated with DpnI (NEB) according to the manufacturer's instructions and transformed into DH5α sub-cloning competent cells (Life Technologies). Colonies were picked, amplified and prepared, as described, and introduction of desired mutation products were confirmed via Sanger sequencing (Source Bioscience).

2.1.2. Mammalian protein expression

Proteins were expressed recombinantly in-house using the HEK 293F expression system (Life Technologies). Cells were maintained in standard Freestyle expression media (Life Technologies) at 37°C with 8% CO_2 under orbital shaking (115 rpm). Cells were suitably passaged/expanded every 2–3 days. Cells were transfected using PEI Max (Polysciences): for 1L of cells at 1 x 10^6 cells/mL, 94 µg of PEI was diluted in 25 mL Opti-MEM (Life Technologies)

and incorporated dropwise into 350 µg expression vector diluted in 25 mL Opti-MEM. After brief vortexing, the mixture was incubated at 25°C for 30 mins and added to the cell culture. After 4–7 days, supernatants were harvested by spinning the culture down (1500g, 15 mins) and supernatant passed through a 0.22 µm filter unit.

2.1.3. Protein purification

Recombinant proteins were purified via several different strategies. Untagged proteins were purified via immunoaffinity chromatography, His-tagged proteins were purified via immobilised metal chromatography and immunoglobin was purified via protein A/G chromatography.

2.1.3.1. Immunoaffinity chromatography

Antibody affinity columns were prepared to capture untagged proteins (for example, gp120 was purified using a 2G12 column and HEL was purified using a D1.3 column). Columns were generated using AminoLink Plus resin according to the manufacturer's instructions (Life Technologies). Briefly, the appropriate amount of resin powder was weighed out (1 g power produces approximately 3.5 mL final volume of resin) and resuspended in 1mM HCl (pH = 3.0). After the resin was re-hydrated, excess HCl was removed in a column via gravity. The resin was washed with 200 mL 10mM HCl. Antibody was prepared in coupling buffer (0.1M $NaHCO_3$, 0.5M NaCl (pH = 8.3)). 5 mL of buffer containing 5–10 mg antibody was prepared per gram of lyophilised power. Coupling solution containing the resin and antibody was mixed end-to-end for 1 h at 25°C. The resin was washed with 5 x resin volume of coupling buffer. 5 x resin volume of

0.1M Tris HCl (pH = 8) was added to the column and rotated end-to-end for 2 h at 25°C to block the unoccupied functional groups on the resin. The beads were subsequently washed as follows: 50 mL high salt buffer (3M MgCl2, 10mM Tris, pH = 8.0), 50 mL PBS, 50 mL glycine buffer (0.1 M glycine, pH = 3.0) and 50 mL PBS.

Supernatants were slowly passed over beads by gravity flow at 4°C and resin was washed with 50 mL PBS. Proteins were eluted with high salt buffer and immediately buffer exchanged into PBS.

2.1.3.2. Immobilised metal affinity chromatography

Nickel affinity chromatography was used to purify His-tagged protein. HisPur Ni-NTA resin (Life Technologies) was used. Briefly, resin was equilibrated with wash buffer (20 mM Tris HCl, 500 mM NaCl, 20 mM, pH = 7.4). Imidazole was added to protein supernatant to a final concentration of 20mM before flowing through the column via gravity. The resin was washed thoroughly with buffer and eluted (20 mM Tris HCl, 500 mM NaCl, 500 mM imidazole, pH = 7.4). The protein was subsequently dialysed into PBS. Nickel resin was regenerated and re-used, according to the manufacturer's instructions.

2.1.3.3. Protein A/G chromatography

Antibodies were purified using Pierce Protein A agarose beads (Life Technologies). Briefly, supernatant was passed through the beads via gravity. After washing the resin with PBS, Ig was eluted using glycine buffer, neutralising

the elutant with 150 µL 1M Tris (pH = 9) per 5mL elution buffer. Antibody was then buffer exchanged into PBS.

2.1.4. Protein quantification

Protein concentrations were determined using a bicinchoninic acid (BCA) quantification assay (Life Technologies), according to the manufacturer's instructions. Protein concentrations were determined according to bovine serum albumin (BSA) standards prepared in-house. All concentrations referred to in this thesis are according to the protein concentration only, without reflection of glycan contributions natively or synthetically conjugated.

2.1.5. Synthesis and conjugation of semi-synthetic glycoconjugates

The development and optimisation of the sugar chemistry pipeline was in large part the work of Drs Xiaochao Xue, Aziz Khan and Guoxuan Sun (Departments of Chemistry and Pharmacology, University of Oxford). Details of these processes are discussed thoroughly elsewhere (Deimel et al., 2023). Brief protocols follow.

2.1.6.1. Generation of the [–amidine-GM3g] glycoconjguate

GM3g-SCN was synthesised from commercially available D-lactose (**Fig 2.1**). Briefly, acetylation in a combination of Ac_2O and NaOAc in reflux gave lactose octaacetate **2** with a yield of 96% and treated acetate **2** with acetic HBr solution at 25°C for 1 h, yielding the bromosugar **3** in 84% after recrystallization from chilled ether. The conversion from **3** to thioacetate **4** was carried out in DMF. Later, CH_3CN was employed as the media to access a readily

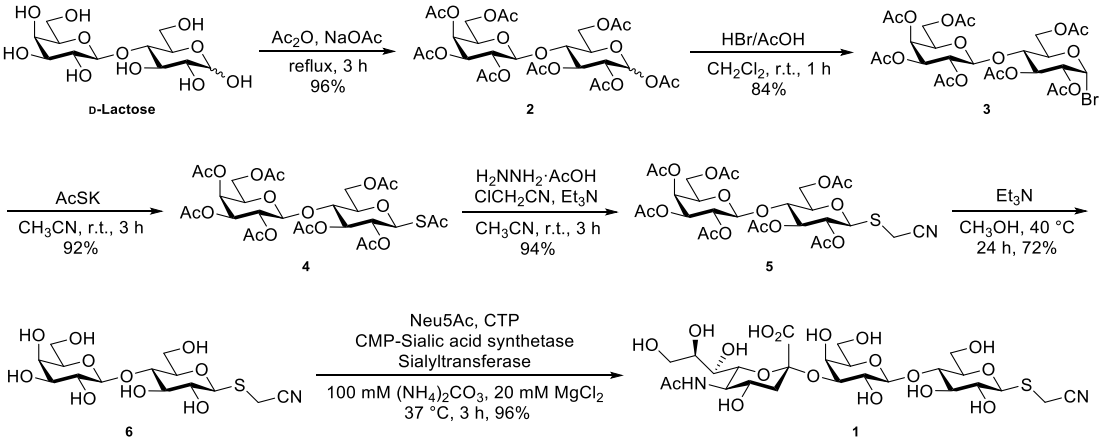


Figure 2.1: Chemoenzymatic synthetic route of cyano-functionalized 3'-GM3g. Adapted from Dr Xiaochao Xue.

workup and purification, the corresponding yield was 92%, which was comparable with product synthesised when DMF was used. Subsequently, selective hydrolysis of the anomeric thioacetate and S_N2 reaction were set up in one-pot, giving the cyano-functionalized lactose **5** in 94% yield; following hydrolysis of acetates in hot alkaline methanol generated **6** in 72% yield, which served the substrate for the enzymatic reaction. **6** was converted GM3g-SCN **1** with *NmCSS* (sialic acid-CMP synthetase from *Neisseria meningitidis*) and *PmST3* (2,3-sialyl-CMP transferase from *Pasteurella multocida*) in the presence of Neu5Ac and CTP (**Fig 2.2**). These protocols were adapted as previously described.

GM3g-SCN (404 mg, 587 μmol) was activated in sodium methoxide solution (20 mM in 29 mL, 1.0 eq. of CH_3ONa) by following the standard protocol (as shown in the preparation of GM3g-imidate **7**). After stirring for 4 days at 25°C, THF (87 mL) or ether (29 mL) was added to precipitate the sugar. The white solid was separated by centrifugation, the supernatant was discharged, and the white

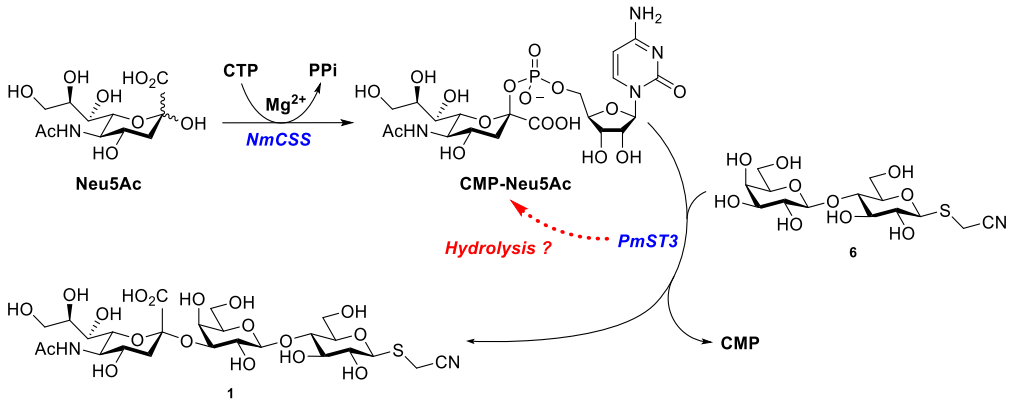


Figure 2.2: Mechanism of 2,3-sialylation in a on-pot two-enzyme system. Adapted from Dr Xiaochao Xue.

residue was then dried under vacuum before being used immediately for protein modification.

The precipitated sugar was dissolved in PBS buffer (2.8 mL, pH = 7.4). A fresh solution of protein in PBS buffer (0.7 mL, 5 mg/mL, pH = 7.4) was added (final concentration of HEL was 1 mg/mL) and the mixture was incubated at 25°C for 12 h (checked by SDS-PAGE and LC_MS if necessary). The reaction was desalted by PD-10 column twice (note: desalting is not sufficient to completely remove sugar. Excess sugar was in the post fraction; GM3g-CN **1** could be recovered by purification). Dialysis was subsequently performed in PBS buffer at 4°C (4 h × 2 and 12 h × 1). The solution was concentrated, sterilized and stored at 4°C. Concentration of HEL-[–amidine-GM3g]$_6$ was analyzed by BCA assay (7.13 mg/mL, 0.6 mL, endotoxin free-PBS buffer, pH = 7.4). Notably, modifications using [–amidine-Le^x] were prepared in an essentially identical manner.

Pure and chemically homogenous products were confirmed by complimentary NMR and chromatography-based methods.

2.1.6.2. Alternative linker conjugates

HEL-[–aminoalkyl-GM3g]$_6$: A mixture of HEL (11 µL, 220 µg, 20 mg/ml in PBS, pH = 7.4), GM3gOCH_2CHO (41.56 µL, 30 mg/ml in H_2O, 20 eq./lysine, 6*lysine), freshly prepared $NaBH_3CN$ solution (23.19 µl, 5 mg/ml in H_2O, 20 eq./lysine, 6*lysine), topped to 220ul with H_2O (144.25 µl, final protein concentration was 1mg/ml) was incubated in 37°C for 24 h without shaking. Then solution was immediately dialyzed to PBS at 4°C.

HEL-[–amide-GM3g]$_6$: 15.83 µL of **S-Short-NHS** (8 eq./lysine, 60mg/mL in DMSO, freshly prepared) was added into HEL (50 µL, 1mg, 20mg/mL in PBS, pH = 7.4) solution, mixed and incubated for 3 h at 25°C. Following immediate desalting into water, protein was concentrated to 2 mg/mL and checked with LC-MS. To a solution of dimeric GM3g **28** (1 mg) in water (75.6 µL), 1.54 µL of TCEP solution (1.0 eq, 0.5 M in water, freshly prepared from TCEP (free acid) solid, neutralized by 3 eq. of NaOH) was added and, after incubation at 25°C for 30 mins, transferred it into 287 µL of iodo-HEL solution (574 µg, 2mg/mL, 6.4 eq. GM3g-SH/Lysine) above. 172 µL of sodium borate (100 mM, pH = 8.5) was added, topped to 1mg/ml (protein solution) with 37 µL of water. This mixture was incubated at RT for 3 h (LC-MS checking) before being dialysed against PBS (pH = 7.4), concentrated, sterilised, and analysed by BCA assay.

2.1.6. Ex vivo drug modification of proteins

Proteins were dialysed into 0.1M $NaCO_3$ (pH =8) and concentration adjusted to 1 mg/mL. PenG was added to a molar ratio of 1:200 per lysine residue of carrier

protein. The mixture was rotated end-to-end at 25°C overnight and dialysed back into PBS.

2.1.7. Evaluation of endotoxin

2.1.7.1. TLR-4 reporter assay

HEK293T-cells transfected with TLR4-CD14-MD2 (Invivogen) were cultured according to the manufacturer's instructions. Briefly, the cells were maintained in supplemented DMEM containing 100 µg/mL Normacin (Invivogen) and selection antibiotics (10 µg/mL Blasticidin and 50 µg/mL Hygrogold (Invivogen)) and split whenever the cells reached 80-90% confluency. To test samples for lipopolysaccharide (LPS) contamination, these cells were plated at 50,000 cells/well in a 96-well flat-bottomed plate in medium without selection antibiotics. Protein samples were then immediately added (final concentration of 50 µg/mL) and the plates left overnight. PBS was used as a negative control in these experiments, whilst Ultrapure-LPS (Invivogen) was used as a positive control. At the end of the incubation, supernatant was collected, and IL-8 production was assessed using a human IL-8 ELISA run according to the manufacturer's instructions (Life Technologies). Briefly, plates were coated overnight at 4°C using 1x capture antibody diluted in coating buffer (PBS) at 50 µL/well. The following day, plates were blocked (1x ELISA/ELISPOT Diluent, 100 µL /well) samples were added (50 µL/well, diluted in 1x ELISA/ELISPOT Diluent) added to the plates for 2 h. At the end of this incubation, plates were washed and 1x detection antibody was added for 1 h, followed by 1x avidin-HRP for 30 mins, both at 50 µL/well. Plates were then developed with TMB substrate, colour

development was stopped with 0.5M H_2SO_4, and absorbance read at 450 and 570 nm.

2.1.7.2. RAW Blue reporter assay

RAW-Blue cells (Invivogen) were cultured according to the manufacturer's instructions, instead using 200 µg/mL Zeocin. To test for pathogen-associated molecular pattern (PAMP) contamination, cells were plated, and samples added as above for overnight incubation. 20 µL of supernatant was then added to 200 µL QUANTI-Blue medium and incubated at 37°C. Absorbance at 630 nm was measured over 1-6 h.

2.1.7.3. Endotoxin clean-up

To remove endotoxin contamination, samples were buffer exchanged into 0.5x PBS and run through a prepacked EndoTrap Red 1 mL column (Lionex) by gravity according to the manufacturer's instructions. Briefly, the column was prepared with 3 column volumes of regeneration buffer and 3 column volumes of 0.5x PBS before adding and eluting sample with 0.5x PBS. Cleaned samples were then retested for contamination and this procedure repeated if necessary. Protein preparations where the reporter endotoxin readouts were less than the < 0.125 ng/mL LPS control was considered clean.

2.1.8. Protein gel electrophoresis

Proteins were evaluated via SDS-PAGE. Samples were run on precast NuPAGE Bis-Tris gels (Life Technologies) with 1X MOPS buffer (Life Technologies) according to the manufacturer's instruction. Proteins were stained using

InstantBlue Coomassie protein stain (Abcam) Molecular weights were manually estimated according to the Novex Sharp protein marker (Life Technologies).

2.1.9. Mass spectrometry (MS)

Ammonia acetate (100 mM, pH = 8.0) buffer was prepared, adjusted pH by using either acetic acid or ammonia hydroxide solution, filtered with a 0.2 μm filter, degassed by sonication, stored at 25°C for use. Purified protein (in PBS buffer) was diluted with ammonia acetate buffer and DTT was added to a final concentration of 10 mM. The optimal concentration for analysis was 0.03 mg/mL, 5 μL was injected.

High Resolution Mass Spectra (HRMS) were recorded on a Bruker Daltronic MicroTOF spectrometer using electrospray ionization (ESI). ProswiftTM RP-2H column (4.6×50 mm SS, Life Technologies) was run at 0.3 mL/min with eluent A (0.1% formic acid in M.Q. water, v/v) and eluent B (0.1% formic acid in acetonitrile, v/v). Method was programmed as follows (10 min): 5% B (1 min), 5% B to 95% B (6 min), 95% B (1 min), 95% B to 5% B (0.1 min), 5% B (1.9 min). The following MS parameters were used: capillary voltage, 3000 V; sample cone, 20 V; desolvation temperature, 200 °C; source temperature, 80 °C; nitrogen desolvation flow, 700 L/h; no cone flow; pusher cycle time, 94; and ion energy, 34 V; m/z scan range 200 to 2100; scan time, 1 s; interscan time, 0.1 s.

m/*z* values are reported in Daltons. Optical rotations were measured on a Perkin-Elmer 241 polarimeter at 589 nm (Na D-line) with a path length of 1.0 dm at ambient temperature and are in units of degree $mL \cdot g^{-1} \cdot dm^{-1}$. The intact protein

liquid chromatography (LC)MS data were analysed using MassLynx (Waters, version 4.1 for Windows).

2.1.9.1 Proteomic analysis of adduct occupancy

Evaluation of the site-specificity and occupancy of PenG adduct formation was conducted by Dr Sean Burnap (Department of Biochemistry, University of Oxford). Briefly, this was conducted using LCMS/MS following in-gel digestion of modified protein, according to previously published protocols (Shevchenko et al., 2006). Peptides were run on a Q Exactive (QE) machine (Life Technologies) connected to an ultimate 3000 high performance liquid chromatography system on a typical 60min gradient using a "top10 ID" method typical for QE. Data were analysed via an open search on MSFragger (Kong et al., 2017).

2.1.10. PNGase F treatment of glycoproteins

To obtain sharper bands and increase signal-to-noise, gp120 proteins were de-glycosylated using PNGase F (New England Biolabs), according to manufacturer's instructions prior to SDS-PAGE.

2.1.11. Liposome synthesis

Liposomes were kindly generated by Dr Erdinc Sezgin. All lipids were from Avanti Polar. Lipid mixtures (phosphatidylglycerol (PG):phosphatidylcholine (PC): cholesterol: GM3 = 39:39:19:3) at 1 mg/mL in chloroform were dried under the flow of nitrogen and rehydrated with buffer (150 mM NaCl, 10 mM HEPES, 2 mM $CaCl_2$) and vortexted to form multilamellar vesicles. Then, suspension of the multilamellar vesicles were sonicated (power 3, duty cycle 40% for 10 mins) using

a Branson Sonifier 250. Liposomes were stored under nitrogen atmosphere to prevent oxidation.

2.2. Animal work and immunisation schedules

2.2.1. Animal handling and maintenance

Unless otherwise indicated, sex-matched wild-type 6–8-week-old pathogen-free BALB/c or C57BL/6 mice were used, purchased from Charles River. All experimentation was conducted in accordance with the institutional, project and personal user licence protocols. Animals were monitored daily and provided standard chow and water *ad libitum*. Immunisation schedules are outlined in the results, and mice were bled periodically from the tail vein. Animals were sacrificed via a rising CO_2 gradient and subsequent cervical dislocation schedule 1 procedure.

2.2.1.1. MD4 mice

For some *in vitro* assays, spleens from MD4 mice were kindly gifted from Dr Tal Arnon. These mice are of a C57BL/6 background have a transgenic BCR of the high-affinity and specific anti-HEL clone, HyHEL10 (Goodnow et al., 1988).

2.2.1.2. Human immune system (HIS) mice

The production and development of HIS mice used in this study was performed by Prof James di Santo and Dr Toshiki Eri, as previously described (Li et al., 2018). This was conducted in BALB/c mice transgenic for mouse thymic stromal lymphopoietin (TSLP) and $Rag2^{-/-}IL2rg^{-/-}Sirpa^{NOD}$. Foetal liver $CD34^{+}$ cells were isolated using an affinity matrix (Miltenyi Biotec) and phenotyped for CD38

expression. Newborn (~4-day-old) pups received sublethal irradiation (3 Gy) and were injected intrahepatically with 5 x 10^4 $CD34^+CD38^-$ liver cells. Mice were maintained for 8 weeks post-transplant prior to use—this provided sufficient time to allow the establishment of the human haemopoietic line and to monitor for rejection.

2.2.1.3. TRIANNI mice

Experiments were also conducted in TRIANNI mice (AbCellera), in collaboration with Dr Dominik Damm and Prof Klaus Üeberla. These mice are of a BALB/c background and have an almost entirely human antibody repertoire, with the mouse V-gene segments substituted for that of a human (VH, Vκ and Vλ). These segments are combined with native, non-coding murine regulatory elements and common chains. These mice allow for antibody discovery against a human germline repertoire (Peter et al., 2022).

2.2.2. Formulation of immunisations

Endotoxin-clean immunogen preparations (antigen dosage indicated in results) were diluted in PBS. Adjuvanted formulations were prepared with 20 µg monophosphoryl lipid A (MPLA) (Polymun Scientific) (a TLR-4 agonising adjuvant) (Mata-Haro et al., 2007), 1:1 Alhydrogel (Invivogen) (Morefield et al., 2005), or 1% Adjuplex (Wegmann et al., 2015) (Merck). Immunisations adjuvated with Alhydrogel were left to rotate end-to-end at 25°C for 30 mins prior to administration to promote antigen:adjuvant absorbance/complexing.

2.3. ELISA

2.3.1. Direct ELISA

Enzyme-linked immunosorbent assays (ELISAs) were performed by coating a target protein in 50 µL at 1 µg/mL in PBS onto 96-well flat-bottom high protein binding plates (PerkinElmer). Wells were washed three times with 200 µL PBS with 0.05% tween-20 (PBST) and blocked with PBST with 2% bovine serum albumin (BSA) (Merck). Wells were incubated with serially-diluted mAbs/sera for 2 h. Plates were washed and 50 µL HRP-conjugated secondary antibody was added (in 1% BSA-TBST) for 1 h (**Table 2.1**). After washing, 50 µL 1-Step Ultra TMB (Life Technologies) substrate was added and after 10 mins (or when the reaction had reach a sufficient intensity), 50 µL 0.5 M H_2SO_4 was added to terminate development. Data were acquired on a Spectramax M5 plate reader (Molecular Devices), evaluating the 450 nm readout minus the respective 570 nm background absorption.

Table 2.1: Secondary reagents used in ELISA.

Reagent	**Clone**	**Manufacturer**	**Dilution**
Goat anti-mouse IgG HRP	Polyclonal	Bio-Rad	1:5000
Rat anti-mouse IgG1 HRP	X56	BD Biosciences	1:1000
Rat anti-mouse IgG2a HRP	R19-15	BD Biosciences	1:1000
Rat anti-mouse IgM HRP	II/41	BD Biosciences	1:1000
Donkey anti-human IgG HRP	Polyclonal	Jackson ImmunoResearch	1:5000
Goat anti-human IgM HRP	Polyclonal	Life Technologies	1:5000
Streptavidin HRP	N/A	Life Technologies	1:500

After subtracting the background, optical density (OD)450-570 data were analysed using GraphPad Prism 9 (version 9.5.1, for Mac). To determine endpoint titres (EPTs), logistic curves were fitted to the data using the [agonist] vs response (variable slope; four parameters) function, with a defined bottom asymptote of 0. EPTs were defined as the intersection where the function OD value was 0.01, confirmed to be greater than 3 x SD above background.

2.3.2. Competition ELISA

Competition ELISAs were performed to titrate soluble ligand binding against anti-serum or a mAb. A serial dilution of soluble ligand was prepared in 2% BSA PBST and 50 µL was preincubated with 50 µL of sample antibody (serum or mAb) to a final concentration of the pre-determined 70% effective concentration (EC_{70}) (as established by direct ELISA). The EC_{70} was chosen as it represents the upper portion of the linear range of antibody binding and is therefore sensitive to competition assays. After 1 h incubation, the mixture was added to a pre-coated and pre-blocked ELISA plate, as described in *Section 2.3.1* for 1 h. Subsequent detection was conducted as per the direct ELISA protocol. Cross-competition IC_{50} values were evaluated by similar logistic regression analysis.

2.3.3. Free primary amine ELISA

Following the conjugation of the synthetic glycoconjugates to a carrier protein, relative free amines were compared to estimate the degree of lysine modification. This protocol was adapted (Hermanson, 2013). Briefly, protein samples (5 µg) in 10 µL PBS were mixed in 40 µL 0.1M sodium bicarbonate buffer. 5% solution of

2,4,6-trinitrobenzenesulfonic acid (TNBSA) was diluted 1:500 in the bicarbonate buffer, and 25 µL of this mixture was added to the protein sample. After 2 h incubation at 37°C. 25 µL 10% SDS and 12.5 µL of 1M HCl was added. The absorbance at 335 nm was measured using a Spectramax M5 spectrophotometer.

2.3.4. Capture cytokine ELISA

Cytokine ELISAs were performed using commercially available kits. Mouse IL-2, IL-4 and IFN-γ in supernatant was measured according to the manufacturer's protocol (all Life Technologies).

2.4. T cell analyses

2.4.1. Preparation of murine single cell suspensions

Splenic single-cell suspensions were prepared. Briefly, spleens were harvested and passed through a 100 µm cell strainer while continuously flushing with complete (c)RPMI media (100 U/mL penicillin (Life Technologies), 100 U/mL streptomycin (Life Technologies), 10 mM N-2-hydroxyethylpiperazine-N-2-ethane sulfonic acid (Life Technologies), 1 mM Na pyruvate (Life Technologies), 2 mM L-Glutamine (Life Technologies), 10% foetal bovine serum (FBS) (Life Technologies), 0.05 mM 2-mercaptoethanol (Sigma) in RPMI (Life Technologies). Suspensions were centrifuged (15 min, 380 g, 4°C), supernatant was discarded, and cells resuspended in red blood cell lysis (RBCL) buffer (Life Technologies). After a 3-min incubation at 25°C, the lysis buffer was diluted 10 x volume with cRPMI and centrifuged. Following two subsequent cRPMI washing steps and a secondary pass through a cell strainer, cells were ready for

downstream analysis. Lymph node (LN) suspensions were as previously outlined, except no RBCL treatment was performed.

2.4.2. Thymidine proliferation assay

Whole splenocyte suspensions (5 x 10^5 cells in 200 µL in a flat-bottom 96-well plate) were stimulated *in vitro* with 10 µg/mL antigen in cRPMI for 16 h. During the final 6 h of stimulation, 20 µL of supplemented RPMI containing 1 µL (0.037mBq) of tritiated thymidine (Perkin Elmer) was added per well and returned to the incubator. Radioactive cells were transferred and lysed on glass filter mats (Perkin Elmer) using a Micro 96 Harvester (Skatron Instruments). Tritium incorporation was measured using Betaplate Scint and a Microbeta Trilux Scintillation counter (both Perkin Elmer).

2.4.3. Intracellular cytokine staining

Whole splenocyte suspensions were similarly stimulated *in vitro* with 10 µg/mL antigen in cRPMI for 16 h. For the final 6 h, 5 µg/mL brefeldin A (Biolegend) was added to all wells to suspend ER–Golgi trafficking and block cytokine secretion. Cells were subsequently washed with PBS with ice-cold 2mM EDTA and stained with TruStain FcX Plus (Biolegend) and LIVE/DEAD Fixable Blue on ice for 30 mins. Surface markers were subsequently stained on ice for 20 mins: anti-mouse CD3-PE (concentration: 1:200, clone: 17A2, manufacturer: Biolegend), anti-mouse CD4-APC (1:200, RM4-5, Biolegend) and anti-mouse CD8-AF700 (1:200, RPA-T8, Biolegend). Following treatment with fixation and permeabilisation buffers (Biolgend), cytokine was stained for using anti-mouse IFN-γ-PE/DAZZLE 954 (1:100, XMG1.2, Biolegend)—this was conducted on ice for 40 mins. Cells

were washed twice with 2% FCS and 0.05% sodium azide in PBS (FB). Data were acquired on the BD Fortessa X-20 (BD Bioscience), collecting 500,000 events per sample.

2.4.4. Tfh quantification

Single cell suspensions derived from draining LNs of 7-days post-prime mice were immediately evaluated by flow cytometry (that is, without *in vitro* restimulation). Cells were stained with LIVE/DEAD Fixable Blue and blocked with TruStain FcX Plus, as previously described. Cell surface staining was subsequently performed on ice for 30 mins, using 100 µL of the following antibody cocktail in FB: anti-mouse CD3-AF647 (1:200, 17A2, Biolegend), anti-mouse CD4-AF700 (1:200, RM4-5, Biolegend), anti-mouse CD44-PE (1:20, IM7, Biolegend), anti-mouse CD62L-FITC (1:200, MEL-14, Biolegend), anti-mouse CXCR5-BV421 (1:20, L138D7, Biolegend) and anti-mouse PD-1-PerCP/Cy5.5 (1:100, 29F.1A12, Biolegend). After washing twice with FB, data were acquired as previously described, except 2 000 000 events were collected per sample.

2.5. Glycan array

These experiments were developed and performed by Prof James Paulson and Dr Ryan McBride. Glycan arrays were custom printed on a MicroGridII (Digilab) using a contact microarray robot equipped with StealthSMP4B microarray pins (Telechem) as previously described (Peng et al., 2017). Briefly, samples of each glycan were diluted to 100 µM in 150 mM Na_3PO_4 buffer, pH 8.4. Aliquots of 10 µL were loaded in 384-well plates and imprinted on NHS-activated glass slides (SlideH, Schott/Nexterion), each containing 6 replicates of each glycan.

Remaining NHS-ester residues were quenched by immersing slides in 50 mM ethanolamine in 50 mM borate buffer, pH 9.2, for 1 h. Blocked slides were washed with water, centrifuged dry, and stored at -20 ˚C until use.

Serum samples were diluted 1:200 in PBST and applied directly to the array for 1 h incubation. Samples were rinsed from the array surface by dipping 4 x each in PBST, PBS and deionized water, respectively. Washed arrays were re-probed with anti-mouse-IgG-AlexaFluor488 (10 µg/mL) for 1h incubation. Following secondary incubation, arrays were washed again by dipping 4 x each in PBST, PBS and deionized water, respectively, and dried by centrifugation. Dried slides were scanned for 488 nm signal on an Innoscan 1100AL scanner (Innopsys) and signal intensities were calculated using Mapix (Innopsys).

2.6. Isolation of single antigen-specific B cells

2.6.1. Molecular probe synthesis

Conjugate-specific probes were generated by fluorescently labelling either GM3g LOG- or PenG-modified gp120. This was achieved by using an NHS-esterified AF647 protein modification kit (Life Technologies). Fluorescent labelling was conducted according to the manufacturer's instructions. Successful modification was confirmed by both SDS-PAGE and subsequent scanning on a ChemiDoc (Bio-Rad), as well as via mass spectrometry.

Protein backbone-specific probes (either HEL or gp120) were generated via tetramerization. First, unmodified protein carriers were biotinylated using EZ-Link Sulfo-NHS-LC-Biotin (Life Technologies). Briefly, the reactive biotin was

dissolved 2 mg/mL in DMSO. 10 µL of dissolved biotin was added to every 100 µL protein in PBS at 1 mg/mL. The reaction was left to incubate overnight at 4°C. Unreacted biotin and DMSO was removed through repeated concentrating with PBS in an Amicon filter column (Merck). The biotinylated product was tetramerised against BV785-modified streptavidin (Biolegend). A 1:4 molar ratio of streptavidin to protein carrier was calculated. Half of the protein carrier was added to the streptavidin and incubated on ice in darkness for 30 mins. Every subsequent 15 mins, 10% of the remain protein was progressively added.

2.6.2. Single cell sorting

BALB/c mice were immunised 4 weeks prior to B cell isolation. Single cell suspensions were generated from the spleen, inguinal lymph nodes and bone marrow (femur and tibia). Splenocyte suspensions were enriched using magnetic anti-mouse CD19 microbeads (Miltenyi Biotec), as outlined in the manufacturer's instructions. Fc receptors were blocked and cells stained with LIVE/DEAD Fixable Blue, as outlined earlier. The following surface stain cocktail was prepared: anti-mouse F4/80-PE (1:200, BM8, Biolegend), anti-mouse Gr-1-PE (1:200, RB6-8C5, Biolegend), anti-mouse CD3-PE (1:200, 17A2, Biolegend), anti-mouse CD4-PE (1:200, RM4-5, Biolegend), anti-mouse CD8-PE (1:200, RPA-T8, Biolegend), anti-mouse B220-eFluor450 (1:100, RA3-6B2, BD Biosciences), anti-mouse IgD-AF700 (1:200, 11-26c.2a, Biolegend), anti-mouse IgM-PE/Cy7 (1:200, R6-60.2, BD Biosciences), anti-mouse IgG1-FITC (1:200, A85-1, BD Biosciences), anti-mouse IgG2a/2b-FITC (1:200, R2-40, BD Bioscience), antigen probes as indicated in the results (10 µg/mL). Cells were stained on ice for 1 h. Cells were washed with FB and sorted immediately on a

BD FACSAriaFusion (BD Biosciences). LIVE/DEAD^{-}DUMP^{-}B220$^{mid–hi}$IgD^{-}(IgM^{+}/IgG^{+})Ag^{+} B cells were singly sorted into MicroAmp Optical 96-Well PCR Plates (Life Technologies) containing 5 µL 1X TCL buffer supplemented with 1% 2-mercaptoethanol. Immediately following sorting, plates were centrifuged at 1,500 g for 1 min. Plates were stored at -80°C until use.

2.6.3. Recovery of variable region sequences

Recovery of the antigen-specific B cell receptor variable regions was carried out, adapted from previous publications (Ho et al., 2016; Viant et al., 2021). The contents of each well were diluted with 10 µL water and 33 µL RNAClean XP beads (Beckman Coulter) and incubated at 25°C to capture RNA. Beads were pulled down under a magnetic field, the liquid fraction was removed and the bead pellet was washed with 70% ethanol 3 times. RNA was eluted from the beads by heating to 65°C for 3 mins following resuspension in elution buffer, containing the following per well: 11.3 µL water, 0.61 µL random 8 nt primers (0.3 mg/mL) (Life Technologies), 0.61 µL NP40 (10%) (Sigma), 0.24 µL RNasin Plus (40 U/µL)(Promega). After elution, reverse transcription mix was added, which contained per well: 2.5 µL water, 3.6 µL 5X SuperScript Buffer (Life Technologies), 0.6 µL dNTP mix (25 mM each) (Life Technologies), 0.24 µL RNasin Plus (40 U/µL) (Promega), 0.3 µL SuperScript III (200 U/µL) (LifeTechnologies). Libraries were generated using the following thermocycling conditions: 42°C for 10 mins, 25°C for 10 mins, 50°C for 60 mins, 94°C for 5 mins and 4°C until ceased.

Variable heavy (VH) and light/kappa (VK) regions were recovered using the primers outlined in **Table 2.2**. Briefly, PCR reactions were setup, with each well containing the following: 0.4 µL Q5 polymerase (2 000 U/mL) (New England Biolabs), 8 µL 5X Q5 reaction buffer (New England Biolabs), 8 µL 5X Q5 high GC enhancer (New England Biolabs), 0.2 µL relevant 5' and 3' primer (100 µM), 0.32 µL dNTP (25 mM each) (Life Technologies), 5 µL cDNA (from previous step), water to 40 µL. The reactions were cycled according to the following program: 94°C for 3 mins, 50 cycles of (94°C for 30 sec, [60°C for HC, 62°C for KC] for 30 sec, 72°C for 45 sec), 72°C for 10 mins, 4°C until ceased. VH PCR products were run on a 1.2% agarose gel and those with a band length of ~450–500 nt were sequenced. VH amplicons were purified using EXO-SAP according to the manufacturer's instructions (Life Technologies). Products were sequenced using Sanger sequencing with the 5' MsVHE primer (Source Bioscience).

Table 2.2: Variable region recovery primers.

Primer name	Primer sequence	PCR round	Source
5' MsVHE	GGGAATTCGAGGTGCAGCTGCAGGAGTCTGG	VH Recovery	(Ho et. al 2016)
3' Cy1 outer (IgG1)	GGAAGGTGTGCACACCGCTGGAC	VH Recovery	(Ho et. al 2016)
3' Cy2b outer (IgG2b)	GGAAGGTGTGCACACTGGAC	VH Recovery	(Ho et. al 2016)
3' Cy2c outer (IgG2c)	GGAAGGTGTGCACACTGCTGGAC	VH Recovery	(Ho et. al 2016)
3' Ca outer (IgA)	GAGGCGAGGGCAGGTGGAAAGTTCACGG	VH Recovery	(Ho et. al 2016)

3' Cm outer (IgM)	AGGGGGCTCTCGCAGGAGACGAGG	VH Recovery	(Ho et. al 2016)
5' VK3	TGCTGCTGCTCTGGGTTCCAG	VK Recovery	(Ho et. al 2016)
5' VK4	ATTWTCAGCTTCCTGCTAATC	VK Recovery	(Ho et. al 2016)
5' VK5	TTTTGCTTTTCTGGATTYCAG	VK Recovery	(Ho et. al 2016)
5' VK6	TCGTGTTKCTSTGGTTGTCTG	VK Recovery	(Ho et. al 2016)
5' VK689	ATGGAATCACAGRCYCWGGT	VK Recovery	(Ho et. al 2016)
5' VK14	TCTTGTTGCTCTGGTTYCCAG	VK Recovery	(Ho et. al 2016)
5' VK19	CAGTTCCTGGGGCTCTTGTTGTTC	VK Recovery	(Ho et. al 2016)
5' VK20	CTCACTAGCTCTTCTCCTC	VK Recovery	(Ho et. al 2016)
3' MCK	GATGGTGGGAAGATGGATACAGTT	VK Recovery	(Ho et. al 2016)

2.6.4. Vectorisation and recombinant mAb expression

In order to incorporate the VH and VK amplicons into expression vectors, a nested PCR was conducted to incorporate overhangs homologous with the expression vectors used (for later homology-based assembly). PCR reactions were setup using Q5, as previously described, except using only 2 µL of amplicon-containing PCR product from the previous round. Primers used are outlined in **Table 2.3**. The reactions were cycled according to the following

program: 94°C for 3 mins, 50 cycles of (94°C for 30 sec, 50°C for 30 sec, 72°C for 45 sec), 72°C for 10 mins, 4°C until ceased. PCR products were run on a 1.2% agarose gel (expected length of ~500 nt) and purified using the PCR clean-up kit (Qiagen) according to the manufacturer's instructions. Depending on the application, amplicons were incorporated into either: i. a human IgG1 backbone expression system, kindly gifted by Prof Patrick Wilson (heavy chain: FJ475055; kappa chain: FJ75056), or ii. a human c-terminally His-tagged IgG1-based Fab expression system kindly gifted by Gabriel Victora. Vectors were assembled using Gibson reactions, as described earlier. Recombinant proteins were expressed in HEK293F cells and appropriately purified, as described earlier.

Table 2.3: Primers to incorporate vector-compatible adaptors to V-region amplicons.

Primer name	Primer sequence	PCR round	Source
T4hmFH_I	CTAGTAGCAACTGCAACCGGTGTAC ATTCTGAWGTGCAGCTGGTGGAGTC	VH cloning	(Viant et. al 2022)
T4hmFH_II	CTAGTAGCAACTGCAACCGGTGTAC ATTCTCAGGTGCAGCTGAAGSAGTC	VH cloning	(Viant et. al 2022)
T4hmFH_III	CTAGTAGCAACTGCAACCGGTGTAC ATTCTGARGTGAAGCTGGTGGARTC	VH cloning	(Viant et. al 2022)
T4hmFH_IV	CTAGTAGCAACTGCAACCGGTGTAC ATTCTCAGGTCCAACTGCAGCAGCC	VH cloning	(Viant et. al 2022)
T4hmFH_V	CTAGTAGCAACTGCAACCGGTGTAC ATTCTSAGGTYCAGCTGCARCAGTC	VH cloning	(Viant et. al 2022)
T4hmFH_VI	CTAGTAGCAACTGCAACCGGTGTAC ATTCTCAAGTGCAGATGAAGGAGTC	VH cloning	(Viant et. al 2022)

T4hmFH_VII	CTAGTAGCAACTGCAACCGGTGTAC ATTCTCAGATCCAGTTGGYGCAGTC	VH cloning	(Viant et. al 2022)
T4hmFH_VIII	CTAGTAGCAACTGCAACCGGTGTAC ATTCTCAGGTCCAACTCCAGCAGCC	VH cloning	(Viant et. al 2022)
T4hmFH_IX	CTAGTAGCAACTGCAACCGGTGTAC ATTCTCAGGTGCAACTGAAGCAGTC	VH cloning	(Viant et. al 2022)
T4hRG_I	CCGATGGGCCCTTGGTCGACGCTGA GGAGACGGTGACCGTGG	VK cloning	(Viant et. al 2022)
T4hRG_II	CCGATGGGCCCTTGGTCGACGCTGA GGAGACTGTGAGAGTGG	VK cloning	(Viant et. al 2022)
T4hRG_III	CCGATGGGCCCTTGGTCGACGCTGA GGAGACAGTGACCAGAG	VK cloning	(Viant et. al 2022)
T4hRG_IV	CCGATGGGCCCTTGGTCGACGCTGA GGAGACGGTGACTGAGG	VK cloning	(Viant et. al 2022)
T4hmFK_I	CTAGTAGCAACTGCAACCGGTGTAC ATTCCGAAAWTGTGCTCACCCAGTC	VK cloning	(Viant et. al 2022)
T4hmFK_II	CTAGTAGCAACTGCAACCGGTGTAC ATTCCCAAATTGTTCTCACCCAGTC	VK cloning	(Viant et. al 2022)
T4hmFK_III	CTAGTAGCAACTGCAACCGGTGTAC ATTCCRACATTGTGCTGACCCAATC	VK cloning	(Viant et. al 2022)
T4hmFK_IV	CTAGTAGCAACTGCAACCGGTGTAC ATTCCGAAACAACTGTGACCCAGTC	VK cloning	(Viant et. al 2022)
T4hmFK_V	CTAGTAGCAACTGCAACCGGTGTAC ATTCCGATATTGTGATGACSCAGGC	VK cloning	(Viant et. al 2022)
T4hmFK_VI	CTAGTAGCAACTGCAACCGGTGTAC ATTCCRRTRTTGTGATGACCCARAC	VK cloning	(Viant et. al 2022)
T4hmFK_VII	CTAGTAGCAACTGCAACCGGTGTAC ATTCCGATATCCAGATGACACAGAC	VK cloning	(Viant et. al 2022)
T4hmFK_VIII	CTAGTAGCAACTGCAACCGGTGTAC ATTCCGACATTGTGATGACMCAGTC	VK cloning	(Viant et. al 2022)

T4hmFK_IX	CTAGTAGCAACTGCAACCGGTGTAC ATTCCGACATCCAGATGACHCAGTC	VK cloning	(Viant et. al 2022)
T4hRK_I	GAAGACAGATGGTGCAGCCACCGTA CGTTTCAGCTCCAGCTTGGTCCC	VK cloning	(Viant et. al 2022)
T4hRK_II	GAAGACAGATGGTGCAGCCACCGTA CGTTTTATTTCCAGTCTGGTCCC	VK cloning	(Viant et. al 2022)
T4hRK_III	GAAGACAGATGGTGCAGCCACCGTA CGTTTKATTTCCARCTTKGTSCC	VK cloning	(Viant et. al 2022)

2.6.5. Immunogenetic analysis

Immunogenic analyses were performed on the VH regions of successfully recovered clones. Sequences were screened against the mouse germline gene segment repertoire using the Immunogenetics Information System (IMGT; https://www.imgt.org/IMGT_vquest/input). These outputs were used to determine both clonality (i.e. their inferred V(D)J configuration) and the SHM frequency. Sequences that returned either no result (indicative of poor sequence read quality) or was unproductive (e.g. premature stop codon) were excluded from our analysis. Clonal lineage trees were determined using GCTree (DeWitt III et al., 2018) and rendered on Adobe Illustrator.

2.7. Isothermal titration calorimetry (ITC)

This assay was conducted by Dr Lucile Moynie. Affinities of Fab BAR1 for the Amidine-GM3g and Lys–amidine-GM3g were measured by isothermal titration calorimetry using an automated PEAQ-ITC instrument (MicroCal) at 25 °C. Titrations were performed using 18 × 2 µL injections of 200-300 µM of the

polysaccharide into 20-30 μM of the protein in PBS buffer. The heats of dilution measured from injection of the ligands into the buffer were subtracted, and titration curves were fitted with one-site binding model.

2.8. X-ray crystallography

The solving of x-ray structures was done by Prof James Naismith and Dr Lucile Moynie. BAR-1 Fab was loaded onto a gel filtration Superdex 200 column (GE Healthcare) in 10 mM Tris-HCl, pH 7.5, 150 mM NaCl. Co-crystals appeared at 20 °C after a few weeks from a hanging drop of 0.1 μL of protein solution (19 mg/mL with 1.2 mM Lys–amidine-GM3g) with 0.1 μL of reservoir solution containing 30% (w/v) PEG MME 2000, 0.1 M potassium thiocyanate in vapor diffusion with reservoir. Crystals were frozen with the same solution containing 16% glycerol and 4 mM Lys–amidine-GM3g. Data were collected at the Diamond light source Oxfordshire (beamlines I24) and were processed with XIA2 (Evans, 2006; Kabsch, 2010; Winn et al., 2011; Winter, 2010; Zhang et al., 2006). The structure was solved by molecular replacement using PHASER and pdb file 6ug7 (Soliman et al., 2020b), and the structure was built with Autobuild program, refined with REFINE of PHENIX with NCS restraints (Liebschner et al., 2019) and adjusted with COOT (Emsley and Cowtan, 2004). Coordinates and topologies of ligands were generated by PRODRG (Schüttelkopf and van Aalten, 2004)

Structures were refined at 1.9 Å. Two Fab molecules are present in the asymmetric unit (H/L and A/B). The two molecules are very similar (rmsd of

0.4852 Angstroms for 213 residues). Final refinement statistics are given in Table 1. Atomic coordinates and structure factors have been deposited in the Protein Data Bank (8BJZ). The quality of all structures was checked with MOLPROBITY (Chen et al., 2010). The Ramachandran statistics are as follows: 98% favoured and 2% allowed.

2.9. Bacterial growth assays

2.9.1. Culturing and maintenance of Streptococcus pneumoniae

The attenuated, unencapsulated lab strain of *S. pneumoniae*, D39 (Δcps2A'-Δcps2H'), was kindly gifted by Drs Carolin Kobras and Matthew Stracey (Lanie et al., 2007). Bacteria was maintained/routinely grown in tryptic soy broth (TSB) (BD Biosciences) at 37°C (standing incubation) in a 5% CO_2 atmosphere.

2.9.2. Liquid minimal inhibitory concentration (MIC) recovery assay

First, serial dilutions of PenG in culture with the D39 *S. pneumoniae* strain revealed a PenG MIC of 0.01 µg/mL (that is, the lowest antibiotic concentration that prevented bacterial growth) (data not shown). In a flat-bottom 96-well plate, 2 ng of PenG in 10 µL PBS was pre-incubated with 10 µL of serially-diluted antisera for 2 h. 180 µL of D39-spiked TSB was added and incubated overnight (such that the final PenG concentration as 0.01 µg/mL). The following day, bacterial growth was measured using a Spectramax M5 plate reader (Molecular Devices), evaluating the 600 nm as a proxy for bacterial density.

2.9.3. Disk diffusion assay

0.1 µg of PenG and mAb (1:50 molar ratio) were spotted onto a paper disk. The disk was placed onto a D39-coated blood agar plate (Merck). Plates were incubated overnight. The following day, the diameter of the kill zone was manually measured with a ruler. Notably, both PenG-raised antibody clones were tested, as well as irrelevant HIV-1-specific antibodies.

2.10. Data processing and statistical analysis

Flow cytometry data were evaluated in FlowJo V.10.8. Sequence data were processed using Geneious Prime Build 2023-01-24, for Mac. Graphs were generated in GraphPad Prism V9.4 and using GCTree (DeWitt III et al., 2018), and later edited in Adobe Illustrator for aesthetics. Statistical analysis was conducted either in GraphPad Prism V.9.4 or in RStudio V.4.1. Chao1 estimates were performed using the RStudio iNEXT package (Hsieh et al., 2016). Statistical test details are provided in the results, figures and associated figure legends.

Chapter 3—Immunogenicity of semi-synthetic GM3g glycoconjugates in mice

3.1 Background

3.1.1 Immunorecessiveness of self-carbohydrate antigens

Self-carbohydrates, as found on glycoproteins and glycolipids, are typically immunorecessive structures, failing to elaborate robust antibody responses, as reviewed in **Chapter 1**. The evolutionary case for lacking glycan-specific B cell antigenicity is intuitively to prevent widespread autoimmunity against endogenously abundant glycans, and thus various serological correlations between self-glycan-reactive immunoglobin and autoimmunity is unsurprising (Dotan et al., 2006; Freedman et al., 2009; Schwarz et al., 2006). I hypothesise that there are two major immune tolerance mechanisms that underpin this phenomenon: 1) absence of germline-encoded carbohydrate-recognising motifs in the germline and 2) negative selective processes that eliminate self-glycan-reactive B cell precursors from entering the mature naïve pool. These and other glycan tolerance mechanisms are discussed in detail throughout **Section 1.4**.

Indeed, pathogens and cancer use glycosylation to shield sensitive functional surfaces from B cell recognition and downstream antibody attack (Hutchins et al., 2017; Rodrigues Mantuano et al., 2020; Vasconcelos-dos-Santos et al., 2015; Watanabe et al., 2020). In these instances, difficulty to raise self-glycan-reactive antibodies limits our ability to harness the immune response against pathogens and cancer, and these settings challenge the vaccine immunology field to develop innovative vaccination design strategies that selectively break glycan tolerance—a challenge that remains largely unmet.

The weak immunogenicity of self-glycans is a feature that has been exploited to develop creative immunogen designs. For example, both HIV-1 Env and IAV hemagglutanin HA have regions that are highly immunodominant, but where antibodies against these regions offer no/limited neutralisation breadth and potency; these epitope clusters, in effect, are hypothesised to detrimentally 'distract' the immune system from functional neutralizable surfaces (Crispin et al., 2018). To overcome this challenge, several pre-clinically tested Env-based immunogens include additional potential *N*-linked glyconsylation sites (PNGSs) in non-neutralizable patches, such that the expressed recombinant protein has epitope-disrupting and immunosilencing bulky glycans (Ringe et al., 2019). This is perhaps best illustrated by the Env-based RC1-4fill immunogen, where this approach was directly shown re-focus the immune response to promote activation of B cell clones that target the neutralisation-relevant regions (Escolano et al., 2019).

3.1.2 Conceptual framework for the glycan blind spot: the BCR–epitope recognition requirement

While there are many factors that contribute to the overall antibody response against a given epitope, a critical condition is that a relevant cognate B cell is represented in the pool: failure for B cells to engage a cognate epitope implies that no antibody response can be elicited. While the B cell repertoire is somewhat diverse (theoretical mouse naïve repertoire of ~3 x 10^6), it is not random (Briney et al., 2019; Rees, 2020). For example, is intuitive that the composition of the B cell repertoire would include BCR structures that are valuable in the recognition of pathogen-/cancer-relevant targets but are not self-reactive. To this end, the germline-encoded V-/D-/J-gene segments themselves must be subject to evolutionary selective pressures, and negative selection mechanisms that kill self-reactive B cell precursors (Nemazee, 2017). These and other functions play a critical role in shaping and skewing the B cell repertoire. The overall outcome is that the naïve repertoire is not diverse enough to recognise the entire set of possible epitopes.

It seems logical that a given self-glycan is likely to be an antigenic target that fails to mount antibody responses, largely due to the autoimmune consequences that may be imparted by broad glycan antibody reactivity. In corroboration of this hypothesis, immunisation with many self-glycans including GM1, GM2, GM3, GD2, GD3 and Le^Y fails to generate antibody responses (Bilodeau et al., 1995; Kudryashov et al., 1998; Livingston et al., 1989; Zhu et al., 2009), suggesting that these structures are unable to engage a relevant B BCR. This proposed *glycan*

blind spot is ultimately the fundamental vaccine design problem being addressed in this study.

3.1.3 SiaLac as a model glycan

A simple model TACA which this study focuses on is the trisaccharide, α-2,3-sialyllactose (also termed SiaLac), expressed on a ceramide tail to form the ganglioside GM3. The glycan component of this ganglioside will hereon in be referred to as GM3g. GM3g is of particular interest for its elevated expression on lung, breast, gastrointestinal, melanoma and neuroectodermal tumours (Blanco et al., 2013; Cavdarli et al., 2019; Lahera et al., 2014; Marquina et al., 1996; Shimizu et al., 2020; Tringali et al., 2014). There is also some *in vivo* and *in vitro* evidence that the mouse-raised anti-GM3 antibody clone 14F7 can facilitate Fc-mediated tumour killing, although the long-term outcomes and clinical tolerability of this clone is not described (Blanco et al., 2013; Carr et al., 2002; Lahera et al., 2014). However, direct immunisation with GM3 rather than passive immunisation with anti-GM3 antibody is ineffective due to its very weak immunogenicity, with experimental studies showing limited success in eliciting *de novo* anti-GM3 antibody responses, including both via administration of GM3 formulations, and GM3g analogues such as various protein carrier:GM3g immunogens (Bitton et al., 2002; Estevez et al., 1999; Guthmann et al., 2004; Livingston et al., 1989; Pan et al., 2005).

Specifically, early mouse immunisation studies using purified GM3 reported a weak antigen-specific IgM response. However, a more conservative interpretation of the data would indicate that the detected signal may not be

above the background/detection limit of the ELISA format used, and that additional controls are necessary to draw conclusions (Livingston et al., 1994, 1989). In the studies using purified GM3, there are confounding immunorecessiveness complications, including the absence of conventional T cell epitopes (peptidic), and thus any potential the B cell response is dependent on help provided via unconventional presentation pathways (such as the lipid-anchoring class I MHC CD1 superfamily) (Gentilini et al., 2016) and subsequent cognate T cell/NKT cell recognition (Lepore et al., 2018; Park et al., 2008).

To overcome this, conjugation of GM3g to carrier proteins such as KLH or bacterial cells has been tested via various linkers (Livingston et al., 1989). While this, in principle, offers a source of associated T cell help within the GM3g-containing antigenic complex to a hypothetical emergent B cell response, it is generally unclear from the serological analyses in these studies whether the antibody responses detected are truly GM3g-specific or an artifact of linker immunogenicity and subsequent cross-reactivity in the assays used. For example, the KLH-methoxyphenylacetate-GM3 antiserum reactivity against HSA-methoxyphenylacetyl-GM3 (Yu et al., 2011a) may be indicative of linker (that is, methoxyphenylacetyl) immunogenicity rather than the target glycan-of-interest. Collectively, there is insufficient evidence in the literature that artificial presentation of GM3g to the immune system promotes a specific glycan-engaging response. This remains an important and unmet goal in the cancer vaccine immunology field.

3.1.4 Rationale for a semi-synthetic glyco-hapten-based vaccination strategy

The failure of autologous glycan formulations (that is, native presentations of TACAs) to generate antibody responses, such as for GM3, implies the absence of a cognate naïve B cell in the repertoire. This has ultimately hindered the translational potential for the targeting of glycans in vaccine design, especially in the context of cancer and viral infections (Berois et al., 2022; Deimel et al., 2022). To dissect this challenge, we used protein editing methods to display GM3g in systematically varied non-native presentation modes by attachment to carrier protein lysine sidechains using diverse chemical linkers. This approach has two hypothetical advantages: 1) the artificial, non-native presentation of GM3g may engage B cell clonal classes that ganglioside GM3 cannot access, and 2) the fixing of the glycan to a carrier protein enables T cell help via the associated peptide, in contrast to the native ceramide-docked glycan presentation. These concepts form the basis of this study (**Fig 3.1**).

3.1.5 Aims

In this chapter, the main aims include to:

a) Chemically and immunologically characterise semi-synthetic GM3g-based antigens for immunisation.
b) Evaluate the immunogenicity of these semi-synthetic glycoconjugates in mice.
c) Determine the glycan specificity of the responses raised against the glycoconjugate and their reactivity with native presentations of GM3g.

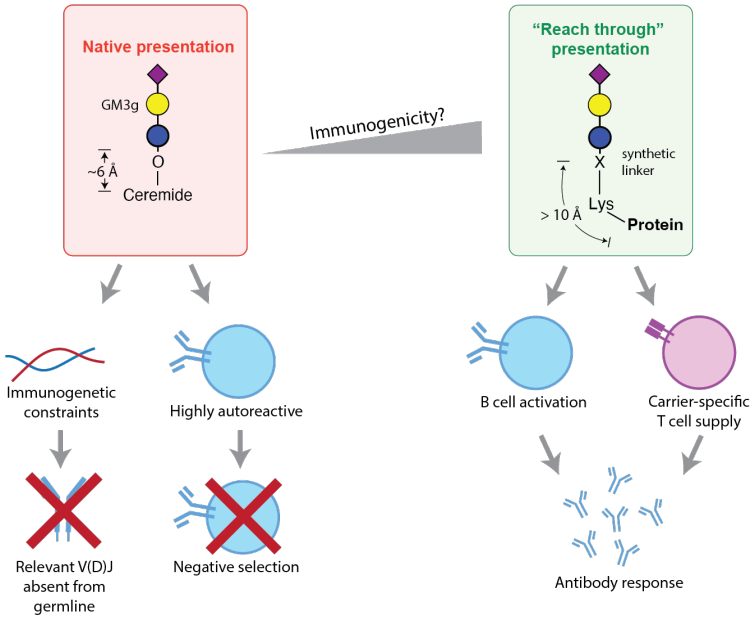


Figure 3.1: Immunological rationale for long orthogonal glycoconjugate vaccine design for classical immunorecessive/immunosilent carbohydrate antigens.

(Left) Native presentations of self-cabrohydrates, such as GM3g, are widely reported to be immunorecessive antigens. One possible explanation is that relevant B cells are absent from the naïve repertoire, including via selection against self-carbohydrate-binding motifs from the germline, and negative selective processes deleting/editing readily self-carbohydrate-reactive clones prior to entering the mature naïve B cell repertoire. (Right). Protein editing methods that artificially display self-glycan GM3g moieties via non-natural linker chemistries may bypass tolerance constraints, engaging B cell clonotypes that native glycan presentations may fail to engage. The conjugation to a carrier protein, in principle, offers Th supply to propagate a hypothetical B cell response.

3.2 Results

3.2.1. Immunogenicity of native GM3 on liposomes

GM3g on ceremide-docked GM3 is a short distance from the membrane (estimated at 6 Å based on native *O*-glycoside, three-bond *O*-hydroxymethyl spaced display from the head group), its native assembly surface (**Fig 3.2a**). Several studies have previously evaluated the immunogenicity of GM3 in a variety of formulations in mice, failing to show a convincing response (Livingston et al., 1994, 1989; Yu et al., 2011a). I first chose to interrogate the inherent immunogenicity in mice of natively-presented GM3g in the context of GM3.

Assembly of GM3-bearing liposomes (PG:PC:Chol:GM3 = 39:39:19:3) created an appropriate macromolecular assembly bearing multi-copy GM3g (**Fig 3.2b**). A control liposome without GM3 was tested as a negative control (PG:PC:Chol:GM3 = 40:40:20:0). Dr Erdinc Sezgin synthesised these liposomes. 6-week-old specific pathogen-free female BALB/c mice were immunised subcutaneously with 20 µg of liposome in formulation with TLR4-agonising MPLA adjuvant (Mata-Haro et al., 2007). Animals were immunised twice and bled periodically (**Fig 3.2c**).

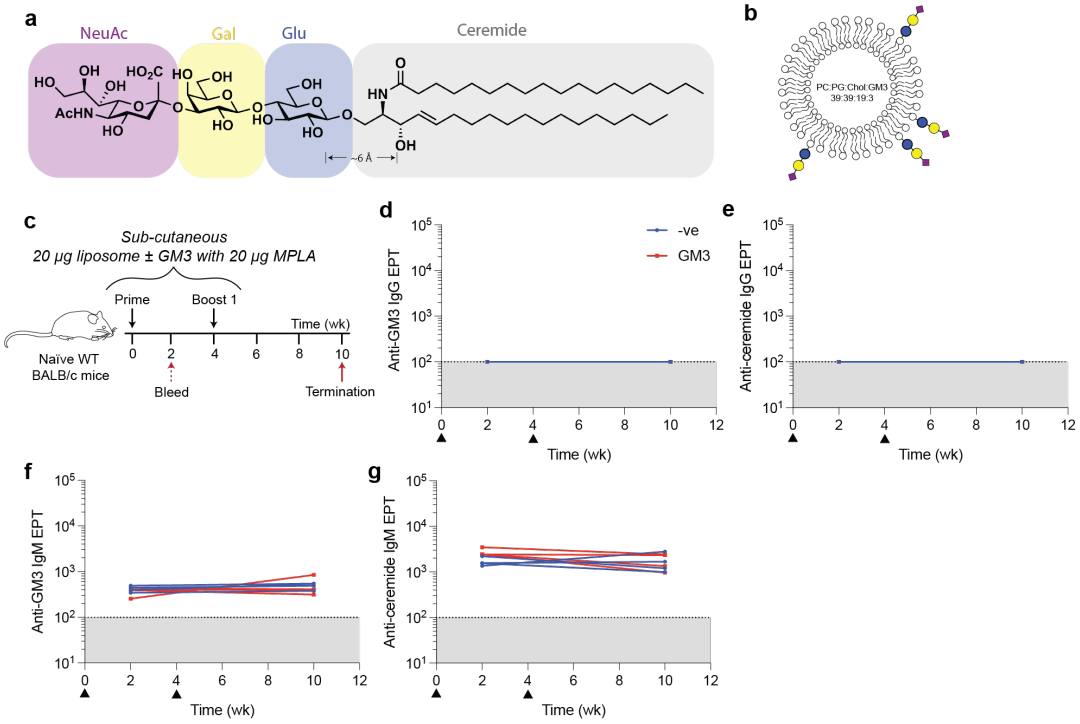


Figure 3.2: Immunogenicity of GM3 liposomes in mice.

(a) Lewis structure of ganglioside and TACA, GM3. **(b)** Graphical representation of GM3 liposome. **(c)** Both male and female 6-week-old BALB/c mice were twice immunized sub-cutaneously with 20 µg of GM3 liposomes or an empty PC:PG:Chol control liposome, along with 20 µg MPLA. Mice were bled periodically. Direct ELISA was performed to evaluate the IgG antibody endpoint titres against both **(d)** GM3 and **(e)** ceramide over time. **(f, g)** IgM titres were similarly measured. Dots represent individual mice, where connecting lines denote the same mouse over time. The grey segment about the y-axis denotes the assay detection limit.

No serum IgG titres were detected against GM3 or ceramide at either timepoint tested, suggesting that no/sub-detectable class-switched antibodies were elicited

against the ganglioside (**Fig 3.2d**). Similarly, no responses against ceramide were found (**Fig 3.2e**). Unsurprisingly given the presumed absence of Th cell help (classically provided by protein within the antigenic complex), no IgG was detected. Notably, there was modest IgM reactivity against GM3 that was equivalent in antiserum of mice immunised with both GM3-containing and control liposome ($P > 0.9999$, Mann-Whitney) (**Fig 3.2f**). Interestingly, there was IgM reactivity against ceramide in both animal groups (**Fig 3.2g**), EPTs against ceramide being greater compared to that against GM3 (median EPT of 2 156 vs 492). These findings are consistent with non-specific IgM binding and the absence of specific GM3g-binding antibodies, reflective of the low-affinity, high-avidity nature of IgM in ELISA formats (James and Tawfik, 2003; Padlan, 1994). A limitation was that pre-immune serum was not acquired for this cohort, and thus it is not clear whether this background serum reactivity to these targets developed post-prime or whether liposome-naïve serum displays the same non-specific reactivity profile.

3.2.2. Differing presentation of GM3g modulates B cell immunogenicity

I next explored an alternative non-native macromolecular assembly upon which to display GM3g. Orthogonal display on macromolecular protein scaffolds has the potential to mimic membrane-like multi-copy-GM3g display, yet allows control of copy-number density, site-specific conjugation and, critically, distance from the surface in terms of longer orthogonal display. The use of precise protein-editing methods via lysine (Lys)-selective (Lee et al., 1976) ‘tag-and-modify’ methods (Chalker et al., 2011) allows GM3g presentation in diverse protein scaffolds. These methods deviate from natural glycoproteins that attach via asparagine (*N*-

) or serine/threonine (*O*-) linkages (Loaeza-Reyes et al., 2021). Synthetic, protein-compatible methods were developed that accessed three presentation modes that were systematically varied for both *O*- *vs* S- glycoside display via amidine [–C(NH)NH–], amide [–C(O)NH–], or aminoalkyl [–$(CH_2)_2$NH–] linkers all at a similar, extended nine/ten-bond length, corresponding to ~11 Å from the peptide backbone (**Fig 3.3**). These long orthogonal glycoconjugates (LOGs) were designed to probe the relative immunogenicity of diverse non-native linkage motifs with features that modulate charge/pKa, hydrogen-bonding ability and hydrophobicity that are absent from the mammalian glycome. Notably, the development of these chemical pipelines has been developed in the laboratory of our collaborators in the Department of Chemistry, University of Oxford over many years and include contributions from Dr. Xiaochao, Xue, Dr Aziz Khan, Dr Guoxuan Sun, Dr Charles Gauthier, Dr Regis Saliba, Dr Karolis Leonavicus and Dr Leanne Minall. Synthetic glycoconjugation of protein products utilised throughout this project was carried out by Dr. Xiaochao Xue, Dr Aziz Khan and Dr Guoxuan Sun unless otherwise indicated.

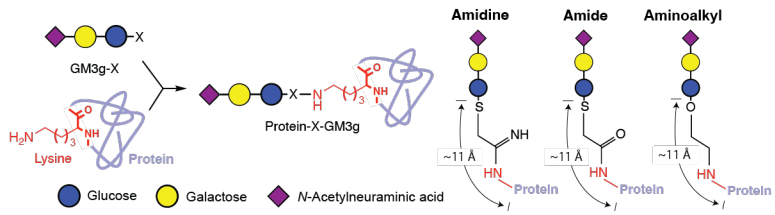


Figure 3.3: Overview of long orthogonal glycoconjugate synthesis.

The precise chemical modification systems used throughout this study involve taking a GM3g-linker construct that can be activated to become selectively reactive with primary amines of lysine sidechains. Resultant semi-synthetic glycoproteins are used as immunogens. Examples of linker chemistries exploited include short amidine, amide and aminoalkyl linkers that protrude ~11Å from the protein backbone.

Each linker strategy developed has a discrete chemical synthesis pipeline. As a representative example used throughout this study, synthesis of the [–amidine-

GM3g] glycoconjugate involves functionalising D-lactose with cyanide, subsequent sialylation and finally activation with imidate (2-imino-2-methoxyl-1-thiol, IME) (**Fig 3.4a**). This product can efficiently couple to primary amines of lysine sidechains of a given carrier protein via a short amidine linkage, an immunogen product that can be tested *in vivo* (**Fig 3.4b**).

First, we coupled the various GM3g glycoconjugates to the model carrier protein HEL (**Fig 3.4c**). HEL is a relatively small (~14 kDa, 129 aa) model antigen that has no native posttranslational modifications (PTMs) when expressed in mammalian cells and has 6 lysine residues. Following the optimising of the modification conditions, significant chemical characterisation was undertaken. For example, HEL-[–amidine-GM3g]$_6$ was run on an SDS-PAGE gel (**Fig 3.4d**). Coomassie gel stain implies successful modification, with a considerable band shift (~19 kDa) compared to the unmodified HEL counterpart. With the assistance of Dr Xue, we performed mass spectrometry on the modified products. For HEL-[–amidine-GM3g]$_6$, the addition of 6 GM3g-amidine glycoconjugates was observed on approximately 95% of HEL molecules (**Fig 3.4e**). This implies that the modification was highly efficient and produced a chemically homogenous product. Notably, while there are 6 lysine residues, the *N*-terminus also has a primary amine group (thus the total number of primary amines is 7). LCMS/MS was not conducted to evaluate whether the terminus was being modified. However, for the purposes of using the glycoconjugate as an antigen, this was not deemed critical for our application.

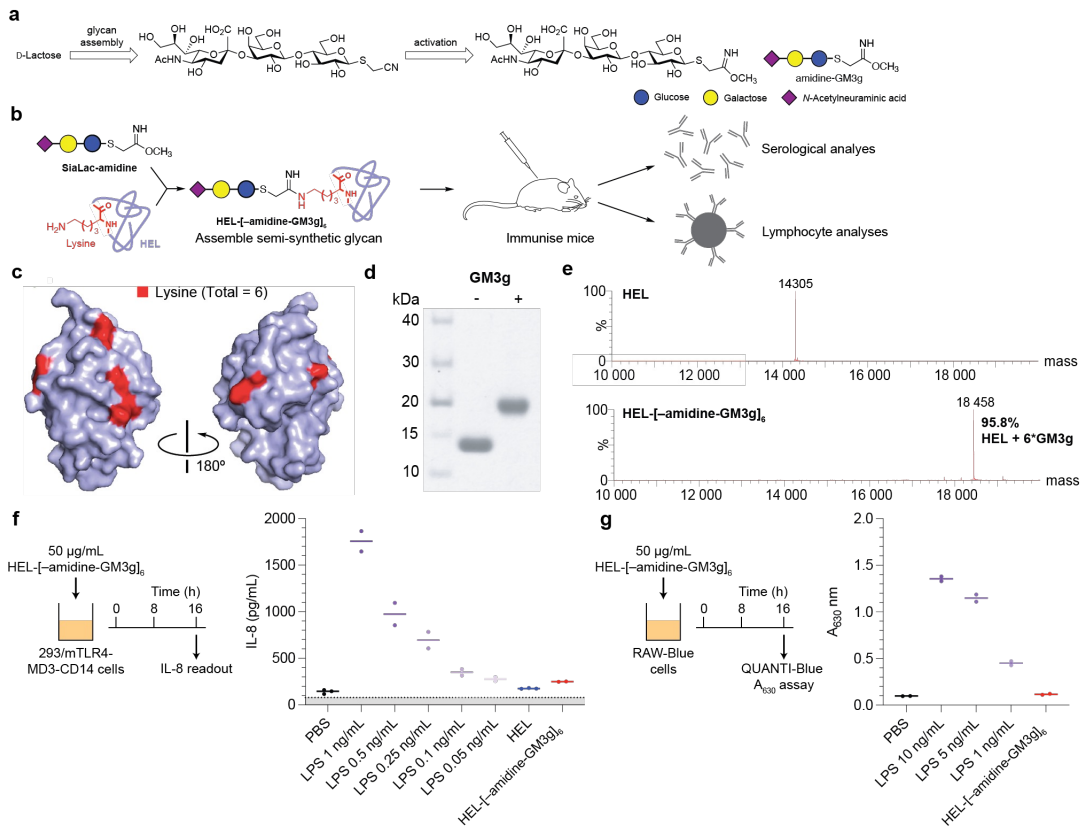


Figure 3.4: Chemical and immunological characterisation of HEL-[–amidine-GM3g]$_6$ preparations.

(a) Synthesis of the amidine-GM3g construct involves functionalising D-lactose with CN and subsequent sialylation. **(b)** The semi-synthetic glycoprotein is then assembled to a carrier protein (in this case, HEL). Mice are immunised and subsequent immune characterisation is performed. **(c)** Surface model of HEL (PDB: 193L). Red denotes lysine sidechains. **(d)** SDS-PAGE was ran on both unmodified and GM3g-modified HEL. **(e)** Mass spectra of HEL-[–amidine-GM3g]$_6$. **(f)** LPS contamination of immnuogens was evaluated using 293/mTLR4-MD3-CD14 cells, which reports TLR4 contamination via IL-8 production. Cells were pre-incubated with 50 µg/mL immunogens or LPS controls and IL-8 was measured via a capture ELISA. **(g)** Broader PAMP/DAMP contamination was tested using RAW-Blue cells, similarly incubating cells with immunogen or LPS controls.

Following chemical characterisation, immunogen preparations were tested for endotoxin contamination. Preparations where the LPS concentration was < 0.05 ng/mL were deemed endotoxin free. LPS contamination was assessed using a highly sensitive TLR4 reporter cell line, 293/mTLR4-MD3-CD14, to which 50 µg/mL HEL-[–amidine-GM3g]$_6$ was added for 16 h and the concentration of IL-8 in supernatant was compared to an LPS control (**Fig 3.4f**). Neither HEL nor HEL-[–amidine-GM3g]$_6$ was found to have an LPS concentration above the set

cut-off. We further screened the cells using the RAW Blue cell line, which is sensitive to a wider array of endotoxins, expressing all TLRs (except TLR5) and with a reporter that is a proxy for NF-κB and AP-1 (Zhang et al., 2015). The immunogen preparations were similarly cultured, and a QUANTI-Blue assay was performed, according to the manufacturer's instructions. The A_{630} nm readout for HEL-[–amidine-GM3g]$_6$ was below the RAW Blue detection limit of 1 ng/mL LPS (**Fig 3.4g**). These chemical and immunological quality control checks were similarly conducted for both the amide and aminoalkyl glycoconjugates (data not shown).

Mice were immunised with the three different HEL-[–X-GM3g]$_6$ LOG antigens in MPLA adjuvant (**Fig 3.5a**). Serum IgG titres against each glycoconjugate were assayed by ELISA against a corresponding LOG constructed from an unrelated protein carrier, such as gp120-[–amidine-GM3g]$_{16}$ (**Fig 3.5b**). This assaying format is similar to that used to test classical hapten-specific antibody responses (Green et al., 1968; Herzenberg and Tokuhisa, 1982). Antibody responses against the autologous LOG were considered a proxy for overall immunogenicity, whereas responses against the heterologous LOG indicated glycan cross-reactivity. High IgG titres were detected against autologous LOGs in antisera from all LOG-immunized mice. Antisera from HEL-[amidine-GM3g]$_6$ and HEL-[amide-GM3g]$_6$ were mutually cross-reactive with each other, reflective of only a small atomic variation (O versus NH) in display (**Fig 3.3**). However, whilst antisera from the aminoalkyl LOG was cross-reactive with both amidine- and amide- LOGs, the converse was not the case: amidine- and amide-LOG antisera were not reactive with the aminoalkyl LOG ($P = 0.0052$, for all; Kruskal-

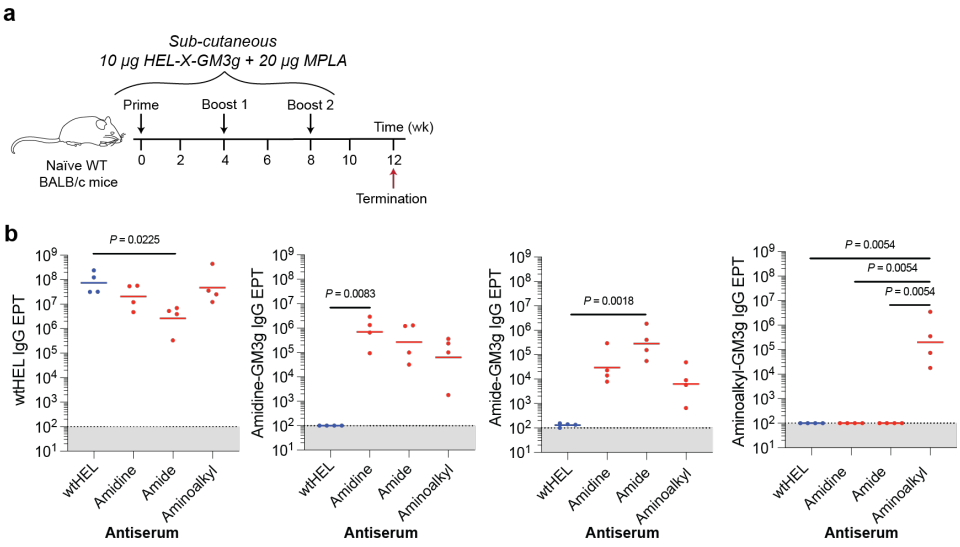


Figure 3.5: Immunogenicity and cross-reactivity of GM3g-based LOGs in mice.

(a) Female 6-week-old BALB/c mice were immunised three times subcutaneously with 10 µg of GM3g LOG-modified HEL with 20 µg MPLA. **(b)** Antisera from the terminal IgG EPTs were evaluated against the HEL protein-backbone, as well as each respective glycoconjugate. LOG-specific antibodies were assayed by screening antibody reactivity against a LOG-modified unrelated protein carrier, such as gp120-[–amidine-GM3g]$_{16}$. Dots represent titres from individual mice and the bar denotes the mean EPT. Data were compared pairwise via Kruskal-Wallis test. The grey represents the assay detection limit.

Wallis test). Antibody titres against the protein carrier HEL revealed high-titre IgG in all immunisation groups, indicating that all methods used to achieve LOG glycoconjugation largely preserved native HEL epitopes. Since the amidine-based LOG provided the highest homologous anti-GM3g titres, we chose to prioritise its investigation going forward.

3.2.3. Evaluation of HEL-[–amidine-GM3g]$_6$ antigenicity and intrinsic immunogenicity of the GM3g modification

Given the anchoring of GM3g to lysine residues, I anticipated that the resultant modified protein, HEL-[–amidine-GM3g]$_6$, would show significant disruption to native protein epitopes. For example, structures of HEL-raised mAbs D1.3, HyHEL-5/HyHEL-9 and HyHEL-10 either contact lysine sidechains or make

contacts proximate to them (**Fig 3.6a,b**) (Cohen et al., 1996; Kenett et al., 1987; Kondo et al., 1999). Antibody binding against both HEL and HEL-[–amidine-GM3g]$_6$ were compared via ELISA (**Fig 3.6c–f**). The data reveal a significant drop in binding for all mAbs except HyHEL10. This was surprising, given that the HyHEL-10 epitope overlaps with K116, indicating the antibody's ability to tolerate the incorporation of the large glycomodification in that position.

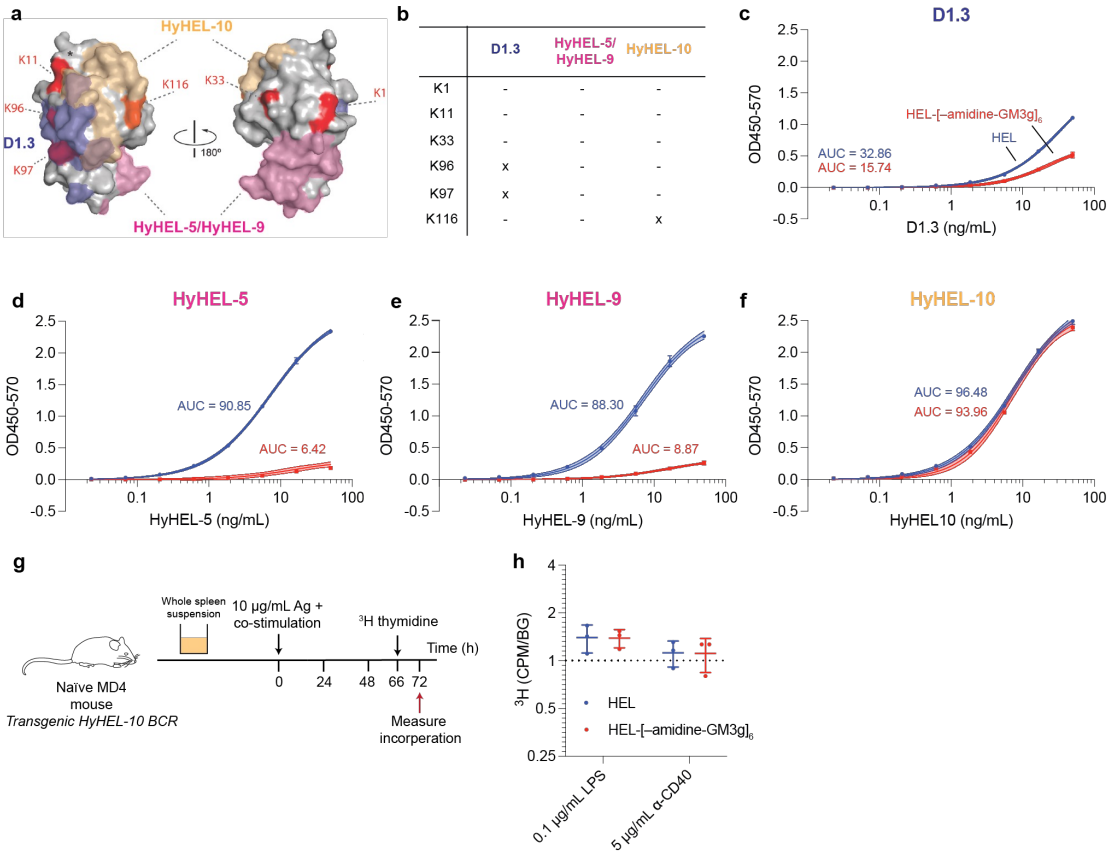


Figure 3.6: Antigenicity of HEL-[–amidine-GM3g]$_6$ and the intrinsic immunogenicity of the LOG.

(a) Surface model of HEL (PDB: 193L) with reported monoclonal antibody epitopes imposed. (b) Lysine overlap with antibody epitopes. **(c–f)** Relative monoclonal antibody binding was assessed via direct ELISA, comparing binding of HEL- and HEL-[–amidine-GM3g]$_6$-coated plates. Logistic functions represent the regression fit (bold) flanked by the 95% confidence interval (light). **(g)** Whole splenocytes from MD4 mice were seeded and stimulated *in vitro* with immunogen and co-stimulatory agents. The culture was later spiked with ^{3}H-thymidine. **(f)** Incorporation of ^{3}H-thymidine was measured and normalized to background. Relative counts per million were presented on a $\log_2$ scale.

It is well-understood that carbohydrates can have either immunopotentiating or immunoinhibitory functions; for example, CD22, a widely expressed lectin which recognises some specific presentations of sialic acid to blunt B cell proliferation (Müller and Nitschke, 2014), or mannose-binding lectins, which modulate proliferation and activation in a variety of immune cell types (Jack et al., 2005; Linehan et al., 2000; Mu et al., 2020). We endeavoured to test whether the GM3g modification had any activation effects on B cells. To crudely test this *in vitro*, we assessed splenocyte proliferation in an MD4 mouse, which has a transgenic HyHEL-10 BCR (kindly gifted by Dr Tal Arnon)(Goodnow et al., 1988). We chose this transgenic animal, since HEL-[–amidine-GM3g]$_6$ retains HyHEL-10 binding integrity. We generated whole spleen suspensions and stimulated them with antigen in the presence of either LPS or anti-CD40, which mimic innate- and adaptive-like co-stimulatory signals, respectively. ^{3}H-thymidine incorporation was measured following 72 h antigen exposure (**Fig 3.6g**). Data were normalised to a non-stimulated control and compared between the treatment conditions. Stimulation with HEL-[–amidine-GM3g]$_6$ was neither significantly better nor worse than HEL alone, irrespective of the co-stimulatory conditions. Although crude, these data are consistent with the GM3g modification failing to impart an intrinsic immunogenic effect.

3.2.4. Evaluation of the glycoconjugate-specific antibody response

To evaluate whether covalent linkage to the carrier protein was required for LOG immunogenicity, we compared immunisation with either LOG HEL-[amidine-GM3g]$_6$ or instead with wtHEL that had been non-covalently mixed with stoichiometrically equivalent (n = 6) amounts of a corresponding, non-conjugated

('free') side-chain-only amidine-GM3g [H_3C–C(NH)NH-GM3g] (**Fig 3.7a,b**). To test GM3g-specific antibodies, cross-reactive IgG titres were measured via ELISA against gp120-[amidine-GM3g]$_{16}$. The HEL-based LOG antiserum had substantial titres of amidine-GM3g-reactive IgG even in the absence of exogenous adjuvant (EPT = 1,430). However, no LOG-specific responses were detected in the groups immunised with mixed, unconjugated HEL-plus-amidine-GM3g ($P < 0.0001$, Tukey's post-hoc) (**Fig 3.7c**). These data imply that LOG immunogenicity is contingent on conjugation of the glycan to a protein carrier to facilitate B cell activation and isotype switching via T cell help, which is an anticipated outcome reflected in classical hapten-carrier biology (Green et al., 1968).

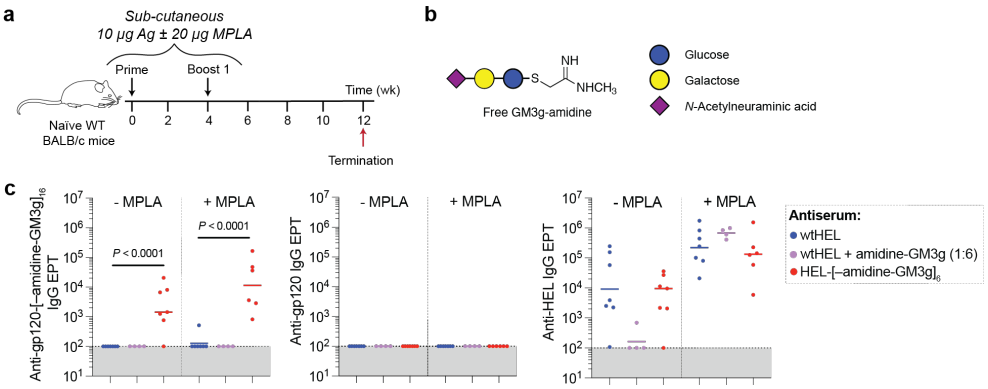


Figure 3.7: Evaluating LOG–protein anchoring in HEL-[–amidine-GM3g]$_6$ immunogenicity.

(a) Female 6-week-old BALB/c mice were immunised subcutaneously with 10 µg of antigen ± 20 µg MPLA. **(b)** Representation of the reductionist, free LOG mimic, methylated GM3g-amidine. Serum IgG EPTs were measured at the terminal timepoint. **(c)** Direct ELISAs were conducted with terminal serum to evaluate the LOG- and backbone-specific antibody titres. Dots represent titres from individual mice and the bar denotes the median. Data are pooled from two independent experiments. Groups were lognormally compared pairwise via a Tukey's post-hoc analysis following a Shapiro–Wilk test.

3.2.5. Precise LOG editing maps the role of glycan site and glycan display stoichiometry in modulating immunogenicity

Given the robust immunogenicity of LOGs, we next set out to better understand the molecular basis for glycan moiety immunogenicity by mapping the functional roles of both glycan site and copy number in precise structure-activity relationships. Importantly, our 'tag-and-modify' LOG construction methods (Chalker et al., 2011) allowed ready LOG 'editing' simply via corresponding control of 'tag' site and copy number.

Having demonstrated the apparent immunodominance of the GM3g-amidine glycoconjugate, I titrated the effects of both the number and spacing of these modifications and assayed the antibody response. To this end, a set of HEL mutants was designed to titrate the effects of LOG number and spatial density by substituting native lysine for arginine (**Fig 3.8a,b**). The rationale for arginine substitution was that it is chemically the most similar with respect to both size and chemical properties (that is, basic), and thus these substitutions were least likely to result in protein misfolding. This allowed for the select removal of modifiable primary amines, and a platform to titrate the role of numbers and spacing in the antibody response.

These mutants were modified with GM3g and run on an SDS-PAGE gel. The results confirmed efficient modification of the proteins (**Fig 3.8c**). Interestingly, modified HEL-[–amidine-GM3g]$_{3p}$ (proximate) ran lower than HEL-[–amidine-GM3g]$_{3d}$ (distal). I hypothesised that this was a product of the proximate GM3g modifications on HEL-[–amidine-GM3g]$_{3d}$, which may effectively form a negative

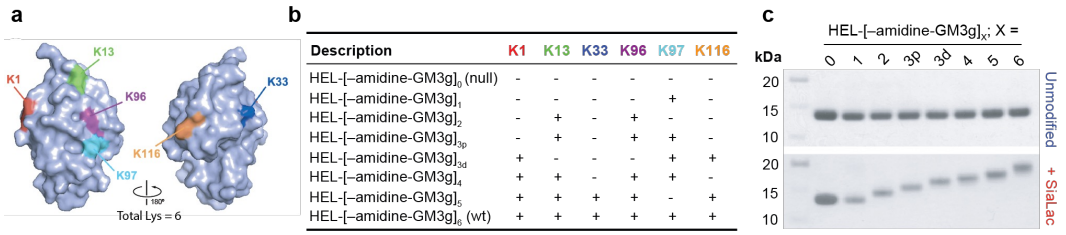


Figure 3.8: Design and modification of HEL mutants.

(a,b) A set of HEL mutants were designed to titrate the impact of LOG copy number and spacing on immunogenicity. '+' denotes presence of the WT lysine sidechain and '-' denotes substitution of arginine. **(c)** Mutants were recombinantly expressed and purified. SDS-PAGE was ran with both unmodified and GM3g-amidine-modified proteins.

pole as a product of the sialic acid, resulting in the band running lower than that of HEL-[–amidine-GM3g]$_{3d}$. MS data ultimately corroborated (**Fig 3.9**). MS analysis revealed efficient modification of all mutants. Interestingly, there was some evidence of N-terminal modification in some of the constructs. For example, HEL-[–amidine-GM3g]$_0$ (where all lysine residues were substituted to arginine), there was an estimated 12% of HEL molecules with a GM3g modification, suggesting that the primary amine at the termini was being partially modified.

Next, animals were immunised with these constructs, according to the immunisation schedule previously described (**Fig 3.7a**). First, IgG endpoint titres were titrated against gp120-[amidine-GM3g]$_{16}$ to determine the glycoconjugate-specific response (**Fig 3.10a**). I had hypothesised that the antibody titre against the glycoconjugate would be proportional to the number of glycoconjugates; for example, that there would effectively be an "avidity boost" imparted by the valency of the carrier protein, making it more likely that the glycoconjugate would crosslink and activate a cognate BCR. Surprisingly, the data instead revealed a "bell curve" with respect to the glycan occupancy in the glycoconjugate-specific

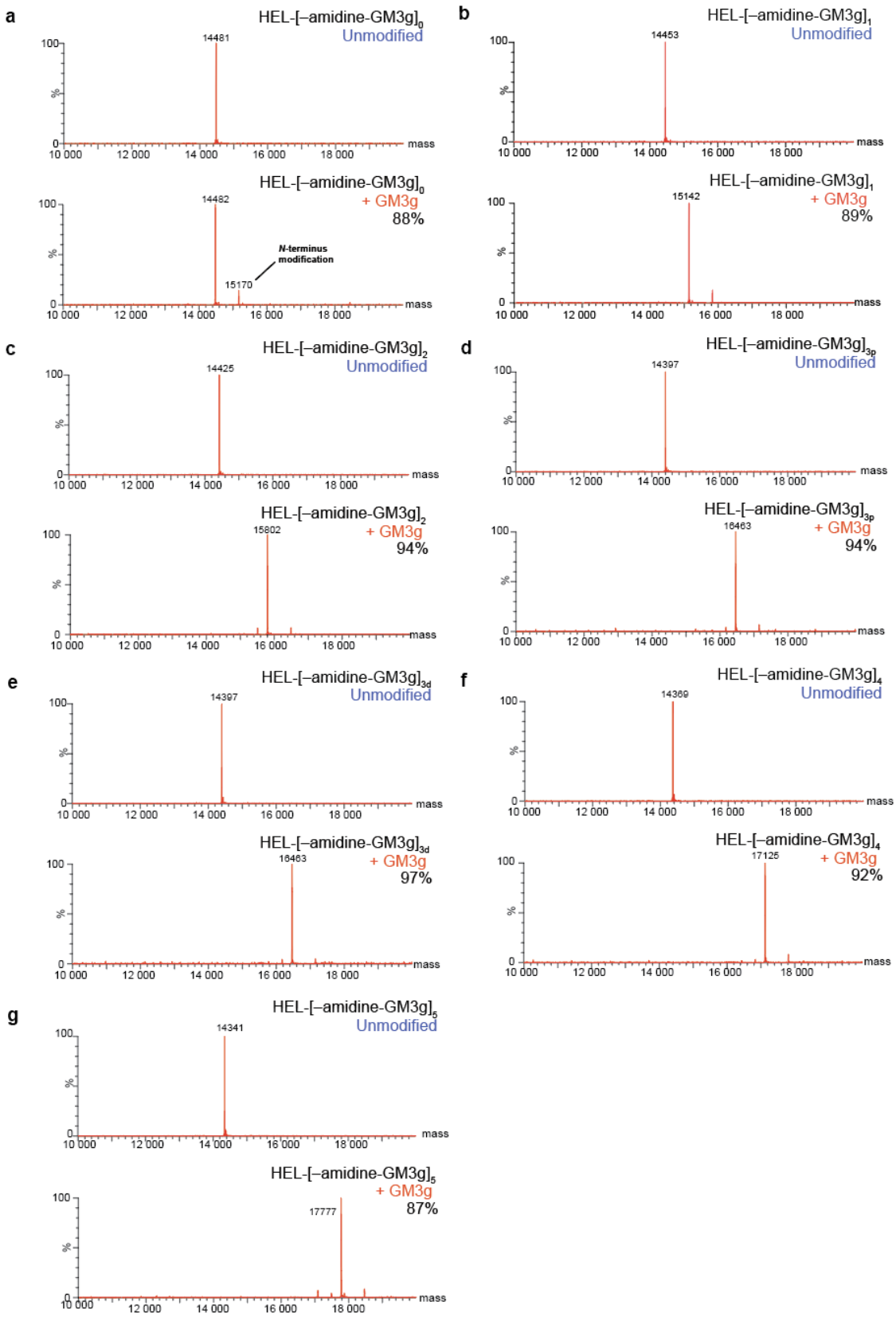


Figure 3.9: Mass spectral analysis of HEL mutants.

(a–g) Mass spectrometry was performed on HEL mutants modified with GM3g and the proportion of fully occupied protein was estimated, as indicated.

endpoint titre with respect to the number of modifications. For example, in the absence of exogenous adjuvant, the optimal number of modifications to deliver the peak endpoint titre was 2–4 (IgG EPT of ~10^6), while 5–6 modifications resulted in 113-fold decrease in the titre, on average ($P < 0.0001$; Mann-Whitney test). These trends were reflected in the adjuvanted groups, although the decrease in titre only occurred in the HEL-[–amidine-GM3g]$_6$ group and not the HEL-[–amidine-GM3g]$_6$ group, potentially suggesting a compensatory feature imparted by MPLA. These trends were similarly reflected in the IgM endpoint titres against the glycoconjugate (**Fig 3.10b**), although these data were more dispersed and thus underpowered compared with the IgG data. By contrast, the antibody response against the protein backbone was found to be an adjuvant rather than modification effect ($P < 0.0001$; Mann-Whitney test) (**Fig 3.10c**).

I next aimed to identify a possible mechanistic underpinning for the relationship between glycan occupancy of the immunogen used and the resultant antibody titre. First, given that glycan occupancy was toggled by mutagenesis, I evaluated whether the protein backbones had differing Th cell immunogenicity profiles—for example, determine whether the arginine substitutions in select HEL mutants introduced immunodominant peptides that drove increased T cell help.

I generated single cell splenocyte suspensions from animals immunised with various modified HEL mutant and adjuvant (which likely bolstered the size of the Th pool, allowing for easier and more sensitive measurement of the Th pool size). Splenocytes were re-stimulated *in vitro* with autologous HEL mutants and cytokine secretion and thymidine proliferation assays were completed (**Fig**

3.11a). No evidence of antigen-induced production of either IL-4 or IL-2 was observed for the groups tested ($P \geq 0.05$, for all; Wilcoxon test) (**Fig3.11b,c**). Similarly, no significant changes in the proliferation indices were observed ($P \geq 0.05$; Kruskal-Wallis test) (**Fig 3.11d**). These data are consistent with no substantial variation in Th cell induction between the different HEL mutants.

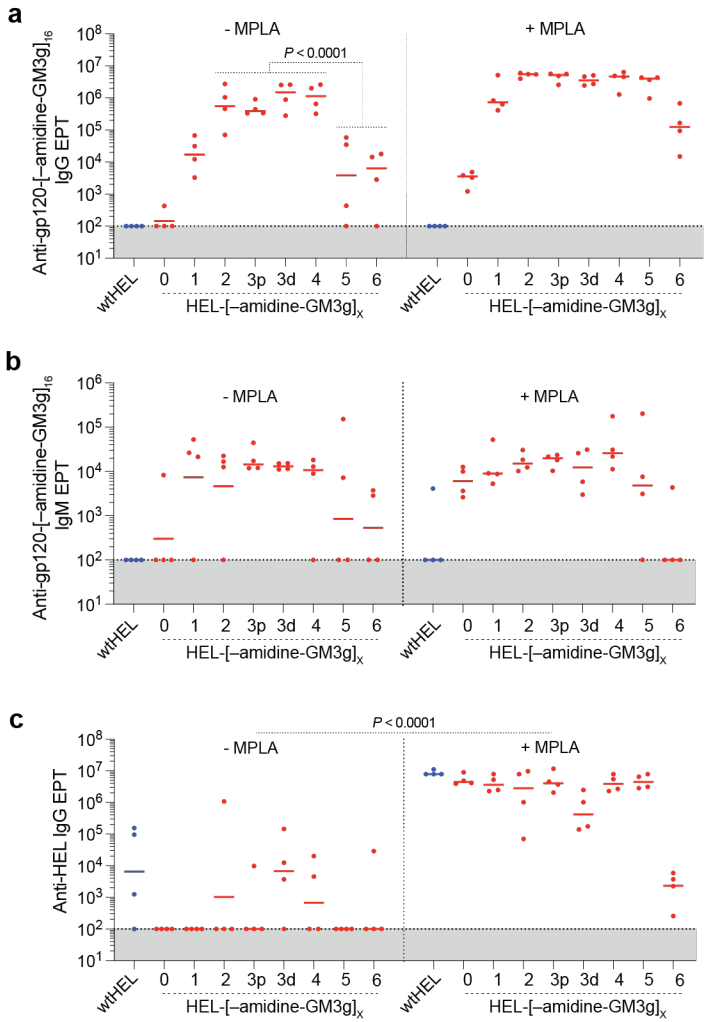


Figure 3.10: Immunogenicity of GM3g-modified HEL mutants.

Female 6-week-old BALB/c mice were immunised twice (0 & 4 weeks) with 10 µg of GM3g-amidine-modified HEL mutant (red) or the wild-type, unmodified control (blue) and bled periodically. Serum **(a)** IgG EPTs were evaluated 8-weeks post-boost and **(b)** IgM endpoint titres were measured 2-weeks post-prime against gp120-[–amidine-GM3g]$_{16}$. Data were clustered into low (0–1), medium (2–4) and high (5–6) LOG modifications and compared pairwise via Kruskal-Wallis tests. **(c)** Terminal IgG EPTs were similarly evaluated against the HEL protein backbone. The adjuvant effect was evaluated via two-way ANOVA. Dots represent data from individual mice (n = 4) and bars represent the geometric mean.

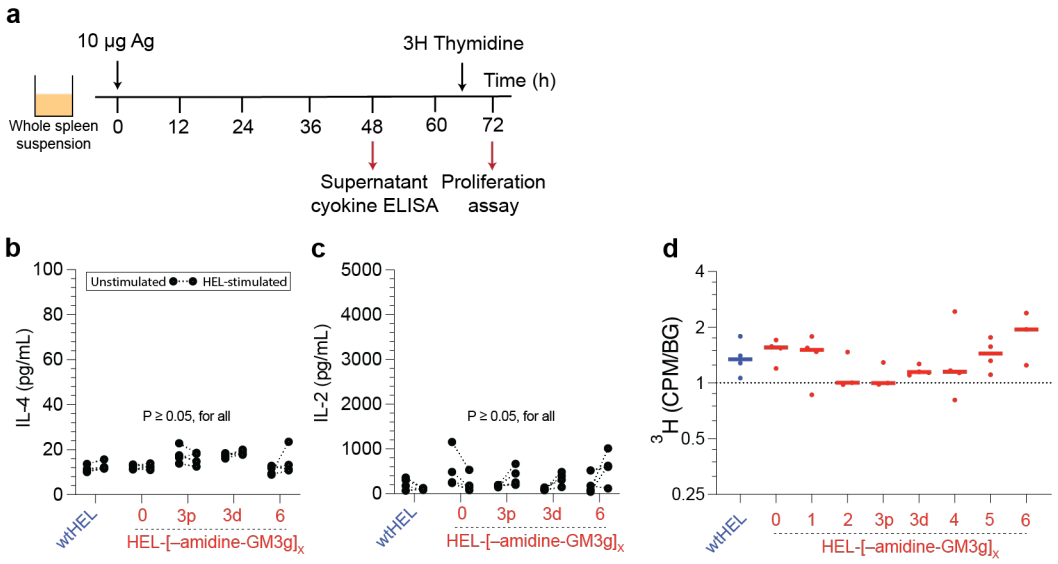


Figure 3.11: T cell immunogenicity of LOG-modified HEL mutants.

(a) Splenocytes were harvested from mice immunised with LOG-modified HEL mutants, according to the immunisation schedule outlined previously. Splenocytes were re-stimulated *in vitro* with autologous antigen and cytokine production and bulk cell proliferation was assayed. Cytokine ELISAs were performed for **(b)** IL-4 and **(c)** IL-2. Data were evaluated by paired Wilcoxon test with Bonferroni correction. **(d)** Background-normalised ^{3}H-thymidine incorporation was contrasted between immunisation conditions.

Given that neither antigen-induced cytokine secretion nor proliferation via thymidine incorporation could be detected, we conducted ICS to determine whether an antigen-specific Th cell population could be quantified via flow cytometry. Splenocytes were stimulated *in vitro* with autologous antigen and cytokine secretory machinery was blocked with brefeldin A (**Fig 12a**) (Vicetti Miguel et al., 2012). IFN-γ production was measured in CD4^{+} T cells (**Fig 12b–d**). There was no evidence of an antigen-specific IFN-γ^{+} population in any of the groups. These data further indicate that HEL is an especially T-immunorecessive antigen in BALB/c mice, an outcome that has similarly been shown in C57BL/6 mice (Grewal et al., 1995). However, the presence of significant IgG endpoint titres implies that a T cell population may have provided help. This suggested

that perhaps the measures to evaluate the Th population were not sensitive enough, or that T cell memory had not established.

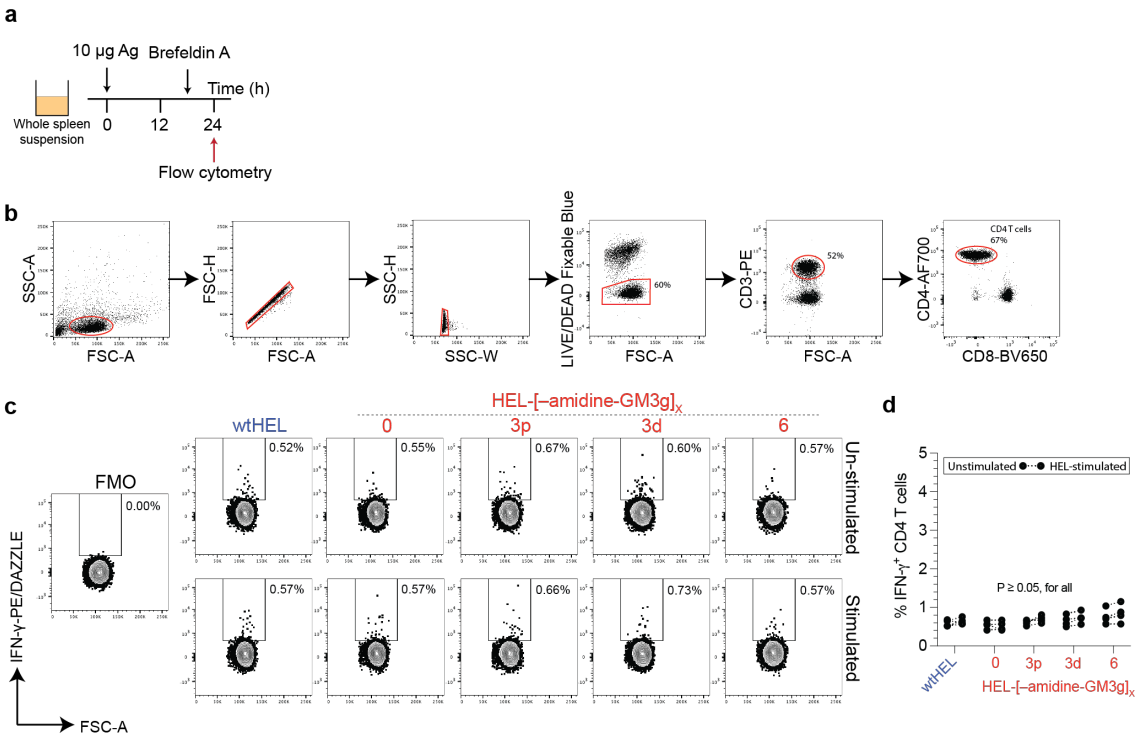


Figure 3.12: Intracellular cytokine staining from HEL mutant-immunised splenocytes.

(a) Whole murine splenocytes were stimulated *in vitro* with 10 µg/mL autologous antigen. Brefeldin A was added in the final 6 h and flow cytometric analysis was performed at 24 h. **(b)** Flow cytometry gating strategy for the pre-gating of live CD4⁺ T cells. **(c,d)** IFN-γ expression on CD4⁺ T cells. Data were evaluated by paired Wilcoxon test with Bonferroni correction.

These findings motivated further investigation as to whether the phenomenon of glycan loading was truly T cell independent. Hence, we took wild-type HEL and altered the GM3g modification conditions to deliberately make the process inefficient by reducing the reaction time such that the median glycan occupancy was 3.7 (**Fig 3.13a**), within the range previously found to elicit high glycoconjugate-specific titres (**Fig 3.10a**). Animals were immunised using the previous schedule (**Fig 3.7a**) and IgG endpoint titres against the glycoconjugate were determined (**Fig 3.13b**). The data similarly show that sugar loading fewer glycoconjugates had a higher endpoint titre (median of ~$10^{5.5}$) compared with

fully occupied HEL (~10^3). This further substantiates the previously reported trend with the HEL mutants, and strongly implies that the differential IgG titres were not a function of the arginine modification altering T-immunodominance.

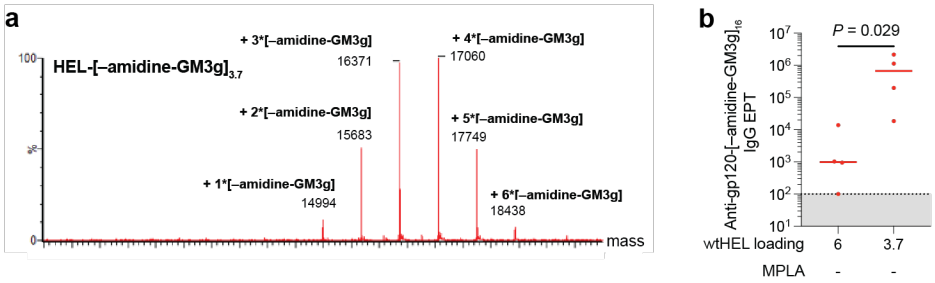


Figure 3.13: Impacts of partial LOG loading on wtHEL on immunogenicity.

(a) Mass spectra of partially modified wtHEL, HEL-[–amidine-GM3g]$_{3.7}$. (b) Mice were immunised under the prime-boost schedule used previously for HEL mutants, and serum terminal IgG EPTs were measure against gp120-[–amidine-GM3g]$_{16}$. Data were compared via a Mann-Whitney test.

3.2.6. Evaluating the immunogenicity of gp120-[–amidine-GM3g]$_{16}$

Having shown that HEL-[–amidine-GM3g]$_6$ elicited antibodies against the glycoconjugate, I next investigated whether alternative protein backbones could deliver a similar outcome. I selected an alternative model carrier protein, a gp120-based construct, which has 26 lysine residues. This carrier protein was similarly modified with the GM3g-amidine glycoconjugate. The modification was evaluated via SDS-PAGE, which revealed a considerable band shift (**Fig 3.14a**); this was conducted both for whole gp120 (which is natively *N*-glycosylated) and PNGase F-treated samples (which removes *N*-linked glycans) to allow for better resolution of the mass gained by the GM3g modification. Notably, gp120 cannot be resolved by mass spectrometry due to the substantial heterogeneity imparted by the N-linked glycans (which cannot be entirely removed by PNGase F), and thus GM3g conjugation efficiency could not be determined via mass spectrometry. However, after application of the same benign editing methods for LOG generation, we estimated via electrophoretic densitometry analysis that the GM3g loading

delivered a mean of approximately 16 modifications. We further conducted (with the assistance of Dr Scarlett Harris) an ELISA that measures free (unmodified) primary amines. The data revealed successful loss of primary amines on gp120-[–amidine-GM3g]$_{16}$ compared with unmodified gp120, indicating successful glycomodification (**Fig 3.14b**).

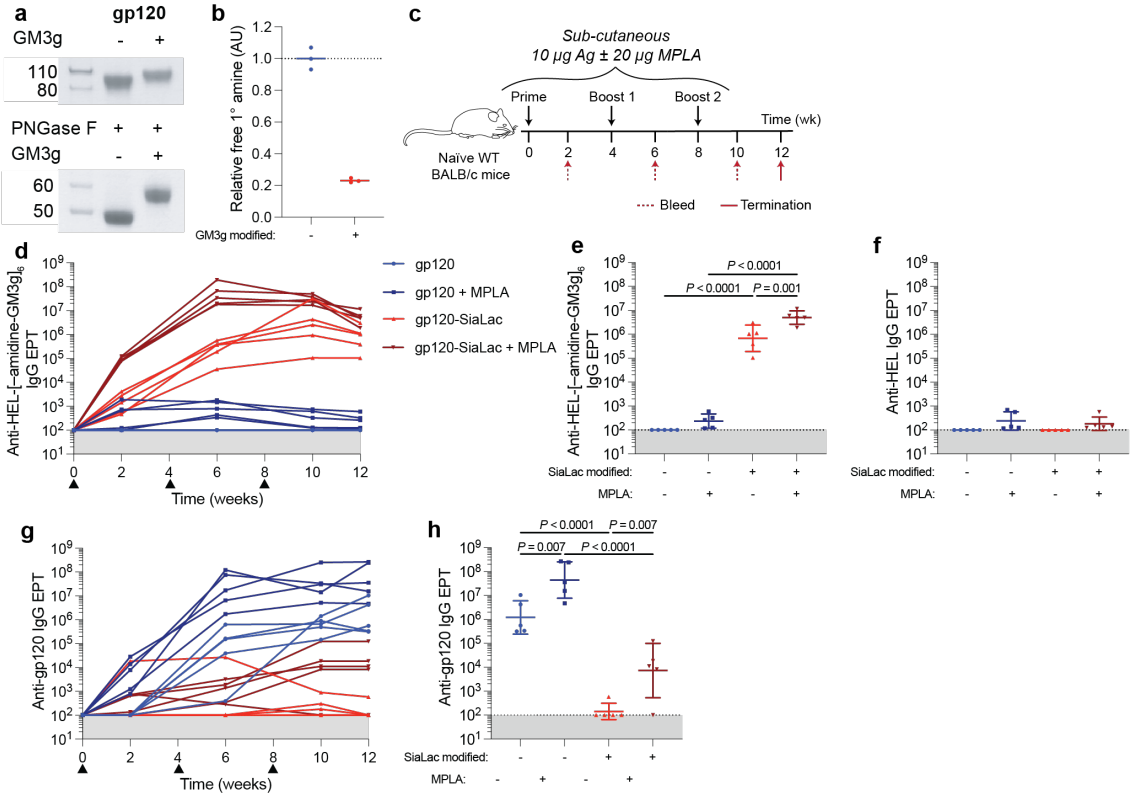


Figure 3.14: Immunogenicity of gp120-[–amidine-GM3g]$_{16}$.

(a) SDS-PAGE of gp120 pre- and post-modification with the [–amidine-GM3g] glycoconjugate. These samples were also ran following PNGaseF treatment (bottom). **(b)** Free amine ELISA of gp120 following glyco-modification. **(c)** Immunisation protocol. **(d)** LOG-specific antibody titres were monitored over time by performing direct ELISAs against HEL-[–amidine-GM3g]$_6$. **(e)** Terminal LOG-specific endpoint titres. (f) Terminal IgG EPTs against HEL. **(g,h)** IgG EPTs against the unmodified protein backbone, gp120. Dots represent biological replicates. Data were compared with Tukey's post-hoc analysis.

Animals were immunised three times and bled periodically throughout the timecourse (**Fig 3.14c**). HEL-[–amidine-GM3g]$_6$-reactive IgG was measured over the timecourse as an indicator of the glycoconjugate-specific antibody response

(**Fig 3.14d**). The results revealed substantial induction of glycoconjugate-specific antibody responses. Animals immunised with gp120-[–amidine-GM3g]$_{16}$ and MPLA elicited a median glycoconjguate-specific IgG endpoint titre of ~10^5 post-prime, plateauing at > $10^{7.5}$ following the first boost. Those that received gp120-[–amidine-GM3g]$_{16}$ and no adjuvant had an endpoint titre of ~10^3 post-prime and ~10^5 post-first-boost. At the terminal timepoint, the MPLA-adjuvanted animals had a glycoconjugate-specific response that was approximately one order of magnitude greater than the unadjuvanted group ($P = 0.01$; Tukey's post-hoc comparison test) (**Fig 3.14e**). Interestingly, the antibody titres in the adjuvanted group appear to reach an asymptote after the first boost, with an additional shot at 8 weeks failing to further bolster the antibody titres (**Fig 3.14d**); this might reflect an antibody feedback/epitope masking mechanism that is an emergent quality of B cell responses that is mechanistically still being fully understood (McNamara et al., 2020; Schaefer-Babajew et al., 2023). Unmodified gp120 antiserum displayed no/background reactivity with HEL-[–amidine-GM3g]$_6$. Both gp120 and gp120-SiaLac antisera similarly displayed no/background reactivity with HEL.

Antibody titres were similarly evaluated against the protein backbone, gp120. Gp120-[–amidine-GM3g]$_{16}$ antisera revealed reduced backbone-reactive IgG EPTs compared with animals that had received unmodified gp120—this was irrespective of adjuvant status ($P < 0.0001$, for both; Tukey's post-hoc comparison test) (**Fig 3.14g,h**). These data imply that GM3g modification disrupted the native surface protein epitopes. This phenomenon was not observed for HEL (**Fig 3.7e**).

Having establish the serological profile of animals immunised with gp120-SiaLac, I next evaluated the memory T cell responses. ICS was conducted as previously described (**Fig 3.12a**), restimulating splenocytes with gp120, gp120-[–amidine-GM3g]$_{16}$ or HEL-[–amidine-GM3g]$_{6}$. This was to interrogate whether the semi-synthetic glycans potentially hindered T cell recall, for example, by affecting antigen processing pathways. An antigen-specific T cell response was detected in animals that had received either gp120 or gp120-[–amidine-GM3g]$_{16}$ *and* MPLA, as indicated by the substantial induction of IFN-γ expression (**Fig 3.15a–c**). Interestingly, in adjuvanted animal groups, both the percentage and absolute number of recalled IFN-γ^{+} CD4 T cells was equivalent whether restimulation was conducted with either gp120 or gp120-[–amidine-GM3g]$_{16}$. ($P > 0.9999$ for all pairwise, Tukey's posthoc). The failure of HEL-[–amidine-GM3g]$_{6}$ to elicit IFN-γ production is unsurprising and reflects the peptide-centric antigenicity model of classical T cell responses. Notably, the interaction effect between GM3g modification and restimulation was insignificant ($P = 0.423$, two-way ANOVA), which crudely reflects that immunisation with GM3 modified vs unmodified gp120 does not affect the size or recallability of the Th cell response.

In addition to ICS, supernatant was harvested from splenocytes re-simulated for 72 h. This allowed for the measurement of a broader panel of cytokines beyond that investigated via ICS. The measured IFN-γ, IL-2 and IL-4 titres reflected the same trends as that observed for ICS (**Fig 3.15d–f**). All three cytokines were

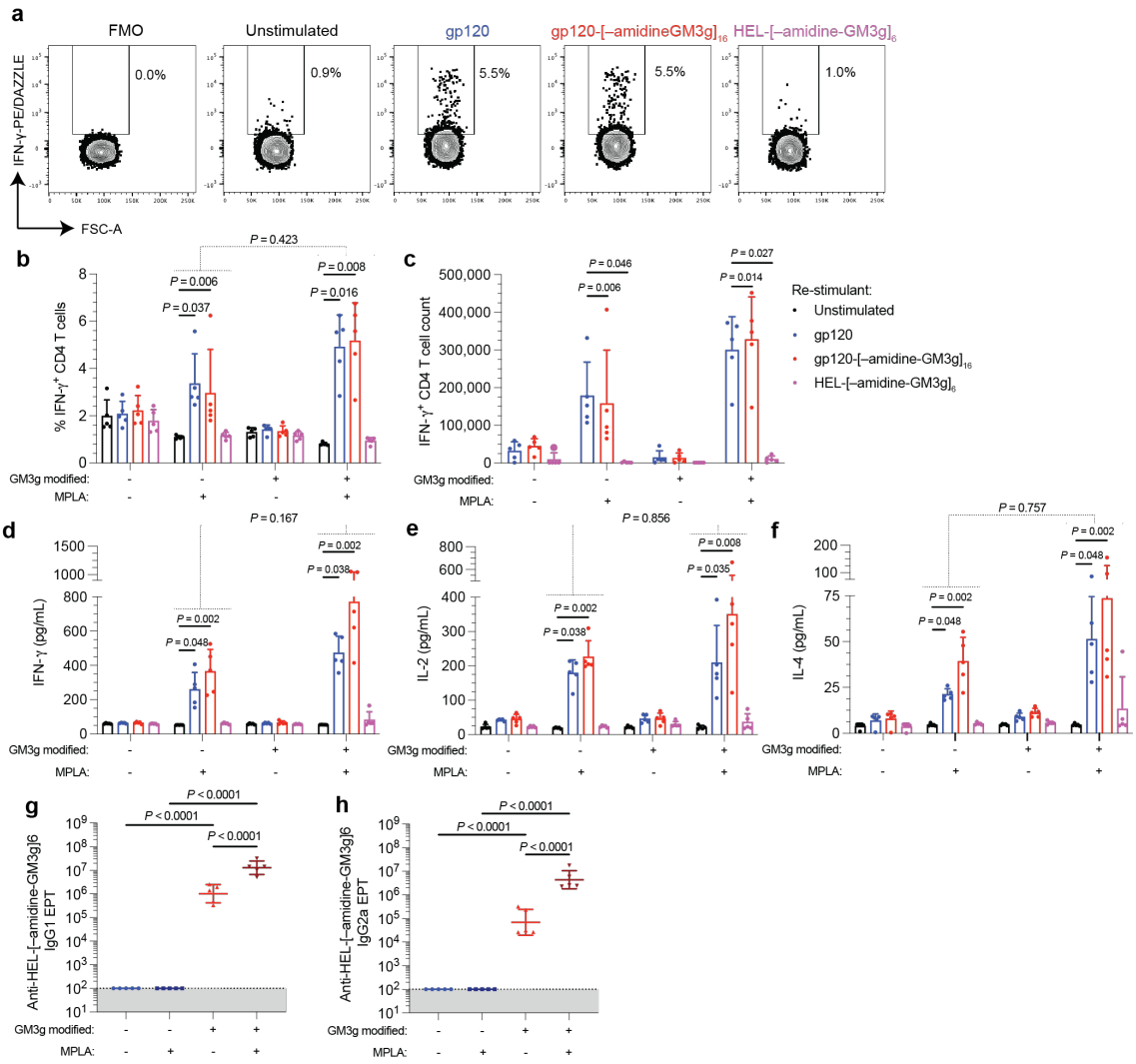


Figure 3.15: T cell responses against gp120-[–amidine-GM3g]$_{16}$.

Splenocytes from gp120-[–amidine-GM3g]$_{16}$-immunised mice were stimulated *in vitro* and Th recall responses were evaluated via ICS or cytokine ELISA, as outlined previously. **(a–c)** IFN-γ expression on CD4$^+$ T cells following 24 h re-stimulation. Cytokine ELISAs were performed on supernatant harvested from 72 h re-stimulated splenocytes, measuring **(d)** IFN-γ , **(e)** IL-2 and **(f)** IL-4. **(g, h)** IgG subclass EPTs were measuring in the terminal timepoint serum. Dots represent data from a single animal. These data were compared via Tukey's post-hoc test, with interaction effects between groups (dotted line) determined via two-way ANOVA.

produced in splenocytes derived from mice that received adjuvanted formulations. We further investigated the effects of the Th on IgG subclass representation. Both glycoconjugate-specific IgG1 and IgG2a EPTs were measured at the terminal timepoint (**Fig 3.15g,h**). The titres for IgG1 were higher than that of IgG2a; in the adjuvanted group, EPTs of 10^7 vs $10^{6.2}$, respectively.

This might reflect the Th2 skewing typical of BALB/c mice (although EPT is an arbitrary readout)(Fukushima et al., 2006a). Titres of both tested IgG subclasses increased with adjuvantation ($P > 0.0001$, for both).

3.2.7. Effects of sex and background on glycoconjugate-specific responses

It is well-documented that sex is a significant biological variable that affects many aspects of the immune system (Klein and Flanagan, 2016). Experiments reported up to this point were conducted using female BALB/c mice, which are known to exaggerate their immune response relative to male mice under various infection and vaccination settings (Alonaizan et al., 2021; Belisle and Strausser, 1981; Fornefett et al., 2018). Therefore, I compared the immunogenicity of both HEL-[–amidine-GM3g]$_6$ in male and female mice. Animals were thrice immunised with 10 µg HEL-[–amidine-GM3g]$_6$ at 4-week intervals ± 20 µg MPLA. The data reveal at the terminal timepoint that the glycoconjugate-specific IgG titres in both sexes were equivalent ($P = 0.9999$, Tukey's posthoc) (**Fig 3.16a,b**). Titres against the HEL protein backbone reflected the glycoconjugate-specific trends (**Fig 3.16c,d**). These data collectively imply that both males and females are similarly responsive to the [–amidine-GM3g] glycoconjugate with respect to IgG EPTs.

BALB/c mice have divergent immunological characteristics compared to other murine backgrounds, including C57BL/6. In general, C57BL.6 mice have a strong Th1 immune response and more readily produces IFN-γ^+ and other Th1-characteristic cytokines, while BALB/c offers a more Th2 phenotype, producing substantial IL-4/IL-13. Indeed, BALB/c mice tend to elaborate a stronger humoral response compared with C57BL/6—this was a model initially established in the

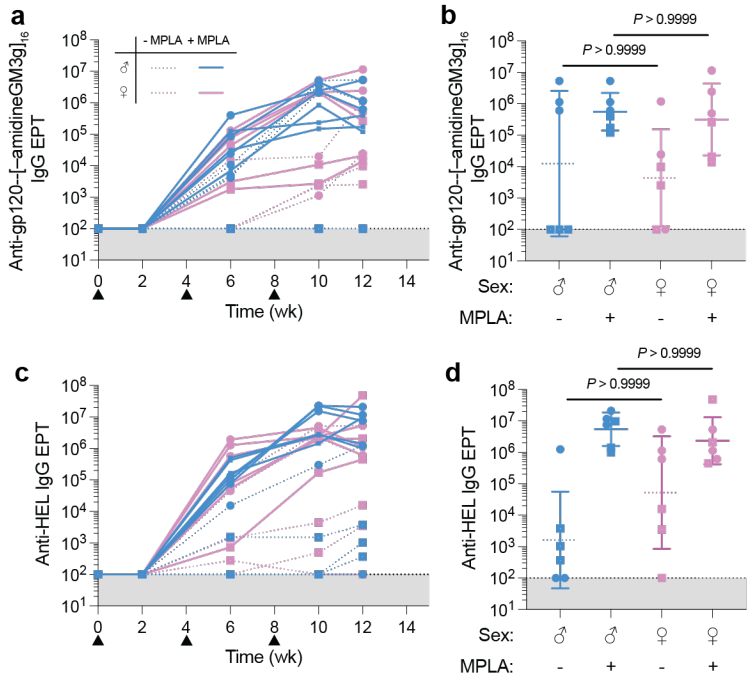


Figure 3.16: Sex and the impact of LOG immunogenicity.

Male and female 6-week-old BALB/c mice were immunised (0, 4 and 8 weeks) with 10 μg HEL-[–amidine-GM3g]$_6$ ± 20 μg MPLA. Mice were bled periodically. IgG EPTs were measured against gp120-[–amidine-GM3g]$_{16}$ **(a)** across the timecourse and **(b)** at the terminal (week 12) timepoint. **(c, d)** Similarly, titres against the HEL protein backbone was measured. Dots represent data from one mouse. Data are pooled from two independent experiments. Data were compared via Kruskal-Wallis test.

context of Leishmania infections (Alexander et al., 1999). Mouse backgrounds also have different germline-encoded T and B cell V- D- and J- gene segments (Bleul et al., 2021; Ferreira et al., 2018; Fukushima et al., 2006b; Mikocziova et al., 2021). For example, C57BL/6 and BALB/c mice are derived from different subspecies of house mouse and thus have highly divergent naïve B cell repertoires, with only five *IGHV* alleles common to both strains, and with BALB/c mice having 164 functional *IGHV* genes and C57BL/6 mice having only 99 (Collins et al., 2015).

Therefore, we also compared the responsiveness of C57BL/6 mice against the LOG-based immunisations with that of BALB/c. Mice were immunised with

gp120-[–amidine-GM3g]$_{16}$ three times with or without MPLA and bled periodically (**Fig 3.17a**). The data reveal that both C57BL/6 and BALB/c mice responded to the glycoconjugate. Notably, in the absence of adjuvant, the post-prime LOG-specific IgG EPTs were undetectable in 3/3 C57BL/6 mice, while unadjuvanted BALB/c mice had detectable serum IgG post-prime (median EPT of approximately 10^4). Following two subsequent boosts, EPTs in both mouse backgrounds were approximately 10^7 irrespective of adjuvantation. These data suggest that the C57BL/6 mice also have LOG-cognate BCRs represented in the naïve repertoire.

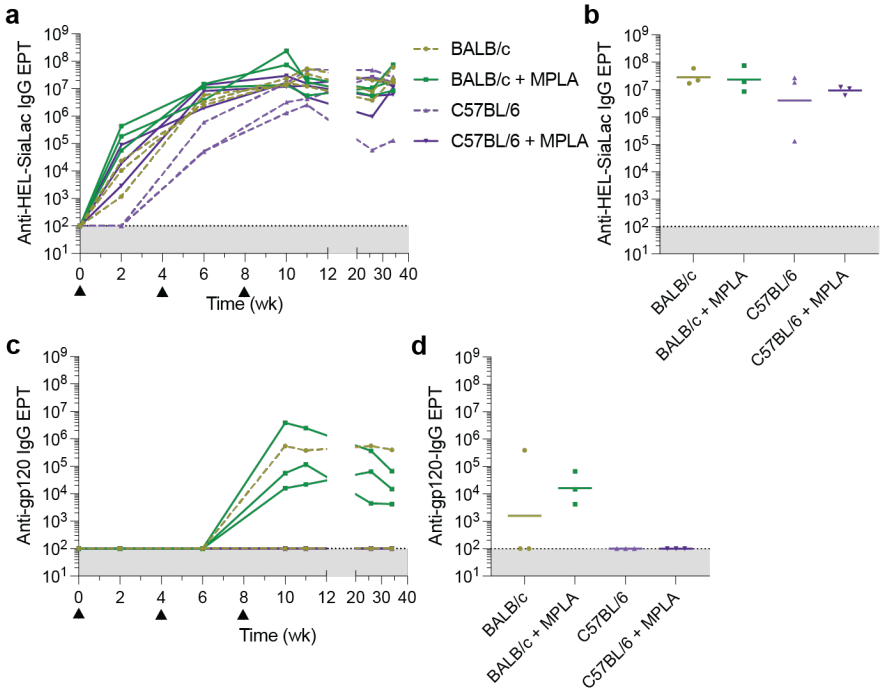


Figure 3.17: Impact of mouse background on LOG-specific antibody responses.

Co-housed BALB/c and C57BL/6 mice were immunised with 10 µg gp120-[–amidine-GM3g]$_{16}$ ± 20 µg MPLA at weeks 0, 4 and 8. Serum IgG EPTs were measured against the glycoconjugate, measuring titres against HEL-[–amidine-GM3g]$_6$ **(a)** across the timecourse and **(b)** at the terminal timepoint. **(c, d)** Titres were similarly measured against the gp120 protein backbone. Dots represent data from a single animal.

As shown in previous gp120-[–amidine-GM3g]16 immunisation experiments, LOG modification represses the response against the protein backbone (presumably by disrupting native protein surfaces) (**Fig 3.14g,h**). The C57BL/6

mice displayed no detectable reactivity with the backbone at the terminal timepoint, while modest IgG EPTs were detected in all adjuvanted BALB/c mice (EPT of approximately 10^4). These data are collectively correspondent with the established advantage of BALB/c mice in mounting humoral responses.

3.2.8. Immunogenicity of [–amidine-GD3] LOGs

Having demonstrated that the amidine-based display of GM3g results in a potent glycoconjugate-specific antibody response, we next aimed to show whether these antibody responses could be similarly elicited against alternative glycans—whether the immunogenicity-bolstering effect of the amidine-based LOG modular formats might be generalisable with other self-glycans. We selected the di-sialyllactose, the glycan of ganlioside TACA, GD3, and modified carrier proteins using the same amidine-based linker chemistry (**Fig 3.18a**)—this was conducted by Dr Guoxuan Sun. First, I screened gp120-[–amidine-GM3g]$_{16}$-raised antiserum against HEL-[–amidine-GD3g]$_6$ via ELISA; this was to ensure that antibodies raised against GM3g were not cross-reactive with GD3g, and thus implying that, if [–amidine-GD3g] happened to be immunogenic in mice, that discrete, sugar-specific clonal populations were being raised. That is, if [–amidine-GM3g]-reactive antibodies were cross-reactive with [–amidine-GD3], then it implies that immunisation with a GD3-based LOG would engage shared B cell clonotypes. Antisera was pooled from 5 mice and screened against HEL-[–amidine-GD3g]$_6$. The data reveal that gp120-[–amidine-GM3g]$_{16}$ antiserum failed to cross-react (**Fig 3.18b**).

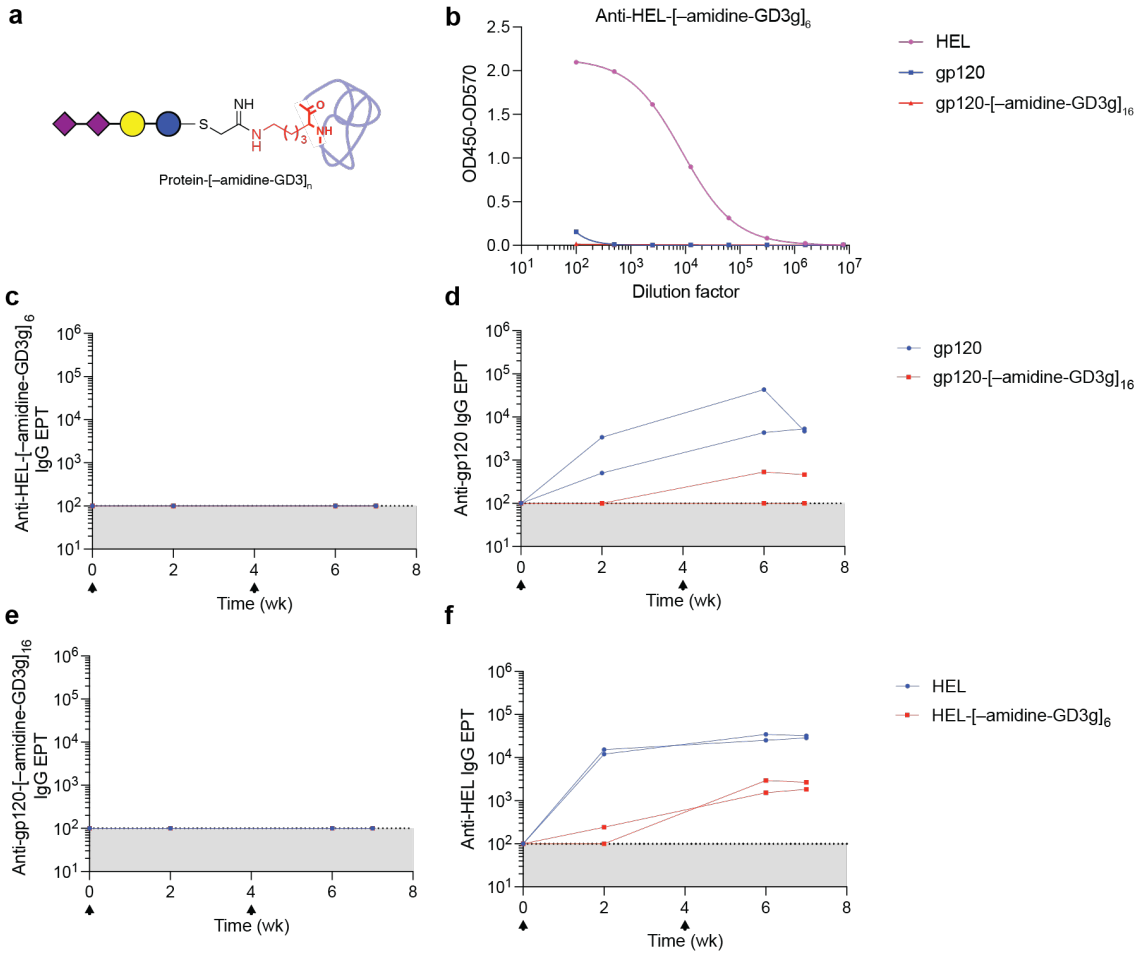


Figure 3.18: Immunogenicity of [–amidine-GD3]-based LOGs.

(a) Model representation of the amidine-based LOG of di-sialyllactose/GD3g. **(b)** Cross-reactivity ELISA; direct ELISA was performed against HEL-[–amidine-GD3g]$_6$, using [–amidine-GM3g]-raised antisera. 6-week-old BALB/c mice were immunised subcutaneously at weeks 0 and 4 with 10 µg of antigen and 20 µg MPLA. **(c, d)** Serum IgG from animals immunised with gp120-[–amidine-GD3]$_{16}$ was screened against both the glycoconjugate and protein backbone. **(e, f)** Antisera raised against HEL-[–amidine-GD3]$_6$ was similarly screened via ELISA. Dots represent data from a single mouse and lines connect titres from the same mouse at different timepoints.

Next, we performed a small pilot experiment to gauge the immunogenicity of [–amidine-GD3g] in mice. Animals were primed and boosted with gp120-[–amidine-GD3g]$_{16}$ and MPLA and serum titres against both the glycoconjguate and protein backbone were monitored over time. No IgG titres were detected against the glycoconjguate over the time course (**Fig 3.18c**). Antibody titres against the protein backbone appear to be blunted by the glycoconjugate, with

mice immunised with gp120 conjugates failing to elicit a detectable backbone response post-prime and only 1/2 having a detectable but titre post-boost (IgG EPT = 527)—this is unlike animals immunised with unmodified gp120, which reached a titre of ~10^4 post-boost (**Fig 3.18d**). This backbone-masking outcome was observed in mice immunised with gp120-[–amidine-GM3g]$_{16}$ (**Fig 3.14g,h**). Further, no glycoconjugate-specific response in HEL-[–amidine-GD3g]$_{16}$ antiserum were detected (**Fig 3.18e,f**). Given that this alternative GD3g glycan was not shown to be immunogenic in this particular LOG format, it was not pursued further.

3.2.9. Evaluating the glycan specificity and linker-dependency of the anti-LOG serological response

'Professional' carbohydrate binding proteins, termed lectins, exhibit low-affinity interactions with their ligands and have relatively poor specificity, binding broad families of carbohydrates. We aimed to establish the reactivity profile of [–amidine-GM3g]-raised antiserum. To this end, we deployed a high-throughout printed glycan array developed by Dr Ryan McBride and Prof James Paulson. This array has a library of 226 mammalian glycans fixed to a plate via a short amide linker (**Fig 3.19a**) (Blixt et al., 2004). When serum is incubated in the wells, antibody binding can subsequently be detected with a fluorescent secondary antibody and MFI can be used as a proxy for serum glycan reactivity. This array was performed using both gp120 and gp120-[–amidine-GM3g]$_{16}$. Surprisingly, cross-reactivity was seen only to very subtly altered glycan features (i.e. α-2,3-sialyllactose and its close counterparts). Specifically, in order of preferential binding: α-2,3 → α-2,6 → monohydroxylated *N*-acetyle-Neu → *N*-glycolyl-Neu or

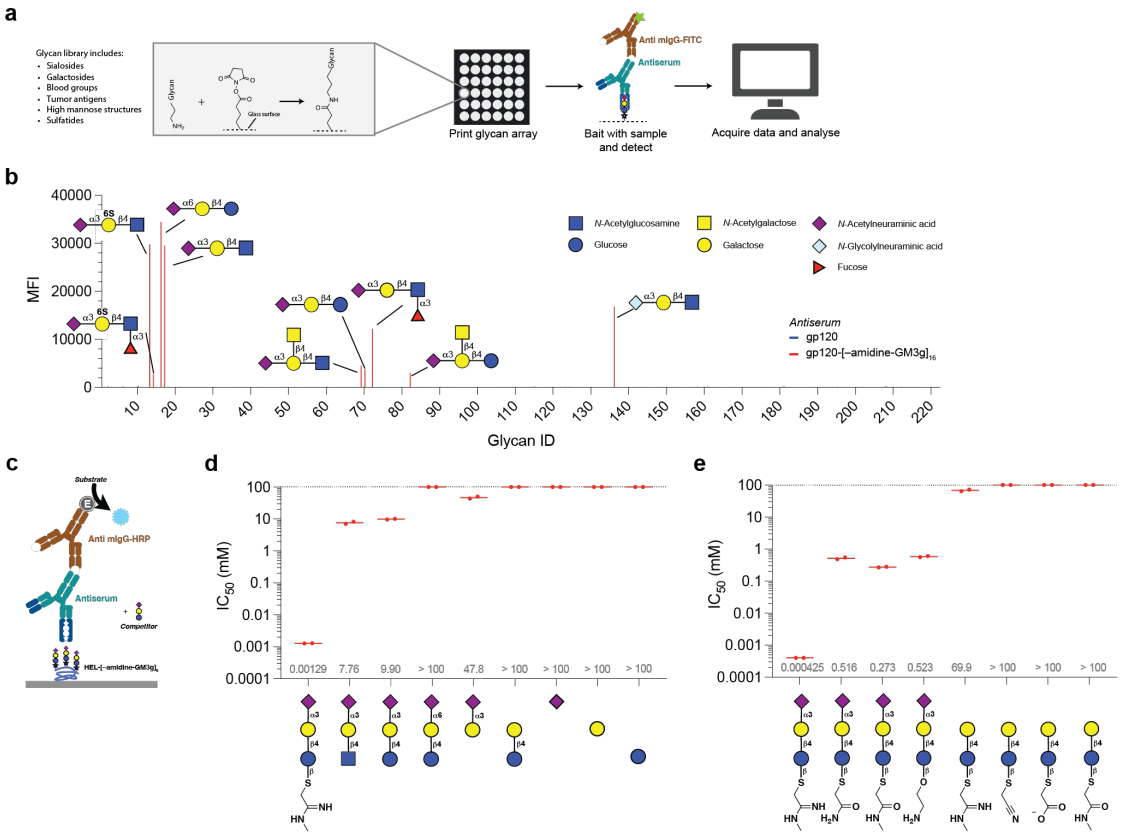


Figure 3.19: Glycan specificity and linker dependencies of [–amidine-GM3g]-raised antiserum.

(a) Design and experimental pipeline of mammalian glycan array. **(b)** Antiserum from gp120 and gp120-[–amidine-GM3g]$_{16}$-immunized mice was screened for reactivity against a mammalian-derived glycan library. **(c)** A competition ELISA format was developed evaluate the relative contribution of link LOG component binding of polyclonal serum. **(d, e)** Soluble glycans and sugar-linker combinations were competed against gp120-[–amidine-GM3g]$_{16}$-raised antiserum for HEL-[–amidine-GM3g]6 binding.

OH-2-Glc → NHAc-2-GalNAc. This striking result implies that the antibody response elicited via the LOG has narrow glycan engagement, demonstrating high specificity to the autologous glycan.

Having shown the narrow glycan specificity imparted by the amidine-based LOG display of GM3g, I next aimed to understand the contribution of the linker in glycoconjugate recognition—that is, whether the antibodies strictly engage the glycan component or whether the antibodies engage a glycan-linker composite epitope. Dr Xiaochao Xue and I developed a soluble competition ELISA format

wherein serum binding of the autologous glycoconjugate could be competed against soluble ligands (**Fig 3.19c**). In this assay, serum from gp120-[–amidine-GM3g]$_{16}$-immunised mice was used. Consistent with the glycan panel analysis, GM3g antiserum bound essentially equivalently to its OH-2-Glc- and NHAc-2-GalNAc variants (IC_{50} of 7.76 mM and 9.90 mM, respectively) (**Fig 3.19d**). Two truncated variants further mapped GM3g specificity and saccharidic moiety dependency: the disaccharide variant SiaGal competed relatively weakly (47.8 mM), implying some role for the 'inner' reducing-end interactions, whereas GM3g disaccharide lacking 'tip' non-reducing-end Sia showed no detectable competition, implying the presence of more critical contacts made with the terminal sialic acid. These findings are later rationalised by our subsequent structural analysis.

Most notably from this assay, the reductionist glycoconjugate mimic, a methylated GM3g-amidine, was roughly 4 orders of magnitude more competitive compared to free GM3g (IC_{50} of 0.0013 vs 9.9). This implied that substantial energetic contributions to glycoconjugate recognition were imparted by linker (**Fig 3.19d**). Although the data imply that the complete GM3g glycan structure is a required component of antibody binding, we also observed broad, significant contributions from differing non-reducing aglycones (**Fig 3.19e**): enhanced binding for amide and aminoalkyl aglycones was potentiated further by the presence of an amidine. Any such potentiation was notably lost in the absence of incorrect glycan (**Fig 3.19e right**), further highlighting the role of tight glycan recognition in driving affinity, despite apparent engagement both of glycan and aliphatic constituents. Thus, although these data suggest that the antibody

response targets the linker-glycan motif, it is nonetheless specific to the GM3g glycan.

Collectively, these data suggest that the polyclonal glycoconjugate-specific antibody pool 1) is highly specific to the autologous GM3g glycan, and 2) has some degree of linker-dependency. Next, we aimed to determine whether these antibodies could recognise native presentations of α-2,3-sialyllactose, such as in the context of GM3, wherein the carbohydrate is ceramide-docked. Notably, the techniques using polyclonal serum and, therefore, bivalent Ig for competition ELISA affects the sensitivity of the cross-reactivity assays: for example, eliminating the avidity effect (for example, by instead using purified Fab) and performing a more sensitive assay (such as biolayer interferometry).

3.2.10. Determining context-dependency in glycan recognition

I endeavoured to screen whether the [–amidine-GM3g] antisera were cross-reactive with GM3. Ganglioside-based ELISAs yield notoriously non-specific signals because of the hydrophobicity of ceramide tails that are “sticky” for antibodies, often resulting in non-specific signal (Bantroch et al., 1994; Péterfi and Kocsis, 2000). This signal is promoted by the inability to use detergent in the ELISA wash solution, which solubilises the glycolipid (Helenius and Simons, 1975; Kragh-Hansen et al., 1998; Young et al., 1983). Thus, careful quality controls were implemented to ensure specificity. For example, plates were coated with either GM3 or ceramide (that is, the non-glycosylated lipid tail) and binding was screened using a commercially available anti-GM3 IgM antibody clone, GMR6 (**Fig 3.20a,b**). Antibody binding was detected against GM3 but not

ceramide using GMR6, but no binding was observed using the respective isotype control. These data imply that the assay setup provided sensitive and specific glycolipid reactivity.

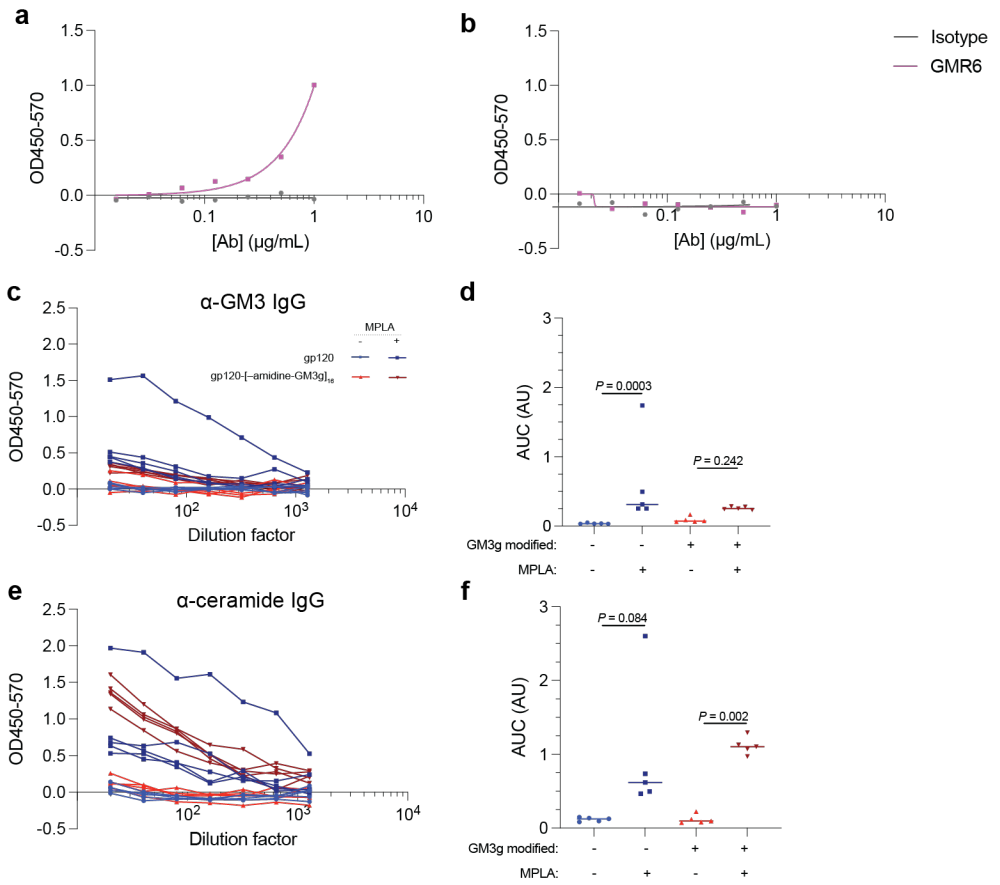


Figure 3.20: Serum reactivity with endogenous ganglioside, GM3.

Anti-GM3g IgM antibody clone, GMR6, was screened against **(a)** GM3 and **(b)** ceramide via direct ELISA. Terminal serum from mice immunised with gp120 or gp120-[–amidine-GM3g]$_{16}$ ± MPLA (scheduled outlined in **Fig 3.14c**) was screened against **(c, d)** GM3 and **(e, f)** ceramide. Area under the curve was measured and groups were contrasted via Kruskal-Wallis test.

Next, antisera from gp120-[–amidine-GM3g]$_{16}$-immunised mice were screened against GM3. Some GM3 reactivity was observed in animals immunised either with gp120 and MPLA or gp120-[–amidine-GM3g]$_{16}$ and MPLA (**Fig 3.20c,d**). This apparent adjuvant-dependent effect was surprising. Notably, sea from mice immunised with unadjuvanted gp120-[–amidine-GM3g]$_{16}$ elicited no elevated

binding compared with the background unadjuvanted gp120 antiserum ($P > 0.9999$, Kruskal-Wallis test), despite unadjuvanted serum exhibiting glycoconjguate-specific IgG titres ~10^5 (**Fig 3.14e**). These data do not indicate specific antibody reactivity with GM3.

These sera were also screened against ceramide, which exhibited a similar adjuvant-dependent reactivity signature (**Fig 3.14e,f**), suggesting that perhaps the adjuvant was driving non-specific antibody responses non-specifically reactive with hydrophobic or other components of the ganglioside. I next investigated whether MPLA itself is immunogenic—whether there might be adjuvant-specific antibody responses that are potentially cross-reactivity with

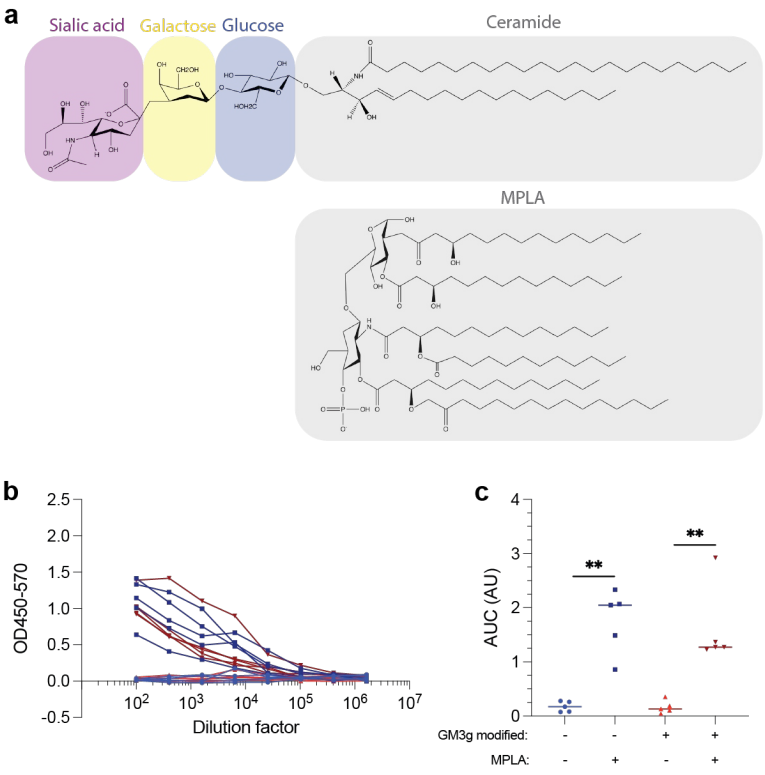


Figure 3.21: Evaluating the adjuvant-reactive antibody response imparted by MPLA.

(a) Lewis structure of GM3 (top) and MPLA (bottom). **(b, c)** IgG reactivity of gp120-[–amidine-GM3g]16-raised antisera was screened against MPLA. Data were compared via Kruskal-Wallis test. *P*-value denotations: '••' $P < 0.01$.

gangliosides. Importantly, however, ceramide and MPLA are structurally highly divergent (**Fig 3.21a**). Surprisingly, we observed considerable MPLA-reactivity (**Fig 3.21b**). Therefore, I conclude that the non-specific signal detected in **Fig 3.20** is an artefact of the adjuvant used in this study.

3.3 Discussion

It has been broadly argued in the literature that there is heavy incentive for immune tolerance of self-glycans, such as via the skewing of the naïve B cell repertoire to avoid the presence of self- or self-like glycan-reactive B cells to prevent the generation of autoreactive antibodies (Deimel et al., 2022; Deimel and Sattentau, 2022; New et al., 2016). This may explain why anti-glycan responses are associated with various autoimmune conditions (Dotan et al., 2006; Temme et al., 2021). Consistent with this, I and others have shown that immunisation with conventional autologous GM3 formulations fail to reliably elicit high-titre antibody response against the ganglioside (Ding et al., 1993; Livingston et al., 1994, 1989).

To address whether the ganglioside GM3-assoiated glycan SiaLac is able to elicit anti-GM3-specific IgG responses, I outline a novel LOG modular format in which native and otherwise immunorecessive/immunosilent glycans can be artificially presented to the immune system via ‘foreign’ linker chemistries. I hypothesised that these immunogens could, in principle, yield two key advantages compared with native TACA display: 1) the non-native presentation of the carbohydrate via a bespoke chemical linker may bypass the tolerogenic constraints that prevent antibodies being raised against native glycan presentations of endogenous

glycoconjugates, and 2) association with a carrier protein within the same antigenic complex allows for associated T cell help. Our discovery that the LOGs tested (amidine, amide and aminoalkyl linkers) permit high-titre GM3g-specific IgG responses indicate that generation of antibodies against self-glycan moieties is readily achievable via the exploitation of these modular formats.

In this study, I focus on the amidine-based LOG, which was shown to develop remarkably high antibody titres against the autologous glycoconjugates, and thoroughly characterise the serological response to [–amidine-GM3g], with particular focus on the determinants of LOG immunogenicity, glycan specificity and contextual dependencies of GM3g recognition. This discussion explores: i) several key observations pertaining to LOG immunogenicity; ii) their implications for B cell biology and vaccine design, and iii) and future directions associated with the development and translational potential of LOG-based vaccinations.

3.3.1. LOG-raised antiserum exhibits narrow glycan reactivity: a comparison with professional carbohydrate binding proteins

Glycobiology has gained significant recent interest, underpinned by substantial technological development that has permitted systematic characterisation, comparison, and modelling of carbohydrate-binding proteins, and their implications for health and disease. These advances have led to the recognition of the remarkable diversity among carbohydrate binding proteins (such as lectins), including their varying glycan specificity profiles (Mattox and Bailey-Kellogg, 2021). For example, galectins are capable of binding broad β-galactosides; galectin-4 can recognise terminal and internal galactose residues,

while tolerating of wide lactosylation, fucosylation, glucosylation and sulphation of galactose, and thus the set of endogenous carbohydrates recognised by galectin-4 is very expansive (Blixt et al., 2004; Hirabayashi et al., 2002). In contrast, for example, human CD22/SigLec7 has high specificity to α-2,6-sialyllactose, failing to appreciably tolerate even the α-2,3-linked counterpart (Blixt et al., 2004). Hence, having demonstrated that the [–amidine-GM3g] was highly immunogenic in mice, it was of interest to determine the glycan reactivity profile of the antibody response.

The evaluation of antiserum glycan specificity was important to understand potential effector antibody functions: if the raised anti-glycan response lacked narrow specificity for the autologous glycan, presumably there would be increased off-target binding that might elevate the risk of autoreactivity. To this end, an array of mammalian glycans was screened against gp120-[–amidine-GM3g]$_{16}$ antisera. The data revealed that the antisera exhibited narrow glycan binding, recognising sialyllated (either the autologous α-2,6- or the α-2,3-counterpart) lactose or *N*-aceytlated lactose, and minor variations of these glycans. The failure for the raised antibodies to cross-react with adjacent sialosides and other glycans suggests that the risk of off-target reactogenicity was minimised.

3.3.2. Context dependent glycan recognition: evaluating the translational potential of the LOG-raised antibody response

I demonstrated via competition ELISA that a reductionist, soluble LOG mimic, methylated amidine-GM3g, outcompeted antiserum binding against the

LOG:protein conjugate far better than GM3g alone, with an IC_{50} approximately 4-orders of magnitude lower. These findings are not necessarily surprising: synthetic linkers have long been reported to themselves impart considerable antigenicity in both mice and humans (Davis and Robinson, 2002; Kim et al., 2000; Kudryashov et al., 1998; Pollard et al., 2009; Rappuoli et al., 2019). Among the most well-characterised is polyethylene glycol (PEG), which is a flexible hydrophilic polymer that can be readily attached to protein, nucleic acids, lipids and small molecules (Lasic, 1997). Studies have consistently shown that pegylated immunogens result in high-titre responses against PEG, or PEG-conjugate composite epitopes (Chen et al., 2021; Ju et al., 2023). Anti-GM3g-based LOG responses are consistent with these findings, indicating that the polyclonal response recognises not only the glycan moiety, but also other elements of the chemical linker.

It was, therefore, unsurprising that there was no detectable cross-reactivity of gp120-[–amidine-GM3g]$_{16}$-raised antisera against the ganglioside GM3, wherein the glycan was docked to a ceramide backbone rather than a synthetic amidine linker. This was determined via ELISA. Notably, I had tested alternative assay formats, such as testing serum binding on GM3g^{+} melanoma line, b16 (Sawada et al., 1998), and GM3 liposomes. However, I was unable to establish a positive control using previously reported available antibody clones specific to GM3 (Kotani et al., 1992). However, my ELISA data (where a reliable positive control antibody was identified) suggests that glycan binding is ‘context dependent’, with linker accommodation likely preventing recognition of endogenous presentations of the autologous glycan and thus blunting any functional antibody effect. Hence,

understanding whether this context dependency could be overcome is a key open question that determines the translational potential of these LOG-based immunogens.

One possible way forward is to establish whether the antibodies raised against the LOG are capable of affinity maturing to become reactive against GM3—that is, determine whether a raised B cell clonotype may “walk” to recognise sugar in native contexts and deliver a functional outcome. Indeed, the contextualisation of glycan recognition may be required; for instance, by reducing antibody dependency on the synthetic linker and instead encourage B cell clones to accommodate the ceramide backbone of GM3, as hypothetically modelled (**Fig 3.22**). This principle has some parallels with classical germline-targeting

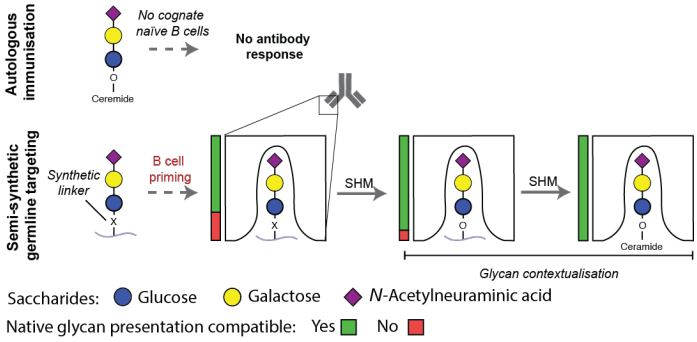


Figure 3.22: Anti-LOG contextualisation model.

LOG responses, such as that raised by [–amidine-GM3g], may fail to recognise native glycan presentations (such as GM3). Germinal centre reactions may be exploited to ‘train’ LOG-specific B cell clones to become reactive with pathology-relevant glycan presentations via iterative SHM rounds.

vaccination strategies, such as that being developed for HIV-1 (Escolano et al., 2019; Steichen et al., 2016).

In the HIV-1 example, immunogens are reverse-engineered to bind inferred germline reverted (iGL) antibody clonotypes with known functional potential

following sufficient SHM. Germline-targeting immunogens are designed to have higher affinity to particular naïve B cell clonotypes with known neutralising potential. In the case of semi-synthetic LOGs, while the artificial glycan display may access B cell clones that native GM3 could not access (in this sense, the linker would be 'throwing a rope' to the naïve B cell repertoire), it is unclear whether there is a possible path for a germinal centre reaction to resolve the context dependency. I envisage that the ability to suitably affinity mature these clones is dependent on two main characteristics. First, the specific antibody clonotype must avoid major clashes with the plasma membrane; for example, if a hypothetical antibody approaches the LOG 'side-on', then the region of the antibody that accommodates the linker component would ultimately clash with the plasma membrane, likely preventing recognition of GM3 ganglioside irrespective of the SHM outcome. Second, there must be a feasible pathway for germinal centre responses to deliver a GM3-reactive outcome through iterative immunisation. This may prove challenging, given the emergent developments around both epitope masking and limited clonal germinal centre recall (Mesin et al., 2020; Schaefer-Babajew et al., 2023) that collectively constrain the extent of 'attention' a germinal centre will give one specific clonotype. Moreover, a hypothetical clone would need to have a relatively low number of mutations to achieve GM3 recognition: in principle, the greater SHM frequency required to deliver a functional, native binding effect, the lower the probability a GC delivers the clonal outcome. These mutations must also be achievable via AID (for example, some codon-to-codon switches are highly unlikely) (Muramatsu et al., 2000, 1999).

Collectively, the serological data evaluated in this chapter suggest that, in order to better understand the response elicited and the potential for the antibody response to become physiologically relevant for reactivity with native GM3g presentations, it is necessary to understand the clonal origins of the antibody response, and associate these data with a structural and biochemical characterisation. This may inform the feasibility of a hypothetical germline-targeted approach to TACA-directed vaccination. This forms the basis of **Chapter 4**.

3.3.3. Relationship between LOG occupancy and immunogenicity: how important is avidity?

The relationship between LOG occupancy on HEL and the downstream LOG-specific IgG EPT was surprising; I hypothesised that the EPTs would be proportional to the number of glyco-modifications per HEL molecule. This was rationalised by the avidity effect, where a greater number of modifications per HEL molecule would improve the probability that a relevant BCR cross-links the immunogen, activates, and drives a downstream humoral response. This, however, was not the case, with the optimal titre being where the number of modifications was ~3–4 [–amidine-GM3g] per HEL molecule, rather than the maximum of 6. The mechanism that underpins this relationship was not found during this study, despite having investigated one possible explanation; I first thought that the substitution of lysine to arginine to modulate LOG occupancy may have inadvertently affected the T cell supply, such as introducing immunodominant $CD4^+$ T cell epitopes. Subsequent experimentation did not support this hypothesis.

There are three alternative explanations that were not investigated here but could be tested. First, there may be a counteracting effect imparted by immunoinhibitory lectin engagement. For example, many lectins, such as CD22/SigLec7, recognise sialic acids and are expressed on both B cells and myeloid cells to actively suppress NF-κB and a promote cell inactivation (Bärenwaldt and Läubli, 2019; Beatson et al., 2016; Crocker et al., 2007; Jandus et al., 2014; Lübbers et al., 2018; Müller and Nitschke, 2014). Perhaps higher valency of GM3g on HEL increases the degree of lectin-mediated immune suppression. Second, there are seemingly some structures are intrinsically inefficient at forming immune complexes and fastening to FDC networks within tertiary lymphoid organs (TLO). The precise conditions that determine immunogen trafficking and FDC localisation are not thoroughly modelled, although size, charge, propensity to deposit complement and availability of IgM are important factors (Irvine and Read, 2020; Read et al., 2022; Tokatlian et al., 2019). Perhaps 'saturation' by the glycomodification in HEL-[–amidine-GM3g]$_6$ compared with HEL-[–amidine-GM3g]$_{3d}$, for instance, may affect immunogen deposition in TLOs. Third, there is some evidence that highly dense spacing of antigen on a solid phase reduces BCR activation, suggesting BCR overstimulation has an inhibitory effect, with spacing of 25–30 nm being optimal with respect to downstream serological readouts (Veneziano et al., 2020).

Notably, modification of gp120, found to have an even greater glycan occupancy (median of 16 [–amidine-GM3g] modifications) delivered very high-titre responses. While this may appear contrary to the trends observed in the HEL

mutant data, these sets cannot be fairly compared: gp120 is highly $CD4^+$ T cell immunodominant in mice, whereas HEL failed to elicit a detectable $CD4^+$ T cell response even in animals immunised with adjuvanted formulations. Therefore, any LOG-specific antibody response mounted against gp120-anchored LOGs are likely highly potentiated by cognate T cell help.

Indeed, while the mechanistic underpinning of LOG valency effects on antibody titres was not resolved in this study, the observation that titres were not proportional to the number of glycomodifications is striking and challenges an avidity-only model for B cell responses.

3.3.4. GM3 but not GD3: the implications of stochasticity in linker–glycan immunogenicity

This study focused on the ganglioside TACA, GM3g, observing that various LOG displays resulted in a glycoconjugate-specific antibody response. The amidine-GM3g display was primarily investigated, as this resulted in the highest antibody titre against the autologous glycoconjugate. Notably, alternative linker displays, such as the aminoalkyl-linked display, resulted in lower autologous glycoconjugate responses. These data imply that there was some degree of stochasticity in the capacity for a given 'reach through', non-self glyconjguate display to elicit a response.

By extension, I anticipated that just because [–amidine-GM3g] might be highly immunogenic, alternative glycan-amidine conjugates may not be. This hypothesis was supported by data acquired following immunisation with [–

amidine-GD3g] (a di-sialyllated counterpart of GM3g), which did not elicit a glycoconjugate-specific polyclonal antibody response (data not shown). In contrast, immunisation with [–amidnine-Le^X] glycoconjugates was found to be immunogenic in mice, eliciting an orthogonal glycan-specific serological reactivity profile compared with [–amidine-GM3g] antisera (Deimel et al. submitted) (these data were acquired by Dr Torben Schiffner and not presented in this thesis).

Based on these data, I hypothesise that the capacity for a given LOG to permit an autologous anti-glycoconjugate-specific response is primarily a feature of the availability of cognate germline B cells in the naïve repertoire—that a given LOG must access, cross-link, and activate a B cell to allow a coordinate LOG-specific response. The implications of a germline-centric model for LOG vaccine efficacy are broad: for example, it implies that murine models will be unlikely to represent the translated outcome in humans, since the germline repertoires of mice and humans are highly divergent. This may explain why several early anti-TACA vaccination designs have failed to translate to humans (Chapman et al., 2000; Holmberg and Sandmaier, 2004; Oyelaran and Gildersleeve, 2010).

3.3.5. Conclusions

The data presented in this study are consistent with the dogma of weak glycan immunogenicity (Livingston and Ragupathi, 2006). However, I explicitly demonstrate that artificially displaying otherwise immunorecessive self-glycan moieties in non-native formats can elicit a cognate glycoconjguate-specific response. The LOG modular formats can impart a significant payoff with respect to immunogenicity which, as we argue in the case of the [–amidine-GM3g]

glycoconjugate, are affected by a penalty to native glycan recognition (**Fig 3.23**). These and other findings suggest that a molecular immunology perspective of the LOG-mediated antibody response (such as performing clonotyping and downstream structural, biophysical and biochemical analyses) may offer insights into why these antibodies may not react with native glycan presentations and suggest a pathway to effective glycoconjugate-based vaccine design.

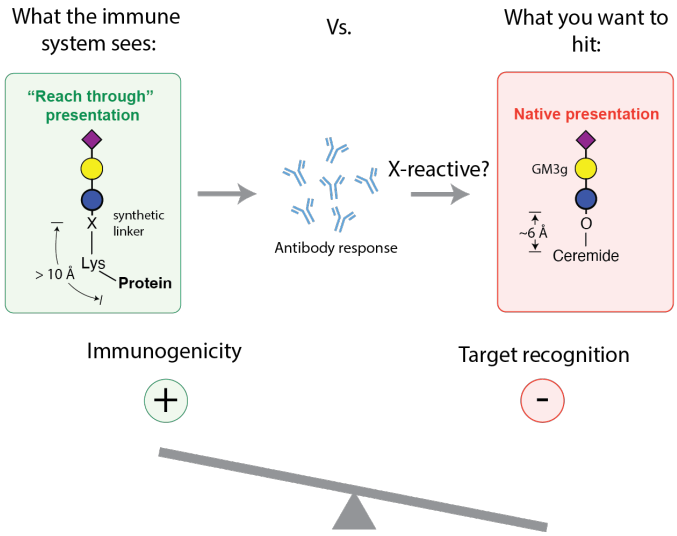


Figure 3.23: Summary model of the impacts of LOGs on the downstream antibody response.

The LOG modular formats of GM3g facilitates high titre antibody responses that native presentations of GM3g fail to elicit. While LOGs such as [–amidine-GM3g] have an immunogenicity payoff, the response fails to react with native presentations. Therefore, the immunogenicity pay-off comes at a penalty to target recognition.

(This page is intentionally left blank)

Chapter 4—Molecular underpinnings of the LOG-specific antibody response

4.1 Background

4.1.1 Introduction to molecular immunology

In **Chapter 3**, I describe a synthetic protein chemistry-based approach to eliciting antibody responses to self-sugar/TACA moieties that are classically highly immunorecessive; the utilisation of protein editing methods to precisely display TACAs via non-native, artificial linker chemistries were shown to bypass tolerance limits that endogenous presentations (e.g. formulations of ganglioside GM3) fail to overcome. The primary LOG system used for this study was lysine-modified with short amidine-docked GM3g (α-2,3-sialyllactose). This glycoconjugate was shown to be highly immunogenic in mice. I hypothesise that these data represent a 'reach-through' model in which these artificial presentations of otherwise immunorecessive glycans can access a subset of naïve B cells that native presentations of the same glycan fail to engage.

This implies that a clonal understanding of the B cell response, namely via isolating and characterising the antigen-specific B population at the molecular level, may offer high-resolution immunogenetic, structural and functional insights into a given antibody response (Viant et al., 2021; von Boehmer et al., 2016). For example, sequencing heavy and light chain variable (VH, VK) regions from antigen-specific single B cells reveals relevant V(D)J configurations that bind the [–amidine-GM3g] LOG, and synthesising and purifying mAbs provides a platform to evaluate binding kinetics, atomic-level structural analyses and epitope mapping, as has been carried out for the HIV-1 envelope glycoprotein in the context of vaccine design (Barnes et al., 2018; Escolano et al., 2017; Gristick et al., 2016; Klein et al., 2012; Leggat et al., 2023; Mouquet et al., 2012; Scheid et al., 2011; Shingai et al., 2014; Viant et al., 2021; Zhou et al., 2010; Zolla-Pazner et al., 2016).

4.1.2 Overview of B cell molecular cloning techniques

The first antibody discovery method was described nearly 50 years ago—hybridoma technology. This method involves the chemical fusing of bulk splenocytes with a mouse myeloma cell line (KÖHLER and MILSTEIN, 1975). The resultant hybridomas are cloned and cultured over iterative rounds to isolate stable monoclonal cell lines that express a mAb of the received originator B lymphocyte. While this immortalisation approach allows for the isolation and purification of monoclonal antibodies against a target of interest, there are several key limitations.

First, hybridoma technology is labour-intensive and relatively low throughput, at best delivering moderate numbers of target-specific mAbs. In part, this is a consequence of the cytotoxicity of the fusing agent, PEG, which kills many relevant hybridomas immediately post-fusion (Kerkis and Zhdanova, 1992; Lane et al., 1984; Lentz, 2007). Moreover, the stability of murine hybridomas is highly variable between clones, with stochastic ablation of antibody productivity, a function of chromosomal loss inherent to myeloma lines (Castillo et al., 1994; Kessler et al., 1993; Weiss and Green, 1967). Second, the time to isolate and select single antibody-secreting clones of interest and produce large-scale cultures is generally in the order of months, making it difficult to rapidly purify significant quantities of mAb for downstream characterisation (Castillo et al., 1994; Kessler et al., 1993). Thus, alternative experimental protocols that overcome these challenges has been a central focus of B cell immunology in recent decades and has given rise to contemporary techniques involving the molecular cloning of V regions from singly sorted target-specific B cells and subsequent recombinant immunoglobin (Ig) synthesis.

Since its initial description in 1996 (Babcook et al., 1996), single B cell antibody cloning techniques have developed rapidly with technological advances. For example, taking advantage of contemporary cell sorters capable of stringent and indexed single-cell isolation; modern high-fidelity molecular cloning tools; Next-Generation sequencing; efficient mammalian protein expression systems; availability of relevant databases for in-depth immunogenic analyses, and improved technology to characterise antibody binding. Collectively, this experimental pipeline has the capability of offering exceptionally efficient

production and characterisation of hundreds of mAbs in a matter of days. This is reflected in recently published methods that allow for highly scalable characterisation of the clonal antibody response in murine models (Carbonetti et al., 2017; Ho et al., 2016; Viant et al., 2021; von Boehmer et al., 2016).

4.1.3 Rationale for a molecular approach to dissecting the anti-GM3g response

In this chapter, I establish and deploy contemporary B cell molecular cloning techniques to isolate and characterise the anti-[–amidine-GM3g] B cell response at the single cell level, as well as characterise monoclonal antibodies against the glycoconjugate. Thorough clonotyping of the response may not only provide an explanation for the immunogenicity imparted by LOG display methods, but also reveal a structural basis for the context-dependency that seemingly restricts antibody function, preventing engagement of endogenous, pathology-relevant glycan presentations.

4.1.4 Aims

In this chapter, the main aims include to:

1. Establish an experimental pipeline to isolate, sequence and recombinantly express LOG-specific B cells.
2. Clonotype the [–amidine-GM3g]-specific B cell response and characterise the effects of the protein backbone on clonal outcomes.
3. Biophysically, biochemically and structurally characterise the prototypical antibody response against the LOG.

4. Rationalise the context-dependency of the B cell response and consider the plausibility of affinity maturing clones to recognise native glycan presentation.
5. Explore the translational potential of LOG-based vaccination.

4.2 Results

4.2.1. Dissecting the clonality of the anti-GM3g-specific antibody response

To evaluate the clonotypes of the LOG-specific response, 6-week-old BALB/c mice were primed subcutaneously with 10 µg of HEL-[–amidine-GM3g]$_6$ adjuvanted with 20 µg of MPLA subcutaneously. After 4 weeks, mice were culled, and the draining inguinal lymph nodes (iLN), spleen and tibial/femoral bone marrow were harvested (**Fig 4.1a**). This time point was selected as it represents the late-/end-stage follicular response, a time point wherein the germinal centre reactions have largely contracted and where the majority of memory B cell export has occurred (Hägglöf et al., 2023; Mesin et al., 2016). Briefly, the overview of the B cell cloning pipeline involves sorting antigen-specific B cell, synthesising single-cell cDNA, PCR amplifying variable regions, sequencing these regions, and subsequently embedding these variable regions into vectors for subsequent recombinant monoclonal antibody expression and purification (**Fig 4.1b**).

IgD$^-$ B cells were pre-gated according to the shown strategy (**Fig 4.1c**). To sort the antigen-specific population, fluorescent antigen probes were synthesised. A dual probe design was used to separate the protein backbone and LOG-specific B cells. To identify LOG-specific clones, the molecular probe was synthesised

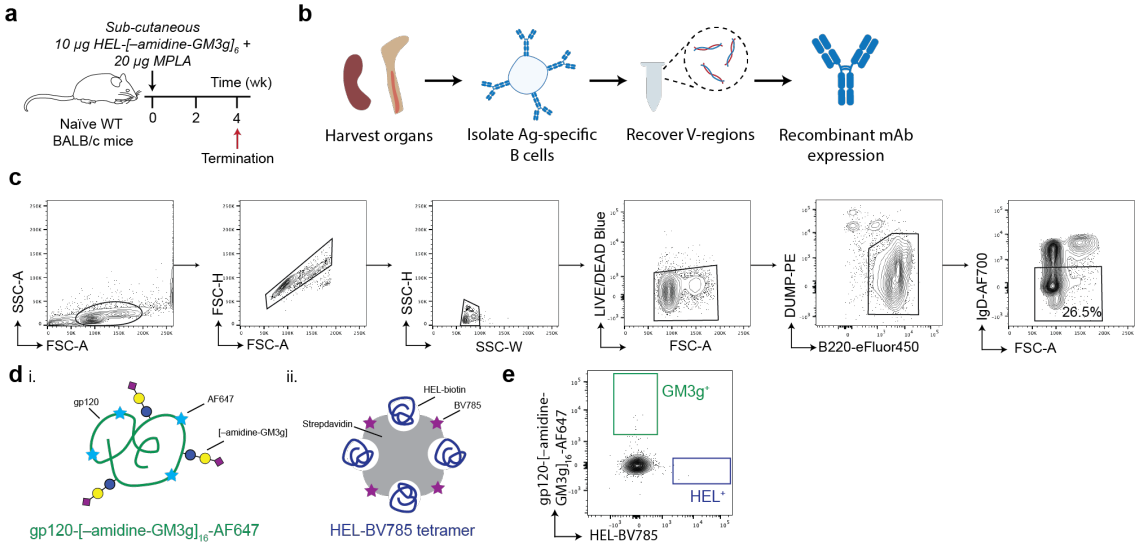


Figure 4.1: Approach to isolate LOG-specific B cells.

(a) Naïve WT 6-week-old BALB/c mice were primed with 10 µg HEL-[–amidine-GM3g]$_6$ and 20 µg MPLA and culled after 4 weeks. **(b)** iLN, spleen and bone marrow were harvested, antigen-specific B cells were sorted, V-regions recovered, and antibodies were expressed recombinantly. **(c)** Non-naïve B cell gating strategy. Data shown are representative of splenocytes that had been pre-enriched for CD19+ cells via MACS. **(d)** i. The LOG-specific probe was synthesized by modifying gp120-[–amidine-GM3g]$_{16}$ with was an AF647-NHS ester. ii. A backbone-specific probe was synthesized by tetramerizing biotinylated HEL to strepdavidin-BV785. **(e)** Probe gating strategy.

using gp120-[–amidine-GM3g]$_{16}$ was prepared, modified with an NHS-esterified AF647 (**Fig 4.1d.i**). Protein backbone-specific clones were identified using a tetramerised HEL, where biotinylated HEL was conjugated to a BV785-modified streptavidin (**Fig 4.1d.ii**). Sorting of antigen-binding B cells was conducted (**Fig 4.1e**).

B cells were sorted from three mice. Interestingly, most B cells isolated were isolated within the GM3g gate rather than the HEL-specific gate (mean of 87%) (**Fig 4.2a**). This may suggest that the LOG is clonally dominant compared with the protein backbone. No antigen-specific B cells were isolated from the iLN, which may suggest that the local follicular response had ceased at this timepoint

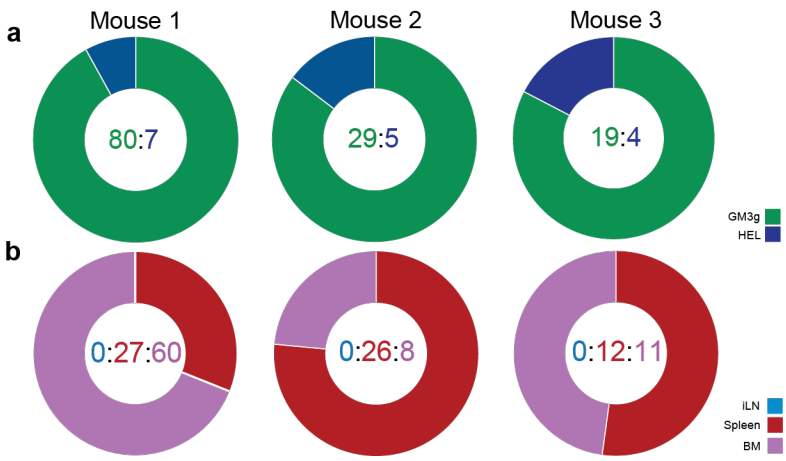


Figure 4.2: Origins of sorted B cells from mice immunised with HEL-[–amidine-GM3g]$_6$.

(a) Breakdown of B cells sorted that fell into either the GM3g gate or HEL backbone gate. **(b)** Location of sorted B cells.

(**Fig 4.2b**). It is likely that this is a function of the limited Th supply imparted by the HEL backbone, as established previously (**Fig 3.11**; **Fig 3.12**).

Heavy chain V-regions were sequenced and aligned against the murine V(D)J germline database (https://www.imgt.org) and inferred gene segments were assigned according to the gene-segment of the best nucleotide similarity (**Fig 4.3a**). This was applied to amplicons isolated against both the LOG- and HEL-based molecular probes, which can be used to infer enriched segments. For example, mouse 1 revealed highly enriched use of V_H segments of an *IGHV2* origin for B cells that bound the GM3g probe (85%), with *IGHV2-3*01* and *IGHV2-9*01* being the two most used gene segments within this *IGHV2* subgroup (**Fig 4.3b**). Meanwhile, D_H and J_H segments were highly diverse among GM3g clones (**Fig 4.3c,d**). Notably, since few clones were sequenced against HEL, enriched clonal classes against the protein backbone could not be inferred. Sequences from both mouse 2 and mouse 3 also indicate significant

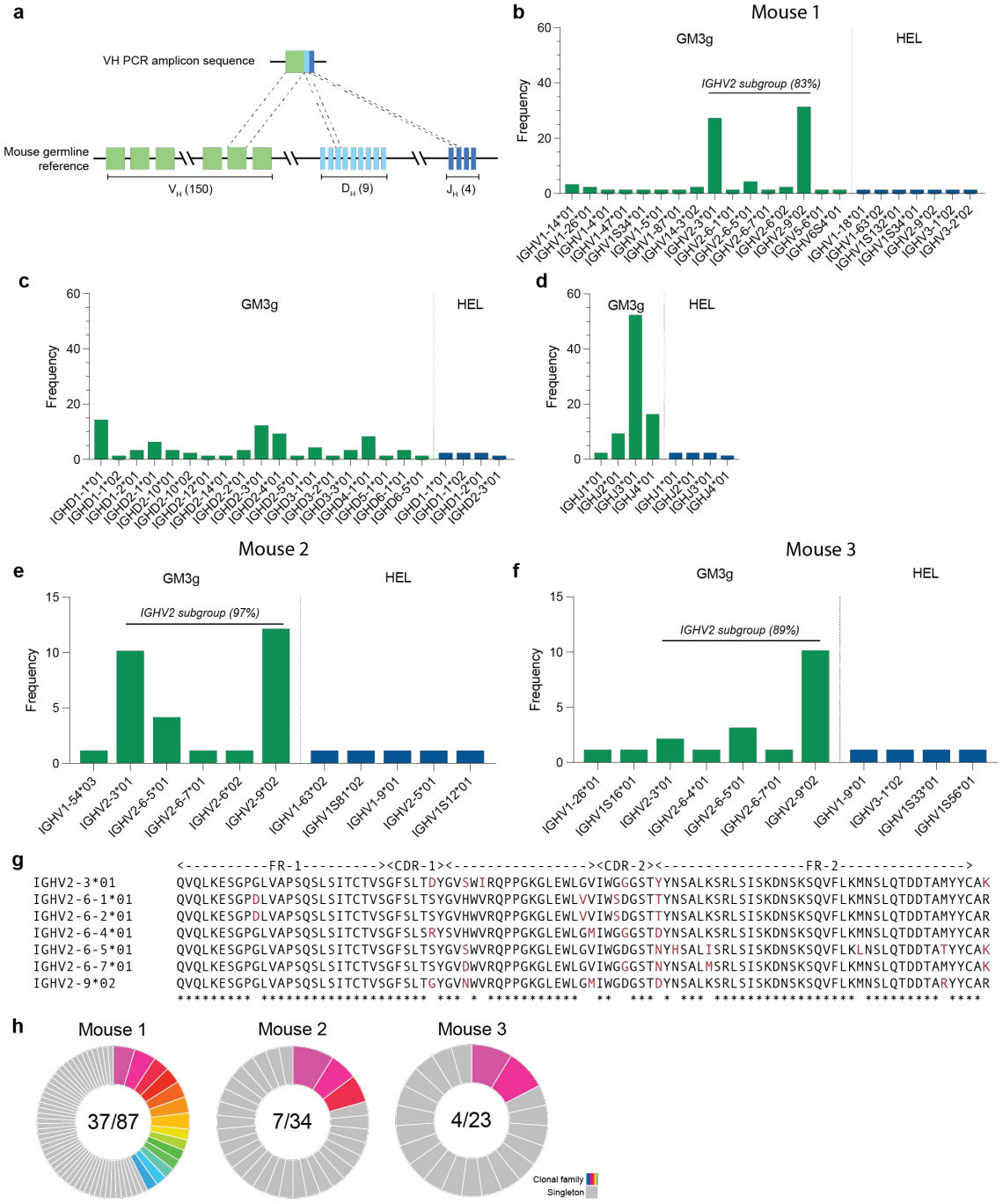


Figure 4.3: Clonal background of [–amidine-GM3g]-specific B cells.

(a) V_H amplicons were compared to the germline-encoded reference gene segments. **(b–d)** Frequency of inferred germline gene segment origins of B cells isolated from mouse 1, partitioned according to their GM3 or HEL probe binding origins. **(e,f)** Mouse 2 and 3 *IGHV*-gene origins. **(g)** Alignment of utilized *IGHV2*-subgroup origin B cells. **(h)** Clonal families. These were clustered according to the inferred $V_HD_HJ_H$ origins.

enrichment of *IGHV2* subgroup VH gene segment use in B cells sorted against the [–amidine-GM3g]-based LOG probe (97% and 89%, respectively) (**Fig 4.3e,f**). These data collectively imply that motifs encoded within the *IGHV2* subgroup are used to engage the glycoconjugate, since their enrichment was observed across all animals immunised with HEL-[–amidine-GM3g]$_6$. Interestingly, the gene segments used within this subgroup encode highly similar amino acid sequences (**Fig 4.3g**), including strong similarity in CDRH1 and CDRH2. This suggests that motifs within these CDRs may be critical for glycoconjugate recognition. Moreover, clonal families were assigned according to the $V_HD_HJ_H$ identities, which implied some clonal expansion (**Fig 4.3h**).

The V_H gene use was compared between mice, which revealed highly related *IGHV2* gene segment proportionality among GM3g-specific B cells (**Fig 4.4a**). Meanwhile, the shared gene segment used among HEL-specific clones was much lower (**Fig 4.4b**). While low sampling numbers (that is, rare HEL-specific B cells) likely contributes to the observed sharing of V gene usage, I envisage that

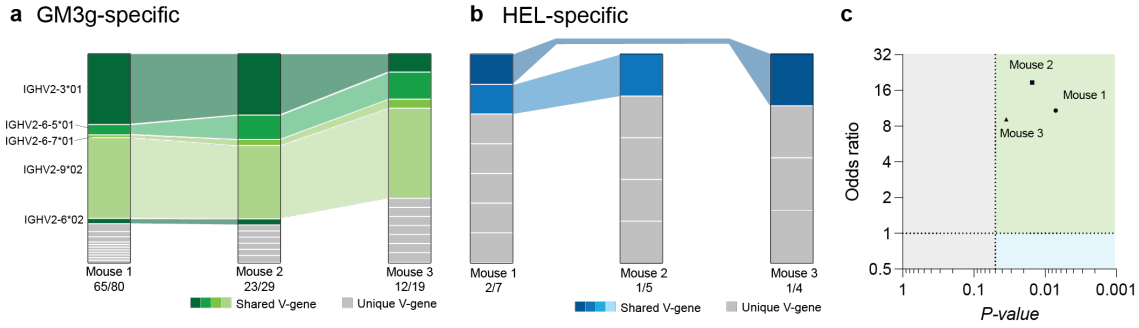


Figure 4.4: V_H gene segment utilization across GM3g-specific B cells.

Bar segments indicate V_H gene segments used by either **(a)** GM3g- or **(b)** HEL-specific B cells. Coloured segments shared across animals denotes shared segments ustilised across individuals. **(c)** Variation in the proportion of shared VH gene segments with respect to target specificity were contrasted via odds ratio and Fisher's exact tests.

the relatively large protein surface area compared to the limited glycan surface probable engages a more diverse set of possible cognate B cells due to their being a greater number of hypothetical epitopes. This is represented by the odds ratio of shared GM3g-specific V-genes compared to that of HEL, indicating a narrower set of V-genes being used (**Fig 4.4c**).

A subset of GM3g-specific antibodies was recombinantly expressed. First, supernatant from transfected cells was screened against gp120-[–amidine-GM3g]$_{16}$ to validate binding (**Fig 4.5a**). Notably, BAR-1, a prototypical *IGHV2-9*02*-background antibody (labeled in the figure), was expanded for later structural and biochemical analysis. Antibodies were subsequently purified and tested against both ceramide and GM3, although no reactivity was observed (**Fig 4.5b**). These data are consistent with earlier polyclonal reactivity data (**Fig 3.20**).

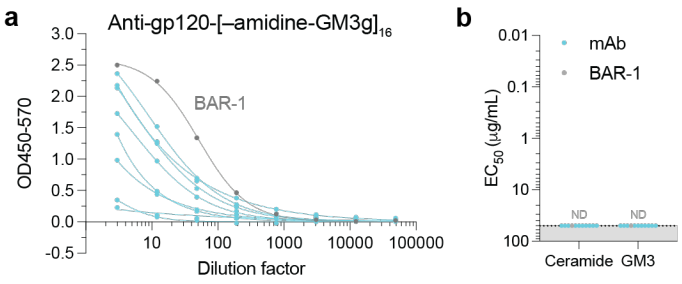


Figure 4.5: Expression and screening of GM3g-specific antibodies.

(a) A subset of *IGHV2*-origin recombinant antibodies was expressed recombinantly, and raw supernatant was screened against gp120-[–amidine-GM3g]$_{16}$. **(b)** Antibodies were purified and screened against both ceramide and GM3. Prototypical antibody later used for structural and biochemical characterisation, BAR-1, is marked grey.

Given the restricted clonal typology of the anti-[–amidine-GM3g] response in the context of the broad tolerance to diverse D_H and J_H genes, the LOG was hypothesised to be engaged by a high frequency of naïve B cells. Although V(D)J

recombination results in a combinatorically diverse B cell repertoire, if a given clonotype is primarily dependent on V_H for binding, while flexibility in D_H and J_H can be tolerated, the proportion of cognate B cells accessible to a given target epitope may increase. To interrogate this, LOG-binding naïve B cells isolated from un-immunised murine splenocytes were evaluated (**Fig 4.6a**). Interestingly, LOG-specific B cells were detected at a high frequency of 0.025% (**Fig 4.6b**). These events were sequenced from one mouse, revealing similar enrichment of the *IGHV2* subgroup (88%) with diverse use of D_H and J_H genes (**Fig 4.6c–e**).

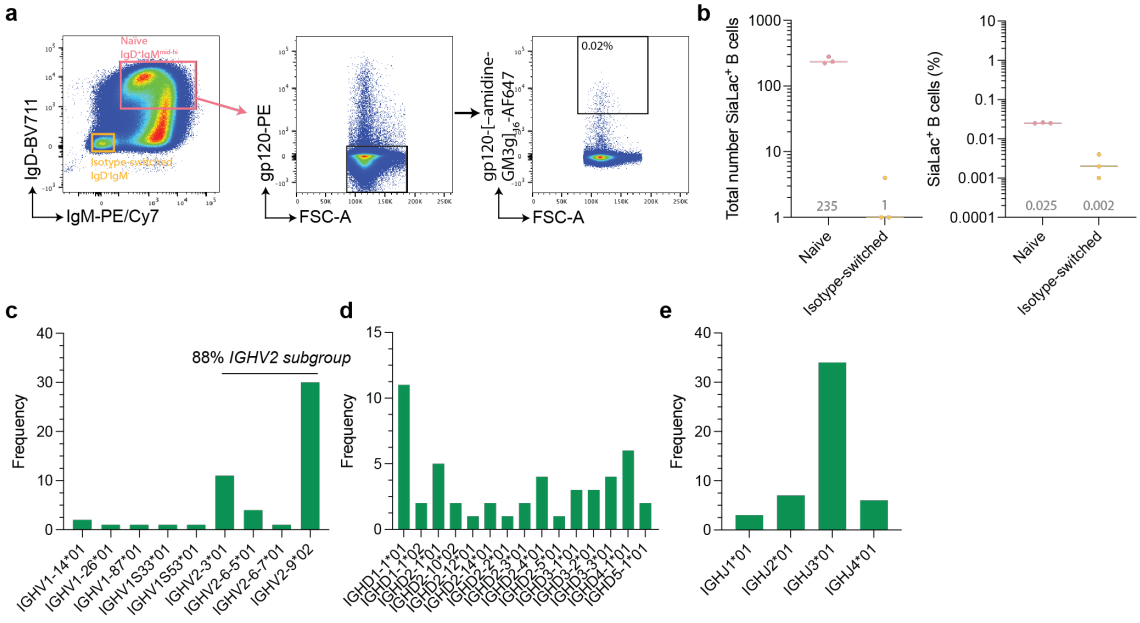


Figure 4.6: Evaluating the frequency of [–amidine-GM3g]-reactive naïve B cells.

(a) Splenocytes from 6-week-old BALB/c mice were harvested, and the frequency of naïve B cells reactive with [–amidine-GM3g] was evaluated. **(b)** Absolute number (left) and percentage (right) of [–amidine-GM3g]$^+$ B cells. **(c–e)** Clonotyping was conducted from a single mouse and frequency of inferred gene segment utilization are shown.

4.2.2. The role of the protein backbone on GM3g-specific outcomes

Having thoroughly clonotyped the glycoconjugate-specific B cell response raised against HEL-[–amidine-GM3g]$_6$, I next aimed to establish whether altering the

protein backbone would affect clonal outcomes. To this end, animals were immunised with gp120-[–amidine-GM3g]$_{16}$ formulated with MPLA, and iLN, spleen and bone marrow were harvest 4-weeks post-prime (**Fig 4.7a**). Cells were sorted using either the gp120-[–amidine-GM3g]$_{16}$-AF647 probe, or a gp120-BV785 tetrameric probe (**Fig 4.7b**). Interestingly, no B cells were sorted against the gp120 protein backbone probe in any mice (for example, mouse 1 yielded 70/70 B cells isolated from the GM3g^{+} gate; **Fig 4.7c**). Consistent with this, terminal sera from none of the three animals screened against both gp120 and HEL-[amidine-GM3g]$_{6}$ (**Fig 4.7d**), gave a detectable IgM or IgG signal against the protein backbone, while significant reactivity was observed against the LOG. These data are also consistent with earlier gp120-[–amidine-GM3g]$_{16}$ immunisations, where detectable gp120-specific titres were only observed post-boost (**Fig 3.14g**).

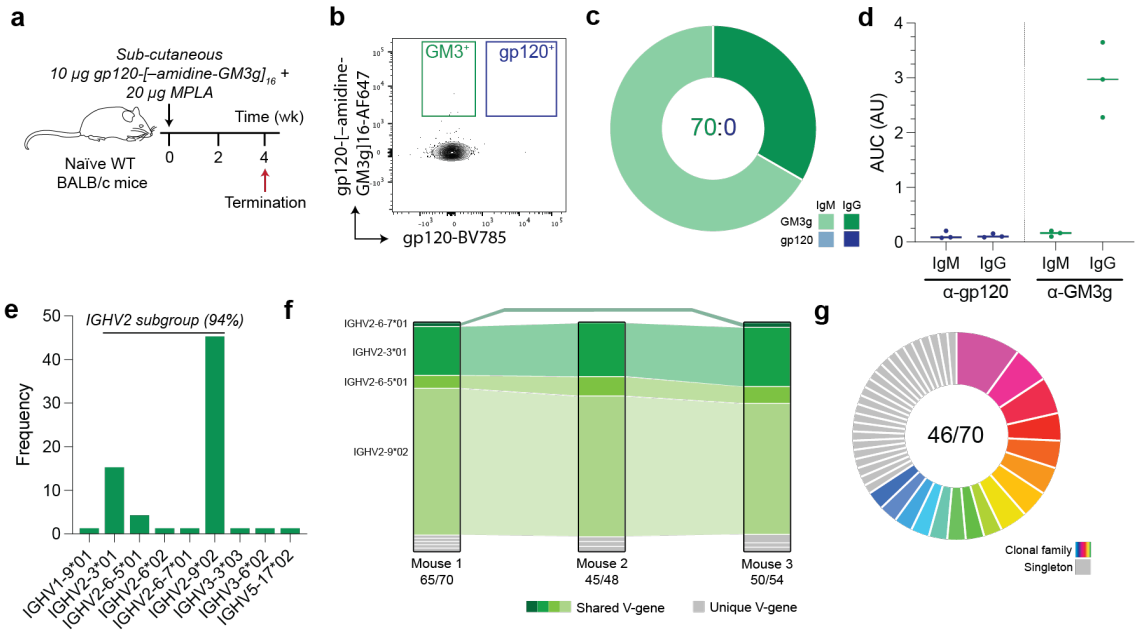


Figure 4.7: Clonotyping of gp120-[–amidine-GM3g]$_{16}$-raised B cells.

(a) Immunisation strategy. **(b)** Probe-based sorting plot. **(c)** Probe specificity and isotype status of sorted B cells. **(d)** Terminal serum reactivity against unmodified gp120 (left) and HEL-[–amidine-GM3g]$_{6}$. **(e)** VH gene utilisation. **(f)** Shared VH gene use across mice. **(g)** Inferred clonal families. **(d,e,g)** Data from Mouse 1.

I hypothesised, since the same LOG was being tested (and thus the same 3D surface epitopes were being recognised by the B cell repertoire), that the same V-gene usage would be observed. Indeed, analysis of the HC variable regions revealed enrichment for the *IGHV2* subgroup as before, and this was observed for all three mice analysed (**Fig 4.7e,f**) and yielded a similar clonal composition (**Fig 4.7g**).

The number of B cells in members of clonal families were greater for animals immunised with the gp120 backbone compared to the HEL-backbone-based LOGs, with an average of 2.67-fold greater proportion of non-singleton B cells (**Fig 4.8a**). This implied that the protein backbone may affect the 'clonal richness' of the B cell response. To test this, chao1 tests were performed; this is a non-parametric statistical test for species richness, which infers that rare species can inform the total/unknown number of unobserved species (**Fig 4.8b**). However, there was no significant effect of protein backbone on the chao1 estimate ($P > 0.9999$), suggesting that the backbone does not impact the total number of clonal families.



Figure 4.8: Evaluation of the protein backbone on clonal richness.

(a) The proportion of non-singleton B cells. **(b)** Visual representation of species richness and chao1. **(c)** Chao1 estimates of clonal richness for each mouse.

Next, SHM rates were evaluated. I observed in the sequences isolated from gp120-[–amidine-GM3g]$_{16}$-immunised mice that the degree of SHM undergone was compartment-specific (**Fig 4.9a**): the mean nucleotide mismatch of VH sequences derived from the lymph node was 6.8, spleen was 1.4 and bone marrow 0.8.

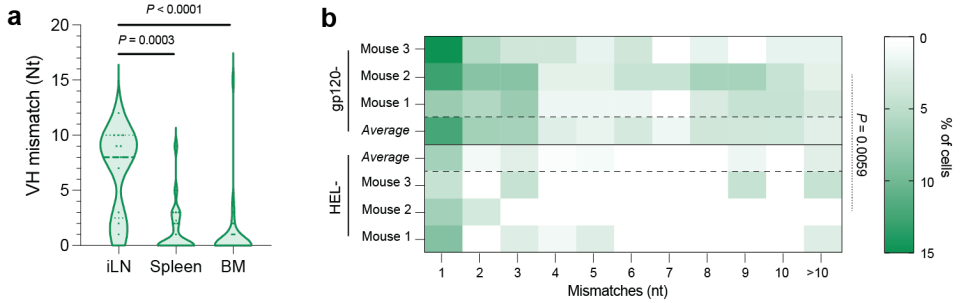


Figure 4.9: Factors affecting SHM rates.

(a) Compartment-dependent VH mismatches from B cell sequences pooled from gp120-[–amidine-GM3g]$_{16}$-immunised mice. Datasets were compared via Kruskal-Wallis test. **(b)** The distribution of VH mismatches was compared with respect to protein backbone. Data were compared using a Kolmogorov–Smirnov test.

I next compared the extent of SHM undergone by GM3g-specific B cells isolated from mice immunised with different protein backbones. Interestingly, the extent of SHM undergone by the clones raised against gp120-[–amidine-GM3g]$_{16}$ was significantly greater than that against HEL-[–amidine-GM3g]$_6$ (P = 0.0059, Kolmogorov–Smirnov test) (**Fig 4.9b**). These data implicate the protein backbone in determining the maintenance of the primary GC reaction conditions.

To understand the cellular underpinnings of the improved GC experience of gp120-[–amidine-GM3g]$_{16}$-raised clones, I measured the induction of Tfh cells with respect to protein carrier. To dissect this, animals were primed subcutaneously with either HEL-[–amidine-GM3g]$_6$ or gp120-[–amidine-GM3g]$_{16}$ with MPLA adjuvant and iLNs were harvested after 7 days (**Fig 4.10a**). This time

point was chosen as it represents the peak effector Tfh response (Lederer et al., 2020). Tfh cells were measured on pre-gated $CD4^{+}CD62L^{-}CD44^{hi}$ T cells (**Fig 4.10b,c**). Interestingly, the cellularity of the iLNs increased compared to the naïve control upon immunisation with either HEL-[–amidine-GM3g]$_6$ or gp120-[–amidine-GM3g]$_{16}$ (**Fig 4.10d**). However, the size of the Tfh cell population was significantly greater among mice immunised with gp120-[–amidine-GM3g]$_{16}$, compared to HEL-[–amidine-GM3g]$_6$, with a 3.6-fold difference in absolute number of Tfh cells (P = 0.045, Mann-Whitney test) (**Fig 4.10e,f**).

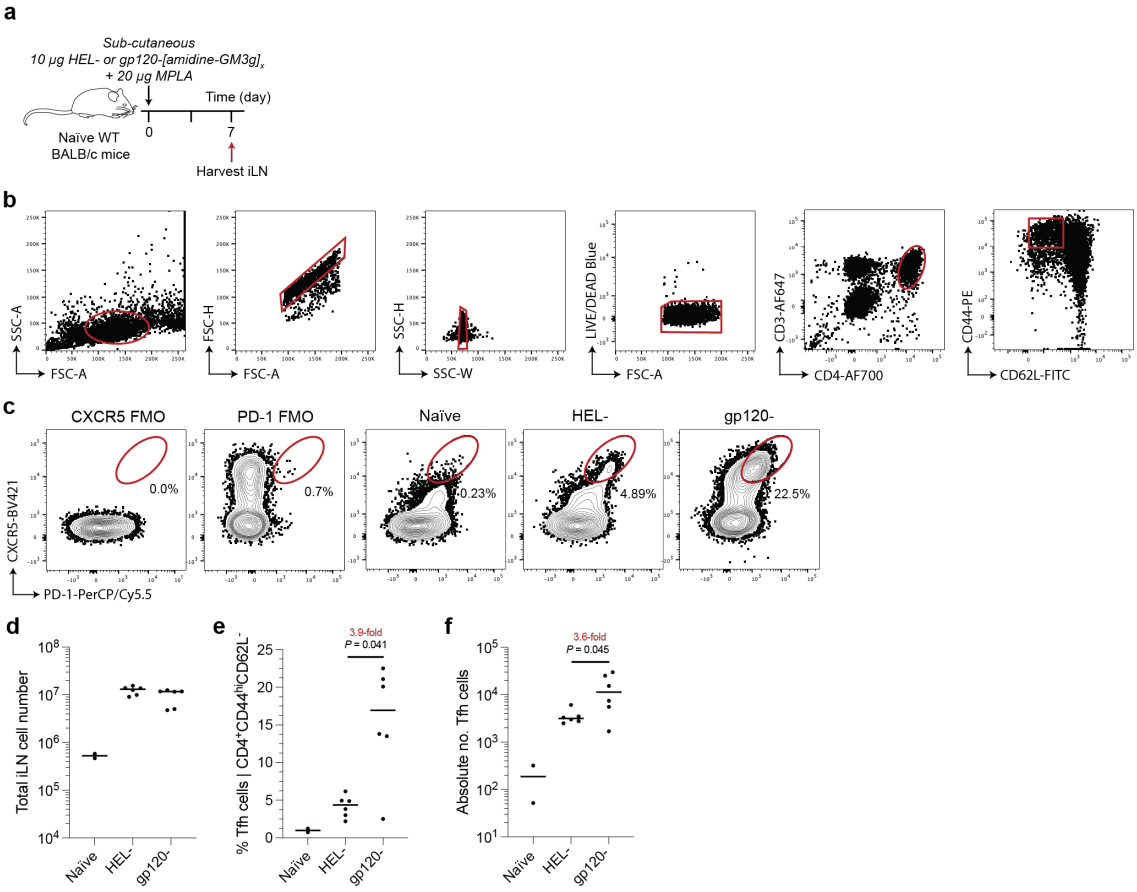


Figure 4.10: Evaluating the differential Tfh supply with respect to protein backbone.

(a) Immunisation strategy. **(b)** T cell pre-gating. **(c)** Representative FACS plots for Tfh selection. **(d)** Total number of iLN cells at the terminal timepoint. **(e,f)** The percentage and absolute number of Tfh cells in the draining iLN. Data were compared via Kruskal-Wallis test.

4.2.3. Evaluating the effects of SHM on GM3g-specific antibody clones

Having shown that B cell clones isolated from mice immunised with gp120-[–amidine-GM3g]$_{16}$ had undergone greater rates of SHM compared with that isolated from HEL-[–amidine-GM3g]$_6$-immunised mice, I next aimed to evaluate whether the SHM had effects of the apparent affinity of antibody clones. First, I evaluated the largest clonal family isolated among gp120-backbone-immunised mice (**Fig 4.11a**). This clonal family was comprised of 12 members and was of the *IGHV2-9*02* background. Phylogenetic analysis of the nucleotide mismatches revealed significant clonal diversification, compared with the iGL revertant. Binding was evaluated via ELISA, reporting the EC_{50} values, as determined by the midpoint between the logistic asymptotes of the ELISA binding curves (**Fig 4.11b**). The respective antibodies were synthesised recombinantly and screened against HEL-[–amidine-GM3g]$_6$ in an ELISA format. Interestingly, compared to the iGL revertant, no significant changes in binding were observed (**Fig 4.11c**). This implied that, despite significant degrees of SHM and resultant diversification in the amino acid sequence, no detectable change to binding was observed against the LOG.

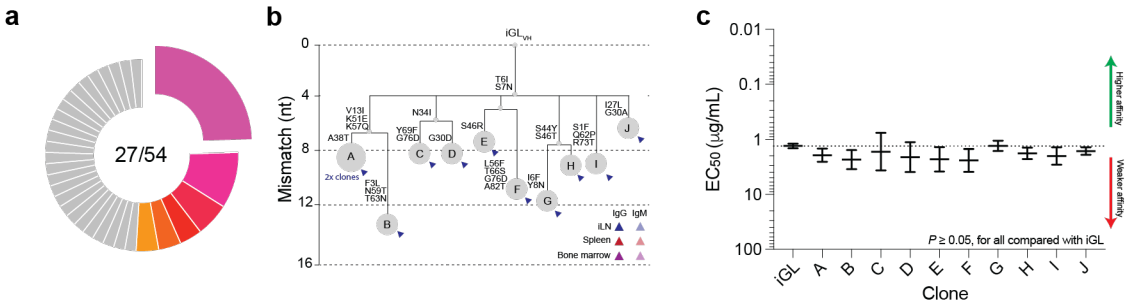


Figure 4.11: Clonal family analysis—the effects of SHM antibody binding.

(a) Clonal families from a gp120-[–amidine-GM3g]$_{16}$-immunised mouse. **(b)** GC tree outlining the phylogeny and amino acid substitutions progressively acquired during SHM. **(c)** Antibodies were recombinantly synthesised and screened against HEL-[–amidine-GM3g]$_6$. EC_{50} values were compared to the iGL as a proxy for relative affinity.

Second, to evaluate the effects of SHM in a non-biased manner, Manhattan plots of the V_H gene segment of all *IGHV2*-origin gene segments were generated to investigate the distribution and enrichment of mutations across the gene segment to identify whether specific substitutions are common across all animals. The data revealed considerable diversification across the gene segment in all animals (**Fig 4.12a**). The most common mutations in the encoded CDRs were at positions T6 and S7, and evaluation of the residue substitutions at these positions indicated that T6I and S7N were the most common outcome across these mice (**Fig 4.12b**). These substitutions were incorporated via mutagenesis into the prototypical BAR-1 antibody (which had WT T6 and S7) via mutagenesis and recombinantly expressed. When screened against HEL-[–amidine-GM3g]$_6$, these antibodies failed to demonstrate improved binding against the target (**Fig 4.12c**). Collectively, these data showed no evidence of increased affinity against the glycoconjugate, despite substantial SHM.

4.2.4. Biophysical, structural and biochemical characterisation of prototypical monoclonal antibody, BAR-1

We generated and purified the Fab of the GM3g-binding BAR-1 clone and quantified binding using surface plasmon resonance (SPR) against an amidine (C(NH)NH)-GM3g-coated surface, bearing the same extended side-chain motif as used in LOGs, generating a K_D = 17 ± 1 μM (**Fig 4.13a**). Next, we synthesised an equivalent soluble ligand, Lys–amidine-GM3g, as a representative minimal LOG motif, and a truncated variant Me–amidine-GM3g and conducted solution-phase ITC, generating a similar K_D = 5.4 ± 1.2 μM (Lys–amidine-GM3g, **Fig 4.13b**). Notably, consistent with the LOG design, rather than display

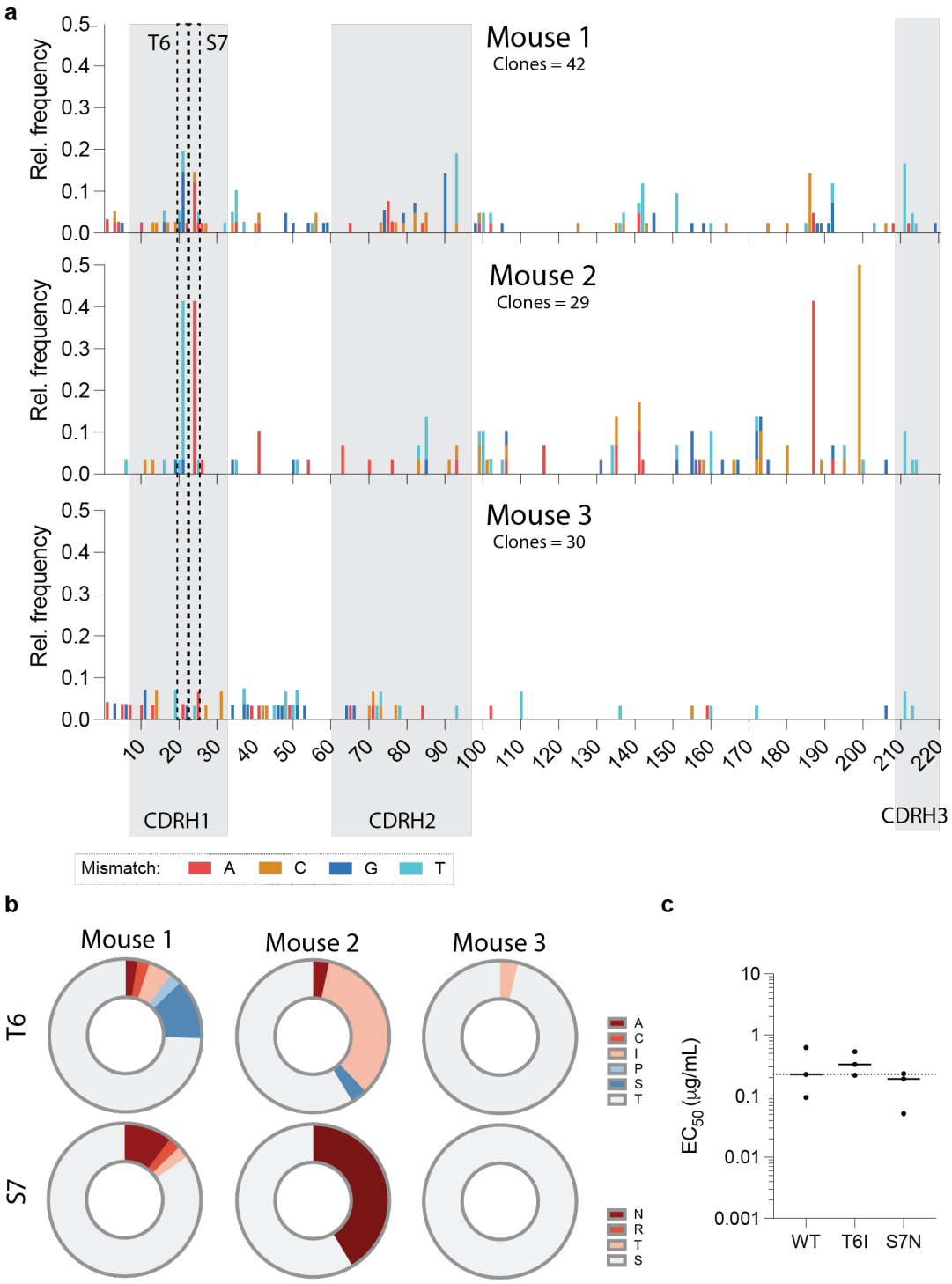


Figure 4.12: Unbiased screening of enriched mutations.

(a) Manhattan plot of V_H mismatches. **(b)** Substitutions of commonly mutated codons. **(c)** Common mutations were incorporated into BAR-1 via site-directed mutagenesis. Mutants were expressed recombinantly and screened against HEL-[–amidine-GM3g]$_6$ via ELISA. EC_{50} values were contrasted with the WT.

entropic cost, both analyses displayed balanced binding thermodynamics (TΔS = -1 kcal/mol and - 5.7 kcal/mol, respectively).

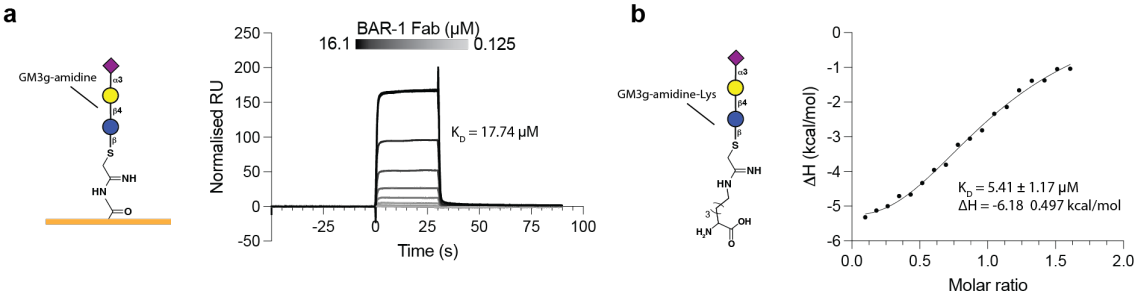


Figure 4.13: Biophysical characterisation of BAR-1.

(a) The binding kinetics of the BAR-1 Fab was evaluated via SPR using an amidine-GM3g-coated chip. **(b)** ITC was conducted with a soluble reductionist LOG mimic, Lys-amidine-GM3g.

Competition ELISAs using these soluble ligands was consistent with that observed using polyclonal sera (**Fig 3.19d**); namely, that binding could be competed out using soluble GM3g, but that soluble Me–amidine-GM3g was more efficient in blocking Ig binding (**Fig 4.14**).

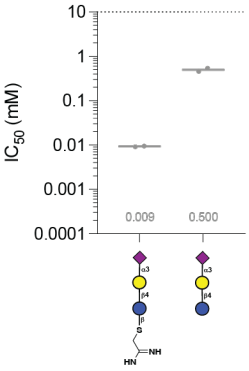


Figure 4.14: Inferred contributions of BAR-1 LOG recognition.

Competition ELISA was conducted using BAR-1 IgG and binding against HEL-[–amidine-GM3g]$_6$ was competed out using soluble ligand. IC_{50} values are shown.

Next, the atomic level basis of the BAR-1:Lys–amidine–GM3g interaction was evaluated via x-ray crystallography. The structure is available on the Protein

Database (PDB: 8BJZ). Dr Lucile Moynie co-crystalised a complex of BAR-1 Fab Lys–amidine-GM3g, and the structure was refined at 1.9 Å resolution. Crystallization of the BAR1•Lys–amidine-GM3g complex revealed a seemingly LOG-specific arrangement in the 3D-structure of the *holo* complex (**Fig 4.15**). First, the antibody approaches the LOG from a 'side-on' angle, with the terminal SiaGal moieties associated with CDRH1/2. The linker was, by contrast, bound by a more flexibly-engaged CDRL3 (**Fig 4.15a**). Notably, this leaves the part of the groove formed by CDRH3, CDRL1 and CDRL2 unoccupied. The antibody binding pocket is largely hydrophobic in character.

As a seemingly key 'foothold' the indole of $Trp57_H$ stacks against the alpha-face of the Gal sugar of GM3g to create a classical pi-CH interaction found in diverse so-called carbohydrate-binding modules (CBMs) (**Fig 4.15b**) (Cantarel et al., 2009; Lombard et al., 2014). This is supported by binding of the tip Neu5Ac sugar of GM3g, which makes five hydrogen bonds to the BAR-1 backbone, including a bidentate interaction of its C-1 carboxylate with amide nitrogen atoms of $Ala58_H$ and $Val59_H$, but notably there is no charge-driven interaction. Several highly coordinated water molecules (W) also contribute to binding, as well as a hydrophobic pi-CH interaction with $Phe37_H$. The reducing-end Glc of GM3g also makes hydrogen bonds to three water molecules, two of which bridge to the protein (including W3 which bridges to $Tyr99_L$, $Asn63_H$ and galactose) but only three direct van der Waal contacts with the protein. The amidine linkage of Lys–amidine-GM3g makes hydrogen bonds to the protein ($Tyr97_L$) and to a water molecule (W5) that bridges to the glucose and, intriguingly, a cation-pi interaction

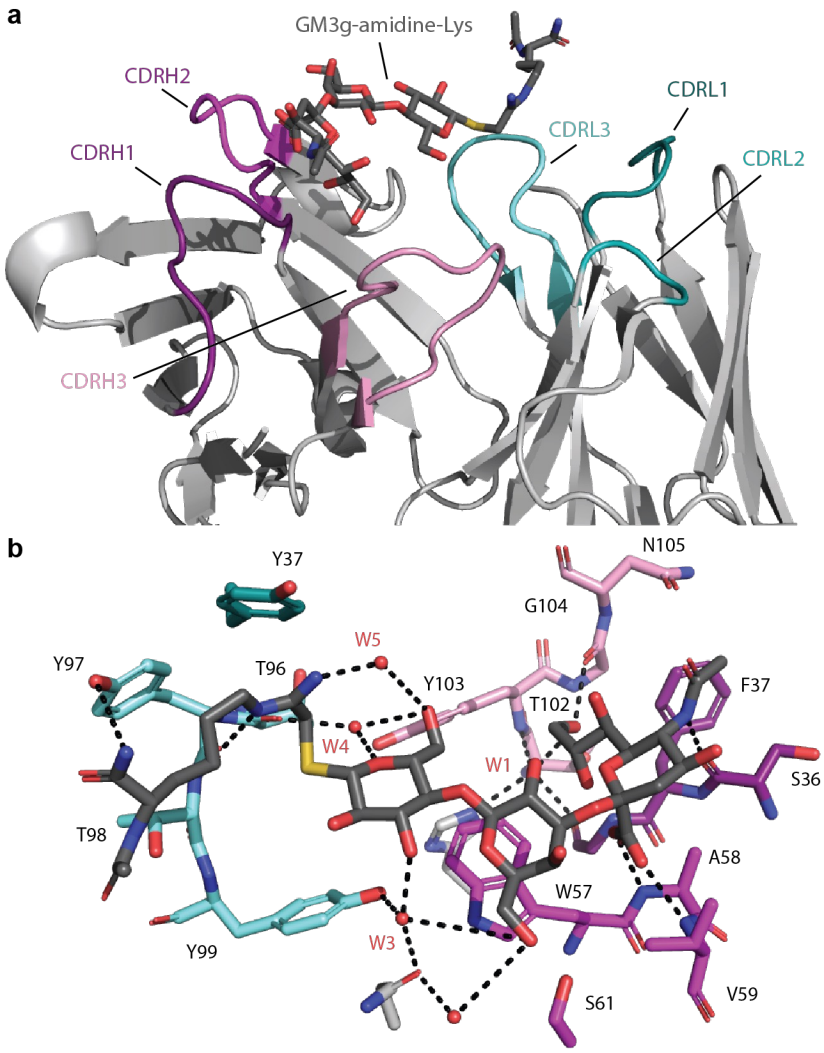


Figure 4.15: BAR-1 x-ray structure.

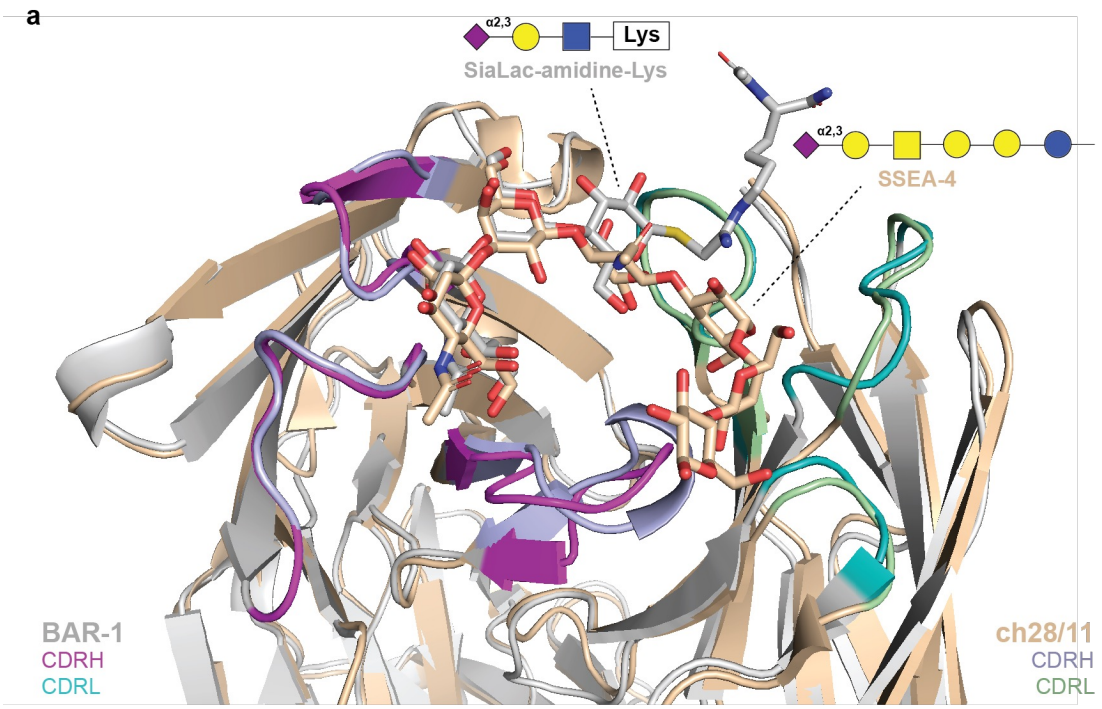
(a) Side view of the 1.9-Å x-ray structure of the BAR-1 Fab bound to the Lys-amidine-GM3g. Both heavy and light chain CDRs are marked. Binding site of GM3g-amidine-Lys. **(b)** Residues within 4.0 Å of the polysaccharide are displayed and hydrogen bonds are shown as black broken lines. Water is marked in red. Lys–amidine-GM3g is shown as sticks.

with $Tyr37_L$ confirming a contribution from the longer amidine linker to binding. The aliphatic side chain of the lysine makes van der Waal contacts with $Tyr97_L$.

Interestingly, the interactions of the tip disaccharide of GM3g, and their positions relative to BAR-1 Fab (including water molecules) are similar to those described for ch28/11 antibody clone (**Fig 4.16a**), which was raised against the SSEA-4 headgroup (a hexasaccharide) (PDB: 6UG7/6UG8) in mice (Soliman et al.,

2020b). The ch28/11 clone is of the same *IGHV* and *IGHJ* origins as BAR-1 (**Fig 4.16b**), which explains why the interacting residues in CDRH1 and CDRH2 in both structures are largely conserved. However, in the hexasaccharide there is a GalNAc in the third position, in contrast to glucose in the ligand studied here. The GalNAc makes hydrogen bonds and multiple van der Waal interactions with the antibody, as well as hydrogen bonds to bridging water molecules (including one like W3). The glucose and the GalNAc rings are offset by a 90° rotation (φ=265) as a result the hexasaccharide forms a U-shape whereas the Lys–C(NH)NH-GM3g adopts a more linear arrangement (φ=47/57). The hexasaccharide engages with the other loops in the ch28/11 alternative light chain, which would otherwise clash with the BAR-1 light chain. This represents a 'mix-and-match' model that the B cell repertoire takes in responding to sub-epitope structures: for example, *IGHV2* subgroup origin gene segments binding a common SiaGal moiety, while other gene segments are substituted to accommodate alternative adjacent epitope components.

To probe specific contributions to binding, I evaluated the residues lining the binding site of BAR-1 through Ala-scanning mutagenesis (**Fig 4.17a,b**). These results revealed several key residues where their substitution ablated antibody binding capacity, and these data were consistent with the x-ray structure of the BAR-1 Fab. For example, substitution of the 'foothold' $Trp57_H$ resulted in reduced binding in line with the observed pi-CH interaction with the Gal moiety of GM3g. Similarly, substitutions of $Phe37_H$, $His50_H$ and $A58_H$ that form either direct or bridging hydrogen bonds also impacted antibody binding. However, mutations in



b

```
HC                  <----------FR1---------><-CDR1-><------FR2------><-CDR2><-
BAR-1          7    VQLKQSGPGLVAPSQSLSITCTVSGFSLTSFGVHWVRQPPGKGLEWLGVIWAVGSTNY  64
ch28/11        7    VQLKESGPGLVAPSQSLSITCTVSGFSLNSYGVSWVRQPPGKGLEWLGVIWGDGSTNY  64
                    **** ************************ ** ****************  *****

                    ---------------FR3-----------------><---CDR3--><---FR4--->
BAR-1         65    NSALMSRLSISKDNSKSQVFLKMNSLQIDDTAMYYCATYGNYGGFAYWGQGTLVTVSS  122
ch28/11       65    HSALMSRLRISKDNSKRQVFLKLNSLQTDDTATYYCTKPGSGYAFAYWGQGTLVTVSS  122
                    ******* ******* ***** ***** **** ***   *    **************


LC                  <-----------FR1---------><-CDR1><------FR2------><2><-----
BAR-1          6    DIQMTQSPKSMSMSVGERVTLSCKASENVHTYVSWYQQKPEQSPKLLIYGASNRYTGV  63
ch28/11        6    ENVLTQSPAIMSASPGEKVTMTCSAS-SSVNYMHWYQQKSSTSPKLWIYDTSKLASGV  62
                    ****  ** * ** **  * **     *  *****   **** **       **

                    -------------FR3-------------><--CDR3-><-FR4->
BAR-1         64    PDRFTGSGSATDFTLTISSVQAEDLADYHCGQTYTYPFTFGSGTKL  109
ch28/11       63    PGRFSGSGSGNSYSLTIRTMEAEDVATYFCFQASGYPLTFGGGTKL  109
                    * ** ****     ***    *** * * * *   ***********
```

Figure 4.16: Structural overlay of BAR-1 and ch28/11.

(a) The x-ray structure of BAR-1 (grey) and SSEA-4-raised ch28/11 (gold) were overlayed as ribbons. Their respective ligands are marked and shown as sticks. **(b)** Amino acid sequence alignments of the two clones.

CDRH3, such as to $Tyr103_H$ did not affect antibody binding. Interestingly, BAR-1 has the CDRH2 residue $Val59_H$, which is deviant from the common residues in that position of similarly isolated GM3g-specific B cells (Gly or Asp are most common) and is a consequence of SHM. However, the substitution of this residue to Ala does not alter antibody binding; these data imply that $Val59_H$ does not significantly contribute to ligand binding. These data are consistent with the

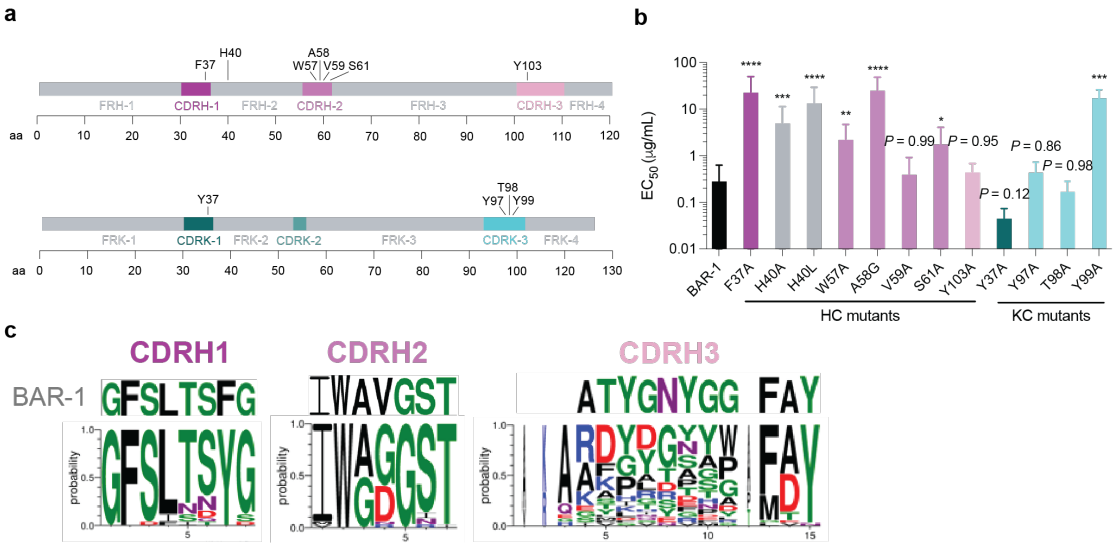


Figure 4.17: Alanine scan of BAR-1.

(a) Primary structure of BAR-1 HC and KC and select residues targeted for alanine scanning. **(b)** Site-directed mutagenesis was conducted on WT BAR-1 and mutants were expressed recombinantly. Mutants were screened against HEL-[–amidine-GM3g]$_6$. Data were compared pairwise via Tukey's posthoc test. *P*-value denotations: '*' $P < 0.05$, '**' $P < 0.01$, '***' $P < 0.001$ and '****' $P < 0.0001$. **(c)** CDRH logo plots of pooled GM3g-specific B cells isolated across mice.

immunogenetics from B cells isolated with the [–amidine-GM3g]-based molecular probe: affinity-critical residues are highly conserved across the BAR-1 antibody class, as indicated by the significant flexibility in CDRH3 (**Fig 3.17c**). Notably, substitutions in the light chains, including Tyr37$_K$, Tyr97$_K$ and Thr98$_K$, were shown to not impact antibody binding, although Tyr99$_H$ mutagenesis was detrimental. These data collectively highlight the definable gene-segment-specific flexibility in the antibody response against the LOG, for example, with the accommodation of diverse D_H- and J_H-encoded CDRH3s.

4.2.5. Predicting the translational potential of the [–amidine-GM3g] LOG

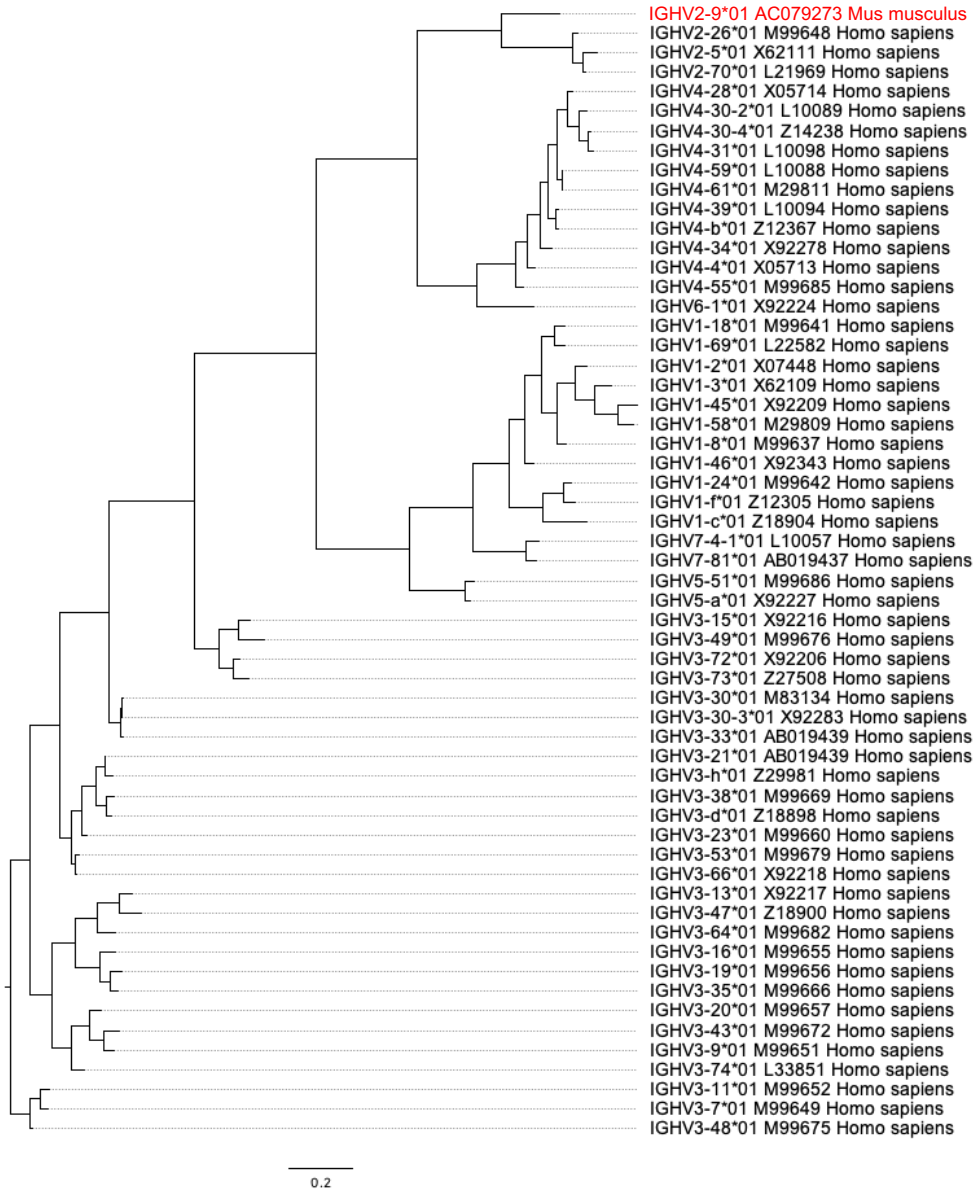
The initial screening and characterisation of LOG immunogenicity was conducted in a murine model. As previously described, the immunogenicity of the [–amidine-GM3g]-based LOG was underpinned by the presence of a definable "BAR-1

class" that depended on *IGHV2* subgroup-encoded lectin-like motifs that engaged the terminal SiaGal moieties. Having demonstrated this in an animal model, I aimed to determine whether these outcomes were likely to be reproducible in humans. Since the germlines between rodents and humans are highly divergent and most V_H gene segments have arisen subsequent to the divergence of the two organisms from their common ancestor (de Bono et al., 2004), I hypothesised that it was unlikely that a human 'cousin' of the BAR-1 class gene segments would be capable of recognising the LOG.

To test this, I first phylogenetically compared the BAR-1 gene segments to gene segments encoded in the human germline to determine the closest relative. For instance, *moIGHV2-9*01* was found to be closest to *huIGHV2-26*01* (**Fig 4.18a**). In this example, the amino acid sequence shared 58% (56/97) identity and 76% (74/97) positive (**Fig 4.18b**). When rationally considering *huIGHV2-26*01*, there were some considerable differences, such as a lengthened CDRH1, that implied that the inferred humanised counterpart for BAR-1 would not bind. However, several key residues were conserved including $Phe37_H$, while other key residues such as $Trp57_H$ were substituted for chemically similar Phe.

I expressed and purified a set of inferred humanised and semi-humanised BAR-1 antibodies—the huBAR-1 series—and compared their binding to that of wild-type BAR-1 (**Fig 4.19**). None of the huBAR-1 antibodies were reactive with gp120-$[$–amidine-GM3g$]_{16}$, suggesting that divergence in the gene segments ablates recognition of the glycoconjugate. Interestingly, even marginal humanisation, such as huBAR-1_V_K_only (wherein the only humanised gene

a



b

```
                  <----------FR1--------><--CDR1--><------FR2------><-CDR2><-
MoIGHV2-9*01   7  VQLKQSGPGLVAPSQSLSITCTVSGFSLTS--FGVHWVRQPPGKGLEWLGVIWAVGSTNY  64
HuIGHV2-26*01  7  VTLKESGPVLVKPTETLTLTCTVSGFSLSNARMGVSWIRQPPGKALEWLAHIFSNDEKSY  66
                  * ** *** ** *   *  *********     ** * ****** ****  *       *

                  ----------------FR3------------------>
MoIGHV2-9*01  65  NSALMSRLSISKDNSKSQVFLKMNSLQIDDTAMYYCAT 105
HuIGHV2-26*01 67  STSLKSRLTISKDTSKSQVVLTMTNMDPVDTATYYCAR 107
                     * *** **** ***** * *      *** ****
```

Figure 4.18: Comparison of murine IGHV2 gene segments with the human germline.

(a) *M. musculus IGHV2-9*01* was phylogenetically compared the subset of closest *H. sapien IGHV* gene segments. **(b)** Amino acid alignment of murine IGHV2-9*01 with human IGHV2-26*01.

segment is *huIGK4-1*01*) failed to react with the LOG. This outcome was surprising, since structural and biochemical analysis of BAR-1 implies a relatively flexible arrangement of the light chain.

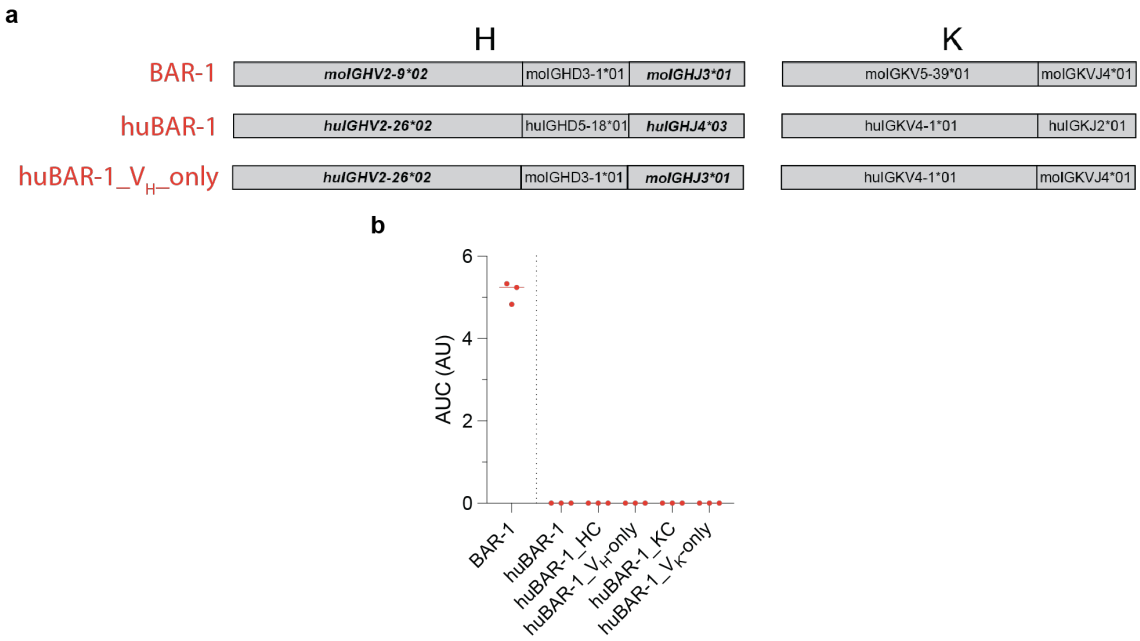


Figure 4.19: Inferred humanisation and partial humanisation of BAR-1.

(a) Human gene segment counterparts phylogenetically inferred. **(b)** Inferred humanised antibodies were recombinantly expressed and screened against gp120-[–amidine-GM3g]$_{16}$.

While attempts to phylogenetically infer a BAR-1-type humanised counterpart failed, it was possible that the human B cell repertoire might offer an alternative germline configurational 'solution' to LOG recognition. To test this, we accessed a humanised immune system (HIS) mouse developed by Drs James di Santo and Toshiki Eri. These mice were generated by sub-lethally irradiating BALB/c Rag2$^{-/-}$ IL2rg$^{-/-}$ Sirpa^{NOD} (BRGS) mice and re-constituting the haemopoietic line with CD34^{+} stem cells isolated from the livers of human foetuses (Li et al., 2018). Mice were immunised with gp120-[–amidine-GM3g]$_{16}$ with and without adjuvant (**Fig 4.20a**). Antibody responses were monitored over time.

No specific antibody titres were detected in any of the mice following three immunisations (**Fig 4.20b**). However, following an additional boost formulated with the potent experimental adjuvant 1% adjuplex (Wegmann et al., 2015), 2/10 mice modestly responded with an IgG antibody titre against the autologous

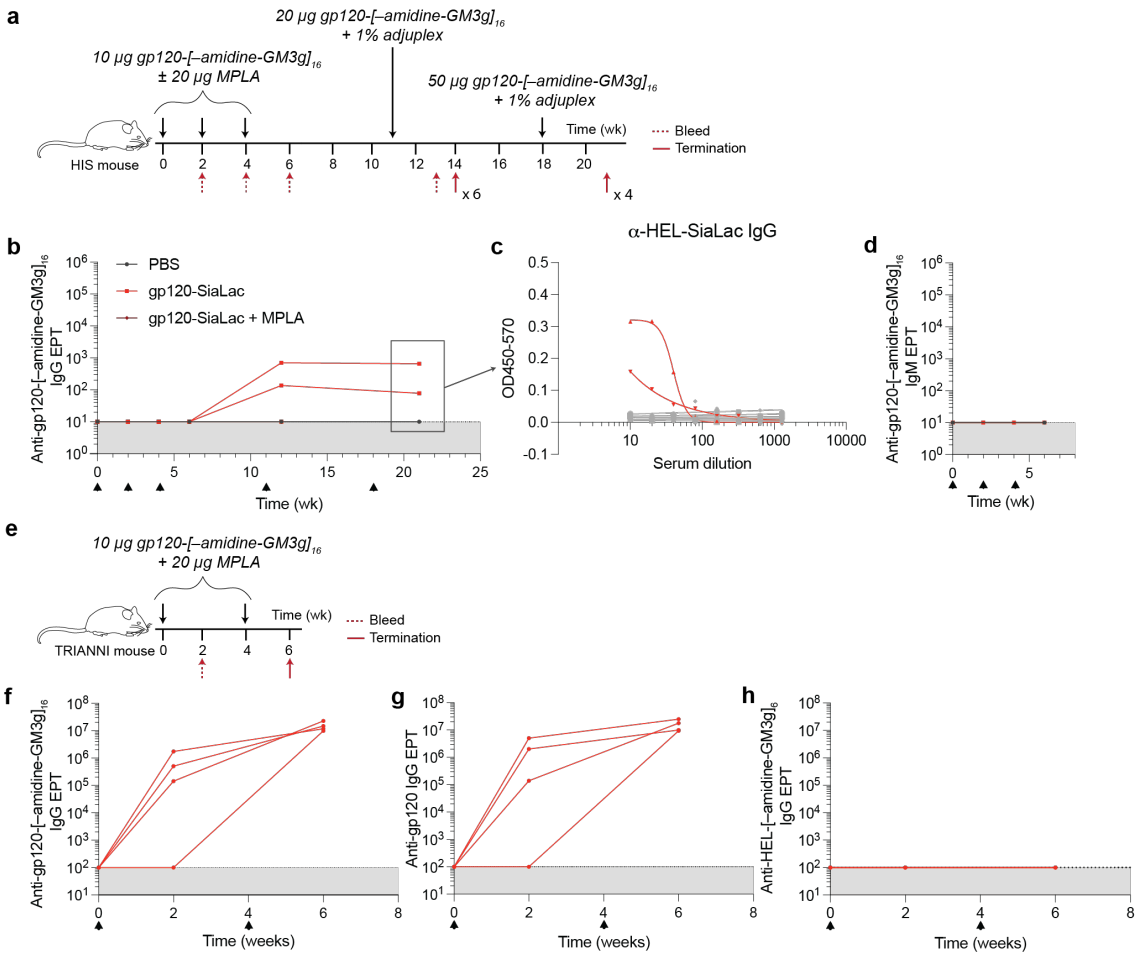


Figure 4.20: Evaluation of [–amidine-GM3g]-based LOGs in humanised animal models.

(a) HIS mouse immunisation protocol. **(b)** Endpoint titres against autologous gp120-[–amidine-GM3g]$_{16}$ were screened over the timecourse. **(c)** LOG-specific antibody titres were screened at the terminal timepoint. **(d)** Initial IgM responses were evaluated over the initial 5-week period. **(e)** TRIANNI mouse immunisation protocol. Serum IgG titres against **(f)** gp120-[–amidine-GM3g]$_{16}$, **(g)** gp120 and **(h)** HEL-[–amidine-GM3g]$_6$ were screened over the timecourse.

gp120-[–amidine-GM3g]$_{16}$ immunogen. There were two interesting observations about these responders: 1) the responding mice were recipients of stem cells from the same human donor, and 2) an additional boost did not further elevate the modest antibody response. To determine whether the antibody responses were reactive with gp120 or the LOG aspects of the antigen, terminal serum from all mice were screened against HEL-[–amidine-GM3g]$_6$, which revealed reactivity from the same two responding mice, suggesting a LOG-specific response. Notably, these HIS mice are highly immunodeficient, struggling to propagate a B

cell response—this is evidenced by the low (~3 order of magnitude less) serum Ig compared with wild-type mice (Li et al., 2018).

Therefore, to test the LOG immunogenicity against a human germline in a less immune-deficient model, we accessed TRIANNI mice from Prof Klaus Überla and Dr Dominik Damm. These mice carry an entire set of human V gene segments (including lambda) and have been shown to clonally recapitulate the human B cell response to a given antigen (Peter et al., 2022). We immunised TRIANNI mice with gp120-[–amidine-GM3g]$_{16}$ in MPLA and, despite a robust response against the gp120 backbone, found that none of the mice generated a response against the LOG post-boost (**Fig 4.20e–h**).

4.3 Discussion

For self-glycans, it is intuitive that there be heavy incentive for the skewing of the naïve B cell repertoire against the induction of self-glycan-reactive antibodies (Deimel et al., 2022; Kim et al., 2000; Livingston and Ragupathi, 2006; Zhu et al., 2009). This is evidenced by the anti-glycan responses being associated with various autoimmune conditions, including Crohns disease and neurodegenerative disorders (Dotan et al., 2006; Polonskaya et al., 2019; Temme et al., 2021). However, the selective breaking of glycan tolerance or passive administration of a glycan-specific antibody may be of significant clinical benefit in certain settings, such as against specific cancers (as reviewed in **Chapter 1**). Previous studies have failed to reliably raise antibodies against self-glycans via vaccination using conventional vaccine formulations of natively presented glycans in both murine models and in the clinic (Chapman et al., 2000;

Krug et al., 2004; Kuduk et al., 1998b; Ragupathi et al., 2006). The phenomenon of self-glycan immunorecessiveness is presumably a function both of biases against germline-encoded, self-glycan reactive V-, D-, J-gene segments/configurations, as well as negative selective processes in primary and tertiary lymphoid organs that delete or modify self-reactive clones (Goodnow et al., 2010; Nemazee, 2000).

To overcome glycan immunorecessiveness, in **Chapter 3** I describe a novel semi-synthetic carbohydrate coupling chemistry that artificially displays GM3g in a non-native manner (via a short amidine linker fixed to the primary amine of lysine sidechains), which was found to be highly immunogenic in mice. In the present study, I dissect the molecular basis for the immunogenicity of LOG, [–amidine-GM3g]: i) the immunogenetic and structural rationale for how non-native presentations of otherwise immunorecessive TACAs via bespoke chemical linkers may bypass the tolerogenic constraints that prevent antibodies being raised against native glycan presentations in endogenous glycoconjugates; ii) the docking of sugar to a protein carrier allows for associated T cell help that can be exploited to toggle the germinal centre experience of B cells; iii) how the clonal response against the LOG ultimately explains the context dependency in glycan recognition, failing to cross-react with native glycan presentations, such as ganglioside, GM3, and iv) the germline-encoded constraints that prevent translatability from murine models to humans. While in this study I focus on the model self-glycan GM3g, I envisage that these outcomes may be broadly generalisable to other self-moieties beyond carbohydrates. To this end, I discuss

the significance and lessons learned from this model, and how my findings might help inform vaccine design moving forward.

4.3.1. Clonal responses to LOGs: lectin-like motifs in the germline

The discovery that the [–amidine-GM3g]-based LOG readily mounted IgG responses in a mouse predominantly via the *IGHV2* subgroup reveals that such modular formats can access a subset of naïve B cell configurations that native presentations of the same glycan do not. These data provide deeply instructive clonotypic response data that challenge the dogma of global self-glycan immunorecessiveness, and instead reveal a context-dependency of glycan reactivity, with non-native (‘orthogonal’ rather than ‘parallel’) presentations readily permitting an autologous response. I dissect this glycoconjugate reactivity by combining serological, immunogenetic, structural, biochemical and biophysical analyses.

For example, the structure of the BAR-1 Fab co-crystalised with reductionist Lys–amiding-GM3g reveals that the sugar portion is recognised by CDRH1 and CDRH2, encoded by the originating germline-encoded *IGHV2* gene segment. There are interactions observed between the glycoconjugate and antibody that closely resemble classical protein–carbohydrate recognition: for example, pi-CH interactions between the beta-face of Gal and the indole ring of Trp is a signature glycan ‘foothold’ motif observed across most mammalian galectins (Rogers et al., 2007; Shao et al., 2022). Moreover, the binding pocket of BAR-1 is conducive of the recruitment of bridging water molecules, and bidentate hydrogen bonding between the carboxylate of the terminal sialic acid with the protein backbone and

the engagement of the methyl of the *N*-acetyl by an aromatic residue. This arrangement is seen for the hexasaccharide binding antibody (ch28/11; an SSEA-4-binding antibody) that is similarly of an *IGHV2*-encoded origin (Soliman et al., 2020b). These data suggest a molecular explanation for how moiety context and presentation affect immunogenicity: the LOG modular format of GM3g effectively 'throws the germline a rope', enabling a unique and definable clonotype to access the GM3g moiety.

4.3.2. Carrier protein toggles GC experience but not LOG-specific clonality

Tfh cells are a specific helper subset that are critical for the formation and maintenance of germinal centres, and thus are highly deterministic of B cell fate and affinity maturation (Chen et al., 2012; Crotty, 2014; Vinuesa et al., 2016b). In line with the fundamental biology of Tfh cells, I observed that the protein carrier had an impact on the B cell outcomes of isolated LOG-specific cells; I contrasted outcomes from two different protein carriers—HEL (which is poor inducer of T cell help) and gp120 (which offers high T cell help). As anticipated, the protein backbone used to carry the [–amidine-GM3g] did not affect the clonotypic response against the LOG, with the same V_H, D_H, J_H gene usage observed. This is unsurprising since LOG antigenicity is unchanged, however, the protein backbone did affect tertiary lymphoid responses against the LOG.

B cells were isolated from mice immunised 4-weeks post-prime, and this reflects a relatively late-/end-stage follicular response (Elsner and Shlomchik, 2020). In mice immunised with HEL-[–amidine-GM3g]$_6$, no GM3g-specific B cells were isolated in the draining iLN, reflecting the cessation of the local secondary

lymphoid organ response. In contrast, many GM3g-specific B cells were isolated from gp120-[–amidine-GM3g]$_{16}$-immunised mice at the same timepoint, reflecting a continuation in the follicular response. I infer that these outcomes were a function of differing Tfh supply by the protein backbone. In corroboration, the extent of somatic hypermutation experienced by GM3g-specific B cells was proportional to the Tfh numbers supplied by the carrier protein. These data are reminiscent of early hapten-carrier studies that similarly implied that hapten-specific antibody affinity was contingent on the carrier protein used (Mitchison, 1971). While our data do not demonstrate improved affinity (as discussed in *Section 4.3.3.*), the change in SHM does imply a carrier effect, and suggests that glycoconjugate or other conjugate-based vaccines should consider the suitability of the Tfh supply imparted by the carrier protein.

Interestingly, while there was a trend whereby the gp120 backbone immunisation was associated with a greater number of non-singleton B cells (which I hypothesised as being reflective of greater extent of T cell-mediated B cell clonal expansion), the backbone did not significantly affect clonal richness; this is unsurprising since data suggests that GCs favour diverse input clones (Hägglöf et al., 2023; Mesin et al., 2020; Schaefer-Babajew et al., 2023). These data are interesting and perhaps reflect a basic germinal centre phenomenon that Tfh supply does not penalise opportunity for new clones to enter the germinal centre.

4.3.3. SHM without affinity maturation: affinity ceiling reached or tertiary negative selective forces?

Outcomes of affinity maturation were evaluated in two different ways. First, members of a large clonal family were expressed and tested against the LOG. Second, to approach this in an unbiased manner, common CDR mutations incorporated during SHM were identified (McNamara et al., 2020), enriched mutations were incorporated into BAR-1 via mutagenesis and relative binding was compared. Interestingly, neither approach identified specific mutations that improved LOG binding. The apparent lack of affinity maturation despite SHM was surprising but may be explained by one of two phenomena.

First, it is possible that the LOG-specific clones may have reached something of an 'affinity ceiling'. For example, BAR-1 was found to have an affinity for the autologous glycoconjugate with a K_D value in the low–mid μM range. This is marginally better than the affinity of GM3g for professional carbohydrate binding lectin CD22/SigLec7 (37.4 μM) (Blixt et al., 2008; Hong et al., 2021; Yamakawa et al., 2020). It could be hypothesised that the nature of the LOG epitope is not conducive to high-affinity interactions based on its structural characteristics: i) the LOG epitope surface area is relatively small compared to the surface of a hypothetical protein epitope and thus the set of possible antigen–antibody interactions is smaller; ii) the GM3g component of the LOG lacks considerable structural rigidity, with flexibility both about the saccharidic bonds and flexibility in the rings (Anggara et al., 2021; Jana and Bandyopadhyay, 2012), and iii) protein–glycan interactions tend to rely on packing and low-energetic hydrogen bonding and hydrophobic interactions rather than electrostatic interactions typical of high-

affinity protein–protein interactions (Deimel et al., 2022). These chemical features of LOGs may cumulatively underpin the apparent lack of affinity maturation.

Second, an alternative (or potentially additional) explanation is that negative selective forces in GCs may delete clones of higher affinity to the carbohydrate. While the mechanistic underpinnings for negative selection within GCs has been long debated (Liu et al., 1997; Victora and Nussenzweig, 2022), it remains unclear how responding cells within tertiary lymphoid organs interpret antigenic signals as negative versus positive.

To test whether a hypothetical positive selective clonal outcome is achievable via SHM, one could perform a directed evolution-based artificial affinity maturation or deep mutational screen, such as the precursory yeast display models previously published (Cherf and Cochran, 2015; Starr et al., 2020). Critically, such a model should use AID to facilitate the incorporation of mutations, since AID has particular mutation hotspots/coldspots, and there are some codon–codon switches AID cannot make (Maul and Gearhart, 2010; Rogozin and Kolchanov, 1992; Wagner et al., 1995). The identification of possible affinity maturational outcomes would suggest that an affinity ceiling is not met, but rather indicate a possible negative selective force acting to delete high-affinity self-glycan-reactive clones.

4.3.4. 'Walking' the BAR-1 class: challenges and feasibility

Structural characterisation of BAR-1 explained why the anti-LOG response fails to cross-react with ganglioside GM3: in the associated clonal class, the orientation of Lys–amidine-GM3g reaches through to the sugar-binding pocket by spanning the V_HV_L interface to be recognised by the CDR3 loop of the V_L domain. In native GM3, the trisaccharide has a glycosidic link in close proximity to the branched arrangement of the ganglioside (displaying stearic acid and sphingosine). A 'reach through' mode observed for Lys–amidine-GM3g would therefore be unavailable to 'self' GM3. Close embedding of GM3 into the membrane creates prohibitive van der Waal clashes for antibody engagement.

These observations invite investigation of heterologous boosting, much like that explored by the HIV-1 antibody-based vaccine research field (Collins et al., 2015; Jardine et al., 2013, 2016; Leggat et al., 2023; Stamatatos et al., 2017; Steichen et al., 2016). For example, subsequent boosting with GM3g coupled via systematically varied LOGs conjugated to different chemical linkers might exploit affinity maturation processes to 'walk' clones towards native glycan reactivity. This is unlike classical germline-targeted approaches, which use isolated and highly mutated antibodies of known functional effect as a template germline clonal class (Escolano et al., 2019; Steichen et al., 2016). In the instance described here, it is not known whether 'up-mutation' of the BAR-1 class can move towards a functional effect to yield native GM3g recognition.

It is also critical to note that emerging data on basic germinal centre mechanics implies that continual recall into the germinal centre is unlikely. First, given the

apparent trend of memory B cells to preferentially re-activate and differentiate into plasmablasts (Mesin et al., 2020), it is unclear how best to continuously refeed GC activity with related heterologous antigens to favour particular affinity maturation outcomes. Relatedly, the production of antibodies by plasmablasts drives 'epitope masking' wherein the 'attention' a GC can give clones competing for a particular epitope will compete with existing systemic antigen-specific Ig (Inoue et al., 2023; McNamara et al., 2020; Schaefer-Babajew et al., 2023). Collectively, given both the structural and GC biology challenges in actively 'walking' these clones *in vivo*, further investigation of this approach seems unlikely to yield a successful outcome.

4.3.5. Translational limitations of the murine model

A key theme for B cell biology and vaccine immunology over the past decade is an appreciation of the germline and clonal underpinnings of an antibody response—that the functional serological response is dependent on suitable naïve B cell representation (Stamatatos et al., 2017). Therefore, as a model for active immunisation, mice (which have a highly divergent germline repertoire compared to that of humans) are unlikely to be useful predictive models for functional antibody translation (de Bono et al., 2004). In this study, I endeavoured to predict whether the human germline could similarly mount an antibody response against the [–amidine-GM3g] LOG. There was minimal induction of a successful outcome—having explored both humanised animal models and rationally predicting the human BAR-1-type clonal counterpart—that a canonical LOG-specific antibody response could be mounted in humans.

4.3.6. Conclusions

In this chapter, I highlight how the LOG modular amidine-based display of GM3g accesses germline-encoded lectin-like motifs (Gabba et al., 2021; Tobola et al., 2018; Topin et al., 2016) present in the murine BCR germline. This not only challenges the dogma associated with the perceived poor immunogenicity of glycans (Livingston and Ragupathi, 2006) but may also provide an explanation for the greatly divergent views and results that have in the past been obtained from immunisations with glycoconjugates (Kim et al., 2000; Livingston et al., 1989; Livingston and Ragupathi, 2006). My data suggest how glycan display can access ‘glycan-ready’ but context-dependent germline BCRs. Having identified and characterised the novel BAR-1 clonal class, I provide an immunogenetic, structural and biochemical explanation for the lack of cross-reactivity with native GM3g presentations. These findings inform how synthetic protein chemistry might be used to ‘fish out’ germline clonal classes otherwise inaccessible to native presentations, and inform the logical design of germline-informed vaccines.

Chapter 5—Antibody responses against β-lactam antibiotics

5.1 Background

5.1.1. Penicillins as haptens

Non-protein, low molecular weight compounds are typically non-immunogenic (Clementi et al., 1991). As exemplified by classical hapten-carrier biology, antibody responses against model haptens like nitrophenol (NP) requires conjugation to a suitable carrier protein (Eisen and Siskind, 1964). The attachment of a hapten to protein means that, within the same antigenic complex, a cognate BCR may cross-link the protein-bound hapten-encompassing epitope, while associated peptidic components can be presented to T cells, imparting linked help to propagate the activated hapten-specific B cell population (Mitchison, 1971).

As outlined in **Section 1.9**, the principle of hapten-carrier immunogenicity may be extended to small-molecule drugs. For example, drugs with chemically

unstable functional groups may form drug–protein conjugates under physiological conditions and result in the production of immune complexes elicit downstream ADA responses. This may have inadvertent pharmacokinetic and pharmacodynamic consequences under certain settings. While the ADA phenomenon is best characterised in the context of antibody-based biologic therapies, where anti-idiotopic effects can reduce drug bioavailability and potentially hinder efficacy (Ben-Horin et al., 2011; Vaisman-Mentesh et al., 2019), the molecular and immunological mechanics of small-molecular-directed ADAs are less well defined.

A model small-molecule drug class that is shown to form adducts *in vivo* is penicillin-type β-lactam antibiotics. Indeed, administration of the drugs, such as PenG, is associated with the production of ADAs in some patients (Lafaye and Lapresle, 1988). Understanding the mechanistic underpinnings of the ADAs and their implications *in vivo* may be clinically relevant, given both the frequency with which PenG is used, and the number of patients who exhibit antibody-mediated hypersensitivity against the drug.

5.1.2. PenG-specific immunity and allergy: gaps in the literature

PenG-specific antibodies are reported in many patients who are treated with the drug; that is, a far greater proportion of patients display ADAs than those who merely exhibit specific IgE-mediated type I hypersensitivity (Lafaye and Lapresle, 1988). While *in vitro* drug modification analyses have determined that the β-lactam ring is highly unstable, readily hydrolysing or combining with amines under certain buffer conditions (Bahmany et al., 2023), the formation and

immunogenicity of penicilloyl adducts *in vivo* are not well-characterised. For instance, while Levine and Ovary in their seminal studies in rabbits showed pre-complexed PenG-adducts to be immunogenic, their model deviates from clincal administration of drug: immunisations were formulated with complete Fruend's adjuvant, foreign protein carriers were used and optimised, and *ex vivo* modification of protein enhances adduct occupancy beyond that which may occur *in vivo* (Levine and Ovary, 1961).

Indeed, despite PenG adducts presumably forming *in vivo* (as evidenced by clinical serology) and the assumed role of these adducts in antibiotic sensitisation, the conditions that affect both i) the coupling of drug *in vivo* and ii) the immunological factors determining a response to these adducts remains unclear. There is significant scope to develop an animal model to investigate these factors, and investigate the clonal B cell responses against these adducts.

5.1.3. Aims

In this chapter, the main aims include to:

1. Determine the chemical coupling conditions that cause the formation of penicilloyl-type adducts on carrier proteins and their relevance to physiology.
2. Develop a murine system to establish the conditions modulating the immunogenicity of PenG adducts, including the effects of the carrier protein.
3. Evaluate the clonotypical response against PenG and predict the functional implications of the antibody products.

5.2 Results

5.2.1. Evaluation of pre-coupled PenG–protein complexes in mice

As previously outlined, PenG is a penicillin-type β-lactam antibiotic drug with constituent β-lactam, haizolidine and benzene functional groups (**Fig 5.1a**). Previous studies have shown that under specific buffer conditions, specifically with carbonate buffers, the β-lactam ring will become highly reactive (Brouwers et al., 2020; Kipper et al., 2018). Studies have reported that this drug will covalently bond with the primary amines of lysine sidechains to form stable penicilloyls, although modifications to both arginine and histidine are also reported (**Fig 5.1b**) (Lapresle and Wal, 1979; Levine and Ovary, 1961; Yvon et al., 1990; Yvon and Wal, 1988).

I first aimed to comprehensively evaluate the immunogenicity of PenG adducts on foreign protein. To this end, I modified HSA with PenG (HSA-PenG) *in vitro* according to modification conditions previously published (Meng et al., 2017b) and immunised mice with this antigen in formulation with alum, bleeding animals periodically (**Fig 5.1c,d**). The IgG EPT against PenG was determined by direct ELISA against a similarly modified unrelated protein, HEL-PenG. The data revealed that immunisation with HSA-PenG in alum resulted in high drug-specific titres post-prime, and the titres compared to the unmodified HSA control were significantly greater (median EPT of 171 [HSA], compared 222,001 [HSA-PenG]; $P = 0.029$, Mann-Whitney test) (**Fig 5.1e,f**). No antibody reactivity was detected against HEL (**Fig 1.5g**). Collectively, these data imply that PenG adducts are immunogenic in mice.

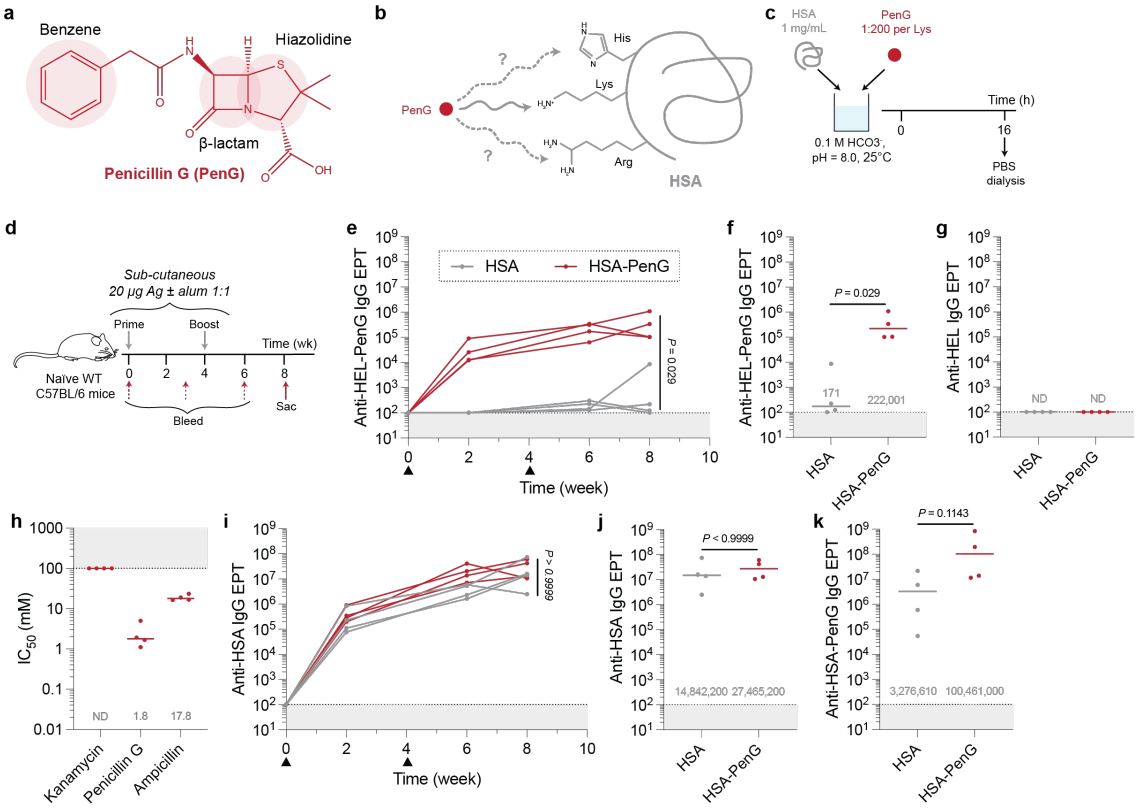


Figure 5.1: Serological response to pre-complexed HSA-PenG in mice.

(a) PenG. **(b)** The drug is stipulated to react preferentially with lysine but my also complex with arginine and histidine. **(c)** Reaction conditions in modifying HSA *in vitro*. **(d)** 6-week-old sex-matched WT C57BL/6 mice were immunised according to the shown schedule. **(e)** IgG EPTs were monitored throughout the timecourse against HEL-PenG to determine the drug adduct-specific titres. Terminal titres against the **(f)** adduct and **(g)** the unmodified HEL negative control. **(h)** Competition ELISAs were conducted using HSA-PenG antisera, wherein dilutions of free drug were screened against a HEL-PenG-coated plate. **(i, j)** IgG EPTs against the unmodified HSA protein backbone, and **(k)** HSA-PenG. Dots represent data from a single mouse. Groups were compared via Mann-Whitney tests.

Next, to evaluate the specificity of the antibody response, a competition ELISA was performed where HSA-PenG antisera binding to HEL-PenG was competed out using soluble antibodies. Interestingly, the median IC_{50} value for PenG was 1.8 mM, and binding was similarly competed out using ampicillin, although competition was approximately an order of magnitude less efficient (17.8 mM) (**Fig 5.1h**). Notably, ampicillin is structurally very similar to penicillin, differing only

by an additional amine group on the acylamino side chain. No competition was detected using kanamycin, a non-β-lactam-type negative control. These data provide some evidence of antibody cross-reactivity with other β-lactam antibiotics, and suggests a low affinity polyclonal serum antibody response.

There were no significant differences in the EPTs against the protein backbone between animals immunised with HSA or HSA-PenG (terminal timepoint: $P > 0.9999$, Mann-Whitney test) (**Fig 5.1i,j**). Although statistically insignificant, titres against HSA-PenG were on average ~3-fold greater in animals immunised with HSA-PenG antigen rather than unmodified HSA ($P = 0.1144$, Mann-Whitney test) (**Fig 5.1k**). This likely reflects both 1) PenG adducts on the plate coat disrupting native HSA epitopes, and 2) HSA-PenG antisera recognising the subset of penicilloyl-containing epitopes.

Having shown that a pre-complexed HSA-PenG antigen was immunogenic in mice, I next characterised the relationship between modification conditions and the frequency of penicilloyl adduct using HEL as a model carrier protein. 16 h incubations at a 1:200 drug-to-lysine ratio was tested in 0.1 M carbonate buffer under various pH conditions. Penicilloyl occupancy was evaluated by mass spectrometry (these data were acquired by Dr Guoxuan Sun). Data revealed a modal penicilloyl adduct number of 3 for pH 6.8–8, and a modal number of 4 for pH of 10–11.7 (**Fig 5.2a**). It is unclear whether the increase in adducts under highly basic conditions is a consequence of more efficient conjugation or whether protein denaturation changed accessibility of PenG target residues. Notably, HEL has 6 lysine residues, and up to 11 penicilloyl adducts detected, suggesting some

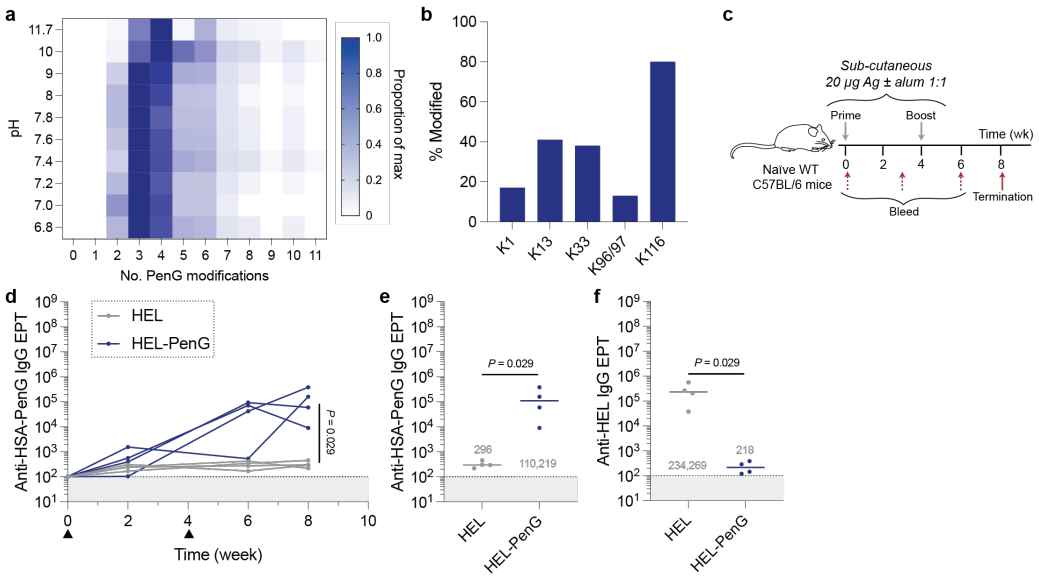


Figure 5.2: Immunogenicity and chemical characterisation of pre-complexed HEL-PenG.

(a) Number of penicillin adducts on HEL were evaluated via mass spectrometry analysis under various pH conditions. **(b)** LCMS/MS mapped the site occupation frequency of penicillin adducts on HEL. **(c)** 6-week-old sex-matched C57BL/6 mice were immunised. IgG EPTs were measured against HSA-PenG as a measure of the PenG adduct-specific response; both **(d)** longitudinal and terminal **(e)** titres are shown. **(f)** Terminal EPTs against the protein backbone. Dots represent data from a single animal. Data were compared via Mann-Whitney tests.

modification of non-lysine residues (likely arginine or histidine). To understand the site-specific modification, LCMS/MS was conducted by Dr Sean Burnap, which revealed that K116 was preferentially modified (82%), while K1 and K96/K97 were infrequently modified (< 20%) (**Fig 5.2b**). Notably, modification under alternative non-carbonate-based buffer systems were also tested; these (such as PBS) were shown to not (or inefficiently) facilitate PenG modification to protein (data not shown).

The immunogenicity of HEL-PenG modified at pH = 8.0 in carbonate buffer was tested in mice, formulated with alum (**Fig 5.2c**). PenG adduct-specific IgG antibody titres were evaluated against HSA-PenG. The data revealed modest titres against the glycoconjugate post-boost, with a terminal median EPT of

110,219, which was significantly greater than the unmodified HEL control (P = 0.029, Mann-Whitney test) (**Fig 5.2d,e**). Interestingly, the PenG-specific EPTs post-prime were relatively low, compared with mice immunised with HSA-PenG—this may be a function of the poor T cell help imparted by HEL, as described throughout **Chapters 3 and 4**. Interestingly, HEL-PenG antiserum had very low titres against the unmodified protein backbone, compared with HEL antisera (P = 0.029, Mann-Whitney test).

Next, lymphocyte proliferation was evaluated via a ^{3}H-thymidine incorporation assay. Whole splenocytes from mice immunised with either HEL-PenG or HSA-PenG (**Fig 5.1d, Fig 5.2c**) were harvested and re-stimulated *in vitro* (**Fig 5.3a**). The data revealed that splenocytes from mice immunised with HSA-PenG stimulated with autologous antigen resulted in a significant increase in ^{3}H incorporation (P = 0.0254, paired t-test with Bonferroni correction) (**Fig 5.3b**). Interestingly, re-stimulation with unmodified HSA did not result in the same outcome, implying that proliferation was dependent on the PenG adduct. No proliferation was detected under any re-stimulatory condition in splenocytes derived from mice immunised with HEL or HEL-PenG, again probably reflecting the weak T cell immunogenicity of HEL.

Cytokine supernatant was screened for IFN-γ production, and these data reflected the proliferation data, with a sharp increase in cytokine production in HSA-PenG-immunised splenocytes re-stimulated with autologous antigen (P = 0.0015) **(Fig 5.3c**). These data imply that the increase in proliferation was likely a function of a peptide-PenG-specific Th population, despite the assay

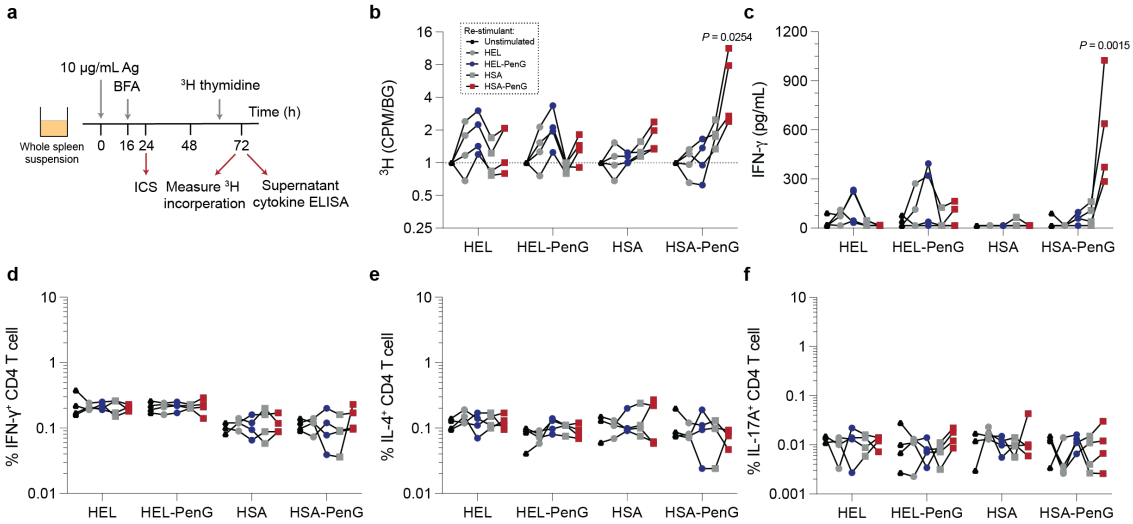


Figure 5.3: Memory splenocyte responses against PenG-modified proteins.

(a) Experimental pipeline for *in vitro* splenocyte re-stimulation assays. **(b)** Incorporation of ^{3}H-thymidine was measured and normalised to background. Relative counts per million were presented on a $\log_2$ scale. **(c)** IFN-γ production in cell supernatant was measured via ELISA. ICS was conducted on re-stimulated splenocytes, reporting the percentage of **(d)** IFN-γ^+, **(e)** IL-4$^+$ and **(f)** IL-17A$^+$ CD4 T cells. Data were compared via paired tests.

being performed on whole splenocytes. ICS was also performed on these splenocytes, although no specific IFN-γ^+, IL-4$^+$ or IL-17A$^+$ antigen-specific CD4 T cell population was detected, likely attributable to the poor sensitivity of the assay (**Fig 5.3d–f**).

5.2.2. Determining the humoral responses following free PenG administration

Having demonstrated the immunogenicity of pre-complexed protein-PenG constructs in formulation with adjuvant, I next aimed to determine whether a drug-specific titre could be measured following the administration of free drug. First, mice were given two week-long courses of antibiotics delivered i.v. daily (**Fig 5.4a**). However, no IgG or IgM responses specific to the drug were detected, when compared to mice given a PBS control (**Fig 5.4b,c**).

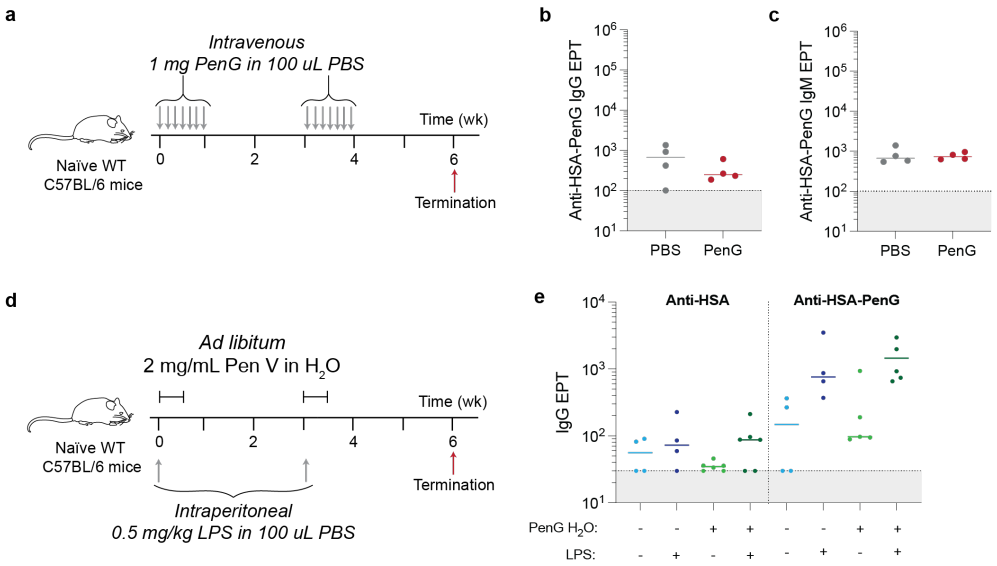


Figure 5.4: Determining the antibody response following free PenG administration.

(a) 6-week-old sex-matched C57BL/6 mice were given two week-long courses of PenG intravenously. Terminal **(b)** IgG and **(c)** IgM EPTs against HSA-PenG were compared. **(d)** Mice were given PenV in drinking water *ad libidum* over two 3.5-day intervals. Some mice were given an intraperitoneal injection of LPS. **(e)** IgG titres against HSA and HSA-PenG were evaluated at the terminal timepoint.

The immunogenicity of orally-administered antibiotic was also evaluated. Here, penicillin V (PenV) was used, which is chemically very similarly to PenG (differing by an ether group in the acylamino side chain). Unlike PenG, PenV is used for oral administration as it does not degrade under the acidic conditions of the stomach (Poschet et al., 1999). Mice were given PenV *ad libitum* for two 3.5-day intervals. Some mice were additionally given an i.p. dose of LPS (0.5 mg/kg) to mimic the systemic increase in endotoxin expected from a bacterial infection, where antibiotics such as PenG are clinically used (**Fig 5.4d**). The innate-immune stimulating effects of the LPS administration was hypothesised to potentiate/'adjuvant' a possible anti-drug response. Despite this, no specific PenG titres were observed, when IgG EPTs were evaluated at the terminal timepoint (**Fig 5.4e**). Interestingly, administration of LPS was shown to increase

the background reactivity of serum: mice given PenG and LPS or drug-free water and LPS only both exhibited modest reactivity against HSA-PenG.

I hypothesised that the failure to initiate a serological response following the administration of free drug may have been a consequence of rapid clearance of the antibiotic in a mouse; for instance, mice have an extremely high cardiac output (20.4 ± 3.4 mL/min) (Kreissl et al., 2006) and renal clearance of PenG is rapid, with a half-life of approximately 15 mins (Erlendsdottir et al., 2001). The fast clearance of the drug may have restricted the time available for endogenous PenG adducts to form in this animal model, or the adducted proteins may have been rapidly cleared, ultimately reducing the probability for B cell cross-linking and adduct uptake/presentation to other immune cell types.

To improve the availability of free drug *in* vivo, I used penicillin G benzathine (PenG-Ben), a formulation of PenG with diphenylethylene diamine that renders PenG poorly soluble (**Fig 5.5a**). When administered intramuscularly, PenG-Ben is slowly hydrolysed (days–weeks) to release PenG systemically (Merad et al., 1998). PenG-Ben was administered intramuscularly to 7 mice. Two courses of three doses were administered (**Fig 5.5b**), and antibody response were evaluated throughout the timecourse. After the initial course, 1/7 mice responded with a PenG-specific IgG EPT, as evidenced by serum reactivity with OVA-PenG but not unmodified OVA (**Fig 5.5c–f**). Notably, after the second course of PenG-Ben, no additional mice responded with a drug-specific titre. Titres in the responding mouse did not elevate, indicating a failure to trigger a boost response. These data suggest an infrequent response following PenG-Ben administration.

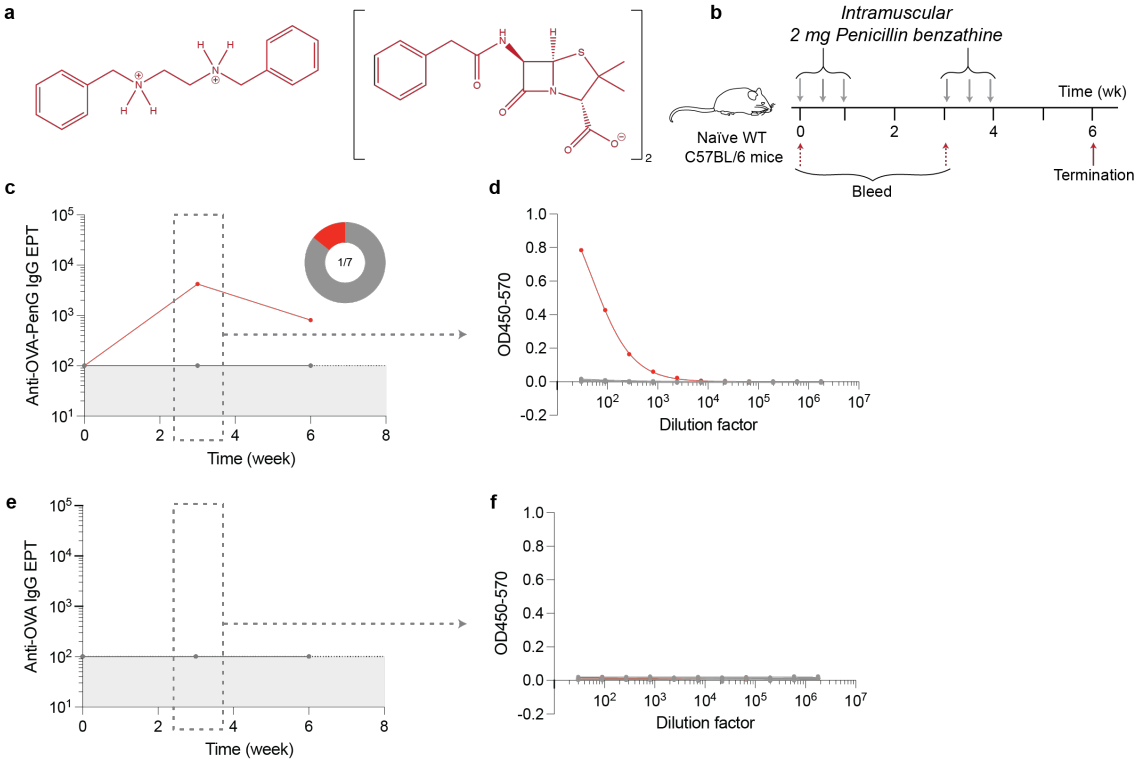


Figure 5.5: Penicillin benzathine administration and its immunogenicity *in vivo*.

(a) PenG-Ben. **(b)** C57BL/6 mice were given two week-long courses of PenG-Ben and the antibody responses were evaluated over time. **(c, d)** Anti-OVA-PenG IgG responses, and **(e, f)** anti-OVA IgG. Dots represent data from a single mouse.

Next, I aimed to establish whether the apparent poor immunogenicity of PenG adducts may have been a function of T cell immunerecessiveness of self-protein-PenG complexes *in vivo*. For example, bulk serum proteins (especially those abundant like mouse serum albumin, MSA) have high T cell tolerance barriers to avoid systemic widespread autoimmunity (Zan-Bar et al., 1978). Therefore, I pre-complexed PenG to MSA using the previously described protocol and immunised mice both with and without alum (**Fig 5.6a**). PenG-specific IgG titres were evaluated using OVA-PenG (**Fig 5.6b,c**). All mice immunised with MSA in alum responded post-boost (4/4), with titres significantly greater than the unmodified MSA in alum control (P = 0.029, Mann-Whitney). 3/4 mice immunised with MSA without adjuvant responded with modest titres (IgG EPT = 10^3–10^4), while one

mouse failed to generate a detectable conjugate-specific response following even a second boost. No antibody responses were detected against MSA in any group (**Fig 5.6d**). These data collectively suggest that penicilloyl-specific antibodies can be raised when fixed to a highly tolerogenic self-protein. However, when comparing drug-specific titres raised against MSA-PenG to that raised against HSA-PenG, it is implied that the self-protein backbone limits antibody production, consistent with the T cell immunerecessiveness of MSA.

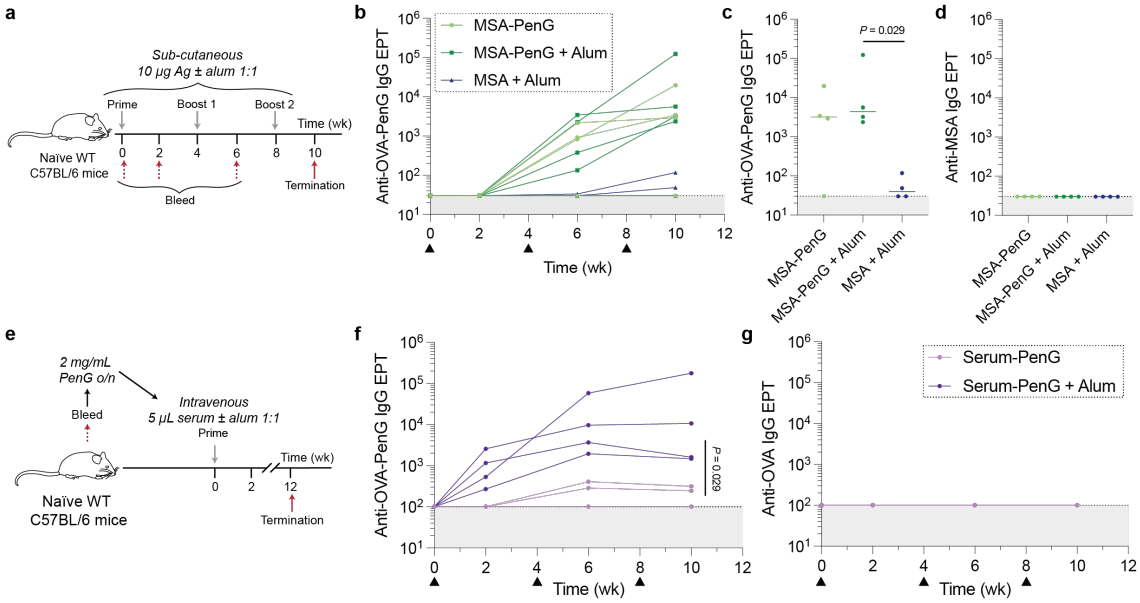


Figure 5.6: Immunogenicity of self-protein modified with PenG.

(a) Mice were immunised with MSA-PenG and bled periodically. IgG EPTs against OVA-PenG were screened throughout **(b)** the timecourse and **(c)** at termination. **(d)** Titres against the unmodified MSA backbone were also evaluated. (e) Mice were bled and bulk serum was modified *ex vivo* overnight with PenG. Modified serum was injected intravenously and mice were bled periodically. IgG EPTs were screened over time against both (f) OVA-PenG and (g) OVA. Dots represent data from a single mouse. Data were compared via Mann-Whitney and, where multiple comparisons were made, a Bonferonni correction was applied.

Next, to confirm that PenG adducts could form in serum and that those adducts are immunogenic, I tested the immunogenicity of bulk-modified serum *ex vivo*. Mice were bled, serum isolated and incubated with 2 mg/mL PenG overnight.

5 µL serum was then diluted in PBS (in some mice formulated with alum) and modified serum (serum-PenG) was reintroduced into the mouse intravenously (**Fig 5.6e**). Mice were immunised three times and bled periodically throughout the timecourse. All mice (4/4) immunised with serum-PenG formulated with adjuvant responded with modest IgG responses against OVA-PenG (median titre of 1.24×10^3 at the terminal timepoint). Only half (2/4) of the mice immunised with serum-PenG without adjuvant responded with OVA-PenG reactivity, and these titres were weak (IgG EPT of ~200). No responses were detected against OVA, the protein backbone control (**Fig 5.6g**). Collectively, these data suggest that the immunogenicity of PenG adducts depend on both the protein backbone used and engagement of the innate immune compartment.

5.2.3. Establishing the B cell clonality against PenG

I next aimed to characterise the B cell response at the molecular level, applying previously described single-cell cloning techniques. Mice were immunised with HSA-PenG in alum and draining iLNs were harvested 2 weeks post-prime (**Fig 5.7a**). Antigen probes were synthesised, similarly to the GM3g-specific clones. Briefly, gp120 was modified with PenG and subsequently fluorescently labelled with an NHS-esterified AF647 dye. A PenG-unmodified gp120-biotin control probe was made by tetramerising with a strepdavidin-PE. PenG-specific IgD^- B cells were sorted according to the gate shown (**Fig 5.7b**). B cells were sorted from four mice and B cell clonality was inferred according to the VH sequences (**Fig 5.7c**).

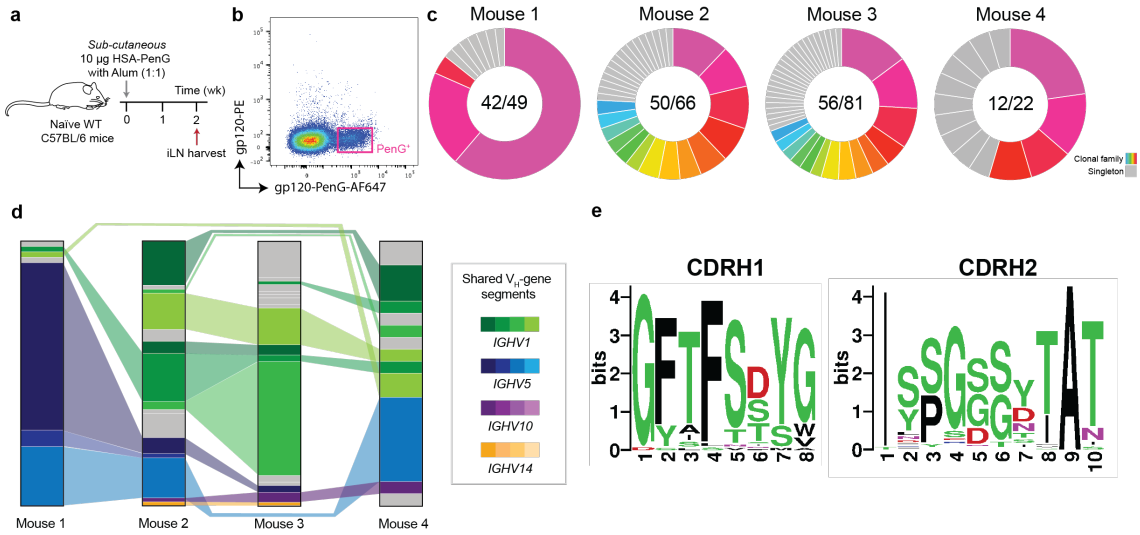


Figure 5.7: Clonotyping of B cells isolated with a PenG-adduct probe.

(a) Immunisation schedule. **(b)** Antigen-specific probe B cell sorting approach on pre-gated IgD^{-} B cells. **(c)** Clonal families were assigned according to the inferred $V_HD_HJ_H$ identities. **(d)** V_H gene segment utilisation across individual mice. Segments of the bars are proportional to the number of B cells isolated with a given VH gene segment origin. Joined segments reflect sharing between individual mice. Coloured segments indicate the subgroup of the shared gene segment. **(e)** Logo plots of the amino acid residues encoded in CDRH1 and CDRH2 across all mice.

Considerable sharing of V_H gene segments was observed between the mice, suggesting similar clonotypes were raised across animals (**Fig 5.7d**). Interestingly, the V_H gene segments utilised were from four phylogenetically similar subgroups: *IGHV1*, *IGHV5*, *IGHV10* and *IGHV14*. This homology is reflected in the conservation of CDRH1 and CDRH2 sequences across mice (**Fig 5.7e**). These data suggest that—much like the BAR-1 clonal class—there are preferred motifs encoded in these gene segments that facilitates binding with the drug.

Interestingly, unlike the BAR-1 clonal class, B cells isolated with the PenG probe exhibited a more defined and ordered CDRH3. For example, CDRH3 length was bimodal, and seemed to either be a short (5–6 aa) or long (17) in length (**Fig**

5.8a). Short CDRH3s were dominated by an 'ARG' moiety of the first three residues, with a diverse c-terminal end (**Fig 5.8d**). The long length class offered a negative N-terminus, a neutral centre, and a positive C-terminus.

The phylogenetics of expanded clones were also evaluated. The two largest isolated from mouse 1 are shown (**Fig 5.9**). The largest clonal family (**Fig 5.9a**) exhibits a 'clonal burst' (that is, many B cells isolated of identical sequence) following acquisition of the S11T mutation, a phenomenon reportedly associated with the acquisition of an affinity-improving mutation that renders the clone more competitive for antigen uptake and T cell help (Tas et al., 2016). This mutation was also found on a separate clade of the same GC tree. The T85S mutation was also identified twice on separate clades.

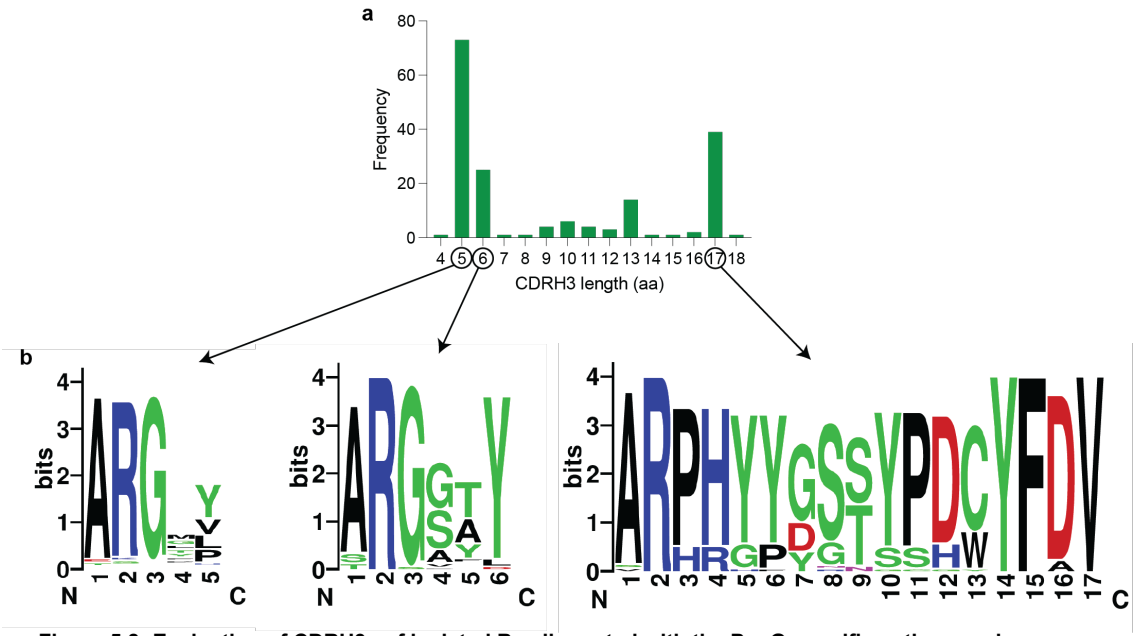


Figure 5.8: Evaluation of CDRH3s of isolated B cells sorted with the PenG-specific antigen probe.

(a) Distribution of CDRH3 length across all mice. (b) Amino acid logo plots of CDRH3s from B cells with lengths 5, 6 and 17.

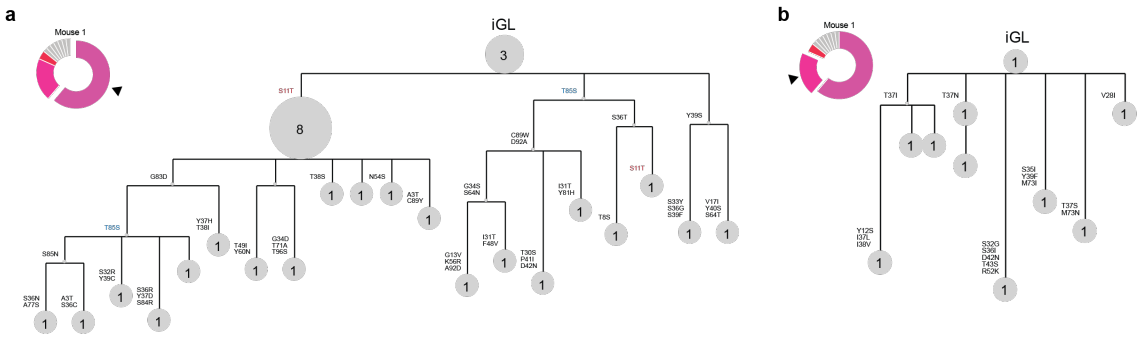


Figure 5.9: Inferred clonal family phylogenetic trees.

(a, b) Two clonal family trees from Mouse 1. Families were inferred and the mutations incorporated are annotated. Node size is proportional to the number of B cells of that identity found.

5.2.4. Characterisation of B cell clones against PenG

Next, the binding analysis of the antibody clones was conducted. A subset of 22 gene segment sets were vectorized and expressed as Fabs. To validate expression, Fabs were coated on an ELISA plate and detected using a serial dilution of biotinylated OVA-PenG that was subsequently detected using streptavidin-HRP (**Fig 5.10a**). All 22/22 Fabs delivered an antigen-specific signal, while the BAR-1 negative control did not. These data suggest that the probe-based sorting approach was highly efficient (**Fig 5.10b**). Interestingly, the range of OD curve distributions was relatively narrow, as exemplified by concentrations of OVA-PenG required to yield an $OD_{450\text{-}570}$=1.25 (an estimate for EC_{70}) (**Fig 5.10c**). These data probably reflect a limited range of affinities against the PenG adduct. Notably, family members from **Fig 5.9a** are represented, and there was no relationship between antibody binding members with S11 and S11T.

I next evaluated whether these antibodies have a drug-sequestering effect. First, a model system was established to determine whether the growth-inhibiting function of PenG could be rescued in a bacterial culture setting (**Fig 5.11a**). This

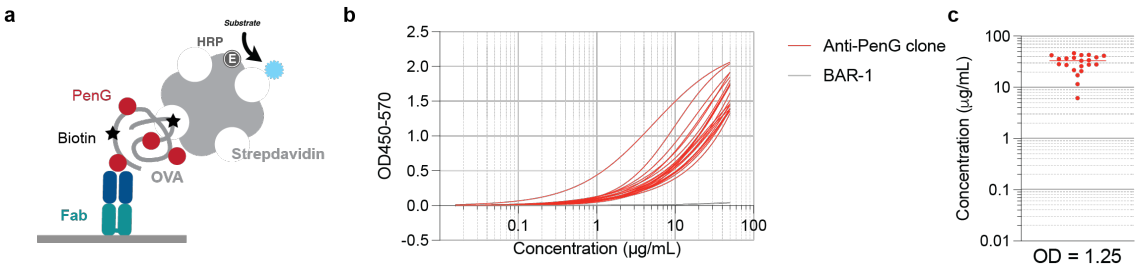


Figure 5.10: Validation of B cell binding specificity.

(a) Fabs were recombinantly expressed and purified, reflecting a subset across all four mice. Binding was assayed by coating a plate with Fab, titrating a serial dilution of biotinylated OVA-Pen and detecting with streptavidin-HRP. **(b)** ELISA data. GM3g LOG-specific clone, BAR-1 Fab, was used as a negative control. **(c)** Concentration of OVA-PenG required for OD = 1.25 was used as an estimate for EC_{70}.

was evaluated using whole antiserum in culture with PenG and an attenuated, unencapsulated lab strain of *S. pneumoniae*, D39 Δcps2A'-Δcps2H (Lanie et al., 2007). This strain was chosen because it was highly sensitive to PenG (minimum inhibitory concentration (MIC) = 0.01 µg/mL, as confirmed in-house (data not shown). MIC-quantities of PenG were pre-incubated with antiserum before adding *S. pneumoniae* in broth and left to incubate overnight (**Fig 5.11b**). OD600 values were compared between cultures incubated with HSA or HSA-PenG antisera. There was no evidence of growth rescue in the HSA-PenG antisera samples ($P > 0.9999$, Kolmogorov-Smirnov test).

To eliminate serum factors (such as iron, which is known to affect bacterial growth) (Kim et al., 2009) and determine whether specific clones have an inhibitory effect, a disk diffusion assay was developed (**Fig 5.11d**). A small subset of PenG-specific clones was expressed as IgG (to impart an avidity effect). 0.1 µg of PenG and IgG to a 1:50 molar ratio was blotted on a paper disk. The disk was placed onto an *S. pneumoniae*-coated agar plate and incubated overnight. The kill zones were compared. None of the clones tested were shown to reduce the antibiotic killing effect, as evidenced by the kill zones of irrelevant negative

antibody controls (**Fig 5.11e**). While these data do not exclude that these antibodies may be directly inhibitory, a drug-sequestering effect was not detected in these assay formats.

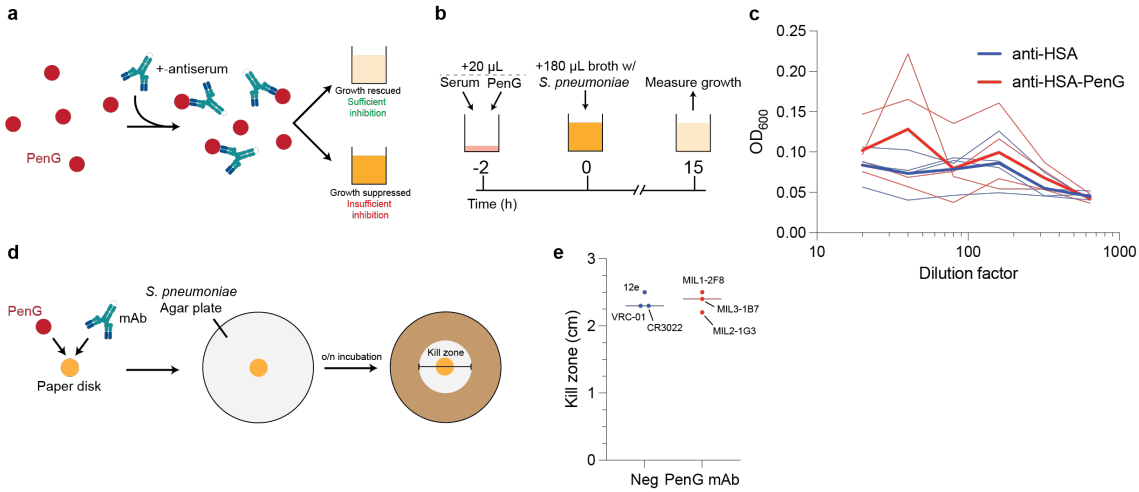


Figure 5.11: Evaluating possible drug-sequestering effects of the antibodies.

(a) Concept for assay to test antibody-mediated sequestering of drug on bacterial growth. **(b)** This assay was established using HSA-PenG antiserum and tested using PenG-sensitive *S. pneumoniae*. **(c)** Growth response to serum serial dilution was measued using OD600 as a proxy. **(d)** Disk diffusion assay setup. **(e)** Kill zones were measured using disks treated with PenG-specific mAbs.

5.3. Discussion

ADAs are reported to have broad pharmacokinetic and pharmacodynamic implications: this includes reducing drug bioavailability by neutralising or by forming immune complexes that are rapidly cleared, and may also mediate drug hypersensitivity (Kavai and Szegedi, 2007; Kohler et al., 2019; Potocnjak et al., 1982). The mechanistic effects of ADAs are best-understood in the context of those against antibody-based therapies, where anti-idiotypic responses can be readily characterised (Ben-Horin et al., 2011; Enrico et al., 2020). However, the immunogenicity of small-molecule, chemically unstable drugs are less clear. In

this study, I evaluated the conditions that determine the immunogenicity of PenG, a model drug that has previously been shown to raise antibody responses after use both experimentally and in the clinic (Lafaye and Lapresle, 1988; Levine and Ovary, 1961).

In **Chapters 3 and 4**, I evaluated in the context of LOG conjugate vaccine design, how protein carriers, conjugate occupancy, and other factors affect the downstream serological response to a given adduct. I applied similar methods to evaluate the conditions of PenG adduct formation and immunogenicity in a mouse model. Here, I discuss the key findings and explore i) the determinants of PenG adduct formation and their immunogenicity, ii) the antibody clonality and their implications for antibody function, and iii) how the clonotyping data could be applied to drug design moving forward.

5.3.1. Factors affecting drug immunogenicity

The set of serological analyses conducted *in vivo* throughout this study suggest that the generation of PenG-specific antibodies is mediated at two key levels: 1) adduct formation and 2) immune engagement (**Fig 5.12**). At each step, I have identified contributing factors that ultimately determine the downstream antibody output.

Antibody responses elicited following the administration of free drug were appreciably weaker or undetectable. This is in contrast to the administration of pre-complexed proteins. even of self-origin, as in the case for MSA and bulk serum. Notably, chemical characterisation data acquired here demonstrate that

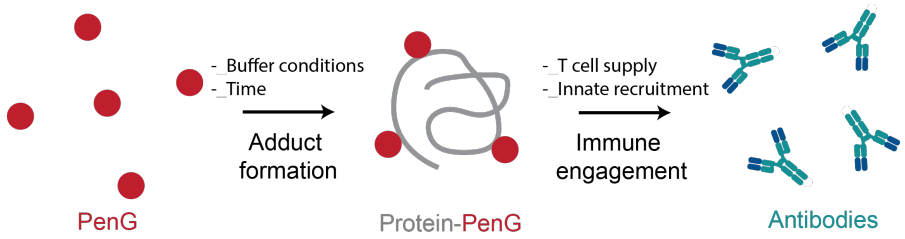


Figure 5.12: Factors affecting antibody responses to PenG.

The production of antibodies against PenG is seemingly determined at two distinct levels. First, the formation of adducts (affected by the reaction buffer conditions and time for protein and free drug to congate). Second, the degree of immune engagement (mediated by T cell help and innate immune compartment recruitment).

PenG adducts form under physiological pH provided adequate buffer conditions (namely, carbonate buffer). Given that serum is carbonate buffered, and that pre-complexing bulk serum with PenG *ex vivo* was shown to deliver modest antibody titres (including in 2/4 mice give serum-PenG without adjuvant), implies that the formation of immunogenic PenG adducts *in vivo* may be temporally or perhaps spatially constrained.

The administration of free drug either intravenously or in water was not shown to elicit an antigen-specific antibody response in mice. These data are incongruent with the human context, where most patients undergoing a standard course of PenG to treat a bacterial infection exhibit anti-penicilloyl IgG antibodies thereafter (Gordon et al., 1994; Lafaye and Lapresle, 1988; Neftel et al., 1984). This difference may be attributed to dosing, where humans are given as much as 6 g of PenG over a 24 h period (Huynh et al., 2023; Metsvaht et al., 2015); mice were given a much smaller dose and the drug could only be administered once per day rather than maintaining a continuous intravenous line. A contributing factor may also be the higher mouse cardiac output and subsequent drug clearance

rate, which results in an extremely short drug half-life (Erlendsdottir et al., 2001; Kreissl et al., 2006).

To compensate for these challenges, I tested the intramuscular administration of PenG-Ben. In 1/7 mice, there was evidence of a penicilloyl-specific antibody response. Interestingly, a subsequent PenG-Ben boost failed to further improve the IgG titre. I hypothesised that this is a consequence of the T cell compartment limiting T cell help. For instance, while a PenG adduct formed post-boost may be recognised by an established memory B cell population, the probability the associated peptide will propagate a Th recall response may be marginal, especially given the diversity of proteins/peptides being modified *in vivo*. This and the infrequency of antibody responses generated post-PenG-Ben administration implies an element of stochasticity in responding to the drug.

Immunological factors both at the innate and adaptive level are also key determinants of antibody responses against PenG adducts. For instance, immunisations with pre-complexed serum-PenG in adjucant were shown to deliver higher drug-specific titres compared to animals given unadjuvanted formulations. This is unsurprising since innate immune engagement is highly potentiating for the adaptive compartment. Interestingly, in a clinical setting where PenG is being administered (that is, where a patient has a bacterial infection), the innate compartment is activated due to the available PAMPs supplied by the offending bacteria (Albiger et al., 2007; Diacovich and Gorvel, 2010; Kubelkova and Macela, 2019). This may partially account for human studies demonstrating that patients undergoing PenG treatment for ongoing

bacterial infections typically mount specific drug-directed antibody responses (Lafaye and Lapresle, 1988).

For anti-LOG responses discussed in prior chapters, the protein carrier affected the T cell help imparted by the LOG-specific B cells, as evidenced both by absolute antibody titres, and the molecular evidence of proportional SHM. I similarly observed in this study that the carrier protein affected the serological outcome: for instance, modest PenG-specific IgG titres were only observed in mice immunised with MSA-PenG in alum post-boost, while high titre responses against HSA-PenG were reported post-prime. These data and others highlight the tolerance barrier imparted by Th cells, with B cell propagation being determined by the immunogenicity of available peptide within the same antigenic complex. Given the self-like character of serum protein, this may further hinder the generation of drug-specific antibodies upon free drug administration.

5.3.2. Relationship between drug conjugation chemistry and antibody function

The bactericidal effects of PenG are imparted by mimicking D-Ala-D-Ala, with the β-lactam suicidally binding to the catalytic site of PGN during bacterial cell wall formation (Blumberg and Strominger, 1974). Therefore, it could be envisaged that the raising of anti-PenG antibodies may have a drug-sequestering effect, potentially reducing the availability of active free drug. However, in this study, I show no evidence of raised clones exhibiting this trait in an *S. pneumoniae* model setup. I hypothesise that clones raised may fail to reduce effective bactericidal activity for one of two reasons.

First, the biophysical characteristics of the antibody clones may be such that effective binding kinetics are insufficient to sequester adequate quantities of free drug. For example, if the affinity is low, the fraction of bound antibody may be small. In the growth rescuing assay, conducted with antiserum reflective of physiological antibody concentrations, no evidence of growth rescue from PenG was detected. Notably, while binding kinetics of these antibodies were not evaluated here (for example, via SPR), the ELISA data does imply relatively weak binding.

Second, I predict that the conjugation chemistry of these antibodies may also have a role in preventing antibody-mediated drug sequestration. For example, even in the disk diffusion assay, where the molar ratio for drug-to-antibody was artificially very high due to the concentration of recombinant antibody used, drug neutralising effects were also not detected. Since the process of forming antigenic complexes requires the β-lactam 'front face' to react with an amino acid sidechain of a carrier protein (Ariza et al., 2012), the B cell compartment only 'sees' a surface 'back face' of the drug (**Fig 5.13**). Therefore, while structural work and saturation transfer analyses (Buchanan et al., 2022) on antibody clones against these drugs are ongoing, I hypothesise that all antibodies raised against PenG will recognise the back face of the drug. Since the β-lactam group is the functionally reactive group (responsible for irreversibly reacting with the catalytic site of PGN), clones raised may not disable the drug. This may be especially relevant in a gram-positive setting, such as *S. pneumoniae*: in gram-negative bacteria, a drug:antibody complex would need to cross a membrane in order to access PGN, thus affecting drug uptake.

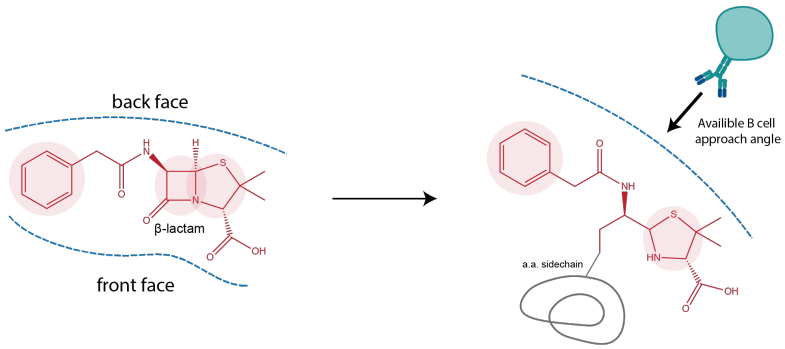


Figure 5.13: Proposed model for how drug conjugation determines B cell recognition sites.

The conjugation of the PenG to amino acid sidechains is mediated by the unfolding of the β-lactam ring and subsequent covalent bonding of the drug to a carrier protein. This 'spending' of the ring may render the front face to the drug inaccessible to B cells.

Collectively, while further structural and biochemical characterisation of the clonotypical response against PenG are pending, these data are consistent with the drug conjugation chemistry determining the pharmacokinetic and functional outcomes of the antibody responses raised.

5.3.3. Future directions: Implications for germline-informed drug design

Given that antibody induction against PenG is associated with drug hypersensitivity (Levine and Ovary, 1961; Stils, 2005), this study may be further expanded to model germline-informed drug design. For example, since the antibody clonotypes raised against PenG adducts are seemingly relatively homogenous (e.g. narrow VH gene utilisation with close amino acid sequence identities in the CDRHs), structural characterisation and other atomic-level evaluations such as saturation transfer analysis may reveal particular drug aspects that are critical for antigen-antibody binding. Therefore, a PenG analogue could potentially be designed that the identified antibody clonal class fails to recognise, while still imparting bactericidal effects. This analogue would represent a penicillin-type β-lactam drug that may be 1) safe for PenG

hypersensitive individuals (in this model, against a mouse germline) and 2) could be used in individuals not yet allergic to avoid subsequent sensitisation.

5.3.4. Conclusions

The administration of unstable small-molecules, such as PenG used to treat bacterial infections, forms immunogenic protein adducts *in vivo*. This has important implications for hypersensitivity in the clinic, although the mechanistic chemical and immunological underpinnings for these allergic phenotypes are poorly understood. Here, I establish a model murine system to dissect the biochemical modulators that determine the serological effect against penicilloyls and detail the clonotypical response against these protein modifications. These findings suggest a possible molecular rationale for the functional effects of these antibodies, as well as to instruct how future drug design may reflect a ‘germline informed’ approach.

Chapter 6—General Discussion

6.1 Thesis summary

In this thesis, I addressed two discrete problems associated with the generation of antibodies against protein adducts, using a combination of classical immune assays and molecular, structural, and biochemical techniques.

First, I consider a fundamental challenge in overcoming tolerance barriers underpinned by antigen lacking both T and B cell antigenicity. In **Chapter 3**, I consider this in the context of self-glycans, which are broadly recognised for their poor immunogenicity. This is exploited by both viruses and cancer. I describe a novel semi-synthetic glycan presentation platform wherein self-glycans—in this instance, the model immunorecessive TACA, GM3g—can be artificially conjugated to a carrier protein via a short bespoke linker. These modular formats were shown to elicit high-titre autologous antibody responses. However, while antibody binding was sugar dependent, no cross-reactivity with native (that is, ceramide-docked) GM3g was detected. These and other data provide evidence

of linker accommodation in the antibody binding mode and steric clashes with native target, membrane-docked GM3, ultimately constraining the translational relevance of the response raised.

To understand the molecular underpinnings of the serological response, in **Chapter 4**, I highlight how the highly immunogenic amidine-based GM3g LOG accesses common germline-encoded lectin-like motifs in the murine germline; by conducting comprehensive clonotyping, I identified how these artificial presentations 'reach through' to the novel BAR-1 clonal class and provide a structural and biochemical rationale for why these antibodies fail to cross-react with native GM3g. While these findings inform how synthetic protein chemistry can raise otherwise inaccessible B cell clonotypes, systematic and iterative stepwise shepherding of these clones would be necessary to modify the context dependency of these clones to potentially deliver a relevant and functional antibody effect *in vivo*.

Second, chemically unstable small-molecule drugs may form protein adducts *in vivo*, which may have implications for allergy and pharmacokinetics. Using PenG as a model, in **Chapter 5**, I evaluated the conditions that determine adduct formation and immunogenicity in mice. Factors affecting antibody production are seemingly influenced both by the extent of adduct formation and the degree of immune engagement. Moreover, I conducted clonotyping and preliminary functional characterisation of antibodies against these adducts.

6.2 LOG-based vaccination: benefits and penalties to improved antigenicity

The LOG system represents a model to circumvent immunorecessiveness against a target antigen. There may be a heavy incentive for the skewing of the naïve repertoire to avoid the presence of self or self-like glycan-reactive B cells to prevent the raising of widespread autoreactive antibodies, which we and other have discussed (Deimel et al., 2022; New et al., 2016). This perspective is supported by evidence of anti-glycan responses associated with various autoimmune conditions (Dotan et al., 2006; Temme et al., 2021). I probe this using the LOG system with model immunorecessive self-glycan, GM3g. Indeed, previous studies have failed to reliably raise high-titre antibodies against GM3 using conventional autologous formulations (Livingston et al., 1994, 1989).

We demonstrate, using a variety of linker chemistries fixed onto the primary amines of lysine sidechains, that GM3g-engaging responses can be readily mounted in a mouse. This implies that the artificial presentation of self-glycans can be exploited to access a subset of naïve B cells that native presentations of the same glycan fail to elaborate. While this marks an important proof-of-principle for our novel LOG-based ‘germline targeting’ framework, the antibody response was not cross-reactive with GM3. This outcome was unsurprising: the immune system raises antibodies against what it recognises. The reactivity of the [–amidine-GM3g]-raised antiserum reflects that the antibodies were raised against a glycan associated with an artificial linker, and thus the accommodation of such linker was a risk associated with this approach. Through subsequent immunogenetic, structural, biochemical and uSTA NMR-based analyses, the

basis for the lack of GM3-reactivity became evident. There was clear clonal accommodation of the linker: the orientation of GM3g across V_H-gene-encoded CDRH1/2 motifs positioned the linker-accommodating kappa chain where ceramide would be found on native GM3. Whether heterologous immunisation strategies might 'walk' these BAR-1 clones to instead accommodate membrane-docked GM3g is untested, but the structural biology and evidence from the HIV-1 field implies that a positive outcome may be unlikely (Mesin et al., 2020; Schaefer-Babajew et al., 2023; Steichen et al., 2016).

Indeed, BAR-1 class recognition of the glycoconjugate is mediated predominantly by the murine *IGHV2* subgroup. The encoded CDRH1/2 ultimately determines the orientation of the glycan, the angle at which the antibody approaches, and the major energetic contributions between the antibody and the carbohydrate. Of note, W57 is in the CDRH2 and stacks with the galactose, effectively providing a 'foothold' for the antibody. This tryptophan-galactose interaction is a hallmark observed across carbohydrate binding proteins, including lectins (Asensio et al., 2013). This study has, therefore, explicitly demonstrated the presence of germline-encoded lectin-like motifs (Gabba et al., 2021; Tobola et al., 2018; Topin et al., 2016) present in the murine germline.

Moreover, the LOG system provided a unique model to titrate the effect of the carrier protein on the adduct-specific antibody response, where a direct relationship between the amount of T cell help could be drawn. While HEL-[–amidine-GM3g]$_6$ and gp120-[–amidine-GM3g]$_{16}$ led to a response against the LOG with the same germline configuration, there was clear toggling of the

germinal centre experience the clones had undergone with respect to the amount of follicular help offered by the different protein backbones. This finding was instructive and informs the ideal LOG design necessary for future heterologous contextualisation boosters; for example, this highlights that a more T-immunodominant backbone is conducive to greater somatic hypermutation rates and, therefore, may improve the odds of achieving successful clonal maturation outcomes. Collectively, these findings demonstrate how synthetic protein chemistry can exploit artificial protein adducts to raise novel antibodies against a target of interest. I propose here that these concepts may be exploited for the logical design of germline-informed conjugate-based vaccines, which may be of broad translational interest for both therapeutic antibody discovery for passive administration, as well as for active vaccination.

6.3 The implications of drug-adduct immunogenicity

Some small-molecule drugs may be chemically unstable *in vivo*. For example, PenG has a β-lactam functional group that has been shown to readily hydrolyse or react with amines under certain buffer conditions (Bahmany et al., 2023). The formation of penicilloyl adducts are believed to be the antigenic drivers of hypersensitivity, including antibody mediated forms (both IgE and IgG) (Lafaye and Lapresle, 1988; Levine and Ovary, 1961). Like antibody responses against LOGs, the generation of ADAs targeting small-molecule drugs is presumably a function of i) cognate B cells cross-reacting epitopes encompassing the drug adducts, and ii) peptide within the antigen complex permitting linked T cell help. However, open questions remain in describing the relationship between the drug–protein conjugation chemistry, the immunogenicity of formed adducts, the

resultant B cell response and the functional antibody effect. Here, I developed a model to investigate these factors using PenG, both free and pre-complexed to carrier proteins, to evaluate the humoral responses in a mouse.

The capacity for drug adducts to form was seemingly highly contingent on the pharmacokinetics of free drug. For example, administration of PenG intravenously or PenV in drinking water failed to elicit detectable drug-specific antibody responses. I hypothesise that this may be a function of rapid drug clearance abetted by the high cardiac output and efficient renal passing of PenG in mice. When pre-incubating serum *ex vivo* with PenG and administering the product intravenously, mice generated antibodies even in the absence of adjuvant: these data imply that the serum buffer conditions are conducive of adduct formation, and that adducts forming on bulk serum proteins are sufficient in generating an antibody response. Moreover, the administration of PenG-Ben, a slow-release formulation of PenG (Merad et al., 1998), resulted in one mouse generating modest IgG titres against the drug. These data highlight the relationship between the pharmacokinetics of chemically unstable small-molecule drugs, the efficiency of the conjugation chemistry and the downstream adaptive outcome.

The data further indicate both innate and adaptive factors that determine the robustness of the serological response to the PenG adducts—these trends reflect that observed against the GM3g-based LOGs. For example, the addition of adjuvant was associated with improved antibody titres. Moreover, selection of

carrier also impacted the serological response. For example, foreign carriers like HSA were associated with high IgG titres post-prime, while conjugation of drug to self-proteins such as MSA resulted in lower titres. These data reflect the role of Th cells in propagating the B cell response.

Antibody induction against PenG and other small-molecule drugs may have considerable clinical interest, both with respect to hypersensitivity and pharmacokinetics (Goh et al., 2021; Tannert et al., 2017; Weiss and Adkinson, 1988). The PenG model explored in this study may be further expanded to consider may the structural, biophysical and biochemical binding modes of the antibodies raised; while clonotyping and preliminary drug-sequestering analyses were conducted, an atomic-level perspective of antibody binding may inform the synthetic design of a model PenG analogue that is 'germline repertoire blind'. For example, the generation of a novel β-lactam antibiotic that cannot be recognised by a given individual's germline B cell repertoire may represent a novel no/low allergenic drug design approach. This is likely highly germline-specific, and thus may need to be tailored for each individual.

6.4 Conclusions

Protein adducts are valuable models both for the development of novel vaccine design approaches and in understanding disease. Moreover, conjugate design provides a unique platform to titrate the effects of adduct spacing/density on the downstream humoral outcome, and the implications of carrier protein in propagating the B cell response. In this thesis, I investigate these immunological

aspects, applying both classical immunoassaying, as well as contemporary molecular B cell techniques. These approaches suggest novel avenues for vaccine design, as well as inform the basis of detrimental clinically-relevant anti-adduct responses against which we might develop rational strategies to mitigate these effects, such as via immune-informed drug design.

References

Abdel-Motal, U.M., Berg, L., Rosén, A., Bengtsson, M., Thorpe, C.J., Kihlberg, J., Dahmén, J., Magnusson, G., Karlsson, K.A., Jondal, M., 1996. Immunization with glycosylated Kb-binding peptides generates carbohydrate-specific, unrestricted cytotoxic T cells. Eur J Immunol 26, 544–551. https://doi.org/10.1002/eji.1830260307

Abraham, E.P., Chain, E., Fletcher, C.M., Florey, H.W., Gardner, A.D., Heatley, N.G., Jennings, M.A., 1992. Further observations on penicillin. 1941. Eur J Clin Pharmacol 42, 3–9.

Akira, S., 2011. Innate immunity and adjuvants. Philosophical Transactions of the Royal Society B: Biological Sciences 366, 2748–2755. https://doi.org/10.1098/rstb.2011.0106

Albiger, B., Dahlberg, S., Henriques-Normark, B., Normark, S., 2007. Role of the innate immune system in host defence against bacterial infections: focus on the Toll-like receptors. J Intern Med 261, 511–528. https://doi.org/10.1111/j.1365-2796.2007.01821.x

Alexander, J., Satoskar, A.R., Russell, D.G., 1999. Leishmania species: models of intracellular parasitism. J Cell Sci 112, 2993–3002. https://doi.org/10.1242/jcs.112.18.2993

Allen, C.D.C., Cyster, J.G., 2008. Follicular dendritic cell networks of primary follicles and germinal centers: Phenotype and function. Semin Immunol 20, 14–25. https://doi.org/10.1016/j.smim.2007.12.001

Alonaizan, R., Woods, S., Hargrave, K.E., Roberts, C.W., 2021. An Exaggerated Immune Response in Female BALB/c Mice Controls Initial Toxoplasma gondii Multiplication but Increases Mortality and Morbidity Relative to Male Mice. Pathogens 10, 1154. https://doi.org/10.3390/pathogens10091154

Alt, F.W., Baltimore, D., 1982. Joining of immunoglobulin heavy chain gene segments: implications from a chromosome with evidence of three D-JH fusions. Proceedings of the National Academy of Sciences 79, 4118–4122. https://doi.org/10.1073/pnas.79.13.4118

Anggara, K., Zhu, Y., Fittolani, G., Yu, Y., Tyrikos-Ergas, T., Delbianco, M., Rauschenbach, S., Abb, S., Seeberger, P.H., Kern, K., 2021. Identifying the origin of local flexibility in a carbohydrate polymer. Proceedings of the National Academy of Sciences 118. https://doi.org/10.1073/pnas.2102168118

Aoshi, T., 2017. Modes of Action for Mucosal Vaccine Adjuvants. Viral Immunol 30, 463–470. https://doi.org/10.1089/vim.2017.0026

Apostolopoulos, V., Pietersz, G.A., Xing, P.-X., Lees, C.J., Michael, M., Bishop, J., McKenzie, I.F.C., 1995. The immunogenicity of MUC1 peptides and fusion protein. Cancer Lett 90, 21–26. https://doi.org/https://doi.org/10.1016/0304-3835(94)03673-7

Apostolopoulos, V., Yuriev, E., Ramsland, P.A., Halton, J., Osinski, C., Li, W., Plebanski, M., Paulsen, H., McKenzie, I.F.C., 2003. A glycopeptide in complex with MHC class I uses the GalNAc residue as an anchor. Proceedings of the National Academy of Sciences 100, 15029–15034. https://doi.org/10.1073/pnas.2432220100

Ariza, A., Garzon, D., Abánades, D.R., de los Ríos, V., Vistoli, G., Torres, M.J., Carini, M., Aldini, G., Pérez-Sala, D., 2012. Protein haptenation by amoxicillin: High resolution mass spectrometry analysis and identification of target proteins in serum. J Proteomics 77, 504–520. https://doi.org/10.1016/j.jprot.2012.09.030

Asensio, J.L., Ardá, A., Cañada, F.J., Jiménez-Barbero, J., 2013. Carbohydrate–Aromatic Interactions. Acc Chem Res 46, 946–954. https://doi.org/10.1021/ar300024d

Astronomo, R.D., Burton, D.R., 2010. Carbohydrate vaccines: developing sweet solutions to sticky situations? Nat Rev Drug Discov 9, 308–324. https://doi.org/10.1038/nrd3012

Avci, F.Y., Kasper, D.L., 2010. How bacterial carbohydrates influence the adaptive immune system. Annu Rev Immunol 28, 107–130. https://doi.org/10.1146/annurev-immunol-030409-101159

Avci, F.Y., Li, X., Tsuji, M., Kasper, D.L., 2013. Carbohydrates and T cells: a sweet twosome. Semin Immunol 25, 146–151. https://doi.org/10.1016/j.smim.2013.05.005

Avery, O.T., Goebel, W.F., 1929. CHEMO-IMMUNOLOGICAL STUDIES ON CONJUGATED CARBOHYDRATE-PROTEINS : II. IMMUNOLOGICAL SPECIFICITY OF SYNTHETIC SUGAR-PROTEIN ANTIGENS. J Exp Med 50, 533–550. https://doi.org/10.1084/jem.50.4.533

Awate, S., Babiuk, L.A., Mutwiri, G., 2013. Mechanisms of action of adjuvants. Front Immunol 4, 114. https://doi.org/10.3389/fimmu.2013.00114

Babcook, J.S., Leslie, K.B., Olsen, O.A., Salmon, R.A., Schrader, J.W., 1996. A novel strategy for generating monoclonal antibodies from single, isolated lymphocytes producing antibodies of defined specificities. Proceedings of the National Academy of Sciences 93, 7843 LP – 7848. https://doi.org/10.1073/pnas.93.15.7843

Bahmany, S., Ewoldt, T.M.J., Abdulla, A., Koch, B.C.P., 2023. Stability of 10 Beta-Lactam Antibiotics in Human Plasma at Different Storage Conditions. Ther Drug Monit 1. https://doi.org/10.1097/FTD.0000000000001100

Bai, L., Deng, S., Reboulet, R., Mathew, R., Teyton, L., Savage, P.B., Bendelac, A., 2013. Natural killer T (NKT)–B-cell interactions promote prolonged antibody responses and long-term memory to pneumococcal capsular polysaccharides. Proceedings of the National Academy of Sciences 110, 16097 LP – 16102. https://doi.org/10.1073/pnas.1303218110

Bantroch, S., Bühler, T., Lam, J.S., 1994. Appropriate coating methods and other conditions for enzyme-linked immunosorbent assay of smooth, rough, and neutral lipopolysaccharides of Pseudomonas aeruginosa. Clinical Diagnostic Laboratory Immunology 1, 55–62. https://doi.org/10.1128/cdli.1.1.55-62.1994

Bärenwaldt, A., Läubli, H., 2019. The sialoglycan-Siglec glyco-immune checkpoint - a target for improving innate and adaptive anti-cancer immunity. Expert Opin Ther Targets 23, 839–853. https://doi.org/10.1080/14728222.2019.1667977

Barnes, C.O., Gristick, H.B., Freund, N.T., Escolano, A., Lyubimov, A.Y., Hartweger, H., West, A.P., Cohen, A.E., Nussenzweig, M.C., Bjorkman, P.J., 2018. Structural characterization of a highly-potent V3-glycan broadly neutralizing antibody bound to natively-glycosylated HIV-1 envelope. Nat Commun 9, 1251. https://doi.org/10.1038/s41467-018-03632-y

Beatson, R., Tajadura-Ortega, V., Achkova, D., Picco, G., Tsourouktsoglou, T.-D., Klausing, S., Hillier, M., Maher, J., Noll, T., Crocker, P.R., Taylor-Papadimitriou, J., Burchell, J.M., 2016. The mucin MUC1 modulates the tumor immunological microenvironment through engagement of the lectin Siglec-9. Nat Immunol 17, 1273–1281. https://doi.org/10.1038/ni.3552

Belisle, E.H., Strausser, H.R., 1981. Sex-Related Immunocompetence of BALB/C Mice. Dev Comp Immunol 5, 661–670. https://doi.org/10.1016/S0145-305X(81)80040-7

Ben-Horin, S., Yavzori, M., Katz, L., Kopylov, U., Picard, O., Fudim, E., Coscas, D., Bar-Meir, S., Goldstein, I., Chowers, Y., 2011. The immunogenic part of infliximab is the F(ab')2, but measuring antibodies to the intact infliximab molecule is more clinically useful. Gut 60, 41–48. https://doi.org/10.1136/gut.2009.201533

Bennett, A.P., Gallacher, G., Landon, J., 1987. The raising and characterisation of antibodies to salicylate. Ann Clin Biochem 24 (Pt 4), 374–84. https://doi.org/10.1177/000456328702400406

Berek, C., Milstein, C., 1987. Mutation Drift and Repertoire Shift in the Maturation of the Immune Response. Immunol Rev 96, 23–41. https://doi.org/10.1111/j.1600-065X.1987.tb00507.x

Berois, N., Pittini, A., Osinaga, E., 2022. Targeting Tumor Glycans for Cancer Therapy: Successes, Limitations, and Perspectives. Cancers (Basel). https://doi.org/10.3390/cancers14030645

Bilodeau, M.T., Park, T.K., Hu, S., Randolph, J.T., Danishefsky, S.J., Livingston, P.O., Zhang, S., 1995. Total Synthesis of a Human Breast

Tumor Associated Antigen. J Am Chem Soc 117, 7840–7841. https://doi.org/10.1021/ja00134a043

Bitton, R.J., Guthmann, M.D., Gabri, M.R., Carnero, A.J.L., Alonso, D.F., Fainboim, L., Gomez, D.E., 2002. Cancer vaccines: an update with special focus on ganglioside antigens. Oncol Rep 9, 267–276.

Bjerregaard-Andersen, K., Abraha, F., Johannesen, H., Oscarson, S., Moreno, E., Krengel, U., 2021. Key role of a structural water molecule for the specificity of 14F7—An antitumor antibody targeting the NeuGc GM3 ganglioside. Glycobiology 31, 1500–1509. https://doi.org/10.1093/glycob/cwab076

Blanco, R., Quintana, Y., Blanco, D., Cedeño, M., Rengifo, C.E., Frómeta, M., Ríos, M., Rengifo, E., Carr, A., 2013. Tissue Reactivity of the 14F7 Mab Raised against N-Glycolyl GM3 Ganglioside in Tumors of Neuroectodermal, Mesodermal, and Epithelial Origin. J Biomark 2013, 602417. https://doi.org/10.1155/2013/602417

Bleul, T., Zhuang, X., Hildebrand, A., Lange, C., Böhringer, D., Schlunck, G., Reinhard, T., Lapp, T., 2021. Different Innate Immune Responses in BALB/c and C57BL/6 Strains following Corneal Transplantation. J Innate Immun 13, 49–59. https://doi.org/10.1159/000509716

Blixt, O., Han, S., Liao, L., Zeng, Y., Hoffmann, J., Futakawa, S., Paulson, J.C., 2008. Sialoside Analogue Arrays for Rapid Identification of High Affinity Siglec Ligands. J Am Chem Soc 130, 6680–6681. https://doi.org/10.1021/ja801052g

Blixt, O., Head, S., Mondala, T., Scanlan, C., Huflejt, M.E., Alvarez, R., Bryan, M.C., Fazio, F., Calarese, D., Stevens, J., Razi, N., Stevens, D.J., Skehel, J.J., van Die, I., Burton, D.R., Wilson, I.A., Cummings, R., Bovin, N., Wong, C.-H., Paulson, J.C., 2004. Printed covalent glycan array for ligand profiling of diverse glycan binding proteins. Proceedings of the National Academy of Sciences 101, 17033–17038. https://doi.org/10.1073/pnas.0407902101

Blumberg, P.M., Strominger, J.L., 1974. Interaction of penicillin with the bacterial cell: penicillin-binding proteins and penicillin-sensitive enzymes. Bacteriol Rev 38, 291–335. https://doi.org/10.1128/br.38.3.291-335.1974

Blumenthal, K.G., Youngster, I., Rabideau, D.J., Parker, R.A., Manning, K.S., Walensky, R.P., Nelson, S.B., 2015. Peripheral blood eosinophilia and

hypersensitivity reactions among patients receiving outpatient parenteral antibiotics. Journal of Allergy and Clinical Immunology 136, 1288-1294.e1. https://doi.org/10.1016/j.jaci.2015.04.005

Brander, C., Mauri-Hellweg, D., Bettens, F., Rolli, H., Goldman, M., Pichler, W.J., 1995. Heterogeneous T cell responses to beta-lactam-modified self-structures are observed in penicillin-allergic individuals. J Immunol 155, 2670–8.

Briney, B., Inderbitzin, A., Joyce, C., Burton, D.R., 2019. Commonality despite exceptional diversity in the baseline human antibody repertoire. Nature 566, 393–397. https://doi.org/10.1038/s41586-019-0879-y

Brochet, X., Lefranc, M.-P., Giudicelli, V., 2008. IMGT/V-QUEST: the highly customized and integrated system for IG and TR standardized V-J and V-D-J sequence analysis. Nucleic Acids Res 36, W503–W508. https://doi.org/10.1093/nar/gkn316

Brouwers, R., Vass, H., Dawson, A., Squires, T., Tavaddod, S., Allen, R.J., 2020. Stability of β-lactam antibiotics in bacterial growth media. PLoS One 15, e0236198. https://doi.org/10.1371/journal.pone.0236198

Buchanan, C.J., Gaunt, B., Harrison, P.J., Yang, Y., Liu, J., Khan, A., Giltrap, A.M., Le Bas, A., Ward, P.N., Gupta, K., Dumoux, M., Tan, T.K., Schimaski, L., Daga, S., Picchiotti, N., Baldassarri, M., Benetti, E., Fallerini, C., Fava, F., Giliberti, A., Koukos, P.I., Davy, M.J., Lakshminarayanan, A., Xue, X., Papadakis, G., Deimel, L.P., Casablancas-Antràs, V., Claridge, T.D.W., Bonvin, A.M.J.J., Sattentau, Q.J., Furini, S., Gori, M., Huo, J., Owens, R.J., Schaffitzel, C., Berger, I., Renieri, A., null, null, Naismith, J.H., Baldwin, A.J., Davis, B.G., 2022. Pathogen-sugar interactions revealed by universal saturation transfer analysis. Science (1979) 377, eabm3125. https://doi.org/10.1126/science.abm3125

Burnet, F.M., 1976. A Modification of Jerne's Theory of Antibody Production using the Concept of Clonal Selection. CA Cancer J Clin 26, 119–121. https://doi.org/10.3322/canjclin.26.2.119

Buskas, T., Li, Y., Boons, G.-J., 2004. The Immunogenicity of the Tumor-Associated Antigen Lewisy May Be Suppressed by a Bifunctional Cross-Linker Required for Coupling to a Carrier Protein. Chemistry – A European

Journal 10, 3517–3524. https://doi.org/https://doi.org/10.1002/chem.200400074

Buskas, T., Thompson, P., Boons, G.-J., 2009. Immunotherapy for cancer: synthetic carbohydrate-based vaccines. Chem. Commun. 5335–5349. https://doi.org/10.1039/B908664C

Butts, C., Socinski, M.A., Mitchell, P.L., Thatcher, N., Havel, L., Krzakowski, M., Nawrocki, S., Ciuleanu, T.-E., Bosquée, L., Trigo, J.M., Spira, A., Tremblay, L., Nyman, J., Ramlau, R., Wickart-Johansson, G., Ellis, P., Gladkov, O., Pereira, J.R., Eberhardt, W.E.E., Helwig, C., Schröder, A., Shepherd, F.A., 2014. Tecemotide (L-BLP25) versus placebo after chemoradiotherapy for stage III non-small-cell lung cancer (START): a randomised, double-blind, phase 3 trial. Lancet Oncol 15, 59–68. https://doi.org/https://doi.org/10.1016/S1470-2045(13)70510-2

Cantarel, B.L., Coutinho, P.M., Rancurel, C., Bernard, T., Lombard, V., Henrissat, B., 2009. The Carbohydrate-Active EnZymes database (CAZy): an expert resource for Glycogenomics. Nucleic Acids Res 37, D233–D238. https://doi.org/10.1093/nar/gkn663

Carbonetti, S., Oliver, B.G., Vigdorovich, V., Dambrauskas, N., Sack, B., Bergl, E., Kappe, S.H.I., Sather, D.N., 2017. A method for the isolation and characterization of functional murine monoclonal antibodies by single B cell cloning. J Immunol Methods 448, 66—73. https://doi.org/10.1016/j.jim.2017.05.010

Carr, A., Mesa, C., del Carmen Arango, M., Vázquez, A.M., Fernández, L.E., 2002. In Vivo and In Vitro Anti-Tumor Effect of 14F7 Monoclonal Antibody. Hybrid Hybridomics 21, 463–468. https://doi.org/10.1089/153685902321043990

Castillo, F.J., Mullen, L.J., Grant, B.C., DeLeon, J., Thrift, J.C., Chang, L.W., Irving, J.M., Burke, D.J., 1994. Hybridoma stability. Dev Biol Stand 83, 55–64.

Cavdarli, S., Groux-Degroote, S., Delannoy, P., 2019. Gangliosides: The Double-Edge Sword of Neuro-Ectodermal Derived Tumors. Biomolecules 9. https://doi.org/10.3390/biom9080311

Chain, E., 1979. The early years of the penicillin discovery. Trends Pharmacol Sci 1, 6–11. https://doi.org/10.1016/0165-6147(79)90004-X

Chalker, J.M., Bernardes, G.J.L., Davis, B.G., 2011. A “tag-and-modify” approach to site-selective protein modification. Acc Chem Res 44, 730–741. https://doi.org/10.1021/ar200056q

Chapman, P.B., Morrissey, D.M., Panageas, K.S., Hamilton, W.B., Zhan, C., Destro, A.N., Williams, L., Israel, R.J., Livingston, P.O., 2000. Induction of antibodies against GM2 ganglioside by immunizing melanoma patients using GM2-keyhole limpet hemocyanin + QS21 vaccine: a dose-response study. Clin Cancer Res 6, 874–879.

Chefalo, P., Pan, Y., Nagy, N., Harding, C., Guo, Z., 2003. Preparation and immunological studies of protein conjugates of N-acylneuraminic acids. Glycoconj J 20, 407–414. https://doi.org/10.1023/B:GLYC.0000033997.01760.b9

Chen, B.-M., Cheng, T.-L., Roffler, S.R., 2021. Polyethylene Glycol Immunogenicity: Theoretical, Clinical, and Practical Aspects of Anti-Polyethylene Glycol Antibodies. ACS Nano 15, 14022–14048. https://doi.org/10.1021/acsnano.1c05922

Chen, M., Guo, Z., Ju, W., Ryffel, B., He, X., Zheng, S.G., 2012. The development and function of follicular helper T cells in immune responses. Cell Mol Immunol 9, 375–379. https://doi.org/10.1038/cmi.2012.18

Chen, S.T., Oliveira, T.Y., Gazumyan, A., Cipolla, M., Nussenzweig, M.C., 2023. B cell receptor signaling in germinal centers prolongs survival and primes B cells for selection. Immunity 56, 547-561.e7. https://doi.org/10.1016/j.immuni.2023.02.003

Chen, V.B., Arendall, W.B., Headd, J.J., Keedy, D.A., Immormino, R.M., Kapral, G.J., Murray, L.W., Richardson, J.S., Richardson, D.C., 2010. MolProbity : all-atom structure validation for macromolecular crystallography. Acta Crystallogr D Biol Crystallogr 66, 12–21. https://doi.org/10.1107/S0907444909042073

Cherf, G.M., Cochran, J.R., 2015. Applications of Yeast Surface Display for Protein Engineering. pp. 155–175. https://doi.org/10.1007/978-1-4939-2748-7_8

Chirmule, N., Jawa, V., Meibohm, B., 2012. Immunogenicity to Therapeutic Proteins: Impact on PK/PD and Efficacy. AAPS J 14, 296–302. https://doi.org/10.1208/s12248-012-9340-y

Clementi, M.E., Marini, S., Condò, S.G., Giardina, B., 1991. Antibodies against small molecules. Ann Ist Super Sanita 27, 139–43.

Cohen, G.H., Sheriff, S., Davies, D.R., 1996. Refined structure of the monoclonal antibody HyHEL-5 with its antigen hen egg-white lysozyme. Acta Crystallogr D Biol Crystallogr 52, 315–326. https://doi.org/10.1107/S0907444995014855

Collins, A.M., Wang, Y., Roskin, K.M., Marquis, C.P., Jackson, K.J.L., 2015. The mouse antibody heavy chain repertoire is germline-focused and highly variable between inbred strains. Philosophical Transactions of the Royal Society B: Biological Sciences 370, 20140236. https://doi.org/10.1098/rstb.2014.0236

Costa, A.F., Campos, D., Reis, C.A., Gomes, C., 2020. Targeting Glycosylation: A New Road for Cancer Drug Discovery. Trends Cancer 6, 757–766. https://doi.org/10.1016/j.trecan.2020.04.002

Crispin, M., Ward, A.B., Wilson, I.A., 2018. Structure and Immune Recognition of the HIV Glycan Shield. Annu Rev Biophys 47, 499–523. https://doi.org/10.1146/annurev-biophys-060414-034156

Crocker, P.R., Paulson, J.C., Varki, A., 2007. Siglecs and their roles in the immune system. Nat Rev Immunol 7, 255–266. https://doi.org/10.1038/nri2056

Crotty, S., 2015. A brief history of T cell help to B cells. Nat Rev Immunol 15, 185–189. https://doi.org/10.1038/nri3803

Crotty, S., 2014. T Follicular Helper Cell Differentiation, Function, and Roles in Disease. Immunity 41, 529–542. https://doi.org/10.1016/j.immuni.2014.10.004

Davis, B.G., Robinson, M.A., 2002. Drug delivery systems based on sugar-macromolecule conjugates. Curr Opin Drug Discov Devel 5, 279–288.

de Bono, B., Madera, M., Chothia, C., 2004. VH Gene Segments in the Mouse and Human Genomes. J Mol Biol 342, 131–143. https://doi.org/10.1016/j.jmb.2004.06.055

DeAngelo, D.J., Jonas, B.A., Liesveld, J.L., Bixby, D.L., Advani, A.S., Marlton, P., Magnani, J.L., Thackray, H.M., Feldman, E.J., O'Dwyer, M.E., Becker, P.S., 2022. Phase 1/2 study of uproleselan added to chemotherapy in

patients with relapsed or refractory acute myeloid leukemia. Blood 139, 1135–1146. https://doi.org/10.1182/blood.2021010721

Deimel, L.P., Sattentau, Q.J., 2022. Shared sugars – parasite glycan homology in HIV-1 vaccine design. Trends Parasitol 38, 498–500. https://doi.org/https://doi.org/10.1016/j.pt.2022.04.001

Deimel, L.P., Xue, X., Khan, A., Moynie, L., Buchanan, C.J., Sun, G., McBride, R., Schuster, H., Gauthier, C., Saliba, R., Leonavicus, K., Minall, L., Bort, G., Russell, R.A., Sezgin, E., Paulson, J.C., Anthony, D.C., Baldwin, A.J., Naismith, J., Schiffner, T., Davis, B.G., Sattentau, Q.J., 2023. Engineered display of ganglioside-sugars on protein elicits a clonally and structurally constrained B cell response. bioRxiv 2023.06.03.543556. https://doi.org/10.1101/2023.06.03.543556

Deimel, L.P., Xue, X., Sattentau, Q.J., 2022. Glycans in HIV-1 vaccine design - engaging the shield. Trends Microbiol. https://doi.org/10.1016/j.tim.2022.02.004

Dengjel, J., Stevanovic, S., 2006. Naturally Presented MHC Ligands Carrying Glycans. Transfusion Medicine and Hemotherapy 33, 38–44. https://doi.org/10.1159/000090194

DeWitt III, W.S., Mesin, L., Victora, G.D., Minin, V.N., Matsen IV, F.A., 2018. Using Genotype Abundance to Improve Phylogenetic Inference. Mol Biol Evol 35, 1253–1265. https://doi.org/10.1093/molbev/msy020

Diacovich, L., Gorvel, J.-P., 2010. Bacterial manipulation of innate immunity to promote infection. Nat Rev Microbiol 8, 117–128. https://doi.org/10.1038/nrmicro2295

Ding, K., Ekberg, T., Zeuthen, J., Teneberg, S., Karlsson, K.-A., Rosén, A., 1993. Monoclonal antibody against a lactose epitope of glycosphingolipids binds to melanoma tumour cells. Glycoconj J 10, 395–405. https://doi.org/10.1007/BF00731044

Dolhofer, R., Wieland, O.H., 1980. Increased glycosylation of serum albumin in diabetes mellitus. Diabetes 29, 417–22. https://doi.org/10.2337/diab.29.6.417

Donovan, R.S., Datti, A., Baek, M.G., Wu, Q., Sas, I.J., Korczak, B., Berger, E.G., Roy, R., Dennis, J.W., 1999. A solid-phase glycosyltransferase assay

for high-throughput screening in drug discovery research. Glycoconj J 16, 607–615. https://doi.org/10.1023/a:1007024916491

Dotan, N., Altstock, R.T., Schwarz, M., Dukler, A., 2006. Anti-glycan antibodies as biomarkers for diagnosis and prognosis. Lupus 15, 442–450. https://doi.org/10.1191/0961203306lu2331oa

Dube, D.H., Bertozzi, C.R., 2005. Glycans in cancer and inflammation — potential for therapeutics and diagnostics. Nat Rev Drug Discov 4, 477–488. https://doi.org/10.1038/nrd1751

Dupnik, K., 2017. What's "hapten"-ing in β-lactam hypersensitivity? Sci Transl Med 9. https://doi.org/10.1126/scitranslmed.aan3774

Eisen, H.N., 2014. Affinity Enhancement of Antibodies: How Low-Affinity Antibodies Produced Early in Immune Responses Are Followed by High-Affinity Antibodies Later and in Memory B-Cell Responses. Cancer Immunol Res 2, 381–392. https://doi.org/10.1158/2326-6066.CIR-14-0029

Eisen, H.N., Siskind, G.W., 1964. Variations in Affinities of Antibodies during the Immune Response *. Biochemistry 3, 996–1008. https://doi.org/10.1021/bi00895a027

Elkon, K., Casali, P., 2008. Nature and functions of autoantibodies. Nat Clin Pract Rheumatol 4, 491–498. https://doi.org/10.1038/ncprheum0895

Elsner, R.A., Shlomchik, M.J., 2020. Germinal Center and Extrafollicular B Cell Responses in Vaccination, Immunity, and Autoimmunity. Immunity 53, 1136–1150. https://doi.org/10.1016/j.immuni.2020.11.006

Emsley, P., Cowtan, K., 2004. Coot: model-building tools for molecular graphics. Acta Crystallogr D Biol Crystallogr 60, 2126–2132. https://doi.org/10.1107/S0907444904019158

Enrico, D., Paci, A., Chaput, N., Karamouza, E., Besse, B., 2020. Antidrug Antibodies Against Immune Checkpoint Blockers: Impairment of Drug Efficacy or Indication of Immune Activation? Clinical Cancer Research 26, 787–792. https://doi.org/10.1158/1078-0432.CCR-19-2337

Erlendsdottir, H., Knudsen, J.D., Odenholt, I., Cars, O., Espersen, F., Frimodt-Møller, N., Fuursted, K., Kristinsson, K.G., Gudmundsson, S., 2001. Penicillin Pharmacodynamics in Four Experimental Pneumococcal Infection Models. Antimicrob Agents Chemother 45, 1078–1085. https://doi.org/10.1128/AAC.45.4.1078-1085.2001

Ertekin, Ö., Pirinçci, Ş., Öztürk, S., 2016. Monoclonal IgA Antibodies for Aflatoxin Immunoassays. Toxins (Basel) 8, 148. https://doi.org/10.3390/toxins8050148

Escolano, A., Dosenovic, P., Nussenzweig, M.C., 2017. Progress toward active or passive HIV-1 vaccination. J Exp Med 214, 3–16. https://doi.org/10.1084/jem.20161765

Escolano, A., Gristick, H.B., Abernathy, M.E., Merkenschlager, J., Gautam, R., Oliveira, T.Y., Pai, J., West, A.P.J., Barnes, C.O., Cohen, A.A., Wang, H., Golijanin, J., Yost, D., Keeffe, J.R., Wang, Z., Zhao, P., Yao, K.-H., Bauer, J., Nogueira, L., Gao, H., Voll, A. v, Montefiori, D.C., Seaman, M.S., Gazumyan, A., Silva, M., McGuire, A.T., Stamatatos, L., Irvine, D.J., Wells, L., Martin, M.A., Bjorkman, P.J., Nussenzweig, M.C., 2019. Immunization expands B cells specific to HIV-1 V3 glycan in mice and macaques. Nature 570, 468–473. https://doi.org/10.1038/s41586-019-1250-z

Estevez, F., Carr, A., Solorzano, L., Valiente, O., Mesa, C., Barroso, O., Sierra, G. V, Fernandez, L.E., 1999. Enhancement of the immune response to poorly immunogenic gangliosides after incorporation into very small size proteoliposomes (VSSP). Vaccine 18, 190–197. https://doi.org/10.1016/s0264-410x(99)00219-4

Evans, P., 2006. Scaling and assessment of data quality. Acta Crystallogr D Biol Crystallogr 62, 72–82. https://doi.org/10.1107/S0907444905036693

Fernández, E.M.S., Navo, C.D., Martínez-Sáez, N., Gonçalves-Pereira, R., Somovilla, V.J., Avenoza, A., Busto, J.H., Bernardes, G.J.L., Jiménez-Osés, G., Corzana, F., Fernández, J.M.G., Mellet, C.O., Peregrina, J.M., 2016. Tn Antigen Mimics Based on sp2-Iminosugars with Affinity for an anti-MUC1 Antibody. Org Lett 18, 3890–3893. https://doi.org/10.1021/acs.orglett.6b01899

Ferreira, B.L., Ferreira, É.R., de Brito, M. V., Salu, B.R., Oliva, M.L. V., Mortara, R.A., Orikaza, C.M., 2018. BALB/c and C57BL/6 Mice Cytokine Responses to Trypanosoma cruzi Infection Are Independent of Parasite Strain Infectivity. Front Microbiol 9. https://doi.org/10.3389/fmicb.2018.00553

Florey, M.E., Adelaide, M.B., Florey, H.W., Adelaide, M.B., 1943. GENERAL AND LOCAL ADMINISTRATION OF PENICILLIN. The Lancet 241, 387–397. https://doi.org/10.1016/S0140-6736(00)41962-8

Fornefett, J., Krause, J., Klose, K., Fingas, F., Hassert, R., Benga, L., Grunwald, T., Müller, U., Schrödl, W., Baums, C.G., 2018. Comparative analysis of humoral immune responses and pathologies of BALB/c and C57BL/6 wildtype mice experimentally infected with a highly virulent Rodentibacter pneumotropicus (Pasteurella pneumotropica) strain. BMC Microbiol 18, 45. https://doi.org/10.1186/s12866-018-1186-8

Freedman, M.S., Laks, J., Dotan, N., Altstock, R.T., Dukler, A., Sindic, C.J.M., 2009. Anti-alpha-glucose-based glycan IgM antibodies predict relapse activity in multiple sclerosis after the first neurological event. Mult Scler 15, 422–430. https://doi.org/10.1177/1352458508101944

Fukushima, A., Yamaguchi, T., Ishida, W., Fukata, K., Taniguchi, T., Liu, F.-T., Ueno, H., 2006a. Genetic background determines susceptibility to experimental immune-mediated blepharoconjunctivitis: Comparison of Balb/c and C57BL/6 mice. Exp Eye Res 82, 210–218. https://doi.org/10.1016/j.exer.2005.06.010

Fukushima, A., Yamaguchi, T., Ishida, W., Fukata, K., Taniguchi, T., Liu, F.-T., Ueno, H., 2006b. Genetic background determines susceptibility to experimental immune-mediated blepharoconjunctivitis: Comparison of Balb/c and C57BL/6 mice. Exp Eye Res 82, 210–218. https://doi.org/10.1016/j.exer.2005.06.010

Gabba, A., Bogucka, A., Luz, J.G., Diniz, A., Coelho, H., Corzana, F., Cañada, F.J., Marcelo, F., Murphy, P. V, Birrane, G., 2021. Crystal Structure of the Carbohydrate Recognition Domain of the Human Macrophage Galactose C-Type Lectin Bound to GalNAc and the Tumor-Associated Tn Antigen. Biochemistry 60, 1327–1336. https://doi.org/10.1021/acs.biochem.1c00009

Gaebler, C., Wang, Z., Lorenzi, J.C.C., Muecksch, F., Finkin, S., Tokuyama, M., Cho, A., Jankovic, M., Schaefer-Babajew, D., Oliveira, T.Y., Cipolla, M., Viant, C., Barnes, C.O., Bram, Y., Breton, G., Hägglöf, T., Mendoza, P., Hurley, A., Turroja, M., Gordon, K., Millard, K.G., Ramos, V., Schmidt, F., Weisblum, Y., Jha, D., Tankelevich, M., Martinez-Delgado, G., Yee, J., Patel, R., Dizon, J., Unson-O'Brien, C., Shimeliovich, I., Robbiani, D.F., Zhao, Z., Gazumyan, A., Schwartz, R.E., Hatziioannou, T., Bjorkman, P.J., Mehandru, S., Bieniasz, P.D., Caskey, M., Nussenzweig, M.C., 2021.

Evolution of antibody immunity to SARS-CoV-2. Nature 591, 639–644. https://doi.org/10.1038/s41586-021-03207-w

Galiza, E.P., Heath, P.T., 2007. Pneumococcal conjugate vaccines. A review. Minerva Med 98, 131–43.

Galli-Stampino, L., Meinjohanns, E., Frische, K., Meldal, M., Jensen, T., Werdelin, O., Mouritsen, S., 1997. T-cell recognition of tumor-associated carbohydrates: the nature of the glycan moiety plays a decisive role in determining glycopeptide immunogenicity. Cancer Res 57, 3214–3222.

Gentilini, M.V., Pérez, M.E., Fernández, P.M., Fainboim, L., Arana, E., 2016. The tumor antigen N-glycolyl-GM3 is a human CD1d ligand capable of mediating B cell and natural killer T cell interaction. Cancer Immunol Immunother 65, 551–562. https://doi.org/10.1007/s00262-016-1812-y

Gessner, B.D., Adegbola, R.A., 2008. The impact of vaccines on pneumonia: Key lessons from Haemophilus influenzae type b conjugate vaccines. Vaccine 26, B3–B8. https://doi.org/10.1016/j.vaccine.2008.04.013

Gibson, D.G., 2011. Enzymatic Assembly of Overlapping DNA Fragments. pp. 349–361. https://doi.org/10.1016/B978-0-12-385120-8.00015-2

Gill, F.A., 1967. The association of increased spontaneous lymphocyte transformation in vitro with clinical manifestations of drug hypersensitivity. J Immunol 98, 778–85.

Glavey, S. v., Huynh, D., Reagan, M.R., Manier, S., Moschetta, M., Kawano, Y., Roccaro, A.M., Ghobrial, I.M., Joshi, L., O'Dwyer, M.E., 2015. The cancer glycome: Carbohydrates as mediators of metastasis. Blood Rev 29, 269–279. https://doi.org/10.1016/j.blre.2015.01.003

Goh, S.J.R., Tuomisto, J.E.E., Purcell, A.W., Mifsud, N.A., Illing, P.T., 2021. The complexity of T cell–mediated penicillin hypersensitivity reactions. Allergy 76, 150–167. https://doi.org/10.1111/all.14355

Goodnow, C.C., Crosbie, J., Adelstein, S., Lavoie, T.B., Smith-Gill, S.J., Brink, R.A., Pritchard-Briscoe, H., Wotherspoon, J.S., Loblay, R.H., Raphael, K., Trent, R.J., Basten, A., 1988. Altered immunoglobulin expression and functional silencing of self-reactive B lymphocytes in transgenic mice. Nature 334, 676–682. https://doi.org/10.1038/334676a0

Goodnow, C.C., Vinuesa, C.G., Randall, K.L., Mackay, F., Brink, R., 2010. Control systems and decision making for antibody production. Nat Immunol 11, 681–688. https://doi.org/10.1038/ni.1900

Gordon, S.M., Eaton, M.E., George, R., Larsen, S., Lukehart, S.A., Kuypers, J., Marra, C.M., Thompson, S., 1994. The Response of Symptomatic Neurosyphilis to High-Dose Intravenous Penicillin G in Patients with Human Immunodeficiency Virus Infection. New England Journal of Medicine 331, 1469–1473. https://doi.org/10.1056/NEJM199412013312201

Green, I., Paul, W.E., Benacerraf, B., 1968. Hapten carrier relationships in the DNP-PLL foreign albumin complex system: induction of tolerance and stimulation of cells in vitro. J Exp Med 127, 43–53. https://doi.org/10.1084/jem.127.1.43

Grewal, I.S., Moudgil, K.D., Sercarz, E.E., 1995. Hindrance of binding to class II major histocompatibility complex molecules by a single amino acid residue contiguous to a determinant leads to crypticity of the determinant as well as lack of response to the protein antigen. Proc Natl Acad Sci U S A 92, 1779–1783. https://doi.org/10.1073/pnas.92.5.1779

Grigalevicius, S., Chierici, S., Renaudet, O., Lo-Man, R., Dériaud, E., Leclerc, C., Dumy, P., 2005. Chemoselective Assembly and Immunological Evaluation of Multiepitopic Glycoconjugates Bearing Clustered Tn Antigen as Synthetic Anticancer Vaccines. Bioconjug Chem 16, 1149–1159. https://doi.org/10.1021/bc050010v

Gristick, H.B., von Boehmer, L., West Jr, A.P., Schamber, M., Gazumyan, A., Golijanin, J., Seaman, M.S., Fätkenheuer, G., Klein, F., Nussenzweig, M.C., Bjorkman, P.J., 2016. Natively glycosylated HIV-1 Env structure reveals new mode for antibody recognition of the CD4-binding site. Nat Struct Mol Biol 23, 906–915. https://doi.org/10.1038/nsmb.3291

Guthmann, M.D., Bitton, R.J., Carnero, A.J.L., Gabri, M.R., Cinat, G., Koliren, L., Lewi, D., Fernandez, L.E., Alonso, D.F., Gómez, D.E., Fainboim, L., 2004. Active specific immunotherapy of melanoma with a GM3 ganglioside-based vaccine: a report on safety and immunogenicity. J Immunother 27, 442–451. https://doi.org/10.1097/00002371-200411000-00004

Hägglöf, T., Cipolla, M., Loewe, M., Chen, S.T., Mesin, L., Hartweger, H., ElTanbouly, M.A., Cho, A., Gazumyan, A., Ramos, V., Stamatatos, L., Oliveira, T.Y., Nussenzweig, M.C., Viant, C., 2023. Continuous germinal center invasion contributes to the diversity of the immune response. Cell 186, 147-161.e15. https://doi.org/10.1016/j.cell.2022.11.032

Haji-Ghassemi, O., Blackler, R.J., Martin Young, N., Evans, S. V, 2015. Antibody recognition of carbohydrate epitopes†. Glycobiology 25, 920–952. https://doi.org/10.1093/glycob/cwv037

Hakomori, S., 2001. Tumor-Associated Carbohydrate Antigens Defining Tumor Malignancy: Basis for Development of Anti-Cancer Vaccines. pp. 369–402. https://doi.org/10.1007/978-1-4615-1267-7_24

Hakomori, S., Kannagi, R., 1983. Glycosphingolipids as tumor-associated and differentiation markers. J Natl Cancer Inst 71, 231–251.

Hakomori, S.I., Murakami, W.T., 1968. Glycolipids of hamster fibroblasts and derived malignant-transformed cell lines. Proc Natl Acad Sci U S A 59, 254–261. https://doi.org/10.1073/pnas.59.1.254

Haurum, J.S., Høier, I.B., Arsequell, G., Neisig, A., Valencia, G., Zeuthen, J., Neefjes, J., Elliott, T., 1999. Presentation of cytosolic glycosylated peptides by human class I major histocompatibility complex molecules in vivo. J Exp Med 190, 145–150. https://doi.org/10.1084/jem.190.1.145

Helenius, A., Simons, K., 1975. Solubilization of membranes by detergents. Biochimica et Biophysica Acta (BBA) - Reviews on Biomembranes 415, 29–79. https://doi.org/10.1016/0304-4157(75)90016-7

Hermanson, G.T., 2013. Chapter 3 - The Reactions of Bioconjugation, in: Hermanson, G.T. (Ed.), Bioconjugate Techniques (Third Edition). Academic Press, Boston, pp. 229–258. https://doi.org/https://doi.org/10.1016/B978-0-12-382239-0.00003-0

Hernández, A.M., Toledo, D., Martínez, D., Griñán, T., Brito, V., Macías, A., Alfonso, S., Rondón, T., Suárez, E., Vázquez, A.M., Pérez, R., 2008. Characterization of the Antibody Response against NeuGcGM3 Ganglioside Elicited in Non-Small Cell Lung Cancer Patients Immunized with an Anti-Idiotype Antibody. The Journal of Immunology 181, 6625–6634. https://doi.org/10.4049/jimmunol.181.9.6625

Herzenberg, L., Tokuhisa, T., 1982. Epitope-specific regulation. I. Carrier-specific induction of suppression for IgG anti-hapten antibody responses. Journal of Experimental Medicine 155, 1730–1740. https://doi.org/10.1084/jem.155.6.1730

Hida, S., Miura, N.N., Adachi, Y., Ohno, N., 2005. Effect of Candida albicans cell wall glucan as adjuvant for induction of autoimmune arthritis in mice. J Autoimmun 25, 93–101. https://doi.org/10.1016/j.jaut.2005.06.002

Hirabayashi, J., Hashidate, T., Arata, Y., Nishi, N., Nakamura, T., Hirashima, M., Urashima, T., Oka, T., Futai, M., Muller, W.E.G., Yagi, F., Kasai, K., 2002. Oligosaccharide specificity of galectins: a search by frontal affinity chromatography. Biochim Biophys Acta 1572, 232–54. https://doi.org/10.1016/s0304-4165(02)00311-2

Ho, I.Y., Bunker, J.J., Erickson, S.A., Neu, K.E., Huang, M., Cortese, M., Pulendran, B., Wilson, P.C., 2016. Refined protocol for generating monoclonal antibodies from single human and murine B cells. J Immunol Methods 438, 67–70. https://doi.org/10.1016/j.jim.2016.09.001

Holmberg, L.A., Sandmaier, B.M., 2004. Vaccination with Theratope (STn-KLH) as treatment for breast cancer. Expert Rev Vaccines 3, 655–663. https://doi.org/10.1586/14760584.3.6.655

Hong, S., Yu, C., Rodrigues, E., Shi, Y., Chen, H., Wang, P., Chapla, D.G., Gao, T., Zhuang, R., Moremen, K.W., Paulson, J.C., Macauley, M.S., Wu, P., 2021. Modulation of Siglec-7 Signaling Via In Situ-Created High-Affinity *cis* -Ligands. ACS Cent Sci 7, 1338–1346. https://doi.org/10.1021/acscentsci.1c00064

Hsieh, T.C., Ma, K.H., Chao, A., 2016. iNEXT: an R package for rarefaction and extrapolation of species diversity (Hill numbers). Methods Ecol Evol 7, 1451–1456. https://doi.org/https://doi.org/10.1111/2041-210X.12613

Hudak, J.E., Canham, S.M., Bertozzi, C.R., 2014. Glycocalyx engineering reveals a Siglec-based mechanism for NK cell immunoevasion. Nat Chem Biol 10, 69–75. https://doi.org/10.1038/nchembio.1388

Hutchins, L.F., Makhoul, I., Emanuel, P.D., Pennisi, A., Siegel, E.R., Jousheghany, F., Guo, X., Pashov, A.D., Monzavi-Karbassi, B., Kieber-Emmons, T., 2017. Targeting tumor-associated carbohydrate antigens: a phase I study of a carbohydrate mimetic-peptide vaccine in stage IV

breast cancer subjects. Oncotarget 8, 99161–99178. https://doi.org/10.18632/oncotarget.21959

Huynh, D., Tung, N., Dam, Q., Tran, T., Hulten, K.G., Harrison, C.J., Kaplan, S.L., Nguyen, A., Do, T.H., Setty, A., Le, J., 2023. Amoxicillin and penicillin G dosing in pediatric community-acquired pneumococcal pneumonia in the era of conjugate pneumococcal vaccines. Pharmacotherapy: The Journal of Human Pharmacology and Drug Therapy. https://doi.org/10.1002/phar.2756

Icart, L.P., Fernandez-Santana, V., Veloso, R.C., Carmenate, T., Sirois, S., Roy, R., Bencomo, V.V., 2008. T-Cell Immunity of Carbohydrates, in: Carbohydrate-Based Vaccines, ACS Symposium Series. American Chemical Society, p. 1. https://doi.org/doi:10.1021/bk-2008-0989.ch001

Iho, S., Maeyama, J., Suzuki, F., 2015. CpG oligodeoxynucleotides as mucosal adjuvants. Hum Vaccin Immunother 11, 755–760. https://doi.org/10.1080/21645515.2014.1004033

Inoue, T., Shinnakasu, R., Kawai, C., Yamamoto, H., Sakakibara, S., Ono, C., Itoh, Y., Terooatea, T., Yamashita, K., Okamoto, T., Hashii, N., Ishii-Watabe, A., Butler, N.S., Matsuura, Y., Matsumoto, H., Otsuka, S., Hiraoka, K., Teshima, T., Murakami, M., Kurosaki, T., 2023. Antibody feedback contributes to facilitating the development of Omicron-reactive memory B cells in SARS-CoV-2 mRNA vaccinees. Journal of Experimental Medicine 220. https://doi.org/10.1084/jem.20221786

Irvine, D.J., Read, B.J., 2020. Shaping humoral immunity to vaccines through antigen-displaying nanoparticles. Curr Opin Immunol 65, 1–6. https://doi.org/10.1016/j.coi.2020.01.007

Jack, D.L., Lee, M.E., Turner, M.W., Klein, N.J., Read, R.C., 2005. Mannose-binding lectin enhances phagocytosis and killing of Neisseria meningitidis by human macrophages. J Leukoc Biol 77, 328–336. https://doi.org/10.1189/jlb.0604342

Jacob, J., Kelsoe, G., Rajewsky, K., Weiss, U., 1991. Intraclonal generation of antibody mutants in germinal centres. Nature 354, 389–392. https://doi.org/10.1038/354389a0

James, L.C., Tawfik, D.S., 2003. The specificity of cross-reactivity: promiscuous antibody binding involves specific hydrogen bonds rather than nonspecific

hydrophobic stickiness. Protein Sci 12, 2183–2193. https://doi.org/10.1110/ps.03172703

Jana, M., Bandyopadhyay, S., 2012. Conformational flexibility of a protein–carbohydrate complex and the structure and ordering of surrounding water. Physical Chemistry Chemical Physics 14, 6628. https://doi.org/10.1039/c2cp24104h

Jandus, C., Boligan, K.F., Chijioke, O., Liu, H., Dahlhaus, M., Démoulins, T., Schneider, C., Wehrli, M., Hunger, R.E., Baerlocher, G.M., Simon, H.-U., Romero, P., Münz, C., von Gunten, S., 2014. Interactions between Siglec-7/9 receptors and ligands influence NK cell-dependent tumor immunosurveillance. J Clin Invest 124, 1810–1820. https://doi.org/10.1172/JCI65899

Jardine, J., Julien, J.-P., Menis, S., Ota, T., Kalyuzhniy, O., McGuire, A., Sok, D., Huang, P.-S., MacPherson, S., Jones, M., Nieusma, T., Mathison, J., Baker, D., Ward, A.B., Burton, D.R., Stamatatos, L., Nemazee, D., Wilson, I.A., Schief, W.R., 2013. Rational HIV Immunogen Design to Target Specific Germline B Cell Receptors. Science (1979) 340, 711 LP – 716. https://doi.org/10.1126/science.1234150

Jardine, J.G., Kulp, D.W., Havenar-Daughton, C., Sarkar, A., Briney, B., Sok, D., Sesterhenn, F., Ereño-Orbea, J., Kalyuzhniy, O., Deresa, I., Hu, X., Spencer, S., Jones, M., Georgeson, E., Adachi, Y., Kubitz, M., deCamp, A.C., Julien, J.-P., Wilson, I.A., Burton, D.R., Crotty, S., Schief, W.R., 2016. HIV-1 broadly neutralizing antibody precursor B cells revealed by germline-targeting immunogen. Science 351, 1458–1463. https://doi.org/10.1126/science.aad9195

Jenner, E., 1821. Letter Addressed to the Medical Profession Generally, Relative to Vaccination. Lond Med Phys J 45, 277–280.

Ju, Y., Carreño, J.M., Simon, V., Dawson, K., Krammer, F., Kent, S.J., 2023. Impact of anti-PEG antibodies induced by SARS-CoV-2 mRNA vaccines. Nat Rev Immunol 23, 135–136. https://doi.org/10.1038/s41577-022-00825-x

Julien, S., Ivetic, A., Grigoriadis, A., QiZe, D., Burford, B., Sproviero, D., Picco, G., Gillett, C., Papp, S.L., Schaffer, L., Tutt, A., Taylor-Papadimitriou, J., Pinder, S.E., Burchell, J.M., 2011. Selectin ligand sialyl-Lewis x antigen

drives metastasis of hormone-dependent breast cancers. Cancer Res 71, 7683–7693. https://doi.org/10.1158/0008-5472.CAN-11-1139

Kabsch, W., 2010. XDS. Acta Crystallogr D Biol Crystallogr 66, 125–132. https://doi.org/10.1107/S0907444909047337

Kannagi, R., Yin, J., Miyazaki, K., Izawa, M., 2008. Current relevance of incomplete synthesis and neo-synthesis for cancer-associated alteration of carbohydrate determinants--Hakomori's concepts revisited. Biochim Biophys Acta 1780, 525–531. https://doi.org/10.1016/j.bbagen.2007.10.007

Karagiannis, S.N., Karagiannis, P., Josephs, D.H., Saul, L., Gilbert, A.E., Upton, N., Gould, H.J., 2013. Immunoglobulin E and Allergy: Antibodies in Immune Inflammation and Treatment. Microbiol Spectr 1. https://doi.org/10.1128/microbiolspec.AID-0006-2012

Kato, T., Ujiie, H., Hatanaka, K.C., Nange, A., Okumura, A., Tsubame, K., Naruchi, K., Sato, M., Kaga, K., Matsuno, Y., Wakasa, S., Hatanaka, Y., 2021. A novel Tn antigen epitope-recognizing antibody for MUC1 predicts clinical outcome in patients with primary lung adenocarcinoma. Oncol Lett 21, 202. https://doi.org/10.3892/ol.2021.12463

Kavai, M., Szegedi, G., 2007. Immune complex clearance by monocytes and macrophages in systemic lupus erythematosus. Autoimmun Rev 6, 497–502. https://doi.org/10.1016/j.autrev.2007.01.017

Kenett, D., Fleminger, G., Katchalski-Katzir, E., Poljak, R.J., 1987. Lysozyme bound to the D1.3 monoclonal antibody retains enzymatic activity in assays using N-acetylglucosamine oligomers as substrate. Mol Immunol 24, 313–316. https://doi.org/10.1016/0161-5890(87)90150-7

Kerkis, A.Yu., Zhdanova, N.S., 1992. Formation and ultrastructure of somatic cell hybrids. Electron Microsc Rev 5, 1–24. https://doi.org/https://doi.org/10.1016/0892-0354(92)90002-8

Kessler, N., Bertrand, S., Aymard, M., 1993. Stability of a Murine Hybridoma Is Dependent on the Clonal Line and Culture Media. In Vitro Cellular & Developmental Biology 29A, 203–207.

Kim, B.J., Park, J.H., Park, T.H., Bronstein, P.A., Schneider, D.J., Cartinhour, S.W., Shuler, M.L., 2009. Effect of Iron Concentration on the Growth Rate of *Pseudomonas syringae* and the Expression of Virulence Factors in *hrp* -

Inducing Minimal Medium. Appl Environ Microbiol 75, 2720–2726. https://doi.org/10.1128/AEM.02738-08

Kim, S.K., Ragupathi, G., Cappello, S., Kagan, E., Livingston, P.O., 2000. Effect of immunological adjuvant combinations on the antibody and T-cell response to vaccination with MUC1-KLH and GD3-KLH conjugates. Vaccine 19, 530–537. https://doi.org/10.1016/s0264-410x(00)00195-x

Kim, Y.J., Varki, A., 1997. Perspectives on the significance of altered glycosylation of glycoproteins in cancer. Glycoconj J 14, 569–576. https://doi.org/10.1023/a:1018580324971

Kipper, K., Barker, C.I.S., Standing, J.F., Sharland, M., Johnston, A., 2018. Development of a Novel Multipenicillin Assay and Assessment of the Impact of Analyte Degradation: Lessons for Scavenged Sampling in Antimicrobial Pharmacokinetic Study Design. Antimicrob Agents Chemother 62. https://doi.org/10.1128/AAC.01540-17

Klein, F., Gaebler, C., Mouquet, H., Sather, D.N., Lehmann, C., Scheid, J.F., Kraft, Z., Liu, Y., Pietzsch, J., Hurley, A., Poignard, P., Feizi, T., Morris, L., Walker, B.D., Fätkenheuer, G., Seaman, M.S., Stamatatos, L., Nussenzweig, M.C., 2012. Broad neutralization by a combination of antibodies recognizing the CD4 binding site and a new conformational epitope on the HIV-1 envelope protein. J Exp Med 209, 1469–1479. https://doi.org/10.1084/jem.20120423

Klein, S.L., Flanagan, K.L., 2016. Sex differences in immune responses. Nat Rev Immunol 16, 626–638. https://doi.org/10.1038/nri.2016.90

KÖHLER, G., MILSTEIN, C., 1975. Continuous cultures of fused cells secreting antibody of predefined specificity. Nature 256, 495–497. https://doi.org/10.1038/256495a0

Kohler, H., Pashov, A., Kieber-Emmons, T., 2019. The Promise of Anti-idiotype Revisited. Front Immunol 10. https://doi.org/10.3389/fimmu.2019.00808

Koike, T., Kimura, N., Miyazaki, K., Yabuta, T., Kumamoto, K., Takenoshita, S., Chen, J., Kobayashi, M., Hosokawa, M., Taniguchi, A., Kojima, T., Ishida, N., Kawakita, M., Yamamoto, H., Takematsu, H., Suzuki, A., Kozutsumi, Y., Kannagi, R., 2004. Hypoxia induces adhesion molecules on cancer cells: A missing link between Warburg effect and induction of selectin-

ligand carbohydrates. Proc Natl Acad Sci U S A 101, 8132–8137. https://doi.org/10.1073/pnas.0402088101

Kondo, H., Shiroishi, M., Matsushima, M., Tsumoto, K., Kumagai, I., 1999. Crystal Structure of Anti-Hen Egg White Lysozyme Antibody (HyHEL-10) Fv-Antigen Complex: LOCAL STRUCTURAL CHANGES IN THE PROTEIN ANTIGEN AND WATER-MEDIATED INTERACTIONS OF FV-ANTIGEN AND LIGHT CHAIN-HEAVY CHAIN INTERFACES*. Journal of Biological Chemistry 274, 27623–27631. https://doi.org/https://doi.org/10.1074/jbc.274.39.27623

Kong, A.T., Leprevost, F. V, Avtonomov, D.M., Mellacheruvu, D., Nesvizhskii, A.I., 2017. MSFragger: ultrafast and comprehensive peptide identification in mass spectrometry–based proteomics. Nat Methods 14, 513–520. https://doi.org/10.1038/nmeth.4256

KONG, K.-F., SCHNEPER, L., MATHEE, K., 2010. Beta-lactam antibiotics: from antibiosis to resistance and bacteriology. APMIS 118, 1–36. https://doi.org/10.1111/j.1600-0463.2009.02563.x

Kotani, M., Ozawa, H., Kawashima, I., Ando, S., Tai, T., 1992. Generation of one set of monoclonal antibodies specific for a-pathway ganglio-series gangliosides. Biochim Biophys Acta 1117, 97–103. https://doi.org/10.1016/0304-4165(92)90168-t

Kragh-Hansen, U., 1990. Structure and ligand binding properties of human serum albumin. Dan Med Bull 37, 57–84.

Kragh-Hansen, U., 1981. Molecular aspects of ligand binding to serum albumin. Pharmacol Rev 33, 17.

Kragh-Hansen, U., le Maire, M., Møller, J. V., 1998. The Mechanism of Detergent Solubilization of Liposomes and Protein-Containing Membranes. Biophys J 75, 2932–2946. https://doi.org/10.1016/S0006-3495(98)77735-5

Kreissl, M.C., Wu, H.-M., Stout, D.B., Ladno, W., Schindler, T.H., Zhang, X., Prior, J.O., Prins, M.L., Chatziioannou, A.F., Huang, S.-C., Schelbert, H.R., 2006. Noninvasive measurement of cardiovascular function in mice with high-temporal-resolution small-animal PET. J Nucl Med 47, 974–80.

Krug, L.M., Ragupathi, G., Hood, C., Kris, M.G., Miller, V.A., Allen, J.R., Keding, S.J., Danishefsky, S.J., Gomez, J., Tyson, L., Pizzo, B., Baez, V., Livingston, P.O., 2004. Vaccination of Patients with Small-Cell Lung

Cancer with Synthetic Fucosyl GM-1 Conjugated to Keyhole Limpet Hemocyanin. Clinical Cancer Research 10, 6094–6100. https://doi.org/10.1158/1078-0432.CCR-04-0482

Krumm, S.A., Doores, K.J., 2020. Targeting Glycans on Human Pathogens for Vaccine Design. Curr Top Microbiol Immunol 428, 129–163. https://doi.org/10.1007/82_2018_103

Kubelkova, K., Macela, A., 2019. Innate Immune Recognition: An Issue More Complex Than Expected. Front Cell Infect Microbiol 9. https://doi.org/10.3389/fcimb.2019.00241

Kudryashov, V., Kim, H.M., Ragupathi, G., Danishefsky, S.J., Livingston, P.O., Lloyd, K.O., 1998. Immunogenicity of synthetic conjugates of Lewis(y) oligosaccharide with proteins in mice: towards the design of anticancer vaccines. Cancer Immunol Immunother 45, 281–6. https://doi.org/10.1007/s002620050444

Kuduk, S.D., Schwarz, J.B., Chen, X.-T., Glunz, P.W., Sames, D., Ragupathi, G., Livingston, P.O., Danishefsky, S.J., 1998a. Synthetic and Immunological Studies on Clustered Modes of Mucin-Related Tn and TF O-Linked Antigens: The Preparation of a Glycopeptide-Based Vaccine for Clinical Trials against Prostate Cancer. J Am Chem Soc 120, 12474–12485. https://doi.org/10.1021/ja9825128

Kuduk, S.D., Schwarz, J.B., Chen, X.-T., Glunz, P.W., Sames, D., Ragupathi, G., Livingston, P.O., Danishefsky, S.J., 1998b. Synthetic and Immunological Studies on Clustered Modes of Mucin-Related Tn and TF O-Linked Antigens: The Preparation of a Glycopeptide-Based Vaccine for Clinical Trials against Prostate Cancer. J Am Chem Soc 120, 12474–12485. https://doi.org/10.1021/ja9825128

Küppers, R., Zhao, M., Hansmann, M.L., Rajewsky, K., 1993. Tracing B cell development in human germinal centres by molecular analysis of single cells picked from histological sections. EMBO J 12, 4955–4967. https://doi.org/10.1002/j.1460-2075.1993.tb06189.x

Lafaye, P., Lapresle, C., 1988. Fixation of penicilloyl groups to albumin and appearance of anti-penicilloyl antibodies in penicillin-treated patients. Journal of Clinical Investigation 82, 7–12. https://doi.org/10.1172/JCI113603

Lahera, T., Calvo, A., Torres, G., Rengifo, C.E., Quintero, S., Arango, M.D.C., Danta, D., Vázquez, J.M., Escobar, X., Carr, A., 2014. Prognostic Role of 14F7 Mab Immunoreactivity against N-Glycolyl GM3 Ganglioside in Colon Cancer. J Oncol 2014, 482301. https://doi.org/10.1155/2014/482301

Landsteiner, K., 2013. The specificity of serological reactions. Courier Corporation.

Landsteiner, K., Jacobs, J., 1936. STUDIES ON THE SENSITIZATION OF ANIMALS WITH SIMPLE CHEMICAL COMPOUNDS. II. J Exp Med 64, 625–39. https://doi.org/10.1084/jem.64.4.625

Lane, R.D., Crissman, R.S., Lachman, M.F., 1984. Comparison of polyethylene glycols as fusogens for producing lymphocyte-myeloma hybrids. J Immunol Methods 72, 71–76. https://doi.org/https://doi.org/10.1016/0022-1759(84)90434-4

Lanie, J.A., Ng, W.-L., Kazmierczak, K.M., Andrzejewski, T.M., Davidsen, T.M., Wayne, K.J., Tettelin, H., Glass, J.I., Winkler, M.E., 2007. Genome sequence of Avery's virulent serotype 2 strain D39 of Streptococcus pneumoniae and comparison with that of unencapsulated laboratory strain R6. J Bacteriol 189, 38–51. https://doi.org/10.1128/JB.01148-06

Lapresle, C., Wal, J.-M., 1979. The binding of penicillin to albumin molecules in bisalbuminemia induced by penicillin therapy. Biochimica et Biophysica Acta (BBA) - General Subjects 586, 106–111. https://doi.org/10.1016/0304-4165(79)90408-2

Larsen, M.T., Kuhlmann, M., Hvam, M.L., Howard, K.A., 2016. Albumin-based drug delivery: harnessing nature to cure disease. Mol Cell Ther 4, 3. https://doi.org/10.1186/s40591-016-0048-8

Lasic, D.D., 1997. The Conformation of Polymers at Interfaces. pp. 31–44. https://doi.org/10.1021/bk-1997-0680.ch003

Lederer, K., Castaño, D., Gómez Atria, D., Oguin, T.H., Wang, S., Manzoni, T.B., Muramatsu, H., Hogan, M.J., Amanat, F., Cherubin, P., Lundgreen, K.A., Tam, Y.K., Fan, S.H.Y., Eisenlohr, L.C., Maillard, I., Weissman, D., Bates, P., Krammer, F., Sempowski, G.D., Pardi, N., Locci, M., 2020. SARS-CoV-2 mRNA Vaccines Foster Potent Antigen-Specific Germinal Center Responses Associated with Neutralizing Antibody Generation. Immunity 53, 1281-1295.e5. https://doi.org/10.1016/j.immuni.2020.11.009

Lee, Y.C., Stowell, C.P., Krantz, M.J., 1976. 2-Imino-2-methoxyethyl 1-thioglycosides: new reagents for attaching sugars to proteins. Biochemistry 15, 3956–3963. https://doi.org/10.1021/bi00663a008

Leggat, D.J., Cohen, K.W., Willis, J.R., Fulp, W.J., deCamp, A.C., Kalyuzhniy, O., Cottrell, C.A., Menis, S., Finak, G., Ballweber-Fleming, L., Srikanth, A., Plyler, J.R., Schiffner, T., Liguori, A., Rahaman, F., Lombardo, A., Philiponis, V., Whaley, R.E., Seese, A., Brand, J., Ruppel, A.M., Hoyland, W., Yates, N.L., Williams, L.D., Greene, K., Gao, H., Mahoney, C.R., Corcoran, M.M., Cagigi, A., Taylor, A., Brown, D.M., Ambrozak, D.R., Sincomb, T., Hu, X., Tingle, R., Georgeson, E., Eskandarzadeh, S., Alavi, N., Lu, D., Mullen, T.-M., Kubitz, M., Groschel, B., Maenza, J., Kolokythas, O., Khati, N., Bethony, J., Crotty, S., Roederer, M., Karlsson Hedestam, G.B., Tomaras, G.D., Montefiori, D., Diemert, D., Koup, R.A., Laufer, D.S., McElrath, M.J., McDermott, A.B., Schief, W.R., 2023. Vaccination induces HIV broadly neutralizing antibody precursors in humans. Science (1979) 378, eadd6502. https://doi.org/10.1126/science.add6502

Lentz, B.R., 2007. PEG as a tool to gain insight into membrane fusion. European Biophysics Journal 36, 315–326. https://doi.org/10.1007/s00249-006-0097-z

Lepore, M., Mori, L., De Libero, G., 2018. The Conventional Nature of Non-MHC-Restricted T Cells. Front Immunol 9. https://doi.org/10.3389/fimmu.2018.01365

Levine, B.B., Ovary, Z., 1961. STUDIES ON THE MECHANISM OF THE FORMATION OF THE PENICILLIN ANTIGEN. Journal of Experimental Medicine 114, 875–940. https://doi.org/10.1084/jem.114.6.875

Li, Y., Masse-Ranson, G., Garcia, Z., Bruel, T., Kök, A., Strick-Marchand, H., Jouvion, G., Serafini, N., Lim, A.I., Dusseaux, M., Hieu, T., Bourgade, F., Toubert, A., Finke, D., Schwartz, O., Bousso, P., Mouquet, H., Di Santo, J.P., 2018. A human immune system mouse model with robust lymph node development. Nat Methods 15, 623–630. https://doi.org/10.1038/s41592-018-0071-6

Liebschner, D., Afonine, P. V., Baker, M.L., Bunkóczi, G., Chen, V.B., Croll, T.I., Hintze, B., Hung, L.-W., Jain, S., McCoy, A.J., Moriarty, N.W., Oeffner, R.D., Poon, B.K., Prisant, M.G., Read, R.J., Richardson, J.S., Richardson,

D.C., Sammito, M.D., Sobolev, O. V., Stockwell, D.H., Terwilliger, T.C., Urzhumtsev, A.G., Videau, L.L., Williams, C.J., Adams, P.D., 2019. Macromolecular structure determination using X-rays, neutrons and electrons: recent developments in Phenix. Acta Crystallogr D Struct Biol 75, 861–877. https://doi.org/10.1107/S2059798319011471

Lin, T.-W., Chang, J.-K., Wu, Y.-R., Sun, T.-H., Cheng, Y.-Y., Ren, C.-T., Pan, M.-H., Wu, J.-L., Chang, K.-H., Yang, H.-I., Chen, C.-M., Wu, C.-Y., Chen, Y.-R., 2023. Ganglioside-focused Glycan Array Reveals Abnormal Anti-GD1b Auto-antibody in Plasma of Preclinical Huntington's Disease. Mol Neurobiol. https://doi.org/10.1007/s12035-023-03307-w

Linehan, S.A., Martínez-Pomares, L., Gordon, S., 2000. Macrophage lectins in host defence. Microbes Infect 2, 279–288. https://doi.org/10.1016/s1286-4579(00)00300-2

Liu, Y.-J., de Bouteiller, O., Fugier-Vivier, I., 1997. Mechanisms of selection and differentiation in germinal centers. Curr Opin Immunol 9, 256–262. https://doi.org/10.1016/S0952-7915(97)80145-8

Livingston, P.O., Ragupathi, G., 2006. Cancer vaccines targeting carbohydrate antigens. Hum Vaccin 2, 137–143. https://doi.org/10.4161/hv.2941

Livingston, P.O., Ritter, G., Calves, M.J., 1989. Antibody response after immunization with the gangliosides GM1, GM2, GM3, GD2 and GD3 in the mouse. Cancer Immunol Immunother 29, 179–184. https://doi.org/10.1007/BF00199993

Livingston, P.O., Wong, G.Y., Adluri, S., Tao, Y., Padavan, M., Parente, R., Hanlon, C., Calves, M.J., Helling, F., Ritter, G., 1994. Improved survival in stage III melanoma patients with GM2 antibodies: a randomized trial of adjuvant vaccination with GM2 ganglioside. Journal of Clinical Oncology 12, 1036–1044. https://doi.org/10.1200/JCO.1994.12.5.1036

Lloyd, K.O., Gordon, C.M., Thampoe, I.J., DiBenedetto, C., 1992. Cell Surface Accessibility of Individual Gangliosides in Malignant Melanoma Cells to Antibodies Is Influenced by the Total Ganglioside Composition of the Cells1. Cancer Res 52, 4948–4953.

Loaeza-Reyes, K.J., Zenteno, E., Moreno-Rodríguez, A., Torres-Rosas, R., Argueta-Figueroa, L., Salinas-Marín, R., Castillo-Real, L.M., Pina-Canseco, S., Cervera, Y.P., 2021. An Overview of Glycosylation and its Impact on

Cardiovascular Health and Disease. Front Mol Biosci 8. https://doi.org/10.3389/fmolb.2021.751637

Lochmatter, P., Beeler, A., Kawabata, T.T., Gerber, B.O., Pichler, W.J., 2009. Drug-specific in vitro release of IL-2, IL-5, IL-13 and IFN-gamma in patients with delayed-type drug hypersensitivity. Allergy 64, 1269–78. https://doi.org/10.1111/j.1398-9995.2009.01985.x

Lombard, V., Golaconda Ramulu, H., Drula, E., Coutinho, P.M., Henrissat, B., 2014. The carbohydrate-active enzymes database (CAZy) in 2013. Nucleic Acids Res 42, D490–D495. https://doi.org/10.1093/nar/gkt1178

Lu, L.L., Suscovich, T.J., Fortune, S.M., Alter, G., 2018. Beyond binding: antibody effector functions in infectious diseases. Nat Rev Immunol 18, 46–61. https://doi.org/10.1038/nri.2017.106

Lübbers, J., Rodríguez, E., van Kooyk, Y., 2018. Modulation of Immune Tolerance via Siglec-Sialic Acid Interactions. Front Immunol 9, 2807. https://doi.org/10.3389/fimmu.2018.02807

Malaker, S.A., Ferracane, M.J., Depontieu, F.R., Zarling, A.L., Shabanowitz, J., Bai, D.L., Topalian, S.L., Engelhard, V.H., Hunt, D.F., 2017. Identification and Characterization of Complex Glycosylated Peptides Presented by the MHC Class II Processing Pathway in Melanoma. J Proteome Res 16, 228–237. https://doi.org/10.1021/acs.jproteome.6b00496

Manz, R.A., Thiel, A., Radbruch, A., 1997. Lifetime of plasma cells in the bone marrow. Nature 388, 133–134. https://doi.org/10.1038/40540

Marquina, G., Waki, H., Fernandez, L.E., Kon, K., Carr, A., Valiente, O., Perez, R., Ando, S., 1996. Gangliosides expressed in human breast cancer. Cancer Res 56, 5165–5171.

Mata-Haro, V., Cekic, C., Martin, M., Chilton, P.M., Casella, C.R., Mitchell, T.C., 2007. The vaccine adjuvant monophosphoryl lipid A as a TRIF-biased agonist of TLR4. Science (1979) 316, 1628–1632. https://doi.org/10.1126/science.1138963

Mattox, D.E., Bailey-Kellogg, C., 2021. Comprehensive analysis of lectin-glycan interactions reveals determinants of lectin specificity. PLoS Comput Biol 17, e1009470. https://doi.org/10.1371/journal.pcbi.1009470

Maul, R.W., Gearhart, P.J., 2010. AID and Somatic Hypermutation. pp. 159–191. https://doi.org/10.1016/S0065-2776(10)05006-6

McNamara, H.A., Idris, A.H., Sutton, H.J., Vistein, R., Flynn, B.J., Cai, Y., Wiehe, K., Lyke, K.E., Chatterjee, D., Kc, N., Chakravarty, S., Lee Sim, B.K., Hoffman, S.L., Bonsignori, M., Seder, R.A., Cockburn, I.A., 2020. Antibody Feedback Limits the Expansion of B Cell Responses to Malaria Vaccination but Drives Diversification of the Humoral Response. Cell Host Microbe 28, 572-585.e7. https://doi.org/10.1016/j.chom.2020.07.001

Meng, X., Al-Attar, Z., Yaseen, F.S., Jenkins, R., Earnshaw, C., Whitaker, P., Peckham, D., French, N.S., Naisbitt, D.J., Park, B.K., 2017a. Definition of the Nature and Hapten Threshold of the β-Lactam Antigen Required for T Cell Activation In Vitro and in Patients. The Journal of Immunology 198, 4217–4227. https://doi.org/10.4049/jimmunol.1700209

Meng, X., Al-Attar, Z., Yaseen, F.S., Jenkins, R., Earnshaw, C., Whitaker, P., Peckham, D., French, N.S., Naisbitt, D.J., Park, B.K., 2017b. Definition of the Nature and Hapten Threshold of the β-Lactam Antigen Required for T Cell Activation In Vitro and in Patients. The Journal of Immunology 198, 4217–4227. https://doi.org/10.4049/jimmunol.1700209

Merad, B., Berrah, H., Miloudi, N., Sami, S., Hireche, K., Kermi, S., Issad, M., De Montclos, H., 1998. [Blood determination of benzathine-penicillin used in acute joint rheumatism prophylaxis]. Arch Inst Pasteur Alger 62, 32–9.

Mesin, L., Ersching, J., Victora, G.D., 2016. Germinal Center B Cell Dynamics. Immunity 45, 471–482. https://doi.org/10.1016/j.immuni.2016.09.001

Mesin, L., Schiepers, A., Ersching, J., Barbulescu, A., Cavazzoni, C.B., Angelini, A., Okada, T., Kurosaki, T., Victora, G.D., 2020. Restricted Clonality and Limited Germinal Center Reentry Characterize Memory B Cell Reactivation by Boosting. Cell 180, 92-106.e11. https://doi.org/10.1016/j.cell.2019.11.032

Metsvaht, T., Nellis, G., Varendi, H., Nunn, A.J., Graham, S., Rieutord, A., Storme, T., McElnay, J., Mulla, H., Turner, M.A., Lutsar, I., 2015. High variability in the dosing of commonly used antibiotics revealed by a Europe-wide point prevalence study: implications for research and dissemination. BMC Pediatr 15, 41. https://doi.org/10.1186/s12887-015-0359-y

Mikocziova, I., Greiff, V., Sollid, L.M., 2021. Immunoglobulin germline gene variation and its impact on human disease. Genes Immun 22, 205–217. https://doi.org/10.1038/s41435-021-00145-5

Mitchison, N.A., 1971. The carrier effect in the secondary response to hapten-protein conjugates. I. Measurement of the effect with transferred cells and objections to the local environment hypothesis. Eur J Immunol 1, 10–17. https://doi.org/10.1002/eji.1830010103

Miyazaki, K., Ohmori, K., Izawa, M., Koike, T., Kumamoto, K., Furukawa, K., Ando, T., Kiso, M., Yamaji, T., Hashimoto, Y., Suzuki, A., Yoshida, A., Takeuchi, M., Kannagi, R., 2004. Loss of disialyl Lewis(a), the ligand for lymphocyte inhibitory receptor sialic acid-binding immunoglobulin-like lectin-7 (Siglec-7) associated with increased sialyl Lewis(a) expression on human colon cancers. Cancer Res 64, 4498–4505. https://doi.org/10.1158/0008-5472.CAN-03-3614

Morbach, H., Eichhorn, E.M., Liese, J.G., Girschick, H.J., 2010. Reference values for B cell subpopulations from infancy to adulthood. Clin Exp Immunol 162, 271–279. https://doi.org/10.1111/j.1365-2249.2010.04206.x

Morefield, G.L., Sokolovska, A., Jiang, D., HogenEsch, H., Robinson, J.P., Hem, S.L., 2005. Role of aluminum-containing adjuvants in antigen internalization by dendritic cells in vitro. Vaccine 23, 1588–1595. https://doi.org/10.1016/j.vaccine.2004.07.050

Mouquet, H., Scharf, L., Euler, Z., Liu, Y., Eden, C., Scheid, J.F., Halper-Stromberg, A., Gnanapragasam, P.N.P., Spencer, D.I.R., Seaman, M.S., Schuitemaker, H., Feizi, T., Nussenzweig, M.C., Bjorkman, P.J., 2012. Complex-type N-glycan recognition by potent broadly neutralizing HIV antibodies. Proc Natl Acad Sci U S A 109, E3268–E3277. https://doi.org/10.1073/pnas.1217207109

Mu, L., Yin, X., Wu, H., Lei, Y., Han, K., Mo, J., Guo, Z., Li, J., Ye, J., 2020. Mannose-Binding Lectin Possesses Agglutination Activity and Promotes Opsonophagocytosis of Macrophages with Calreticulin Interaction in an Early Vertebrate. The Journal of Immunology ji2000256. https://doi.org/10.4049/jimmunol.2000256

Müller, J., Nitschke, L., 2014. The role of CD22 and Siglec-G in B-cell tolerance and autoimmune disease. Nat Rev Rheumatol 10, 422–428. https://doi.org/10.1038/nrrheum.2014.54

Muramatsu, M., Kinoshita, K., Fagarasan, S., Yamada, S., Shinkai, Y., Honjo, T., 2000. Class Switch Recombination and Hypermutation Require Activation-Induced Cytidine Deaminase (AID), a Potential RNA Editing Enzyme. Cell 102, 553–563. https://doi.org/10.1016/S0092-8674(00)00078-7

Muramatsu, M., Sankaranand, V.S., Anant, S., Sugai, M., Kinoshita, K., Davidson, N.O., Honjo, T., 1999. Specific Expression of Activation-induced Cytidine Deaminase (AID), a Novel Member of the RNA-editing Deaminase Family in Germinal Center B Cells. Journal of Biological Chemistry 274, 18470–18476. https://doi.org/10.1074/jbc.274.26.18470

Nativi, C., Papi, F., Roelens, S., 2019. Tn antigen analogues: the synthetic way to “upgrade” an attracting tumour associated carbohydrate antigen (TACA). Chemical Communications 55, 7729–7736. https://doi.org/10.1039/C9CC02920F

Nazha, B., Inal, C., Owonikoko, T.K., 2020. Disialoganglioside GD2 Expression in Solid Tumors and Role as a Target for Cancer Therapy. Front Oncol 10, 1000. https://doi.org/10.3389/fonc.2020.01000

Neftel, K.A., Wälti, M., Schulthess, H.K., Gubler, J., 1984. Adverse reactions following intravenous penicillin-G relate to degradation of the drug in vitro. Klin Wochenschr 62, 25–29. https://doi.org/10.1007/BF01725189

Nemazee, D., 2017. Mechanisms of central tolerance for B cells. Nat Rev Immunol 17, 281–294. https://doi.org/10.1038/nri.2017.19

Nemazee, D., 2000. Receptor Selection in B and T Lymphocytes. Annu Rev Immunol 18, 19–51. https://doi.org/10.1146/annurev.immunol.18.1.19

New, J.S., King, R.G., Kearney, J.F., 2016. Manipulation of the glycan-specific natural antibody repertoire for immunotherapy. Immunol Rev 270, 32–50. https://doi.org/10.1111/imr.12397

Ni, J., Song, H., Wang, Y., Stamatos, N.M., Wang, L.-X., 2006. Toward a Carbohydrate-Based HIV-1 Vaccine: Synthesis and Immunological Studies of Oligomannose-Containing Glycoconjugates. Bioconjug Chem 17, 493–500. https://doi.org/10.1021/bc0502816

Nieuwenhuis, P., Opstelten, D., 1984. Functional anatomy of germinal centers. American Journal of Anatomy 170, 421–435. https://doi.org/10.1002/aja.1001700315

Nutt, S.L., Hodgkin, P.D., Tarlinton, D.M., Corcoran, L.M., 2015. The generation of antibody-secreting plasma cells. Nat Rev Immunol 15, 160–171. https://doi.org/10.1038/nri3795

O'Cearbhaill, R., Ragupathi, G., Zhu, J., Wan, Q., Mironov, S., Yang, G., Spassova, M., Iasonos, A., Kravetz, S., Ouerfelli, O., Spriggs, D., Danishefsky, S., Sabbatini, P., 2016. A Phase I Study of Unimolecular Pentavalent (Globo-H-GM2-sTn-TF-Tn) Immunization of Patients with Epithelial Ovarian, Fallopian Tube, or Peritoneal Cancer in First Remission. Cancers (Basel) 8, 46. https://doi.org/10.3390/cancers8040046

Oyelaran, O., Gildersleeve, J.C., 2010. Evaluation of human antibody responses to keyhole limpet hemocyanin on a carbohydrate microarray. Proteomics Clin Appl 4, 285–294. https://doi.org/10.1002/prca.200900130

Padlan, E.A., 1994. Anatomy of the antibody molecule. Mol Immunol 31, 169–217. https://doi.org/10.1016/0161-5890(94)90001-9

Palmer, M., Parker, J., Modi, S., Butts, C., Smylie, M., Meikle, A., Kehoe, M., MacLean, G., Longenecker, M., 2001. Phase I Study of the BLP25 (MUC1 Peptide) Liposomal Vaccine for Active Specific Immunotherapy in Stage IIIB/IV Non–Small-Cell Lung Cancer. Clin Lung Cancer 3, 49–57. https://doi.org/https://doi.org/10.3816/CLC.2001.n.018

Pan, Y., Chefalo, P., Nagy, N., Harding, C., Guo, Z., 2005. Synthesis and immunological properties of N-modified GM3 antigens as therapeutic cancer vaccines. J Med Chem 48, 875–883. https://doi.org/10.1021/jm0494422

Park, J.-E., Wu, D.Y., Prendes, M., Lu, S.X., Ragupathi, G., Schrantz, N., Chapman, P.B., 2008. Fine specificity of natural killer T cells against GD3 ganglioside and identification of GM3 as an inhibitory natural killer T-cell ligand. Immunology 123, 145–155. https://doi.org/10.1111/j.1365-2567.2007.02760.x

Pellicci, D.G., Clarke, A.J., Patel, O., Mallevaey, T., Beddoe, T., Le Nours, J., Uldrich, A.P., McCluskey, J., Besra, G.S., Porcelli, S.A., Gapin, L., Godfrey, D.I., Rossjohn, J., 2011. Recognition of β-linked self glycolipids

mediated by natural killer T cell antigen receptors. Nat Immunol 12, 827–833. https://doi.org/10.1038/ni.2076

Pender, M.P., Csurhes, P.A., Wolfe, N.P., Hooper, K.D., Good, M.F., McCombe, P.A., Greer, J.M., 2003. Increased circulating T cell reactivity to GM3 and GQ1b gangliosides in primary progressive multiple sclerosis. J Clin Neurosci 10, 63–66. https://doi.org/10.1016/s0967-5868(02)00270-9

Peng, W., de Vries, R.P., Grant, O.C., Thompson, A.J., McBride, R., Tsogtbaatar, B., Lee, P.S., Razi, N., Wilson, I.A., Woods, R.J., Paulson, J.C., 2017. Recent H3N2 Viruses Have Evolved Specificity for Extended, Branched Human-type Receptors, Conferring Potential for Increased Avidity. Cell Host Microbe 21, 23–34. https://doi.org/10.1016/j.chom.2016.11.004

Peter, A.S., Roth, E., Schulz, S.R., Fraedrich, K., Steinmetz, T., Damm, D., Hauke, M., Richel, E., Mueller-Schmucker, S., Habenicht, K., Eberlein, V., Issmail, L., Uhlig, N., Dolles, S., Grüner, E., Peterhoff, D., Ciesek, S., Hoffmann, M., Pöhlmann, S., McKay, P.F., Shattock, R.J., Wölfel, R., Socher, E., Wagner, R., Eichler, J., Sticht, H., Schuh, W., Neipel, F., Ensser, A., Mielenz, D., Tenbusch, M., Winkler, T.H., Grunwald, T., Überla, K., Jäck, H., 2022. A pair of noncompeting neutralizing human monoclonal antibodies protecting from disease in a SARS-CoV-2 infection model. Eur J Immunol 52, 770–783. https://doi.org/10.1002/eji.202149374

Péterfi, Z., Kocsis, B., 2000. Comparison of Blocking Agents for an Elisa for Lps. J Immunoassay 21, 341–354. https://doi.org/10.1080/01971520009349541

Peters, T., 1985. Serum Albumin. pp. 161–245. https://doi.org/10.1016/S0065-3233(08)60065-0

Pollard, A.J., Perrett, K.P., Beverley, P.C., 2009. Maintaining protection against invasive bacteria with protein-polysaccharide conjugate vaccines. Nat Rev Immunol 9, 213–220. https://doi.org/10.1038/nri2494

Polonskaya, Z., Savage, P.B., Finn, M.G., Teyton, L., 2019. High-affinity anti-glycan antibodies: challenges and strategies. Curr Opin Immunol 59, 65–71. https://doi.org/10.1016/j.coi.2019.03.004

Poschet, J.F., Hammond, S.M., Fairclough, P.D., 1999. Characterisation of penicillin G uptake in human small intestinal brush border membrane vesicles. Gut 44, 620. https://doi.org/10.1136/gut.44.5.620

Posey, A.D.J., Schwab, R.D., Boesteanu, A.C., Steentoft, C., Mandel, U., Engels, B., Stone, J.D., Madsen, T.D., Schreiber, K., Haines, K.M., Cogdill, A.P., Chen, T.J., Song, D., Scholler, J., Kranz, D.M., Feldman, M.D., Young, R., Keith, B., Schreiber, H., Clausen, H., Johnson, L.A., June, C.H., 2016. Engineered CAR T Cells Targeting the Cancer-Associated Tn-Glycoform of the Membrane Mucin MUC1 Control Adenocarcinoma. Immunity 44, 1444–1454. https://doi.org/10.1016/j.immuni.2016.05.014

Potocnjak, P., Zavala, F., Nussenzweig, R., Nussenzweig, V., 1982. Inhibition of Idiotype—Anti-Idiotype Interaction for Detection of a Parasite Antigen: a New Immunoassay. Science (1979) 215, 1637–1639. https://doi.org/10.1126/science.6122269

Pratt, K., 2018. Anti-Drug Antibodies: Emerging Approaches to Predict, Reduce or Reverse Biotherapeutic Immunogenicity. Antibodies 7, 19. https://doi.org/10.3390/antib7020019

Prüss, H., 2021. Autoantibodies in neurological disease. Nat Rev Immunol 21, 798–813. https://doi.org/10.1038/s41577-021-00543-w

Ragupathi, G., Koide, F., Livingston, P.O., Cho, Y.S., Endo, A., Wan, Q., Spassova, M.K., Keding, S.J., Allen, J., Ouerfelli, O., Wilson, R.M., Danishefsky, S.J., 2006. Preparation and Evaluation of Unimolecular Pentavalent and Hexavalent Antigenic Constructs Targeting Prostate and Breast Cancer: A Synthetic Route to Anticancer Vaccine Candidates. J Am Chem Soc 128, 2715–2725. https://doi.org/10.1021/ja057244+

Rampoldi, F., Ullrich, L., Prinz, I., 2020. Revisiting the Interaction of γδ T-Cells and B-Cells. Cells 9. https://doi.org/10.3390/cells9030743

Rappuoli, R., De Gregorio, E., Costantino, P., 2019. On the mechanisms of conjugate vaccines. Proc Natl Acad Sci U S A 116, 14–16. https://doi.org/10.1073/pnas.1819612116

Ravindranath, M.H., Kelley, M.C., Jones, R.C., Amiri, A.A., Bauer, P.M., Morton, D.L., 1998. Ratio of IgG:IgM antibodies to sialyl Lewis(x) and GM3 correlates with tumor growth after immunization with melanoma-cell vaccine with different adjuvants in mice. Int J Cancer 75, 117–124.

https://doi.org/10.1002/(sici)1097-0215(19980105)75:1<117::aid-ijc18>3.0.co;2-d

Read, B.J., Won, L., Kraft, J.C., Sappington, I., Aung, A., Wu, S., Bals, J., Chen, C., Lee, K.K., Lingwood, D., King, N.P., Irvine, D.J., 2022. Mannose-binding lectin and complement mediate follicular localization and enhanced immunogenicity of diverse protein nanoparticle immunogens. Cell Rep 38, 110217. https://doi.org/10.1016/j.celrep.2021.110217

Rees, A.R., 2020. Understanding the human antibody repertoire. MAbs 12, 1729683. https://doi.org/10.1080/19420862.2020.1729683

Reily, C., Stewart, T.J., Renfrow, M.B., Novak, J., 2019. Glycosylation in health and disease. Nat Rev Nephrol 15, 346–366. https://doi.org/10.1038/s41581-019-0129-4

Rillahan, C.D., Brown, S.J., Register, A.C., Rosen, H., Paulson, J.C., 2011. High-throughput screening for inhibitors of sialyl- and fucosyltransferases. Angew Chem Int Ed Engl 50, 12534–12537. https://doi.org/10.1002/anie.201105065

Ringe, R.P., Pugach, P., Cottrell, C.A., LaBranche, C.C., Seabright, G.E., Ketas, T.J., Ozorowski, G., Kumar, S., Schorcht, A., van Gils, M.J., Crispin, M., Montefiori, D.C., Wilson, I.A., Ward, A.B., Sanders, R.W., Klasse, P.J., Moore, J.P., 2019. Closing and Opening Holes in the Glycan Shield of HIV-1 Envelope Glycoprotein SOSIP Trimers Can Redirect the Neutralizing Antibody Response to the Newly Unmasked Epitopes. J Virol 93. https://doi.org/10.1128/JVI.01656-18

Robbiani, D.F., Gaebler, C., Muecksch, F., Lorenzi, J.C.C., Wang, Z., Cho, A., Agudelo, M., Barnes, C.O., Gazumyan, A., Finkin, S., Hägglöf, T., Oliveira, T.Y., Viant, C., Hurley, A., Hoffmann, H.-H., Millard, K.G., Kost, R.G., Cipolla, M., Gordon, K., Bianchini, F., Chen, S.T., Ramos, V., Patel, R., Dizon, J., Shimeliovich, I., Mendoza, P., Hartweger, H., Nogueira, L., Pack, M., Horowitz, J., Schmidt, F., Weisblum, Y., Michailidis, E., Ashbrook, A.W., Waltari, E., Pak, J.E., Huey-Tubman, K.E., Koranda, N., Hoffman, P.R., West, A.P., Rice, C.M., Hatziioannou, T., Bjorkman, P.J., Bieniasz, P.D., Caskey, M., Nussenzweig, M.C., 2020. Convergent antibody responses to SARS-CoV-2 in convalescent individuals. Nature 584, 437–442. https://doi.org/10.1038/s41586-020-2456-9

Rodrigues Mantuano, N., Natoli, M., Zippelius, A., Läubli, H., 2020. Tumor-associated carbohydrates and immunomodulatory lectins as targets for cancer immunotherapy. J Immunother Cancer 8, e001222. https://doi.org/10.1136/jitc-2020-001222

Rogers, M.S., Tyler, E.M., Akyumani, N., Kurtis, C.R., Spooner, R.K., Deacon, S.E., Tamber, S., Firbank, S.J., Mahmoud, K., Knowles, P.F., Phillips, S.E. V., McPherson, M.J., Dooley, D.M., 2007. The Stacking Tryptophan of Galactose Oxidase: A Second-Coordination Sphere Residue that Has Profound Effects on Tyrosyl Radical Behavior and Enzyme Catalysis †. Biochemistry 46, 4606–4618. https://doi.org/10.1021/bi062139d

Rogozin, I.B., Kolchanov, N.A., 1992. Somatic hypermutagenesis in immunoglobulin genes. II. Influence of neighbouring base sequences on mutagenesis. Biochim Biophys Acta 1171, 11–8. https://doi.org/10.1016/0167-4781(92)90134-l

Ruutu, M., Thomas, G., Steck, R., Degli-Esposti, M.A., Zinkernagel, M.S., Alexander, K., Velasco, J., Strutton, G., Tran, A., Benham, H., Rehaume, L., Wilson, R.J., Kikly, K., Davies, J., Pettit, A.R., Brown, M.A., McGuckin, M.A., Thomas, R., 2012. β-glucan triggers spondylarthritis and Crohn's disease-like ileitis in SKG mice. Arthritis Rheum 64, 2211–22. https://doi.org/10.1002/art.34423

Sabbatini, P.J., Ragupathi, G., Hood, C., Aghajanian, C.A., Juretzka, M., Iasonos, A., Hensley, M.L., Spassova, M.K., Ouerfelli, O., Spriggs, D.R., Tew, W.P., Konner, J., Clausen, H., Abu Rustum, N., Dansihefsky, S.J., Livingston, P.O., 2007. Pilot Study of a Heptavalent Vaccine-Keyhole Limpet Hemocyanin Conjugate plus QS21 in Patients with Epithelial Ovarian, Fallopian Tube, or Peritoneal Cancer. Clinical Cancer Research 13, 4170–4177. https://doi.org/10.1158/1078-0432.CCR-06-2949

Sawada, M., Moriya, S., Shineha, R., Satomi, S., Miyagi, T., 1998. Comparative study of sialidase activity and G(M3) content in B16 melanoma variants with different metastatic potential. Acta Biochim Pol 45, 343–9.

Schaefer-Babajew, D., Wang, Z., Muecksch, F., Cho, A., Loewe, M., Cipolla, M., Raspe, R., Johnson, B., Canis, M., DaSilva, J., Ramos, V., Turroja, M., Millard, K.G., Schmidt, F., Witte, L., Dizon, J., Shimeliovich, I., Yao, K.-H., Oliveira, T.Y., Gazumyan, A., Gaebler, C., Bieniasz, P.D., Hatziioannou, T.,

Caskey, M., Nussenzweig, M.C., 2023. Antibody feedback regulates immune memory after SARS-CoV-2 mRNA vaccination. Nature 613, 735–742. https://doi.org/10.1038/s41586-022-05609-w

Scheid, J.F., Mouquet, H., Ueberheide, B., Diskin, R., Klein, F., Oliveira, T.Y.K., Pietzsch, J., Fenyo, D., Abadir, A., Velinzon, K., Hurley, A., Myung, S., Boulad, F., Poignard, P., Burton, D.R., Pereyra, F., Ho, D.D., Walker, B.D., Seaman, M.S., Bjorkman, P.J., Chait, B.T., Nussenzweig, M.C., 2011. Sequence and structural convergence of broad and potent HIV antibodies that mimic CD4 binding. Science 333, 1633–1637. https://doi.org/10.1126/science.1207227

Schoel, B., Sprenger, S., Kaufmann, S.H., 1994. Phosphate is essential for stimulation of V gamma 9V delta 2 T lymphocytes by mycobacterial low molecular weight ligand. Eur J Immunol 24, 1886–1892. https://doi.org/10.1002/eji.1830240826

Schüttelkopf, A.W., van Aalten, D.M.F., 2004. PRODRG: a tool for high-throughput crystallography of protein–ligand complexes. Acta Crystallogr D Biol Crystallogr 60, 1355–1363. https://doi.org/10.1107/S0907444904011679

Schwarz, M., Spector, L., Gortler, M., Weisshaus, O., Glass-Marmor, L., Karni, A., Dotan, N., Miller, A., 2006. Serum anti-Glc(alpha1,4)Glc(alpha) antibodies as a biomarker for relapsing-remitting multiple sclerosis. J Neurol Sci 244, 59–68. https://doi.org/10.1016/j.jns.2005.12.006

Shao, J., Kuiper, B.P., Thunnissen, A.-M.W.H., Cool, R.H., Zhou, L., Huang, C., Dijkstra, B.W., Broos, J., 2022. The Role of Tryptophan in π Interactions in Proteins: An Experimental Approach. J Am Chem Soc 144, 13815–13822. https://doi.org/10.1021/jacs.2c04986

Shevchenko, A., Tomas, H., Havli, J., Olsen, J. V, Mann, M., 2006. In-gel digestion for mass spectrometric characterization of proteins and proteomes. Nat Protoc 1, 2856–2860. https://doi.org/10.1038/nprot.2006.468

Shimizu, T., Nagane, M., Suzuki, M., Yamauchi, A., Kato, K., Kawashima, N., Nemoto, Y., Maruo, T., Kawakami, Y., Yamashita, T., 2020. Tumor hypoxia regulates ganglioside GM3 synthase, which contributes to oxidative stress

resistance in malignant melanoma. Biochim Biophys Acta Gen Subj 1864, 129723. https://doi.org/10.1016/j.bbagen.2020.129723

Shingai, M., Donau, O.K., Plishka, R.J., Buckler-White, A., Mascola, J.R., Nabel, G.J., Nason, M.C., Montefiori, D., Moldt, B., Poignard, P., Diskin, R., Bjorkman, P.J., Eckhaus, M.A., Klein, F., Mouquet, H., Cetrulo Lorenzi, J.C., Gazumyan, A., Burton, D.R., Nussenzweig, M.C., Martin, M.A., Nishimura, Y., 2014. Passive transfer of modest titers of potent and broadly neutralizing anti-HIV monoclonal antibodies block SHIV infection in macaques. J Exp Med 211, 2061–2074. https://doi.org/10.1084/jem.20132494

Soliman, C., Chua, J.X., Vankemmelbeke, M., McIntosh, R.S., Guy, A.J., Spendlove, I., Durrant, L.G., Ramsland, P.A., 2020a. The terminal sialic acid of stage-specific embryonic antigen-4 has a crucial role in binding to a cancer-targeting antibody. Journal of Biological Chemistry 295, 1009–1020. https://doi.org/10.1074/jbc.RA119.011518

Soliman, C., Chua, J.X., Vankemmelbeke, M., McIntosh, R.S., Guy, A.J., Spendlove, I., Durrant, L.G., Ramsland, P.A., 2020b. The terminal sialic acid of stage-specific embryonic antigen-4 has a crucial role in binding to a cancer-targeting antibody. Journal of Biological Chemistry 295, 1009–1020. https://doi.org/10.1074/jbc.RA119.011518

Song, C., Zheng, X.-J., Liu, C.-C., Zhou, Y., Ye, X.-S., 2017. A cancer vaccine based on fluorine-modified sialyl-Tn induces robust immune responses in a murine model. Oncotarget 8, 47330–47343. https://doi.org/10.18632/oncotarget.17646

Speir, J.A., Abdel-Motal, U.M., Jondal, M., Wilson, I.A., 1999. Crystal structure of an MHC class I presented glycopeptide that generates carbohydrate-specific CTL. Immunity 10, 51–61. https://doi.org/10.1016/s1074-7613(00)80006-0

Stamatatos, L., Pancera, M., McGuire, A.T., 2017. Germline-targeting immunogens. Immunol Rev 275, 203–216. https://doi.org/10.1111/imr.12483

Starr, T.N., Greaney, A.J., Hilton, S.K., Ellis, D., Crawford, K.H.D., Dingens, A.S., Navarro, M.J., Bowen, J.E., Tortorici, M.A., Walls, A.C., King, N.P., Veesler, D., Bloom, J.D., 2020. Deep Mutational Scanning of SARS-CoV-2

Receptor Binding Domain Reveals Constraints on Folding and ACE2 Binding. Cell 182, 1295-1310.e20. https://doi.org/10.1016/j.cell.2020.08.012

Steichen, J.M., Kulp, D.W., Tokatlian, T., Escolano, A., Dosenovic, P., Stanfield, R.L., McCoy, L.E., Ozorowski, G., Hu, X., Kalyuzhniy, O., Briney, B., Schiffner, T., Garces, F., Freund, N.T., Gitlin, A.D., Menis, S., Georgeson, E., Kubitz, M., Adachi, Y., Jones, M., Mutafyan, A.A., Yun, D.S., Mayer, C.T., Ward, A.B., Burton, D.R., Wilson, I.A., Irvine, D.J., Nussenzweig, M.C., Schief, W.R., 2016. HIV Vaccine Design to Target Germline Precursors of Glycan-Dependent Broadly Neutralizing Antibodies. Immunity 45, 483–496. https://doi.org/10.1016/j.immuni.2016.08.016

Stils, H.F., 2005. Adjuvants and Antibody Production: Dispelling the Myths Associated with Freund's Complete and Other Adjuvants. ILAR J 46, 280–293. https://doi.org/10.1093/ilar.46.3.280

Sun, L., Paschall, A. V, Middleton, D.R., Ishihara, M., Ozdilek, A., Wantuch, P.L., Aceil, J., Duke, J.A., LaBranche, C.C., Tiemeyer, M., Avci, F.Y., 2020. Glycopeptide epitope facilitates HIV-1 envelope specific humoral immune responses by eliciting T cell help. Nat Commun 11, 2550. https://doi.org/10.1038/s41467-020-16319-0

Sun, X., Stefanetti, G., Berti, F., Kasper, D.L., 2019. Polysaccharide structure dictates mechanism of adaptive immune response to glycoconjugate vaccines. Proc Natl Acad Sci U S A 116, 193–198. https://doi.org/10.1073/pnas.1816401115

Tannert, L.K., Mortz, C.G., Skov, P.S., Bindslev-Jensen, C., 2017. Positive Skin Test or Specific IgE to Penicillin Does Not Reliably Predict Penicillin Allergy. J Allergy Clin Immunol Pract 5, 676–683. https://doi.org/10.1016/j.jaip.2017.03.014

Tas, J.M.J., Mesin, L., Pasqual, G., Targ, S., Jacobsen, J.T., Mano, Y.M., Chen, C.S., Weill, J.-C., Reynaud, C.-A., Browne, E.P., Meyer-Hermann, M., Victora, G.D., 2016. Visualizing antibody affinity maturation in germinal centers. Science (1979) 351, 1048–1054. https://doi.org/10.1126/science.aad3439

Tei, K., Kawakami-Kimura, N., Taguchi, O., Kumamoto, K., Higashiyama, S., Taniguchi, N., Toda, K., Kawata, R., Hisa, Y., Kannagi, R., 2002. Roles of cell adhesion molecules in tumor angiogenesis induced by cotransplantation of cancer and endothelial cells to nude rats. Cancer Res 62, 6289–6296.

Temme, J.S., Butler, D.L., Gildersleeve, J.C., 2021. Anti-glycan antibodies: roles in human disease. Biochemical Journal 478, 1485–1509. https://doi.org/10.1042/BCJ20200610

Tizard, I.R., 2021. Adjuvants and adjuvanticity. Vaccines for Veterinarians. https://doi.org/10.1016/B978-0-323-68299-2.00016-2

Tobola, F., Lelimousin, M., Varrot, A., Gillon, E., Darnhofer, B., Blixt, O., Birner-Gruenberger, R., Imberty, A., Wiltschi, B., 2018. Effect of Noncanonical Amino Acids on Protein–Carbohydrate Interactions: Structure, Dynamics, and Carbohydrate Affinity of a Lectin Engineered with Fluorinated Tryptophan Analogs. ACS Chem Biol 13, 2211–2219. https://doi.org/10.1021/acschembio.8b00377

Tokatlian, T., Read, B.J., Jones, C.A., Kulp, D.W., Menis, S., Chang, J.Y.H., Steichen, J.M., Kumari, S., Allen, J.D., Dane, E.L., Liguori, A., Sangesland, M., Lingwood, D., Crispin, M., Schief, W.R., Irvine, D.J., 2019. Innate immune recognition of glycans targets HIV nanoparticle immunogens to germinal centers. Science (1979) 363, 649–654. https://doi.org/10.1126/science.aat9120

Tonegawa, S., 1983. Somatic generation of antibody diversity. Nature 302, 575–581. https://doi.org/10.1038/302575a0

Topin, J., Lelimousin, M., Arnaud, J., Audfray, A., Pérez, S., Varrot, A., Imberty, A., 2016. The Hidden Conformation of Lewis x, a Human Histo-Blood Group Antigen, Is a Determinant for Recognition by Pathogen Lectins. ACS Chem Biol 11, 2011–2020. https://doi.org/10.1021/acschembio.6b00333

Trabbic, K.R., Kleski, K.A., Barchi, J.J.Jr., 2021. Stable Gold-Nanoparticle-Based Vaccine for the Targeted Delivery of Tumor-Associated Glycopeptide Antigens. ACS Bio & Med Chem Au 1, 31–43. https://doi.org/10.1021/acsbiomedchemau.1c00021

Trinchera, M., Aronica, A., Dall'Olio, F., 2017. Selectin Ligands Sialyl-Lewis a and Sialyl-Lewis x in Gastrointestinal Cancers. Biology (Basel) 6. https://doi.org/10.3390/biology6010016

Tringali, C., Silvestri, I., Testa, F., Baldassari, P., Anastasia, L., Mortarini, R., Anichini, A., López-Requena, A., Tettamanti, G., Venerando, B., 2014. Molecular subtyping of metastatic melanoma based on cell ganglioside metabolism profiles. BMC Cancer 14, 560. https://doi.org/10.1186/1471-2407-14-560

Vaisman-Mentesh, A., Rosenstein, S., Yavzori, M., Dror, Y., Fudim, E., Ungar, B., Kopylov, U., Picard, O., Kigel, A., Ben-Horin, S., Benhar, I., Wine, Y., 2019. Molecular Landscape of Anti-Drug Antibodies Reveals the Mechanism of the Immune Response Following Treatment With TNFα Antagonists. Front Immunol 10. https://doi.org/10.3389/fimmu.2019.02921

Varki, A., 2017. Biological roles of glycans. Glycobiology 27, 3–49. https://doi.org/10.1093/glycob/cww086

Varki, A., 2016. Biological roles of glycans. Glycobiology 27, 3–49. https://doi.org/10.1093/glycob/cww086

Vasconcelos-dos-Santos, A., Oliveira, I.A., Lucena, M.C., Mantuano, N.R., Whelan, S.A., Dias, W.B., Todeschini, A.R., 2015. Biosynthetic Machinery Involved in Aberrant Glycosylation: Promising Targets for Developing of Drugs Against Cancer. Front Oncol 5, 138. https://doi.org/10.3389/fonc.2015.00138

Veneziano, R., Moyer, T.J., Stone, M.B., Wamhoff, E.-C., Read, B.J., Mukherjee, S., Shepherd, T.R., Das, J., Schief, W.R., Irvine, D.J., Bathe, M., 2020. Role of nanoscale antigen organization on B-cell activation probed using DNA origami. Nat Nanotechnol 15, 716–723. https://doi.org/10.1038/s41565-020-0719-0

Viant, C., Escolano, A., Chen, S.T., Nussenzweig, M.C., 2021. Sequencing, cloning, and antigen binding analysis of monoclonal antibodies isolated from single mouse B cells. STAR Protoc 2, 100389. https://doi.org/https://doi.org/10.1016/j.xpro.2021.100389

Vicetti Miguel, R.D., Maryak, S.A., Cherpes, T.L., 2012. Brefeldin A, but not monensin, enables flow cytometric detection of interleukin-4 within

peripheral T cells responding to ex vivo stimulation with Chlamydia trachomatis. J Immunol Methods 384, 191–195.

Victora, G.D., Nussenzweig, M.C., 2022. Germinal Centers. Annu Rev Immunol 40, 413–442. https://doi.org/10.1146/annurev-immunol-120419-022408

Vinuesa, C.G., Linterman, M.A., Yu, D., MacLennan, I.C.M., 2016a. Follicular Helper T Cells. Annu Rev Immunol 34, 335–368. https://doi.org/10.1146/annurev-immunol-041015-055605

Vinuesa, C.G., Linterman, M.A., Yu, D., MacLennan, I.C.M., 2016b. Follicular Helper T Cells. Annu Rev Immunol 34, 335–368. https://doi.org/10.1146/annurev-immunol-041015-055605

von Boehmer, L., Liu, C., Ackerman, S., Gitlin, A.D., Wang, Q., Gazumyan, A., Nussenzweig, M.C., 2016. Sequencing and cloning of antigen-specific antibodies from mouse memory B cells. Nat Protoc 11, 1908–1923. https://doi.org/10.1038/nprot.2016.102

Vultaggio, A., Nencini, F., Pratesi, S., Petroni, G., Maggi, E., Matucci, A., 2014. Manifestations of Antidrug Antibodies Response: Hypersensitivity and Infusion Reactions. Journal of Interferon & Cytokine Research 34, 946–952. https://doi.org/10.1089/jir.2012.0139

Wagner, S., Mersch, C., Hoffmann-Röder, A., 2010. Fluorinated Glycosyl Amino Acids for Mucin-Like Glycopeptide Antigen Analogues. Chemistry – A European Journal 16, 7319–7330. https://doi.org/https://doi.org/10.1002/chem.200903294

Wagner, S.D., Milstein, C., Neuberger, M.S., 1995. Codon bias targets mutation. Nature 376, 732–732. https://doi.org/10.1038/376732a0

Walker, J.E., 1976. Lysine residue 199 of human serum albumin is modified by acetylsalicylic acid. FEBS Lett 66, 173–175. https://doi.org/10.1016/0014-5793(76)80496-6

Ward, A.B., Wilson, I.A., 2017. The HIV-1 envelope glycoprotein structure: nailing down a moving target. Immunol Rev 275, 21–32. https://doi.org/10.1111/imr.12507

Watanabe, Y., Berndsen, Z.T., Raghwani, J., Seabright, G.E., Allen, J.D., Pybus, O.G., McLellan, J.S., Wilson, I.A., Bowden, T.A., Ward, A.B., Crispin, M., 2020. Vulnerabilities in coronavirus glycan shields despite

extensive glycosylation. Nat Commun 11, 2688. https://doi.org/10.1038/s41467-020-16567-0

Wegmann, F., Moghaddam, A.E., Schiffner, T., Gartlan, K.H., Powell, T.J., Russell, R.A., Baart, M., Carrow, E.W., Sattentau, Q.J., 2015. The Carbomer-Lecithin Adjuvant Adjuplex Has Potent Immunoactivating Properties and Elicits Protective Adaptive Immunity against Influenza Virus Challenge in Mice. Clinical and Vaccine Immunology 22, 1004–1012. https://doi.org/10.1128/CVI.00736-14

WEIGERT, M.G., CESARI, I.M., YONKOVICH, S.J., COHN, M., 1970. Variability in the Lambda Light Chain Sequences of Mouse Antibody. Nature 228, 1045–1047. https://doi.org/10.1038/2281045a0

Weiss, M.C., Green, H., 1967. Human-mouse hybrid cell lines containing partial complements of human chromosomes and functioning human genes. Proceedings of the National Academy of Sciences 58, 1104 LP – 1111. https://doi.org/10.1073/pnas.58.3.1104

WEISS, M.E., ADKINSON, N.F., 1988. Immediate hypersensitivity reactions to penicillin and related antibiotics. Clinical <html_ent glyph="@amp;" ascii="&"/> Experimental Allergy 18, 515–540. https://doi.org/10.1111/j.1365-2222.1988.tb02904.x

Werdelin, O., Meldal, M., Jensen, T., 2002. Processing of glycans on glycoprotein and glycopeptide antigens in antigen-presenting cells. Proc Natl Acad Sci U S A 99, 9611–9613. https://doi.org/10.1073/pnas.152345899

Whitaker, P., Meng, X., Lavergne, S.N., El-Ghaiesh, S., Monshi, M., Earnshaw, C., Peckham, D., Gooi, J., Conway, S., Pirmohamed, M., Jenkins, R.E., Naisbitt, D.J., Park, B.K., 2011. Mass spectrometric characterization of circulating and functional antigens derived from piperacillin in patients with cystic fibrosis. J Immunol 187, 200–11. https://doi.org/10.4049/jimmunol.1100647

Wieczorek, M., Abualrous, E.T., Sticht, J., Álvaro-Benito, M., Stolzenberg, S., Noé, F., Freund, C., 2017. Major Histocompatibility Complex (MHC) Class I and MHC Class II Proteins: Conformational Plasticity in Antigen Presentation. Front Immunol 8, 292.

Wilson, R.M., Danishefsky, S.J., 2013. A Vision for Vaccines Built from Fully Synthetic Tumor-Associated Antigens: From the Laboratory to the Clinic. J Am Chem Soc 135, 14462–14472. https://doi.org/10.1021/ja405932r

Winn, M.D., Ballard, C.C., Cowtan, K.D., Dodson, E.J., Emsley, P., Evans, P.R., Keegan, R.M., Krissinel, E.B., Leslie, A.G.W., McCoy, A., McNicholas, S.J., Murshudov, G.N., Pannu, N.S., Potterton, E.A., Powell, H.R., Read, R.J., Vagin, A., Wilson, K.S., 2011. Overview of the CCP 4 suite and current developments. Acta Crystallogr D Biol Crystallogr 67, 235–242. https://doi.org/10.1107/S0907444910045749

Winter, G., 2010. xia2: an expert system for macromolecular crystallography data reduction. J Appl Crystallogr 43, 186–190. https://doi.org/10.1107/S0021889809045701

Xia, J., Xue, J., Locke, R.D., Chandrasekaran, E. v, Srikrishnan, T., Matta, K.L., 2006. Synthesis of Fluorinated Mucin Core 2 Branched Oligosaccharides with the Potential of Novel Substrates and Enzyme Inhibitors for Glycosyltransferases and Sulfotransferases. J Org Chem 71, 3696–3706. https://doi.org/10.1021/jo052626j

Yamakawa, N., Yasuda, Y., Yoshimura, A., Goshima, A., Crocker, P.R., Vergoten, G., Nishiura, Y., Takahashi, T., Hanashima, S., Matsumoto, K., Yamaguchi, Y., Tanaka, H., Kitajima, K., Sato, C., 2020. Discovery of a new sialic acid binding region that regulates Siglec-7. Sci Rep 10, 8647. https://doi.org/10.1038/s41598-020-64887-4

Yolaç, E., Pınarbaşı, A., Ertekin, Ö., Güloğlu, F.B., Öztürk, S., 2012. Improving the approaches to increase the immunogenicity of Staphylococcal enteretoksin B. N Biotechnol 29, S223. https://doi.org/10.1016/j.nbt.2012.08.627

Young, M., Dinda, M., Singer, M., 1983. Effect of Tween 80 on lipid vesicle permeability. Biochimica et Biophysica Acta (BBA) - Biomembranes 735, 429–432. https://doi.org/10.1016/0005-2736(83)90158-X

Yu, S., Wang, Q., Zhang, J., Wu, Q., Guo, Z., 2011a. Synthesis and Evaluation of Protein Conjugates of GM3 Derivatives Carrying Modified Sialic Acids as Highly Immunogenic Cancer Vaccine Candidates. Medchemcomm 2, 524–530. https://doi.org/10.1039/C1MD00033K

Yu, S., Wang, Q., Zhang, J., Wu, Q., Guo, Z., 2011b. Synthesis and evaluation of protein conjugates of GM3 derivatives carrying modified sialic acids as highly immunogenic cancer vaccine candidates. Medchemcomm 2, 524. https://doi.org/10.1039/c1md00033k

Yuki, N., Yamada, M., Tagawa, Y., Takahashi, H., Handa, S., 1997. Pathogenesis of the neurotoxicity caused by anti-GD2 antibody therapy. J Neurol Sci 149, 127–130. https://doi.org/10.1016/S0022-510X(97)05390-2

Yvon, M., Anglade, P., Wal, J.-M., 1990. Identification of the binding sites of benzyl penicilloyl, the allergenic metabolite of penicillin, on the serum albumin molecule. FEBS Lett 263, 237–240. https://doi.org/10.1016/0014-5793(90)81382-X

Yvon, M., Wal, J.-M., 1988. Identification of lysine residue 199 of human serum albumin as a binding site for benzylpenicilloyl groups. FEBS Lett 239, 237–240. https://doi.org/10.1016/0014-5793(88)80924-4

Zan-Bar, I., Murphy, D.B., Strober, S., 1978. Cellular basis of tolerance to serum albumin in adult mice. I. characterization of T suppressor and T helper cells. J Immunol 120, 497–506.

Zhang, Y., Karki, R., Igwe, O.J., 2015. Toll-like receptor 4 signaling: A common pathway for interactions between prooxidants and extracellular disulfide high mobility group box 1 (HMGB1) protein-coupled activation. Biochem Pharmacol 98, 132–143. https://doi.org/10.1016/j.bcp.2015.08.109

Zhang, Z., Sauter, N.K., van den Bedem, H., Snell, G., Deacon, A.M., 2006. Automated diffraction image analysis and spot searching for high-throughput crystal screening. J Appl Crystallogr 39, 112–119. https://doi.org/10.1107/S0021889805040677

Zhou, T., Georgiev, I., Wu, X., Yang, Z.-Y., Dai, K., Finzi, A., Kwon, Y. Do, Scheid, J.F., Shi, W., Xu, L., Yang, Y., Zhu, J., Nussenzweig, M.C., Sodroski, J., Shapiro, L., Nabel, G.J., Mascola, J.R., Kwong, P.D., 2010. Structural basis for broad and potent neutralization of HIV-1 by antibody VRC01. Science 329, 811–817. https://doi.org/10.1126/science.1192819

Zhu, H., Rollier, C.S., Pollard, A.J., 2021. Recent advances in lipopolysaccharide-based glycoconjugate vaccines. Expert Rev Vaccines 1–24. https://doi.org/10.1080/14760584.2021.1984889

Zhu, J., Wan, Q., Lee, D., Yang, G., Spassova, M.K., Ouerfelli, O., Ragupathi, G., Damani, P., Livingston, P.O., Danishefsky, S.J., 2009. From Synthesis to Biologics: Preclinical Data on a Chemistry Derived Anticancer Vaccine. J Am Chem Soc 131, 9298–9303. https://doi.org/10.1021/ja901415s

Zolla-Pazner, S., Cohen, S.S., Boyd, D., Kong, X.-P., Seaman, M., Nussenzweig, M., Klein, F., Overbaugh, J., Totrov, M., 2016. Structure/Function Studies Involving the V3 Region of the HIV-1 Envelope Delineate Multiple Factors That Affect Neutralization Sensitivity. J Virol 90, 636–649. https://doi.org/10.1128/JVI.01645-15